ELECTROCHEMICAL STUDIES ON COMPARATIVE COMPLEXATION BEHAVIOUR OF HALOGEN SUBSTITUTED ACETATE IONS

A THESIS

SUBMITTED IN FULFILMENT OF THE REQUIREMENTS

FOR THE DEGREE OF

DOCTOR OF PHILOSOPHY

BUNDELKHAND UNIVERSITY

JHANSI, U. P.

March, 1988

t1586

8613

BY

SHAILENDRA KUMAR GUPTA

M. Sc;

Postgraduate Department of Chemistry, Dayanand Vedic College,

ORAI - 285001 (U. P.)

ACKNOWLEDGEMENTS.

First of all I express my sincere gratitude and indebtedness to Dr. S. C. Khurana, M.Sc. Ph.D., Postgraduate Department of Chemistry, Dayanand Vedic College, Orai for his valuable and inspiring guidance throughout the progress of this work.

I would be failing in my duty if I do not express my sincere sense of gratitute to my beloved parents and wife without whose blessings and constant encouragement this work would not have been possible.

I am grateful to the Principal and Dr. S. P. Saxena Reader and Head of Department of Chemistry of my institution for providing laboratory facilities.

I am also thankful to Dr. Dhirendra Singh Chandel of Govt. Science College, Gwalior for his unfailing interest in completion of this work.

I would also like to offer my thanks to all the colleagues of the Department for their affection and guidance

Last but not the least, I take this opportunity to record my thanks to all persons who worked with me and also who have been directly or indirectly helpful to me.

S. K. Gupta

(Shailendra Kumar Gupta)
Post Graduate Department of Chemistry,
Dayanand Vedic College
Orai

Orai
Dated: 4th March, 1988.

CERTIFICATE.

This is to certify that Shri Shailendra Kumar Gupta, a candidate for the degree of Doctor of Philosophy in Chemistry of Bundelkhand University, Jhansi, has worked under my guidance on, ' Electrochemical studies on Comparative Complexation behaviour of halogen substituted acetate ions.'

It is my firm opinion that he has taken enough pains to make the thesis upto the standard both in respect of contents and literary presentation.

I further certify that to the best of my knowledge, the work and approach is entirely original and it has not been carried out in the same manner or form anywhere else.

Shri Gupta has put in more than two hundred days of work in the Chemical laboratory of Dayanand Vedic College, Orai.

9.3.88

(S. C. Khurana)
M.Sc.Ph.D.
Postgraduate Department of Chemistry
Dayanand Vedic College, Orai.

ORAI
Dated: 9.3.88

CONTENTS

CHAPTER VI CADMIUM COMPLEXES

CHAPTER I

POLAROGRAPHY

Introduction and Developments

Just sixty five years ago, in the year 1922, Prof. J. Heyrovsky[1] of Prague, Czechoslovakia, discovered a versatile analytical technique which has gained unique prominence among the modern instrumental methods. Prof. Heyrovsky was rightly awarded the prestigious Nobel Prize in 1959 for this wonderful discovery. The method of polarography, as it commonly came to be known, consists of a unique type of electrolysis in that it involves the current voltage relationships at a dropping mercury electrode in contrast to stationary electrodes used earlier.

Ordinarily, electrolysis involves the transfer of ions to and fro from the electrode followed by the electrochemical processes which essentially involve the exchange of electrons at the electrode surface. In polarography mass transfer process is solely dependent upon natural diffusion to the exclusion of convection and migration processes. The effect due to migration is eliminated by using an excess of a supporting electrolyte while suppression of convection effects is achieved by electrolysing the test solutions in adequately controlled thermostat and protecting the apparatus from vibration and shock. In addition, the electrolysis is carried out for a very short duration such that the resultant change in concentration of the electroreducible or oxidisable species present in the bulk of the solution is assumed to be nil for purposes of theoretical treatment of the data. It is, therefore, essential that the dropping mercury electrode has micro dimensions

so that it is readily polarised and the other has a relatively large surface area which inhibits its ready polarisation. Under such conditions, any change in current with applied potential is connected directly with the electrolytic process occurring at the microelectrode (DME).

Though the current voltage curves obtained by polarography are quite different from those obtained by usual methods, many useful interpretations can be available from the study of these current voltage data.

A SIMPLE POLAROGRAPHIC CIRCUIT :

A simple polarographic circuit consists of an instrument assembled according to the diagram shown in figure 1.1. The test solution is placed in a cell A and the dropping mercury electrode B, which usually serves as a cathode, is dipped into it. The mercury pool at the bottom of the cell or any other half cell of known potential is made the anode. The dropping mercury electrode is connected to the negative pole of a battery F through a galvanometer G while the mercury pool or the other reference electrode C in the cell is joined through the sliding contact D of the rheostat E to the positive terminal of the battery.

The voltage applied across the electrolytic cell can be gradually varied from zero to the maximum emf of the battery with the help of slide contact on the rheostat. A variable shunt S attached to the galvanometer serves to read a wide range of current values. The galvanometer readings

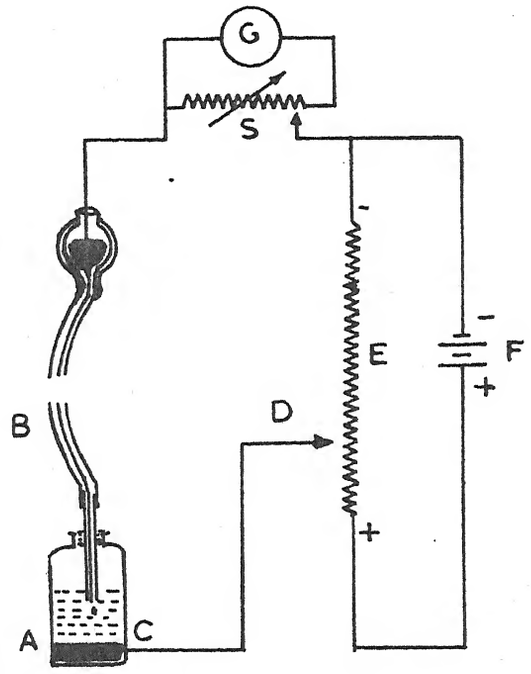

FIG. I. I SIMPLE CIRCUIT DIAGRAM FOR POLAROGRAPHIC ANALYSIS.

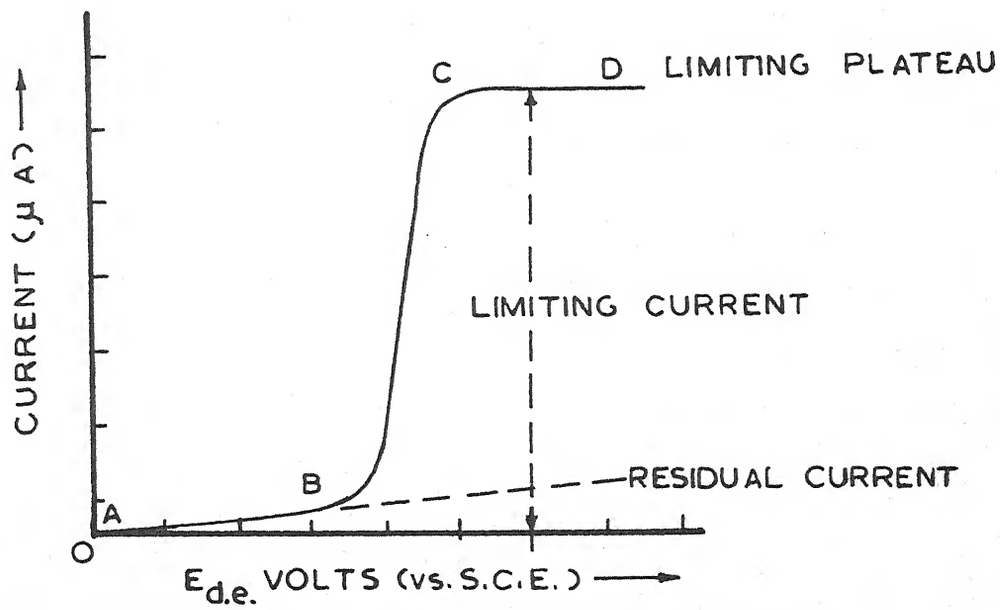

FIG. I. 2 A TYPICAL CURRENT - VOLTAGE CURVE.

oscillate between a maximum and a minimum value on account of change in surface area as each drop grows in size and falls. It is usual practice to record the average current at each applied potential.

Essentially, the technique consists in gradually increasing the applied potential and noting the corresponding galvanometer reading. A current voltage curve can thus be constructed by plotting current along the vertical axis and applied voltage along the horizontal axis.

POLAROGRAM - THE CURRENT VOLTAGE CURVE :

Figure 1.2 represents a typical current-voltage curve or a polarogram when an electroreducible species is present in the test solution. The shape of the curve reveals that at lower potentials, a small practically constant current flows. This small current is called the residual current. A further increase in applied potential results in sudden rise in current value when the ions begin to discharge at the DME. As a result, the solution surrounding the cathode becomes rapidly depleted of ions and concentration polarisation occurs. The concentration of the ions at the electrode surface drops until it becomes practically nil. Since the rate of reduction increases as more cathodic potential is applied, a point is eventually reached when all the ions reaching the electrode are reduced as fast as they diffuse through the concentration gradient so that current attains a maximum value. A further increase in potential can cause no further increase in overall reduction rate which is controlled

by the rate of diffusion. The current at this stage is called the limiting current.

THE LIMITING CURRENT :

The total or the limiting current consists of three contributions which are described below :

1. Residual current :

Generally this current is regarded as sum of two components. It is, predominantly, due to the potential required to charge the electrical double layer round the each drop while a small contribution is made by some reducible impurities present in the supporting electrolyte. The former and the latter are known as the 'condenser' and the 'faradaic' current respectively. Since the ultimate sensitivity is dependent upon the magnitude of residual current, it is a usual practice to study the test solution along with a blank solution.

2. The migration current :

The existence of a potential gradient across the electrodes results in electrostatic attraction of ions to oppositely charged electrodes causing what is known as the migration current. This is apart from the contribution due to diffusive force arising out of the concentration gradient. The magnitude of migration current component is dependent upon the transport number and the charge of the reducible ions. All practical polarographic work is done under conditions that serve to render the migration current negligible by carrying out studies

in presence of excess (at least 50 times) of a supporting electrolyte with ions of high transport number. Under such conditions, the transport number of the electroactive ion becomes practically nil resulting in almost complete elimination of the migration current. The addition of excess supporting electrolyte also decreases the cell current considerably minimising the iR drop so that the potential applied externally is practically equal to the potential drop across the electrodes.

3. The diffusion current :

When the migration current has been eliminated and the residual current substracted from the total limiting current, the remaining component reflects the flow of current due to reduction of electroactive ions that reach the cathode solely due to diffusion. This is known as the diffusion current.

From the experimental findings of Kemula[2], Ilcovic[3-4] derived the following relationship :

$$i_d = 706\ nCD^{1/2}\ m^{2/3}t^{1/6} \quad \text{for instantaneous current} \quad (1)$$

and $$i_d = 607\ nCD^{1/2}\ m^{2/3}t^{1/6} \quad \text{for mean current} \quad (2)$$

where

i_d = diffusion current in microamperes

n = number of electrons involved in the reduction/ oxidation of one particle (molecule or ion) of the electroactive species.

C = concentration of the electroactive species in millimoles l^{-1}

m = rate of flow of mercury through the capillary in mg sec^{-1}

t = drop time in seconds.

Thus with all the factors remaining constant, under given experimental conditions, the diffusion current is directly proportional to the concentration of the electroactive material.

Several workers have proposed that Ilcovic equation should be modified to account for the spherical diffusion to the DME rather than linear diffusion which Ilcovic assumed to derive equations (1) and (2). Lingane and Loverbridge[5] derived the following equation considering spherical diffusion

$$i_d = 607\ nD^{1/2}Cm^{2/3}t^{1/6} \quad [\ 1+Ad^{1/2}t^{1/6}/m^{1/3}\ ] \qquad (3)$$

and suggested the value of A to be 39. Strehlow and Von Stackelberg[6], however, have given A = 17 for the same equation. A little later Koutecky[7] formulated the equation

$$i_d = 607nD^{1/2}Cm^{2/3}t^{1/6} \quad 1 + 34D^{1/2}t^{1/6}/m^{1/3} + 100(Dt^{1/3}/m^{2/3}) \qquad (4)$$

in which the the third term in the parentheses is negligibly small.

Several other attempts[8-12] to derive a modified Ilcovic equation to account for spherical diffusion have ended up in equations similar to (4) differing only in the numerical value of A.

FACTORS AFFECTING DIFFUSION CURRENT :

1. Concentration of the depolarizer :

Subject to the absence of any side reactions other than reduction/oxidation, the diffusion current is directly proportional to concentration of the depolarizer[13] i.e. the electroactive species.

2. Diffusion coefficient of the depolarizer :

In a given media, the size of a depolarizer particle is constant. Therefore, under identical conditions (composition of media and temperature), the diffusion co-efficient of the depolarizer should not vary causing little effect on the diffusion current.

3. Capillary characteristics :

The concentration and diffusion co-efficient remaining constant, the diffusion current is proportional to $m^{2/3}t^{1/6}$ (Ilcovic equation). But since the rate of flow of mercury (m) through the DME is proportional to the pressure and drop time (t) is inversely proportional to this pressure, mt does not vary significantly with change in height of the mercury column or the mercury pressure. It has been shown[14] that $m^{2/3}t^{1/6}$ is proportional to $h_{corr.}^{1/2}$ (square root of corrected height of mercury column). Therefore, from Ilcovic equation (1)

$$i_d/h_{corr.}^{1/2} = \text{constant} \qquad \text{-----} \qquad (5)$$

This relationship is widely used to ascertain the

diffusion controlled nature of a polarographic wave.

4. Temperature :

A change in temperature of the test solution influences viscosity, density, interfacial tension of mercury and the diffusion coefficient of the depolarizer. Contribution due to the first three factors is negligibly small. Effect of temperature on change in the diffusion co-efficient (2-3% $deg.^{-1}$) should, however, be considered. This is of the order of 1-1.5% per degree rise in temperature for diffusion current. Making allowance for the other factors, the temperature co-efficient of i_d should not exceed 2% deg^{-1} provided the reduction/oxidation is solely diffusion controlled.

5. Nature of the media :

While studying reduction of metal ions, it is seen that in presence of a complexing agent, the diffusion current is found to decrease due, largely, to an increase in size and hence a decrease in diffusion co-efficient of the species which diffuse to the DME. Larger the size of the ligand, smaller is the diffusion current.

In general, increased viscosity due to the presence of a non-aqueous component in the media tends to decrease diffusion current obeying the relation $i_d \propto \eta^{-1/2}$.

POLAROGRAPHIC MAXIMA :

A polarographic maxima may be defined as an abnormal increase in current at the top of a polarogram followed by a

decrease until at sufficiently negative potentials the value of limiting current is reached. The shape of the maxima may vary from an acute peak to a rounded hump. The maxima may be classified into two types : the streaming and the non-streaming type. On account of vigorous motion of solution round the mercury drop, larger number of ions reach the cathode than those due only to diffusion resulting in an abrupt rise in current which is classified as the streaming type. Non-streaming maxima have a catalytic origin. Addition of small quantity of a surface active substance such as gelatin[15], Triton X-100[16] etc. serves to eliminate the maxima. Large concentration of a maxima-suppressor should be avoided to obtain reliable results; otherwise, a gross change in diffusion current and a shift in the position of the wave considerably distorts the results. 0.005%, 0.002% and 0.004% are the maximum permissible concentrations of gelatin, triton-X-100 and methyl red respectively.

KINETIC CURRENT :

In some cases, a chemical reaction preceding the electrode reaction produces an electroactive species which is subsequently reduced at the DME. The height of the wave is then partly or wholly governed by the rate of preceding reaction. The component of the total current which is observed due to the chemical reaction is called the kinetic current. For example Y is chemically converted into electroactive O which is then reduced to R as follows :

$$Y \underset{k_b}{\overset{k_f}{\rightleftharpoons}} O + ne \longrightarrow R$$

Kinetic current is, therefore, proportional to the concentration of the depolarizer. An excellent derivation of kinetic current is given by Delahay[17].

ADSORPTION CURRENT :

Adsorption current is observed when either the electroactive species or the product of the electrode reaction is adsorbed on the surface of the mercury electrode indicating itself as a pre-wave or a post-wave[18] respectively. The adsorption wave is independent of the concentration of the electro-active species though proportional to the height of the mercury column.

CATLYTIC CURRENT :

Catalytic current is generally observed when the presence of an external substance called a catalyst regenerates the original electroactive species from the electrode reaction. This regenerated species is again available for electrode reduction. Some times the catalyst may produce a different substance which is also reducible.

$$O + ne \rightleftharpoons R$$

$$R + X \underset{}{\overset{k_f}{\rightleftharpoons}} O$$

Catalytic waves are characterised by non-linear dependence on the catalyst concentration. Exceedingly small concentrations of the original electroactive substance may be determined from catalytic considerations[19-20].

HALF WAVE POTENTIAL :

The ease of reduction/oxidation for different substances is reflected by a parameter called the half wave potential ($E_{1/2}$) which may be defined as the potential at which the current due to reduction/oxidation of the substance responsible for the wave is half as large as the plateau[21]. In a given media, $E_{1/2}$ of a substance is the characteristic property of that substance at a definite temperature. It is independent of concentration of the depolarizer, size of the mercury drop, the drop-time and the galvanometer sensitivity. It is the usual practice to prefix a positive or a negative sign on $E_{1/2}$ according whether the potential is more positive or more negative than the potential of the saturated calomel electrode (SCE) which usually serves as a reference electrode.

FACTORS AFFECTING HALF WAVE POTENTIAL :

The effects of various experimental variables on the half wave potential are discussed below :

For a reversible reduction, the $E_{1/2}$ changes to an extent of $\pm$ 2 mV per degree rise in temperature. For an irreversible wave, however, this change may exceed several millivolts.

Half wave potential for a reversible wave is independent of the concentration of the depolarizer. The capillary characteristics m and t also do not affect the half wave potential. A negligibly small dependence on $m^{1/3}t^{1/6}$ is observed

when the diffusion co-efficients of the oxidised and reduced forms differ. This is, too , dismal to be taken into consideration.

$E_{1/2}$ becomes more anodic as t increases in the case of totally irreversible wave.

Nature of the media significantly affects the half wave potential. Complexing nature of the supporting electrolyte shifts the $E_{1/2}$ to more negative side. Effect of pH, specially in the reduction of organic compounds, plays an important role.

Variation of half wave potential in the non-aqueous media has been investigated by Amis[22] and Schaap[23]. Kirchmayer[24] has related the $E_{1/2}$ of reduction of a metal ion to the structure of amalgam formed. Effect of ionic strength on $E_{1/2}$ has been studied by Sellers and Vandenborgh[25-26]. Zahradnik and Parkamyr[27] have reviewed the correlation between $E_{1/2}$ and quantum mechanical characteristics of the depolarizer.

MODERN DEVELOPMENTS :

Soon after the initial development of polarography, automatic recording of polarograms was introduced first by Heyrovsky and Shikata[28] using a photographically recording instrument which was later conveniently made a pen-recording type. There are now many methods using the dropping mercury electrode, though bearing no resemblance with classical polarography. Thanks to the development of new methods the limit of sensitivity now stands extended from 10^{-5} M. In addition greater resolution of successive waves is possible. Such advances have greatly extended

the varsatility and speed of polarography as an analytical implement.

The following lines give a brief resume of the modern polarographic technique as a development of the classical method.

OSCILLOGRAPHIC POLAROGRAPHY :

In this technique rapid changes in the electrical system are displayed on a cathode ray osciloscope (CRO). It consists of essentially two techniques discussed below :

(i) Oscillographic polarography with controlled current :

In this method first developed by Heyrovsky and Forejt[29], the current is controlled and potential variations with time are investigated. A fifty c/s sine wave A.C. voltage of about 100 V is applied across the polarographic cell and a large variable resistance. The large resistance accounts for the most part of the voltage drop. A DC voltage is superimposed upon the AC voltage across the cell to determine the AC potential sweep. A stationary potential time curve is obtained on the CRO screen if the frequency of time sweep is synchronized with that of the AC voltage. The curve, so obtained, is a 'double' polarogram in which the potential range is swept out in both forward and backward directions.

A comparative study of these curves provides useful information regarding electrode processes.

(ii) Oscillographic polarography with controlled potential :

Much of the credit for this technique should go to

Davis and Seaborn[30-31]. A controlled drop-life, usually, of the order of 7 seconds is adjusted. It is presumed that for a drop life of 7 seconds, no significant change in surface area of the drop takes place for the last two seconds during which period, a rapid voltage sweep is applied and consequent changes in current are observed on the CRO screen. In this case, stationary current voltage curve is obtained. The curve appears to be a conventional DC polarogram with a maxima which is due to the rapid stripping of the depolarizer from the vicinity of the DME during rapid voltage sweep (0.5 V/2s). The peak height (i_p) is directly proportional to the concentration of the depolarizer.

ALTERNATING CURRENT POLAROGRAPHY :

Four main types of AC polarography are discussed below :

1. Sinusoidal AC polarography :

This technique owes its development to the work done by Breyer and coworkers[32]. A small sinusoidal low frequency alternating potential is superimposed on the applied DC potential in a polarographic circuit. The resultant current consists of two parts (a) DC part related to mean potential E of the electrode (b) an AC part which gives a peaked curve when the alternating component of the cell current is plotted against the applied DC voltage. This peak height is directly proportional to the concentration of the depolarizer.

2. Square wave polarography :

This method was developed by Barker and Jenkins[33] to

overcome the effect of interference from capacity current in Bryer's method. They applied 225 c/s square wave voltage of less than 30 mV on a slowly changing DC voltage so that at the end of each half cycle there is a superior faradaic to non-faradaic current ratio. This facilitates resolution of peaks separated by as little as 45 mV. Components in mixtures with component ratio of the order of 1:20,000 can be estimated efficiently. Determinations as low as 10^{-8} M are possible though the technique does not provide excellent results for irreversible reductions. Another fault in the technique makes itself felt due to capillary response at the detachment of each drop, a small quantity of the electrolyte is drawn into the tip of the capillary-causing an unstable response on the recorder.

3. Pulse polarography :

In this method the 'capillary response' referred to in the previous method was eliminated by Barker and coworkers[34] by applying voltage pulse at some specific instance in the drop life. Introduction of such pulse technique kept the 'capillary response' at a minimum even when working at high sensitivity.

4. Radio frequency polarography :

In squar-wave polarography, the instability of the response produced by small defects[35] in the dropping mercury electrode results in limited sensitivity of the instrument. A radio frequency attachment has been developed which virtually eliminates any response due to electrode defects. In this technique

an amplitude modulated radio frequency current of 200 kc/s is passed through the cell. The radio frequency current is fully modulated by a squar-wave voltage taken from the circuits of the polarograph and the polarograph measures the magnitude of the low frequency alternating current caused by faradaic rectification[36-37] at the interface of the electrode and the solution. Such measurements result in better sensitivity for reversible as well as irreversible processes. It is very useful in estimation of concentrations as low as 10^{-9} M.

APPLICATIONS OF POLAROGRAPHY :

From the usual current voltage curves obtained in polarography, useful information can be gathered as regards some specific characteristics such as half wave potential magnitude and nature of current and extent of electron participation that are associated with a particular electroactive species. Some times these parameters help us in having an insight into the electrode mechanism and kinetics of the reduction/oxidation. Industry and research make gainful use of the determinations of the order of 10^{-9} M. Components of mixtures with high component ratios can now be estimated with precision. Electroactivity of some classes of organic compounds has introduced polarography to biochemical research.

In metallurgy, polarography plays a useful role in the analysis of raw materials and alloys. Traces of metals in alloys control their physical properties and determination is all the more important. Polarographic determination of traces of lead and

cadmium in copper[38], chrome in steel[39], alkali metals, aluminium, cadmium, zinc, lead and copper in zinc ores[40], manganese and iron in iron ores have been reported.

Organic compounds with conjugated systems containing a quinoid structure e.g. quinone-hydroquinone system and some redox indicators e.g. methylene blue have been studied polarographically. Study of aldehydes, ketones, mono-saccharides, unsaturated acids, nitro and amino compounds, imines, oximes and certain other heterocyclic compounds have been investigated to obtain their reduction waves. Recently, polarography of some mercapto acids has been reported.

Polarography has been usefully employed in the fields of pharmacy and biochemistry. Determination of vitamins, morphine barbital in medicinal preparations and analysis of etheric oil[41] are few examples of applications of polarography in this field.

In food industry, determination of quality and origin of honey, lead in tinned food, aldehydes in spirit, ascorbic acid in fruits and vegetables and iodine in table salts[42] embrace some of the numerous polarographic applications.

All these determinations derive advantage from small sample requirement, speed, sensitivity and selectivity of the method of polarography, thus, demonstrating that the technique has unlimited scope in the explorations in and advancement of scientific knowledge which ultimately serves the mankind as a whole. As a tribute to the versality of polarography as an

excellent tool of analysis, Prof. J. Heyrovsky was awarded the Nobel Prize in 1959.

In short, this new marvellous technique has opened a new era in probing various electrochemical equilibria in pure and applied chemistry as indicated by nearly two to three hundred papers being published every year in this discipline. Many useful reviews on the method have been presented by Muller[43], Zuman[44] and Taylor[45] and various others in Heyrovsky honour issue[46] of Talanta published in December 1965.

LITERATURE CITED

1. J. Heyrovsky, Chem. Listy, 16, 256 (1922).
2. W. Kemula, Trabojos IX, Congr. inter. quim. pura y aplicada, Tomo II, 297 (Madrid) 1934.
3. D. Ilcovic, Collection Czechoslov. Chem. Communs., 6, 498 (1934).
4. D. Ilcovic, J. Chim. Phys., 35, 129 (1938).
5. J.J. Lingane and B.A. Loverbridge, J. Am. Chem. Soc., 72, 438 (1950).
6. H. Srehlov and M. Stackelberg, Z. Elektrochem., 54, 51 (1950).
7. J. Koutecky, Ceskoslovensky cas. fys. 2, 117 (1952).
8. M. Stackelberg, Z. Elektrochem., 57, 338 (1953).
9. M. Stackelberg and V. T oome, Z. Elektrochem., 58, 226 (1954).
10. T. Kambara and I. Tachi, Bull. Chem. Soc. Jap., 23, 226 (1950).
11. R.S. Subrahmanya, Can. J. Chem., 40, 296 (1962).
12. H. Matsuda, Bjll. Chem. Soc. Jap., 36, 342 (1953).
13. L. Meites and T. Meites, J. Am. Chem. Soc., 72, 3686 (1950).
14. L. Meites, Polarographic Techniques 2nd edition, Interscience Publisher, New York, London, Sydney (1965).
15. I.M. Kolthoff and J.J. Lingane, 'Polarography' end edition, Interscience, New York, London (1953).
16. L. Meites and T. Meites, J. Am. Chem. Soc., 73, 177 (1951).
17. P. Delahay, J. Am. Chem. Soc., 74, 3506 (1952).
18. J. Brdicka, Z. Elektrochem., 48, 278 (1942).
19. W.E. Harris and I.M. Kolthoff, J. Am. Chem. Soc., 67, 1484 (1945).

LITERATURE CITED

1. J. Heyrovsky, Chem. Listy, 16, 256 (1922).
2. W. Kemula, Trabojos IX, Congr. inter. quim. pura y aplicada, Tomo II, 297 (Madrid) 1934.
3. D. Ilcovic, Collection Czechoslov. Chem. Communs., 6, 498 (1934).
4. D. Ilcovic, J. Chim. Phys., 35, 129 (1938).
5. J.J. Lingane and B.A. Loverbridge, J. Am. Chem. Soc., 72, 438 (1950).
6. H. Srehlov and M. Stackelberg, Z. Elektrochem., 54, 51 (1950).
7. J. Koutecky, Ceskoslovensky cas. fys. 2, 117 (1952).
8. M. Stackelberg, Z. Elektrochem., 57, 338 (1953).
9. M. Stackelberg and V. T oome, Z. Elektrochem., 58, 226 (1954).
10. T. Kambara and I. Tachi, Bull. Chem. Soc. Jap., 23, 226 (1950).
11. R.S. Subrahmanya, Can. J. Chem., 40, 296 (1962).
12. H. Matsuda, Bjll. Chem. Soc. Jap., 36, 342 (1953).
13. L. Meites and T. Meites, J. Am. Chem. Soc., 72, 3686 (1950).
14. L. Meites, Polarographic Techniques 2nd edition, Interscience Publisher, New York, London, Sydney (1965).
15. I.M. Kolthoff and J.J. Lingane, 'Polarography' end edition, Interscience, New York, London (1953).
16. L. Meites and T. Meites, J. Am. Chem. Soc., 73, 177 (1951).
17. P. Delahay, J. Am. Chem. Soc., 74, 3506 (1952).
18. J. Brdicka, Z. Elektrochem., 48, 278 (1942).
19. W.E. Harris and I.M. Kolthoff, J. Am. Chem. Soc., 67, 1484 (1945).

20. A.T. Violanda and W.D. Cooke, Anal. Chem., 36, 2287 (1964).

21. J. Heyrovsky and D. Ilkovic, Colln. Czech. Chem. Commun., 7, 198 (1935).

22. E.S. Amis, J. Electroanal. Chem., 8, 413 (1964).

23. W.B. Schaap, J. Am. Chem. Soc., 82, 1837 (1960).

24. H.R. Kirchmayer, Electrochim. Acta, 9, 459 (1964).

25. N.E. Vandenborgh and D.E. Sellers, J. Am. Chem. Soc., 86, 1934 (1964).

26. Idem - ibid., 87, 1206 and 1396 (1965).

27. C. Parkanyi and R. Zahradnik, Talanta, 12, 1889 (1965).

28. J. Heyrovsky and M. Shikata, Recl. Trav. Chim. Pays. Bas Belg., 44, 496 (1925).

29. J. Heyrovsky and J. Forejt, Z. Phys. Chem., 193, 77 (1943).

30. H.M. Davis and J.E. Seaborn, Electron Engng., 26, 314 (1953).

31. Idem, 'Advances and polarography', I.S.Longmuir, Pergamon Press (Oxofrd), p. 239 (1960).

32. B. Breyer et.al, Aust. J. Scient. Res., A/3, 558 (1950).

33. G.C. Barker and I.L. Jenkins, Analyst, 77, 685 (1952).

34. G.C. Barker and A.W. Gardner, Z. Analyt. Chem., 173, 79 (1960).

35. G.C. Barker, Anal. Chim. Acta, 18, 118 (1958).

36. G.C. Barker, R.L. Faircloth and A.W. Gardner, Nature, 181, 247 (1958).

37. G.C. Barker, Trans. Symp. Electrode Process, philadelphia (1959).

38. M. Spalenka, Z. Analyt. Chem., 126, 49 (1943).

39. M. Spalenka, Anal. Chim. Acta, 2, 533 (1948).

40. R. Kraus and U.V. Novak, Colln. Czech. Chem. Commun., 10, 534 (1938).

41. B. Bitter, Colln. Czech. Chem. Commun., 15, 677 (1950).

42. J.V.A. Novak, Colln. Czech. Chem. Commun., 19, 177 (1954).

43. O.H. Muller, J. Chem. Edu., 41, 320 (1964).

44. P. Zuman, 'Advances in Analytical Chemistry and Instrumentation', C.N. Reilley, Willey, New York, p. 219 (1963).

45. J.K. Taylor, J. Assoc. Office Ag. Chemist, 47, 21 (1964).

46. Talanta No. 12, 1061-1379 (1965).

CHAPTER II

Section (A)-Theoretical Aspects

Section (B)-Instrumentation

THE NATURE OF ELECTRODE PROCESSES :

Consider a simple electrochemical reduction process A + ne = B occurring at the DME. Such a process may be conveniently classified into two extreme types. One is the class of reversible reactions in which the depolarizer ions reaching the electrode are reduced instantaneously. The electron transfer process is so rapid that thermodynamic equilibrium is very nearly attained at every instant during the life time of a drop. In such reversible reactions, the equilibrium is represented by Nernst equation. On the other hand, totally irreversible processes are so slow that thermodynamic equilibrium is only partially attained during the life time of each drop. For these processes, the rate of electron transfer governs the current-voltage relationships. In between these two classes lie a continuous spectrum of electrode processes. Any sharp line of demarcation between the two classes is, therefore, not possible.

Despite the empirical nature of this classification, much valuable thermodynamic information is available from polarographic data on reversible processes. Kinetics of rate determining step for irreversible process are also conveniently evaluated.

REVERSIBLE PROCESSES :

1. Reversible processes involving simple or complex metal ions and metals soluble in mercury :

The following equation represents the reduction of a

simple metal ion or an aquo-complex metal ion to give an amalgam

$$M^{n+} + ne + Hg = M(Hg)$$

Since as already discussed, the thermodynamic equilibrium is rapidly attained, Nernst equation is applicable.

$$E_{de} = E_s^o - \frac{RT}{nF} \ln \frac{[Red]^o}{[OX]^o} \qquad (1)$$

where $[Red]^o$ and $[OX]^o$ denote the concentrations of the reduced and the oxidised form of the depolarizer at the electrode surface, E_s^o the standard oxidation - reduction potential of the system, E_{de} the potential of the DME. Both the potentials are conveniently referred to a saturated calomel electrode (SCE).

Under this category, equations for three types of electrode processes can be formulated which are discussed below :

(i) Equation for a cathodic wave :

A cathodic wave is observed if the depolarizer accepts electrons from the dropping electrode. Here the oxidation state of the depolarizer is lowered, or, in other words, the depolarizer is reduced. The equation for a cathodic wave was first derived by Heyrovsky and Ilcovic[1] and the simplest mathematical expression for the same is as follows :

$$E = E^o - \frac{RT}{nF} \ln \frac{i}{i_d - i} \qquad (2)$$

(ii) Equation for an anodic wave :

An anodic wave is observed if the dropping electrode accepts electrons from the depolarizer so that the oxidation state of the depolarizer is increased, in other words, it is oxidised. The polarogram is a curve beneath the galvanometer zero line. For an anodic wave, the expression in its simplest form may be written as under :

$$E = E^{o} - \frac{RT}{nF} \ln \frac{i_d - i}{i} \qquad (3)$$

(iii) Equation for a cathodic-anodic wave :

In presence of both the oxidised and the reduced forms of the depolarizer which have the same half wave potential, a composite cathodic-anodic wave is observed. The polarogram extends on both sides of the galvanometer zero line. The portion above the zero line corresponds to reduction while the portion below it corresponds to oxidation of the depolarizer. The expression for such a reversible polarographic wave may be represented as follows :

$$E = E^{o} - \frac{RT}{nF} \ln \frac{i - I_d}{i_d - i} \qquad \ldots\ldots \quad (4)$$

where I_d = cathodic diffusion current and i_d is anodic diffusion current.

As already defined, the potential corresponding to one half of diffusion current represents the half wave potential ($E_{1/2}$). The equation for half wave potential for the cathodic,

anodic and cathodic anodic wave is readily derived by substituting $i_d/2$ for i for the first two types and $I_d+i_d/2$ for the third type. At this stage

$$E_{de} = E_{1/2} = E_o \quad \ldots\ldots \quad (5)$$

The half wave potential for such polarographically reversible waves is independent of the concentration of the depolarizer, the DME characterisitics and the galvanometer sensitivity. $E_{1/2}$ characterises a depolarizer in a given media at a definite temperature.

2. Reversible processes involving a solid insoluble in mercury :

If the product of electrode reaction is insoluble in mercury as well as in the solution phase, the current would be independent of its activity rather than proportional to it. Thus for the reversible polarographic reduction of a depolarizer to a solid product insoluble in mercury, the Nernst equation would take the form

$$E_{de} = E^o_M - \frac{RT}{nF} \ln \frac{1}{f_s C^o_s} \quad \ldots\ldots \quad (6)$$

Where E^o_M is the standard potential for the reduction of the depolarizer.

Introducing the half wave potential term for the condition $i = i_d/2$, the expression has been derived as -

$$E_{de} = E_{1/2} - \frac{RT}{nF} \ln \frac{i_d}{2} + \frac{RT}{nF} \ln (i_d - i) \quad \ldots\ldots \quad (7)$$

Where $E_{1/2}$ of the depolarizer varies with its concentration and the plot of E_{de} vs. ln $(i_d - i)$ should be a straight line with a slope of $\frac{RT}{nF}$ V.

3. Reversible processes involving only dissolved species :

If the depolarizer as well as the reduction/oxidation product are in solution phase, the DME acts as an inert electrode. The half wave potential, is reversible and therefore, Nernst equation is applicable. The expression given below for such a reversible polarographic reduction is identical with that for process involving products which form amalgam with mercury :

$$E_{de} = E_{1/2} - \frac{RT}{nF} \ln \frac{i}{i_d - i} \quad \ldots\ldots \quad (8)$$

The equations for ano-dic and the composite cathodic-anodic waves are likewise analogous to the first type of electrode processes.

CRITERIA OF REVERSIBILITY

From the treatment of the equations for reversible electrode processes it has been possible to derive various criteria governing reversibility of polarographic reduction/oxidation. It is always useful and accurate to use more than one criterian in combination with each other to establish reversibility. Some of the most widely accepted criteria are as under :

1. For a reversible reaction, the cathodic wave obtained from the oxidised form alone, the anodic wave obtained from the

reduced form alone and the composite wave obtained from the mixture of the two forms should all have the same half wave potential. This is the fundamental criterian and must be used whereever possible.

2. The most commonly used auxiliary criterian is the slopes of 'log plots'. Except in the case where solid products are formed, for each reversible system, the assumption of reversibility leads to the following equations at 25° C :

$$E_{de} = E_{1/2} - \frac{0.059}{n} \log. \frac{i}{(i_d)_c - i} \quad \text{(cathodic wave)} \qquad (9)$$

$$E_{de} = E_{1/2} - \frac{0.059}{n} \log. \frac{(i_d)_a - i}{i} \quad \text{(anodic wave)} \qquad (10)$$

and

$$E_{de} = E_{1/2} = \frac{0.059}{n} \log. \frac{i-(i_d)_a}{(i_d)_c - i} \quad \text{(composite wave)} \qquad (11)$$

It, therefore, follows from the above equations that the plots of E_{de} vs. the log. term should be straight lines with a slope equal to $\frac{0.059}{n}$ V for a reversible wave.

3. The much more easy measurement of $E_{1/4}$ and $E_{3/4}$, which are applied potentials corresponding to $i_d/4$ and $3i_d/4$, helps in testing the reversible character for a reduction/oxidation wave. Obviously,

$$E_{1/4} = E_{1/2} - \frac{0.059}{n} \log. \frac{i_d/4}{i_d - i_d/4}$$

$$= E_{1/2} - \frac{0.059}{n} \log. \frac{1}{3} \quad \ldots \quad (12)$$

While

$$E_{3/4} = E_{1/2} - \frac{0.059}{n} \log. 3 \quad \ldots \quad (13)$$

so that $$E_{3/4} - E_{1/4} = - \frac{0.0564}{n} \quad \ldots \quad (14)$$

Therefore, $(E_{3/4} - E_{1/4})$ should have a value $-56.4/n$ mV for a reversible cathodic wave; for a reversible anodic wave, it is equal to $+ \frac{56.4}{n}$ mV.

4. Another criterian, though most reliable, has been rarely used. The half wave potential for a reversible wave may be written in the form, at 25° C.

$$E_{1/2} = E^{\circ} - \frac{0.059}{n} \log. \frac{D_o^{1/2}}{D_R^{1/2}} \quad \ldots \quad (15)$$

The log. term should be numerically equal to the logarithm of the ratio of cathodic and anodic diffusion current constants which can be evaluated experimentally. If the formal potential of the couple is known, $E_{1/2}$ can be calculated. For a reversible wave, therefore, this calculated value of $E_{1/2}$ should coincide with the experimental value of $E_{1/2}$.

5. The temperature co-efficient of half-wave potential for a reversible wave is usually small being of the order of $\pm$ 2 mV/degree. Irreversible waves have a much larger value[2].

6. $E_{1/2}$ for a reversible wave is always practically independent of drop time[3-4].

7. Lastly, $E_{1/2}$ is independent of depolarizer

concentration for a reversible wave. Though not a useful criterian in itself, it indirectly establishes the irreversibility of a wave for any appreciable variation in $E_{1/2}$ with concentration is taken as conclusive proof of irreversibility.

IRREVERSIBLE PROCESSES :

The half wave potential of the anodic and the cathodic wave does not coincide within the limits of experimental error very unlike that in the case of a reversible half reaction. The electron transfer process is slow unlike reversible process where it is very rapid. Over a large part of an irreversible wave the rate and, therefore, the current, is controlled mainly by the electrode reaction rate which is slow as compared to the rate of diffusion. This, certainly, holds over the lower potential range. However, as the potential is increased, the reaction rate increases until in the region approaching limiting current, it is comparable with that of diffusion. At limiting current stage, the electrode reaction is very rapid and there diffusion becomes rate determining. It is, therefore, logical that Ilcovic equation should be applicable to irreversible processes as well.

It has been established[3-4] that for an irreversible wave the half wave potential is a function of drop-time.

Several authors[5-13] have provided useful treatments for irreversible waves in order to study reaction kinetics at the DME.

QUASI-REVERSIBLE PROCESSES :

In the preceding pages, we have discussed the two extreme types of electrode processes; the reversible and the completely irreversible.

It is sometimes seen that the plot of log. i/i_d-i vs. E_{de} is a curve rather than a straight line expected for a reversible process (slope 0.059/n) and a completely irreversible process (slope = $0.059/\alpha n$).

In the case of totally irreversible processes, the reverse reaction does not operate at all. For quasi-reversible processes, however, the forward and the backward reaction rates are comparable.

The methods for determining kinetic parameters for such a wave have been suggested by Matsuda[14-15], Koryta[16] and Stromberg[17].

POLAROGRAPHY OF METAL COMPLEXES :

A metal ion in solution is assumed to be solvated complex with solvent molecules acting as ligand. Addition of a ligand, other than solvent molecules results in a shift in half wave potential, almost invariably to more negative side, with a simultaneous change in diffusion current almost always becoming smaller. The shift in $E_{1/2}$ in presence of a ligand is probably due to the necessity to liberate metal ion from the complex which can then be reduced at the DME. This requires energy and hence the cathodic shift. The decrease in diffusion

current is accounted for by the increased bulk of the diffusing species.

Study of metal complexes by polarography involves determination of changes in half wave potential and diffusion current as a function of ligand concentration. The data so obtained enable us to establish composition, stability and other thermodynamic data for complex species in solution.

Heyrovsky and Ilcovic were the first to suggest the usefulness of polarography in the study of metal complexes. Since then several authors have provided useful theoretical treatments to carry out systematic study of complexes formed in solution by any conceivable combination of a metal ion with ligands.

For the sake of brevity, only those methods would be discussed which have actually been employed in the investigations.

I. THE METHOD OF LINGANE[18] :

(Single complex formation)

This method is applicable when only one complex species exists in solution i.e. there is no stepwise complex formation.

The half-cell reaction for the reduction of such a complex may be represented as

$$MX_p^{(n-pb)} + ne + Hg \rightleftharpoons M(Hg) + p(x)^{b-} \qquad (16)$$

Where MX_p is a complex of the metal ion or M^{n+} with ligand x^{b-} carrying a charge (n-pb).

The half-cell reaction may be broken up into two simpler reactions :

$$MX_p^{(n-pb)+} \rightleftharpoons M^{n+} + p(X)^{b-} \quad \ldots\ldots \quad (17)$$

and $$M^{n+} + ne + Hg \rightleftharpoons M(Hg) \quad \ldots\ldots \quad (18)$$

If the electrode reduction is reversible, the potential of the dropping electrode at any point is given by

$$E_{de} = E_a^o - \frac{RT}{nF} \ln \frac{C_a^o f_a}{C_M^o f_M} \quad \ldots\ldots \quad (19)$$

Where C_a^o is the concentration of the amalgam formed on the surface of the DME and f_a its activity co-efficient. C_M^o is the concentration of the simple metal ion at the electrode surface and f_M its activity. E_A^o is the standard potential of the amalgam.

The overall thermodynamic stability constant β_{MX_p} of the complex MX_p is given by

$$\beta_{MX_p} = \frac{[MX_p]}{[M][X]^p} \quad \ldots\ldots \quad (20)$$

Where charges have been omitted for convenience and square bracket terms represent activities.

or $$\beta_{MX_p} = \frac{C_{MX_p} \cdot f_{MX_p}}{C_M f_M \cdot C_X^p f_X^p} \quad \ldots\ldots \quad (21)$$

At specified concentrations of metal ion and ligand,

the concentration of the complex in the bulk of the solution is given by

$$C_{MX_p} = \frac{\beta_{MX_p} \cdot C_M f_M \cdot C_X^p f_X^p}{f_{MX_p}} \quad \ldots\ldots \quad (22)$$

and the same at the electrode surface will be

$$C^o_{MX_p} = \frac{\beta_{MX_p} \cdot C^o_M f_M \cdot C_X^p f_X^p}{f_{MX_p}} \quad \ldots\ldots \quad (23)$$

The previous equation is valid when it is presumed that the concentration of the ligand is large and equitably distributed throughout the bulk of the solution with the same value of activity co-efficient both in the bulk and the electrode surface. We can now substitute for $C^o_M f_M$ from equation (23) into equation (19) to give :

$$E_{de} = E^o_a - \frac{RT}{nF} \ln \frac{C^o_a f_a \beta_{MX_p} C_X^p f_X^p}{f_{MX_p} C^o_{MX_p}} \quad \ldots \quad (24)$$

The particles diffusing to the electrode are complex ions and therefore the mean current at any part of the wave is given by

$$i = KI_{MX_p} (C_{MX_p} - C^o_{MX_p}) \quad \ldots \quad (25)$$

Where K and I_{MX_p} are respectively the capillary constant ($m^{2/3} t^{1/6}$) and diffusion current constant ($607 D^{1/2}$) of

the species MX_p. When $C^o_{MX_p} = 0$, the limiting diffusion current is obtained :

$$i_d = KI_{MX_p} \cdot C_{MX_p} \qquad \ldots \qquad (26)$$

A similar relation holds in terms of concentration of metal atoms within the mercury, viz.

$$i = KI_a C^o_a \qquad \ldots \qquad (27)$$

Where I_a is the diffusion current constant of the metal atoms in the amalgam.

Thus substituting for C^o_a from equation (27) into equation (24), we get

$$E = E^o_a - \frac{RT}{nF} \ln \frac{i.f_a}{KI_a} \cdot \frac{\beta_{MX_p} \cdot C^p_X f^p_X}{f_{MX_p} \cdot C^o_{MX_p}} \qquad \ldots \qquad (28)$$

Combining equations (25) and (26),

$$C^o_{MX_p} = \frac{i_d - i}{KI_{MX_p}} \qquad \ldots \qquad (29)$$

Substituting for $C^o_{MX_p}$ in equation (28) gives

$$E = E^o_a - \frac{RT}{nF} \ln \frac{i\, f_a}{KI_a} \cdot \frac{KI_{MX_p}}{i_d - i} \cdot \frac{\beta_{MX_p} \cdot C^p_X f^p_X}{f_{MX_p}} \qquad \ldots \qquad (30)$$

Or

$$E = E_a^o - \frac{RT}{nF} \ln \frac{I_{MX_p} \cdot f_a}{I_a} \cdot \left(\frac{i}{i_d - i}\right) \cdot \frac{\beta_{MX_p} C_X^p f_X^p}{f_{MX_p}} \qquad (31)$$

The expression for half-wave potential of a reduction wave is conveniently obtained by substituting $i = i_d/2$

$$(E_{1/2})_c = E_a^o = \frac{RT}{nF} \ln f_a \cdot \frac{I_{MX_p}}{I_a} \cdot \frac{\beta_{MX_p} \cdot C_X^p f_X^p}{f_{MX_p}} \qquad (32)$$

For a simple metal ion I_{MX_p} becomes I_M and $C_X^p f_X^p = 0$ so that the expression (32) becomes

$$(E_{1/2})_s = E_A^o - \frac{RT}{nF} \ln \frac{f_a}{f_M} \cdot \frac{I_M}{I_a} \qquad \ldots \qquad (33)$$

Therefore, the shift in half wave potential in presence of an excess of the ligand is given by

$$(E_{1/2})_s - (E_{1/2})_c = \Delta E_{1/2} = \frac{2.303RT}{nF} \log. \frac{f_M I_{MX_p}}{I_M} \cdot \frac{\beta_{MX_p} \cdot C_X^p f_X^p}{f_{MX_p}} \qquad (34)$$

For convenience, we shall neglect here a small decrease in diffusion current constant of the metal ion due to complex formation so that I_M and I_{MX_p} are approximately equal. Now assuming that the free ligand concentration is equal to the analytical concentration and that activity co-efficients may be dropped i.e. $f_M f_M^p / f_{MX_p} \sim 1$ if ionic strength is held constant, the equation (34) is simplified to a form originally used by Lingane, viz :

$$\Delta E_{1/2} = \frac{2.303RT}{nF} \log. \beta_{MX_p} . C_X^p \quad \ldots \quad (35)$$

$$\text{or } \Delta E_{1/2} = \frac{2.303RT}{nF} \log. \beta_{MX_p} + p \frac{2.303RT}{nF} \log. C_X \quad \ldots \quad (36)$$

In practice, the total shift in $E_{1/2}$ by the presence of one mole of the ligand is obtained by extrapolating the value of -log. C_X to zero in a plot of $-E_{1/2}$ vs. -log. C_X so that the last term in equation (36) conveniently becomes zero.

From equation (36), it is obvious that the rate of change of half-wave potential with increase in ligand concentration may be written as

$$\frac{d(E_{1/2})_c}{d(E_{1/2})_s} = - p \frac{2.303RT}{nF} \quad \ldots \quad (37)$$

The co-ordination number p of the complex is readily available from equation (37).

II. METHOD OF DEFORD AND HUME[19] :
(Stepwise complex formation)

This method is the first serious attempt to study polarographically step equilibria between successively formed complexes in solution. This method has now been modified to suit practical determinations. The basic theory in deriving the required expression is almost similar to that in the method of Lingane.

The reduction of successive complexes may be represented in the following form :

$$M^{n+} \rightleftharpoons MX \rightleftharpoons MX_2 \rightleftharpoons \cdots\cdots MX_N$$

$$\Big\updownarrow E^{o},n \qquad \ldots\ldots \quad (38)$$

$$M(Hg)$$

This representation signifies the fact that for a reversible reduction, it is not possible to point out the exact species which is actually involved in the electrode process.

DeFord and Hume have defined an experimentally determinable function $F_o(X)$ such that

$$F_o(X) = \text{antilog}\left[\frac{0.4343nF}{RT}\Delta E_{1/2} + \log I_M/I_c\right] \qquad (39)$$

$$= f_M \sum_{O}^{N} \frac{\beta_{MX_p}[X]^p f_{X_p}}{f_{MX_p}} \qquad \ldots \qquad (40)$$

where f_M, f_{X_p} and f_{MX_p} are the activity co-efficient terms of the respective species.

According to Irving[20], activity co-efficients may dropped if ionic strength is held constant. Therefore, equation (40) becomes

$$F_O(X) = 1 + \beta_1[X] + \beta_2[X]^2 + \cdots\cdots \beta_N[X]^N \qquad (41)$$

The numerical value $F_o(X)$ function corresponding to each concentration of the ligand is available from equation (39) by substituting experimental data. The stability constants

β_1, β_2 ..... β_N are then determined by graphical extrapolation me thod as devised by Leden[21].

A curved plot of $F_o(X)$ versus $[X]$ would have an intercept on $F_o(X)$ axis equal to unity and a limiting slope of β_1. This is a preliminary value of β_1. A new function $F_1(X)$ may now be defined as

$$F_1(X) = \frac{F_o(X)-1}{[X]} \quad \ldots\ldots \quad (42)$$

Here again, a plot of $F_1(X)$ versus $[X]$ has an intercept on $F_1(X)$ axis equal to β_1 and a limiting slope of β_2. In addition to the confirmation of β_1 value, a clue is now available as to the approximate value of β_2.

Similarly a function $F_2(X)$ is defined as

$$F_2(X) = \frac{F_1(X) - \beta_1}{[X]} \quad \ldots\ldots \quad (43)$$

and values of β_2 and β_3 (preliminary) are obtained.

This procedure is continued until for the penultimate complex MX_{N-1} $F_{N-1}(X)$ function is given by

$$F_{N-1}(X) = \frac{F_{N-2}(X)-\beta_{N-2}}{[X]} = \beta_{N-1} + \beta_N(X) \quad \ldots\ldots \quad (44)$$

Here the plot of $F_{N-1}(X)$ vs. $[X]$ is a straight line with a slope equal to β_N. The straight line nature of the plot signifies that penultimate complex has been reached. The final function $F_N(X)$ is independent of ligand concentration as shown

$$F_N(X) = \frac{F_{N-1}(X) - \beta_{N-1}}{[X]} = \beta_N \quad \ldots\ldots \quad (45)$$

so that a plot of $F_N(X)$ vs. β_N is a straight line parallel to X axis.

In practice one has a very good idea where a point is departing from normal where the line of the curve should pass to obtain best results, An accurate determination of $F_0(X)$ which depends predominently on $E_{\frac{1}{2}}$ values ,is indispensable since the higher functions are very sensitive to slight deviations in it . Errors in F(X) functions ,being cumulative result in high deviations in the final stages causing difficulties in drawing of curves and the results become unreliable. However, practice and foresight are essential if maximum accuracy of the results is to be obtained from the $F_0(X)$ data. It is,therefore, useful to attempt measurement of $E_{\frac{1}{2}}$ to the nearest 0.1 mV.

It is noteworthy, that in our deviations, activity co-efficient terms have been ignored. It is convenient to keep activity co-efficient terms and constant (so that these cancel out) rather than attempting their approximate calculation by tedious methods. This is achieved by holding the ionic strength constant for each system. These stability constants are not true thermodynamic values but hold good only in a media of some ionic strength. The condition is more favourable if the ligand is an uncharged molecule.

Section B

I N S T R U M E N T A T I O N

POLAROGRAPH:

A simple circuit of a polarograph is depicted in Figure 2.1.

A manual polarograph with scalamp galvanometer as current recorder with automatic arrangement of standardisation was used for recording current-voltage variations. The polarographic unit was standardised with a W.G. Pye Vernier potentiometer N 7568.

DROPPING MERCURY ELECTRODE :

The dropping mercury electrode consists of a glass capillary connected to a reservoir of mercury by means of a flexible tubing . The reservoir , the tubing and the capillary are filled with doubly distilled mercury. The reservoir and the capillary are clamped to a stand so that either can be raised or lowered as the situation warrants. A short platinum wire sealed at the end of a glass tube which is dipped in the reservoir serves to connect the DME with the polarograph proper.

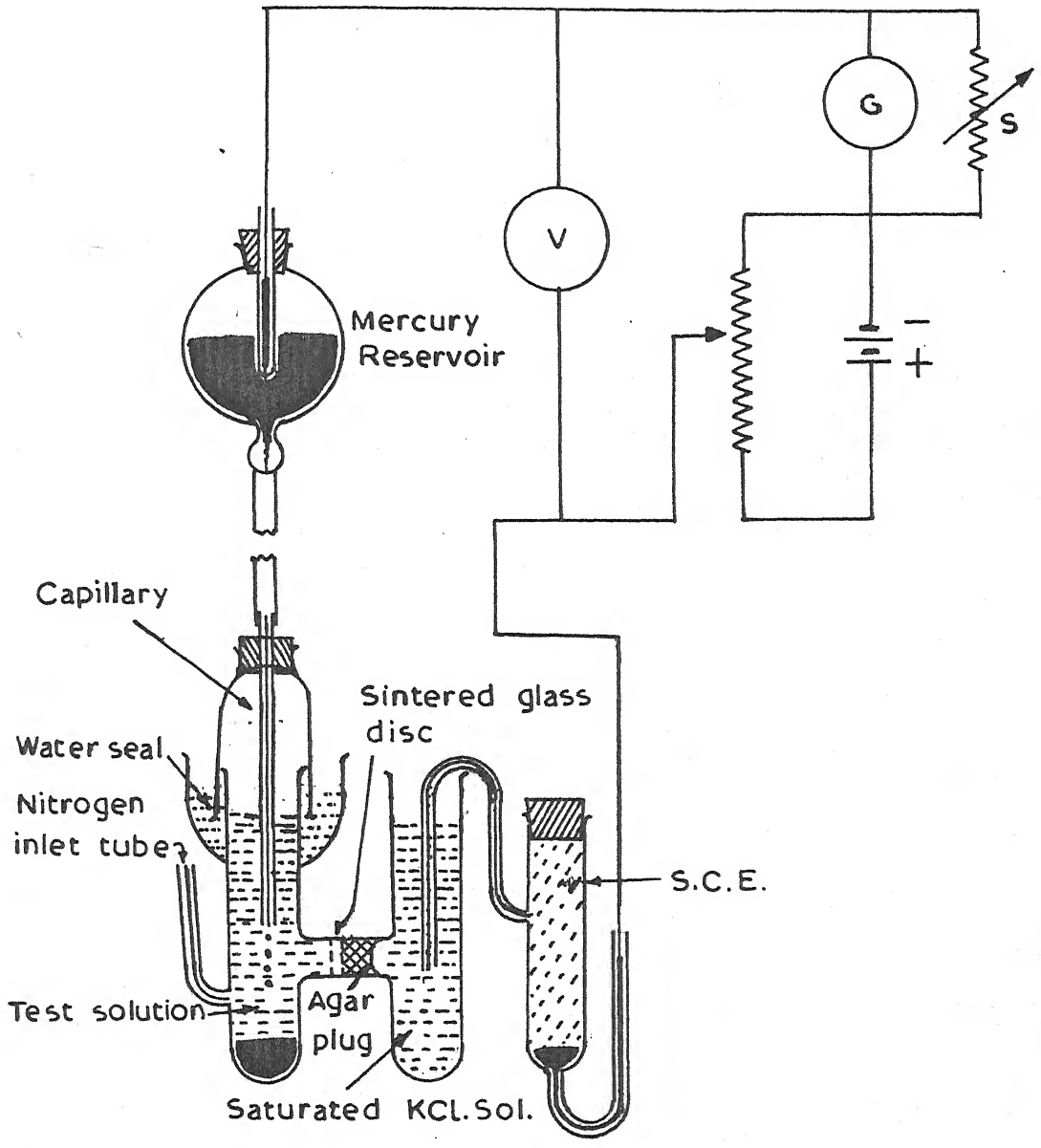

FIG. 2.1. H. CELL IN POLAROGRAPHIC CIRCUIT.

REFERENCE ELECTRODE

The saturated calomel electrode largely satisfies the requirement that its potential remains unaltered during the variations in applied potential. Hence, the saturated calomel electrode was used as reference electrode throughout the investigations.

POLAROGRAPHIC H-CELL

As shown in figure 2.1, an H-Cell comprises two compartments: One for the test solution and the other for saturated potassium chloride solution where the SCE is dipped. The compartment for test solution is also provided with a side tube which allows streaming hydrogen through the test solution for expelling dissolved oxygen.

The two compartments are separated by means of a sintered glass disc in combination with KCl saturated agar-agar bridge.

THERMOSTAT

An Ultra-Thermostat Type NBE was used to maintain the temperature throughout the investigations.

EXPERIMENTAL PROCEDURE:

First of all, 'm' and 't' are measured. The capillary

is dipped into 0.1 M potassium chloride at a given height of mercury reservoir, and the time required for the detachment of 10 drops is measured by means of a stop watch. 'm' is determined by collecting the dropping mercury for a known time and weighing the same after completely drying it.

The thermostated H-cell is filled with the test solution and purified hydrogen is passed through it for about ten minutes. The capillary is now dipped into the solution, the circuit is completed by dipping the SCE in the KCl compartment of the H-cell. Gradually increasing potential is now applied and the corresponding current values are read on the galvanometer.

COMPUTATIONS :

For each current voltage curve (polarogram) the half wave potential was obtained from intercept on the potential axis in the plot of $-E_{de}$ vs. -log. i/i_d-i. Since multiple complex formation had taken place in each system, the method of DeFord and Hume[19] as improved by Irving[20] was applied to determine overall formation constants.

The formation constants were determined at two temperatures and thermodynamic functions were computed from the following relationships :

$$\Delta G = -2.303\ RT \log. \beta_1$$

$$\Delta G = \Delta H - T\Delta S$$

$$\Delta H = 2.303\ RT_1T_2 \left(\log. \beta_{T_2} - \beta_{T_1}\right) \Big/ (T_2 - T_1)$$

Where

ΔG = Change in free energy

ΔH = Change in enthalpy or heat content

ΔS = Change in entropy

R = Universal gas constant

T = Absolute temperature, ^{o}K

β = Overall formation constant

β_{T_1} = Overall formation constant at the lower temperature

β_{T_2} = Overall formation constant at the higher temperagure

T_1 = Lower temperature, ^{o}K

T_2 = Higher temperature, ^{o}K

LITERATURE CITED

1. J. Heyrovsky and D. Ilcovic, Coll. Czech. Chem., Commun., 7, 198 (1935).
2. I.M. Kolthoff and J.J. Lingane, 'Polarography', 2nd ed., Interscience, New York, London (1953).
3. H. Strehlow and M.V. Stakelberg, J. Electrochem., 55, 244 (1951).
4. J.K. Taylor and S.W. Smith, J. Research Natl. Bur. Standard, 56, 143 (1956).
5. J. Koutecky, Coll. Czech. Chem. Commun., 18, 597 (1953).
6. J. Weber and J. Koutecky, Coll. Czech. Chem. Commun., 20, 980 (1955).
7. H.A. Laitinen and W.J. Subcasky, J. Am. Chem. Soc., 80, 26023 (1958).
8. L. Meites and Y. Israel, J. Am. Chem. Soc., 83, 4903 (1961).
9. P. Delahay, J. Am. Chem. Soc., 75, 1190 and 1430 (1953).
10. P. Delahay, J. Am. Chem. Soc., 73, 4944 (1951).
11. N.N. Meimann, J. Koutecky and J. Cizeck, Zh. Fig. Khim., 22, 1454 (1948).
12. K.B. Oldham and E. Parry, Anal. Chim., 40, 65 (1968).
13. J.E.B. Randles, Can. J. Chem., 37, 238 (1959).
14. H. Matsuda and Y. Ayabe, Bull. Chem. Soc. Jap., 29, 134 (1956).
15. H. Matsuda and Y. Ayabe, Z. Elektrochem., 63, 1164 (1959).
16. J. Kosyta, Z. Physik. Chem. (Leipzig) Sonderheft, 157 (1958).

17. A.G. Stromberg, Zh. Fig. Khim., 36, 2714 (1962).

18. J.J. Lingane, Chem. Rev., 29, 1 (1941).

19. D.D. DeFord and D.N. Hume, J.Am. Chem. Soc., 73, 5321 (1951).

20. H. Irving, 'Advances in Polarography' I.S. Longmuir, Pergamon Press, Oxford, 49 (1960).

21. I. Leden, Z. phys. Chem., 188, 160 (1941).

Abbreviations used in the text

$FA\bar{c}$. - monofluoroacetate ion

$F_2A\bar{c}$. - difluoroacetate ion

$F_3A\bar{c}$, - trifluoroacetate ion

$ClA\bar{c}$. - monochloroacetate ion

$Cl_2A\bar{c}$. - dichloroacetate ion

$Cl_3A\bar{c}$. - trichloroacetate ion

$BrA\bar{c}$. - monobromoacetate ion

$Br_2A\bar{c}$. - dibromoacetate ion

$IA\bar{c}$. - monoiodoacetate ion

β_1 - Overall Stability constant or formation constant for 1:1 complex.

β_2 - Overall formation constant of 1:2 complex.

K_2 - Step wise formation constant of the 1:2 complex and equals β_2/β_1

DME - Dropping mercury electrode

E_{de} - Potential of dropping electrode.

$h_{eff.}$ or $h_{corr.}$ - Effective or corrected height of mercury column of the DME.

$E_{\frac{1}{2}}$ - Half wave potential

i_d - Diffusion current.

ΔG - Change in free energy.

ΔH - Change in enthalpy or heat content.

ΔS - Change in entropy .

μ - ~~Dielectric constant.~~ Ionic strength

$X_nA\bar{c}$. - Halosubstituted acetate ion.

$F_j(X)$ - DeFord and Hume function

mM - millimolar.

mV - millivolt.

8613

CHAPTER III

Cu(II) Complexes with

(a) acetate ion

(b) mono-, di- and trifluoroacetate ions

(c) mono-, di- and trichloroacetate ions

(d) mono- and dibromoacetate ions

(e) monoiodoacetate ion

3.1 INTRODUCTION :

Copper(II) has been established to form fairly stable complexes with most of the ligands depending upon their basic character. Acetate ion does not form very strong complexes with this metal ion as borne out by a number of investigations. Thus, Tanaka, Saito and Ogino[1] have investigated copper acetate complexes polarographically to find that two complexes (with log β_1 = 1.30 and log β_2 = 2.04) are formed. Kolat and Powell[2] have studied the copper acetate complexes at the glass electrode obtaining similar results. Potentiometric studies on these complexes have also been made by Swinarki et.al[3] and Archer and Monk[4] while Aditya[5] studied them spectrophotometrically in 50% dioxan.

Halocarboxylic acids are stronger acids than acetic acid. Consequently, their conjugate base, the haloacetate ion, is expected to form weaker complexes due to reduced basic character. Thus, potentiometric studies on copper-monochloroacetate complex have been made by H. Erlenmeyer and co-workers[6] in 50% dioxan. The composition and stability of Cu(II) complexes with bromo- and iodoacetate ions were determined by John Eva[7] using spectrophotometric and potentiometric methods. The Cu(II) monochloroacetate complex has also been investigated polarographically and potentiometrically by Vidya and Banerji[8]. Although various other references[9-12] are available on acetate and haloacetate complexes of Copper(II), literature appears to be silent on

a systematic study of various halogen substituted acetate complexes with the Cu(II) ion.

It was, therefore, thought worthwile to undertake a systematic study of various fluoro-, chloro-, bromo- and iodoacetate complexes with Copper(II) polarographically to determine their nature of reduction at DME, and determine their composition, formation constants and thermodynamic parameters under identical conditions. This is expected to go a long way in understanding the effect of different halogen substitutions in the acetate ion on its basicity and hence the complex forming ability with the metal ion under investigation.

3.2 EXPERIMENTAL :

All chemicals of analytical reagent grade purity were used. K & K (USA), Fluka (Swiss), BDH (UK) and Riedel (German) brand halogen substituted acids were used. Their sodium salts were prepared by using a dilute solution of sodium bicarbonate. Care had to be taken in handling haloacetic acids as they cause serious burns and blisters on the skin. Semi-micro burette was used to add the required quantity of their sodium salt solutions.

All solutions were made in double distilled conductivity water. Sodium perchlorate at 1.0M concentration was the supporting electrolyte used. Its concentration was correspondingly reduced in presence of increasing concentration

of ligand to maintain the ionic strength constant at 1.0M. The concentration of Copper(II) ions was kept constant at 0.9 mM while 0.002% gelatin, in final solutions, just sufficed to suppress the maxima observed.

The polarographic examination of the test solutions was carried out by placing them in a thermostated H-cell coupled with a saturated calomel electrode. Prior to the polarographic examination of each test solution, hydrogen gas was passed for about ten minutes to remove dissolved oxygen. The potential of the dropping mercury electrode (DME) was then gradually increased and change in current recorded in each case.

The half wave potentials were determined from the intercepts on the potential axis in the plots of $-E_{de}$ vs. $-\log. \frac{i}{i_d - i}$.

The capillary had the following characteristics in 0.1 M sodium perchlorate in the open circuit :

$$m = 2.43 \text{ mg/sec}$$

$$t = 2.9 \text{ sec}$$

$$h_{corr.} = 53 \text{ cm}$$

During the recording of the polarograms, the temperature was maintained constant 30° C and 40° C to obtain two sets of the data.

3.3 RESULTS :

3.3.01 Copper/acetate system :

(a) Nature of reduction : The reduction of Cu(II) in acetate

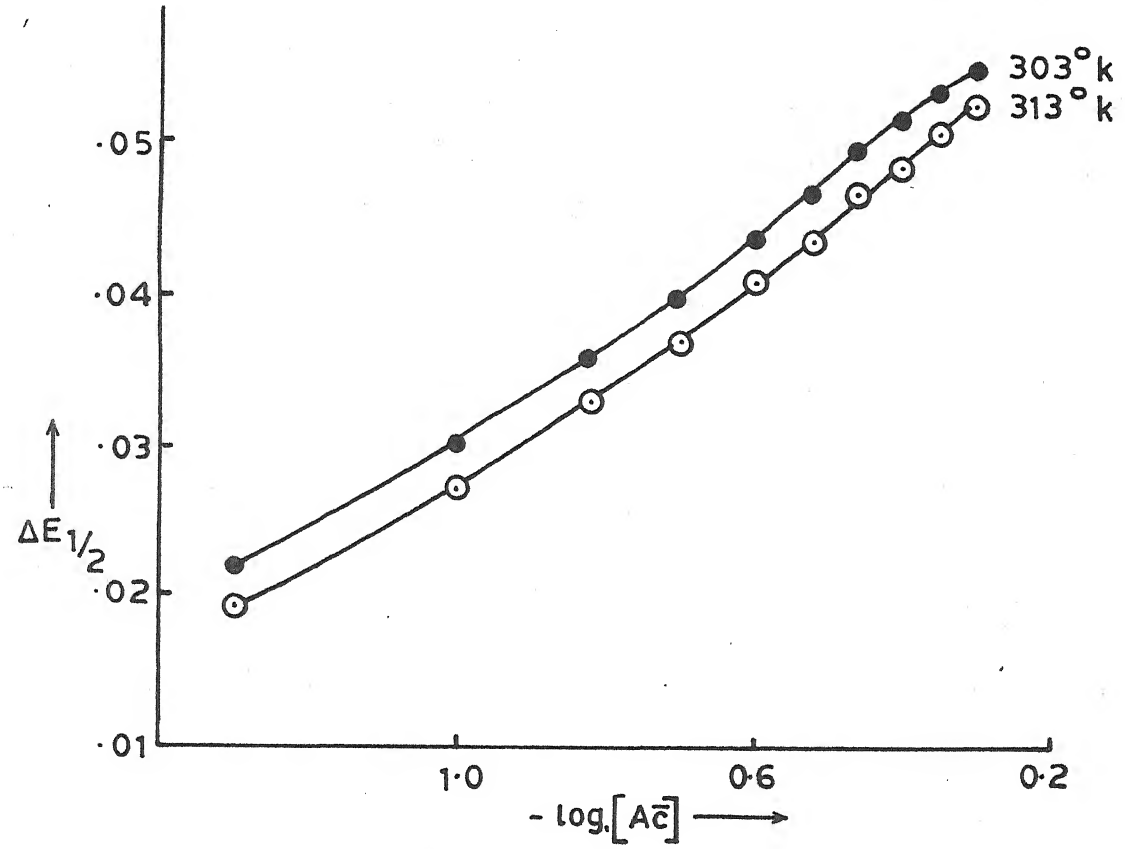

Fig. 3·01 - Plot of $\Delta E_{1/2}$. Vs. $-\log.[A\bar{c}]$; Cu(Ac̄.) system.

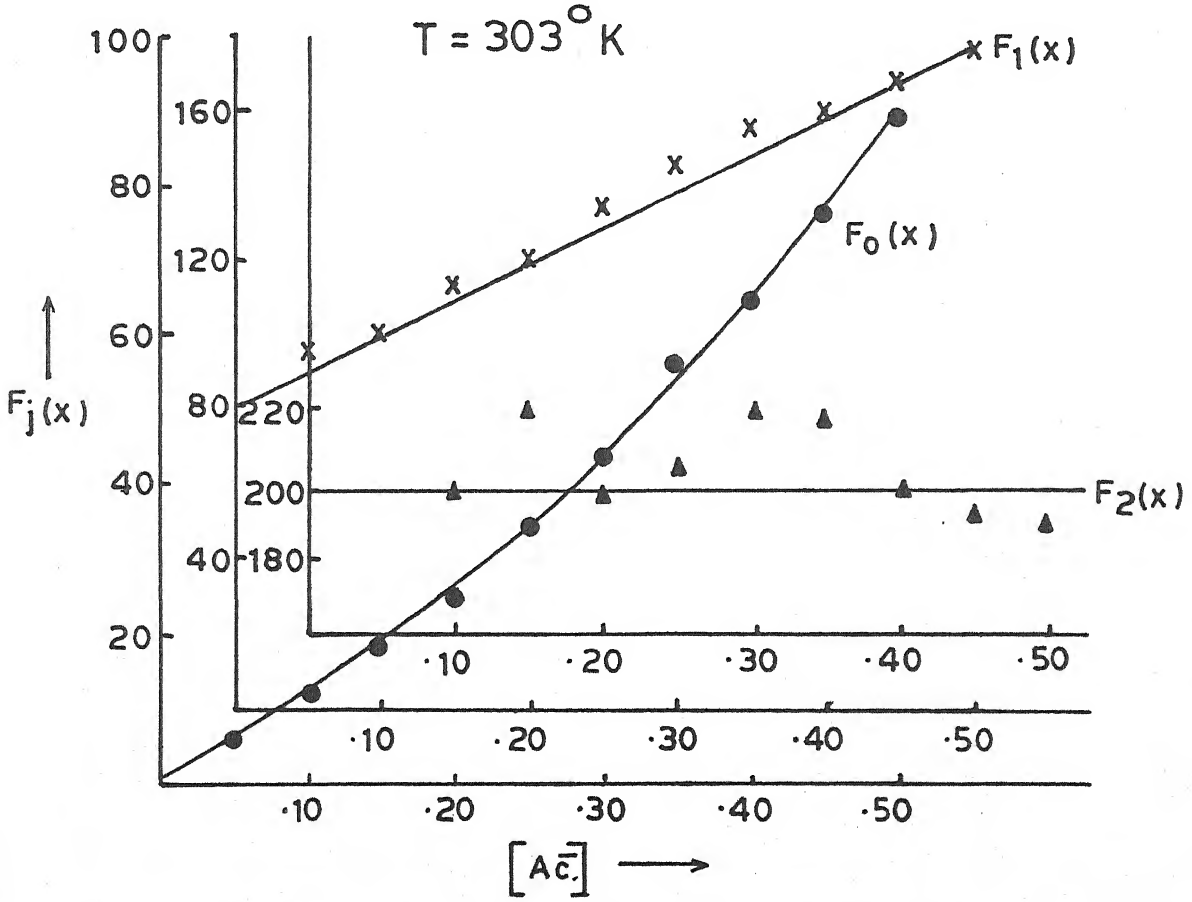

Fig. 3·02 - Plot of $F_j(x)$ Vs. $[A\bar{c}.]$; Cu(Ac̄.) system.

Table 3.01

Polarographic data for copper acetate system

Concn. of Zn^{++} ions = 0.9 mM Ionic strength = 1.0 M ($NaClO_4$)
$E_{1/2}$ of Cu^{++} ions = 0.012 vs. SCE Temperature = 303° K
Slopes of plots of $-E_{de}$ vs.-log. i/i_d-i = 30-31 mV

$[Ac^-]$ (M)	$\Delta E_{1/2}$ (V)	log. I_M/I_C	$F_0(X)$	$F_1(X)$	$F_2(X)$
0.05	0.022	0.0291	5.76	95.20	-
0.10	0.030	0.0445	11.00	100.00	200.0
0.15	0.0.36	0.0571	17.98	113.20	221.3
0.20	0.040	0.0669	24.98	119.90	199.5
0.25	0.044	0.0735	34.46	133.84	212.16
0.30	0.047	0.803	44.04	146.80	222.6
0.35	0.050	0.0837	55.85	156.71	219.17
0.40	0.052	0.0837	65.10	160.25	200.62
0.45	0.054	0.0871	76.48	167.73	194.95
0.50	0.056	0.0871	89.15	176.30	192.6

$\beta_1 = 80$ $\beta_2 = 198$

Table 3.02

Polarographic data for copper acetate system

Concn. of Cu^{++} ions = 0.9 mM Ionic strength = 1.0 M ($NaClO_4$)
$E_{1/2}$ of Cu^{++} ions = 0.016 V vs. SCE Temperature = 313° K
Slopes of plots of $-E_{de}$ vs.-log. i/i_d-i=30-31 mV

$[Ac^-]$ (M)	$\Delta E_{1/2}$ (V)	log. I_M/I_C	$F_0(X)$	$F_1(X)$	$F_2(X)$
0.05	0.019	0.0347	4.43	68.6	-
0.10	0.027	0.0517	8.34	73.4	150.0
0.15	0.033	0.0635	13.37	82.46	159.73
0.20	0.037	0.0725	18.37	86.85	141.75
0.25	0.041	0.0817	25.24	96.96	153.84
0.30	0.044	0.0880	31.98	103.26	149.2
0.35	0.047	0.0943	40.54	112.97	155.62
0.40	0.049	0.975	47.37	115.92	143.55
0.45	0.051	0.1007	55.36	120.8	138.4
0.50	0.053	0.1007	64.20	126.4	135.8

$\beta_1 = 58.5$ $\beta_2 = 144$

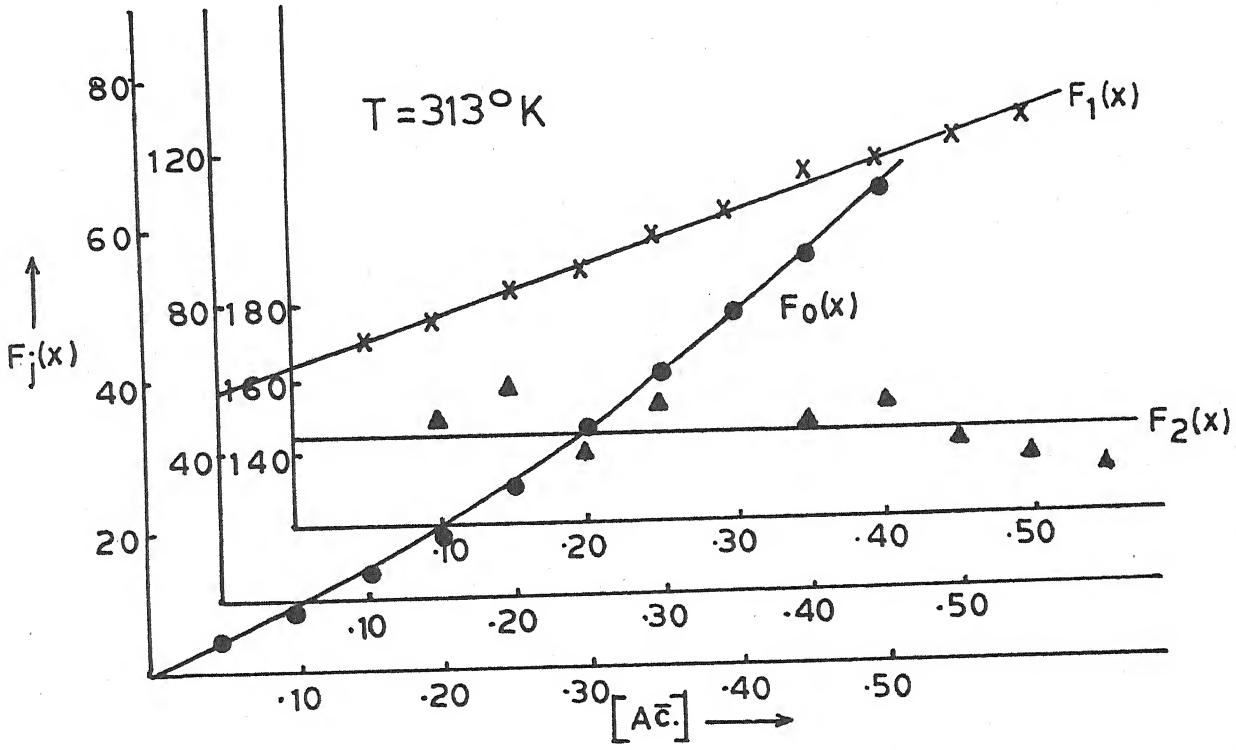

Fig. 3·03 - Plot of $F_j(x)$ Vs. $[A\bar{c}.]$; Cu ($A\bar{c}.$) system.

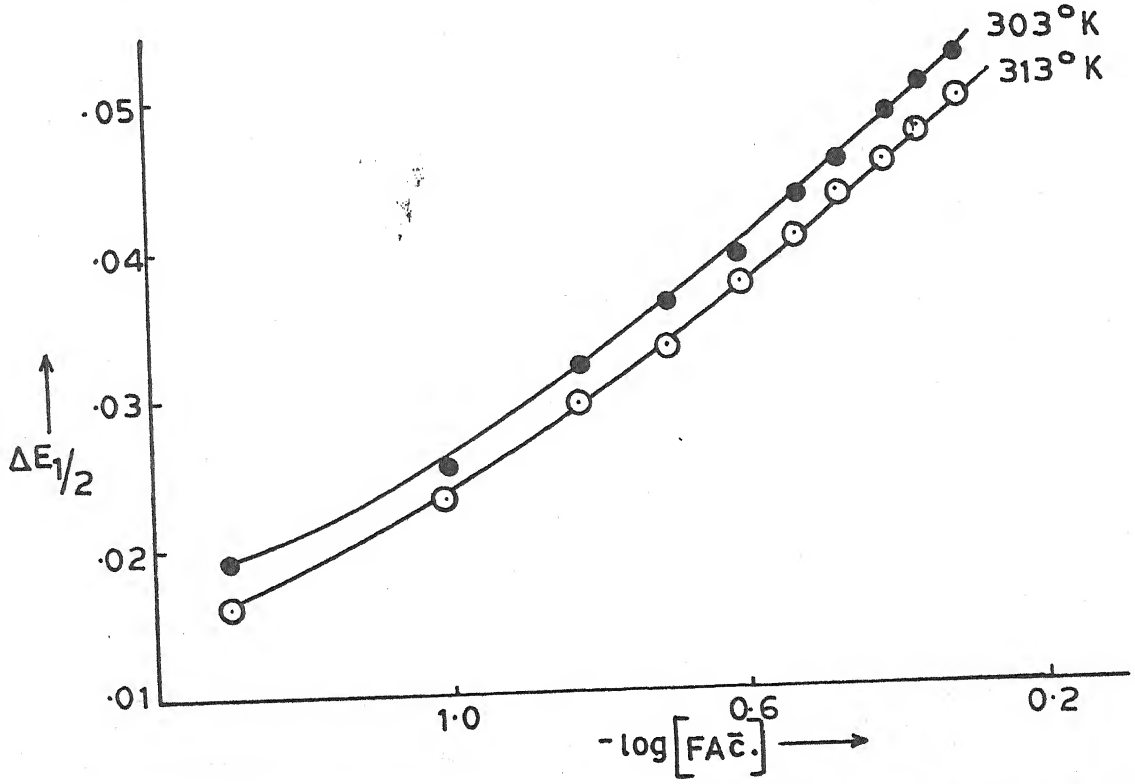

Fig. 3·04 - Plot of $\Delta E_{1/2}$ Vs. $-\log[FA\bar{c}.]$; Cu($FA\bar{c}.$) system.

presented in the table 3.01 and $F_j(X)$ functions plotted in figure 3.02.

(c) Effect of temperature :- Earlier in this section, the temperature co-efficient of $E_{1/2}$ and i_d were used to establish the reversibility and diffusion controlled nature of the reduction at DME.

The stability constants of the copper/acetate complexes were also determined at 313° K to enable us to compute the thermodynamic parameters. The stability constants of the 1:1 and 1:2 complexes at this temperature were found to be 58.5 and 144 respectively. The corresponding polarographic data have been included in table 3.02 and the $F_j(X)$ functions plotted in figure 3.03.

The values of different thermodynamic parameters have been calculated and presented in table 3.03.

Table 3.03

Copper acetate system

Temperature (° K)	log β_1	- ΔG (kj)	- ΔH (kj)	- ΔS (kj deg^{-1})x10^3
303	1.9030	11.0408		45.0102
			24.6789	
313	1.7671	10.5907		45.0102

3.3.02 Copper monofluoroacetate system :

(a) Nature of reduction : The well defined polarographic waves for the reduction of Cu(II) in presence monofluoroacetate ions (sodium monofluoroacetate) were found to be reversible involving two electrons from the linearity and slopes (30 mV) of the plots of $-E_{de}$ vs. -log. i/i_d-i and the temperature co-efficient of $E_{1/2}$ which was of the order of 0.2 - 0.3 mV per degree centigrade. That the reduction was entirely diffusion controlled was inferred from the temperature co-efficient of diffusion current (0.3 $\pm$ 0.1 percent per degree centigrade) and the linearity of curves in the plots of diffusion current and square root of effective height of the mercury column of the DME.

(b) Effect of ligand concentration : When solution containing 0.9 mM Cu(II) ions, 0.002% gelatin, increasing amounts of monofluoroacetate ions (FAc^-.) and requisite amounts of sodium perchlorate were polarographed at 303° K, a cathodic shift in $E_{1/2}$ and reduction in i_d was observed which indicated complex formation. From the curved nature of plot of $\Delta E_{1/2}$ vs. -log $[FAc^-]$ (fig. 3.04) multiple complex formation was inferred and the method of DeFord and Hume as improved by Irving was applied to determine the stability constants of the complexes formed. The overall stability constant values were found to be 58.5 for $[Cu(FAc.)]^+$ and 142 for $[Cu(FAc.)_2]$ complexes. The relevant polarographic data are listed in table 3.04 and the

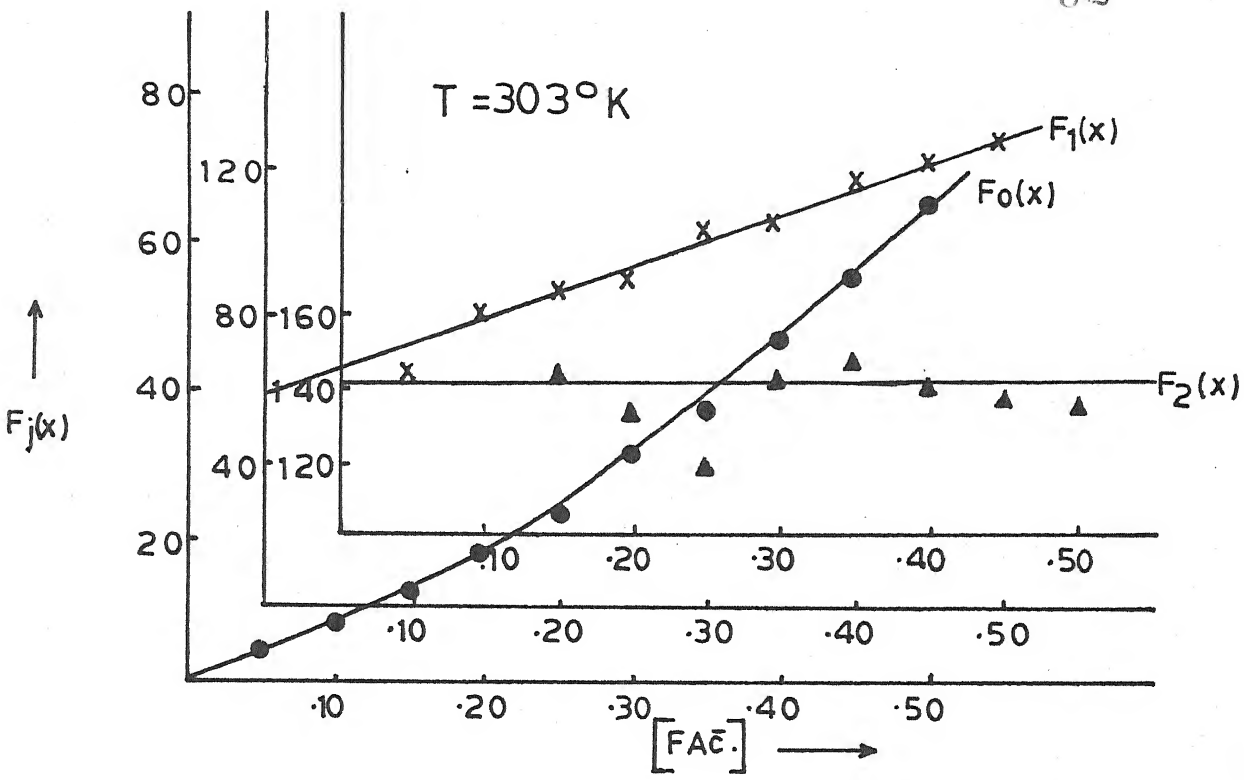

Fig. 3·05 - Plot of $F_j(x)$ Vs. $[FA\bar{c}.]$; Cu(FAc̄.) system.

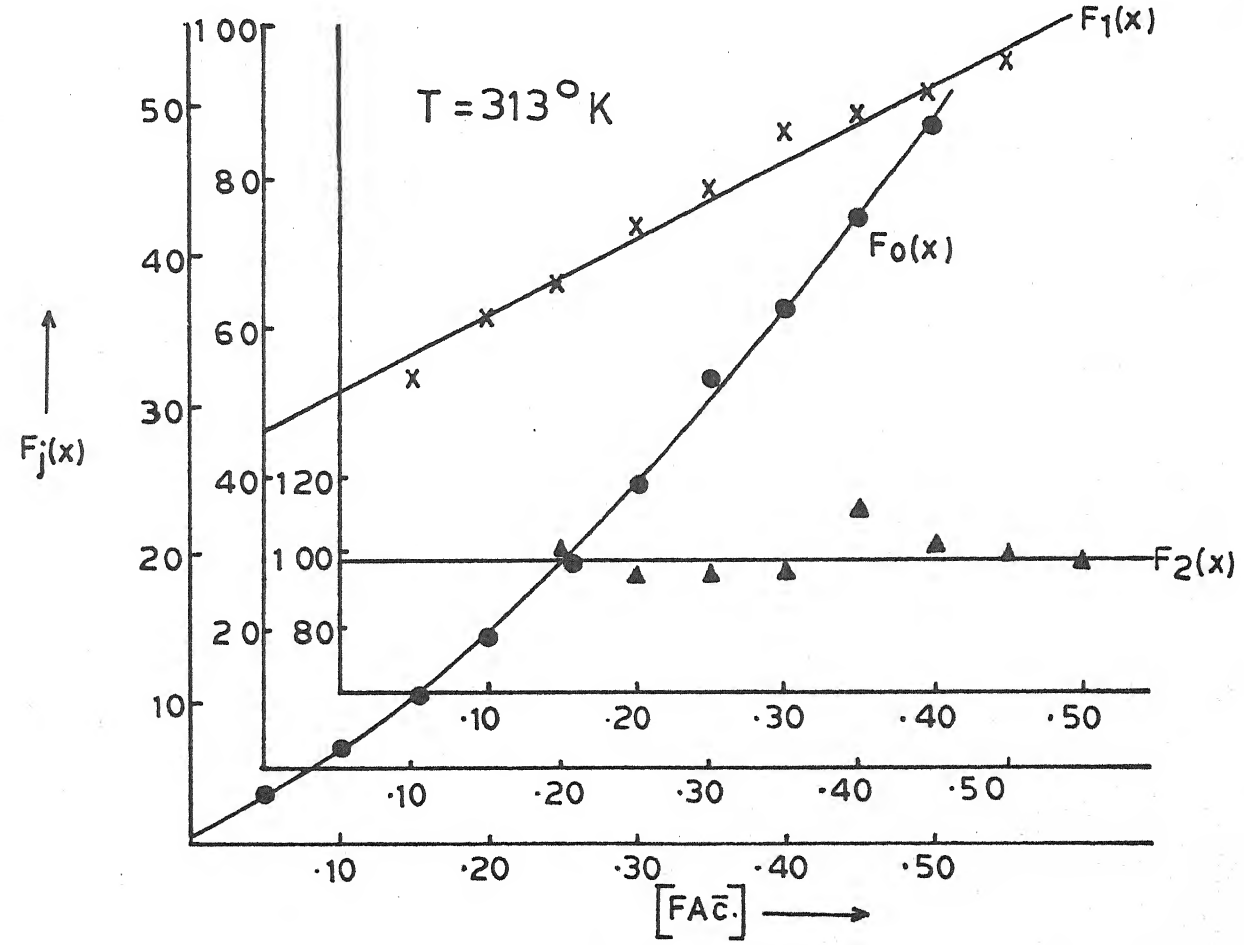

Fig. 3·06 - Plot of $F_j(x)$ Vs. $[FA\bar{c}.]$; Cu(FAc̄.) system.

Table 3.04

Polarographic data for copper monofluoroacetate system

Concn. of Cu^{++} ions = 0.9 mM Ionic strength = 1.0 M ($NaClO_4$)

$E_{1/2}$ of Cu^{++} ion = 0.012 V vs. SCE Temperature = 303° K

Slopes of plots of $-E_{de}$ vs.-log. i/i_d-i = 30-31 mV

$[FA\bar{c}.]$ (M)	$\Delta E_{1/2}$ (V)	log I_M/I_C	$F_0(X)$	$F_1(X)$	$F_2(X)$
0.05	0.019	0.0234	4.52	-	-
0.10	0.025	0.0388	7.42	64.2	-
0.15	0.032	0.0515	13.06	80.4	146.0
0.20	0.036	0.0612	18.15	85.75	136.25
0.25	0.039	0.0679	23.19	88.76	121.04
0.30	0.043	0.0712	31.75	102.5	146.6
0.35	0.045	0.0746	37.29	103.68	150.6
0.40	0.048	0.0780	47.30	115.75	143.1
0.45	0.050	0.0814	55.57	121.26	139.4
0.50	0.052	0.0814	64.77	127.54	138.0

$\beta_1 = 58.5$ $\beta_2 = 142$

Table 3.05

Polarographic data for copper monofluoroacetate system

Concn. of Cu^{++} ions = 0.9 mM Ionic strength = 1.0 M ($NaClO_4$)

$E_{1/2}$ of Cu^{++} ion = 0.016 V vs. SCE Temperature = 313° K

Slopes of plots of $-E_{de}$ vs.-log. i/i_d-i = 30-31 mV

$[FA\bar{c}.]$ (M)	$\Delta E_{1/2}$ (V)	log I_M/I_C	$F_0(X)$	$F_1(X)$	$F_2(X)$
0.05	0.016	0.0460	3.64	-	-
0.10	0.023	0.0605	6.32	53.2	-
0.15	0.029	0.0725	10.15	61.0	100.0
0.20	0.033	0.0817	13.94	64.7	93.5
0.25	0.037	0.0911	19.17	72.68	106.7
0.30	0.040	0.0475	24.30	77.66	105.5
0.35	0.043	0.1040	30.82	85.2	112.0
0.40	0.045	0.1040	35.74	86.85	102.1
0.45	0.047	0.1073	41.77	90.6	99.1
0.40	0.049	0.1073	48.45	94.9	97.8

$\beta_1 = 46$ $\beta_2 = 96$

$F_j(X)$ function plotted in figure 3.05.

(c) Effect of temperature : The temperature co-efficients of $E_{1/2}$ and i_d, already listed earlier in this section, have been used to infer the reversibility and diffus-ion controlled nature of the reduction of copper monofluoroacetate complexes at the DME.

The stability constants of these complexes were also determined at 313° K and were found to be 46 and 96 for $[Cu\ (FAc.)]^+$ and $[Cu\ (FAc.)_2]$ complexes respectively. The relevant polarographic data appears in table 3.05 and the $F_j(X)$ functions find place in figure 3.06.

From the knowledge of stability constants at two temperatures, it was possible to compute thermodynamic parameters viz. ΔG, ΔH and ΔS which are listed in table 3.06.

Table 3.06

Copper monofluoroacetate system

Temperature (° K)	log β_1	$-\Delta G$ (kj)	$-\Delta H$ (kj)	$-\Delta S$ (kj deg^{-1})x10^3
303	1.7671	10.2523		28.7336
			18.9586	
313	1.6627	9.9650		28.7335

3.3.03 Copper difluoroacetate system :

(a) Nature of reduction : That the reduction of Cu(II) in difluoroacetate medium is reversible involving two electrons and is entirely diffusion controlled was inferred from linearity of plots of $-E_{de}$ vs. $-\log i/i_d - i$ with slopes of 30-31 mV, temperature co-efficients of $E_{1/2}$ (0.4 ± 0.1 mV per degree centigrade) and i_d (0.4 ± 0.1 percent per degree centigrade) and linearity of plot of i_d against the square root of effective height of mercury column of the DME.

(b) Effect of ligand concentration : When the concentration of difluoroacetate ions is increased in test solutions containing 0.9 mM Cu(II) ions, 0.002% gelatin and requisite amount of sodium perchlorate to maintain ionic strength constant at 1.0 M, the $E_{1/2}$ registers a gradual shift in the cathodic direction accompanied by reduction in i_d. This implies complex formation. The plot of $\Delta E_{1/2}$ vs. $-\log. [F_2Ac^-.]$ is a curve (figure 3.07) indicating successive complex formation. The method of DeFord and Hume, as improved by Irving, was therefore used to compute the overall stability constants which were found to be 28 and 194 for 1:1 and 1:2 complexes respectively at 303^o K. The polarographic data find place in table 3.07 while the $F_j(X)$ functions are depicted in figure 3.08.

(c) Effect of temperature : The temperature co-efficient of $E_{1/2}$ and i_d, already referred to earlier in this section,

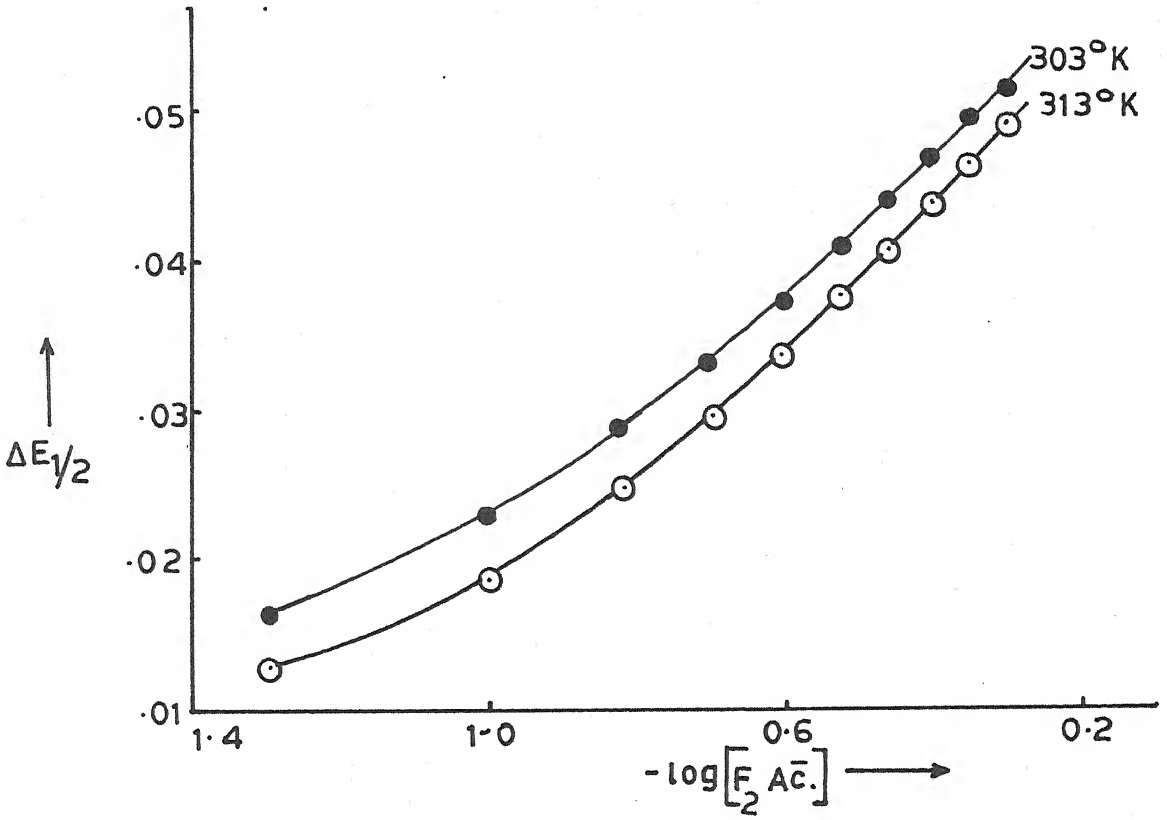

Fig. 3·07 - Plot of $\Delta E_{1/2}$ Vs. $-\log[F_2 Ac.]$; Cu(F_2 Ac.) system.

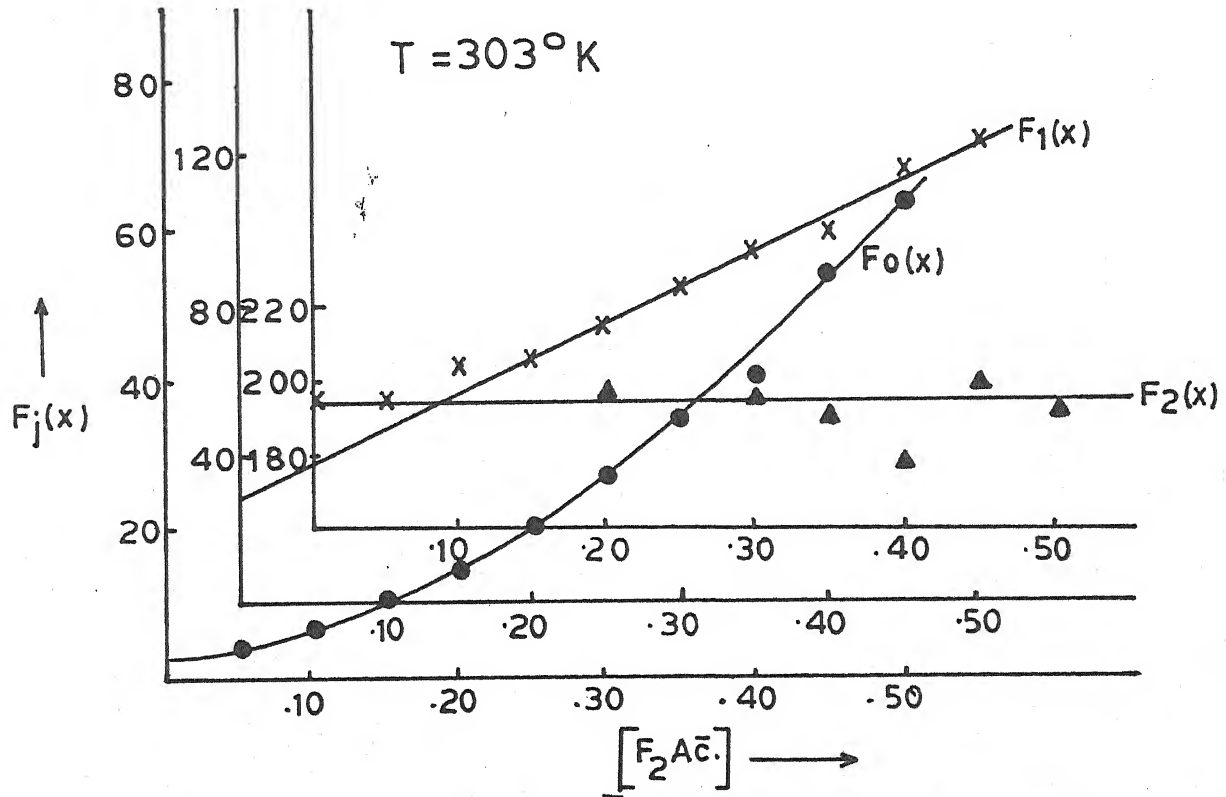

Fig. 3·08 - Plot of $F_j(x)$ Vs. $[F_2 Ac.]$; Cu (F_2Ac.) system.

Table 3.07

Polarographic data for copper difluroacetate system

Concn. of Cu^{++} ions = 0.9 mM Ionic strength = 1.0 M ($NaClO_4$)
$E_{1/2}$ of Cu^{++} ions = 0.012 V vs. SCE Temperature = 303° K
Slopes of plots of $-E_{de}$ vs. $-\log. i/i_d - i$ = 30-31 mV

$[F_2Ac^-.]$ (M)	$\Delta E_{1/2}$ (V)	$\log. I_M/I_C$	$F_0(X)$	$F_1(X)$	$F_2(X)$
0.05	0.016	0.0354	3.69	53.8	-
0.10	0.023	0.0479	6.50	55.0	-
0.15	0.029	0.0575	10.52	63.46	-
0.20	0.033	0.0641	14.51	67.5	197.5
0.25	0.037	0.0674	19.87	75.48	189.9
0.30	0.041	0.0707	27.20	87.33	197.7
0.35	0.044	0.0741	34.50	95.71	193.4
0.40	0.047	0.0741	40.92	100.0	180.0
0.45	0.050	0.0741	54.63	119.17	202.6
0.50	0.052	0.0741	63.68	125.36	194.7

$\beta_1 = 28$ $\beta_2 = 194$

Table 3.08

Polarographic data for copper difluoroacetate system

Concn. of Cu^{++} ions = 0.9 mM Ionic strength = 1.0 M ($NaClO_4$)
$E_{1/2}$ of Cu^{++} ions = 0.016 V vs. SCE Temperature = 313° K
Slopes of plots of $-E_{de}$ vs. $-\log. i/i_d - i$ = 30-31 mV

$[F_2Ac^-.]$ (M)	$\Delta E_{1/2}$ (V)	$\log. I_M/I_C$	$F_0(X)$	$F_1(X)$	$F_2(X)$
0.05	0.013	0.0237	2.76	-	-
0.10	0.019	0.0375	4.46	34.6	131.0
0.15	0.025	0.0489	7.14	40.93	129.5
0.20	0.030	0.0547	10.49	47.45	129.7
0.25	0.034	0.0605	14.30	53.2	126.8
0.30	0.038	0.0635	19.37	61.25	132.4
0.35	0.041	0.0665	24.37	66.77	129.4
0.40	0.044	0.0695	30.65	74.12	131.5
0.45	0.047	0.0725	38.56	83.46	137.7
0.50	0.050	0.0755	48.50	95.0	147.0

$\beta_1 = 21.5$ $\beta_2 = 131$

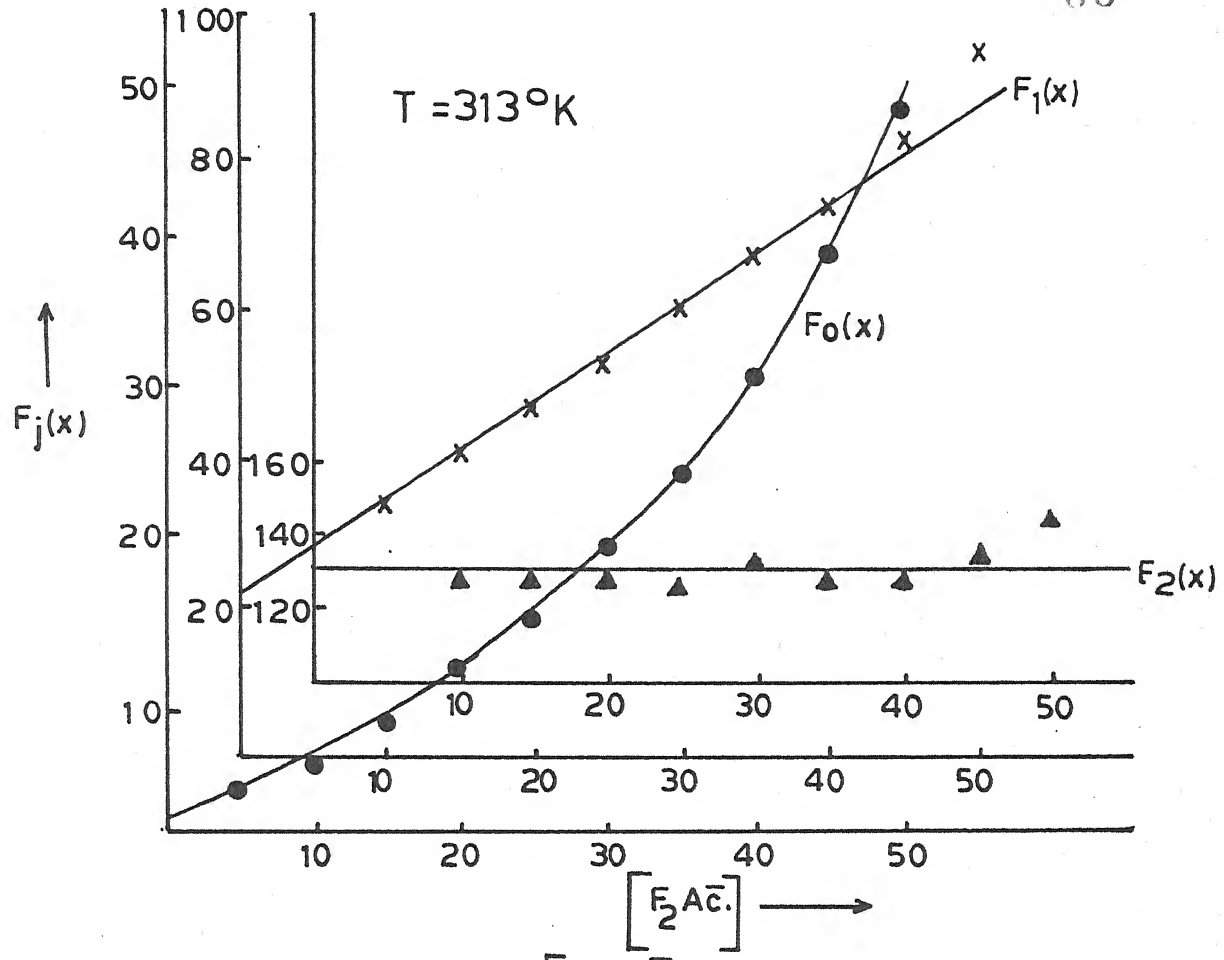

Fig. 3·09 - Plot of $F_j(x)$ Vs. $[F_2 Ac.]$; Cu ($F_2 Ac.$) system.

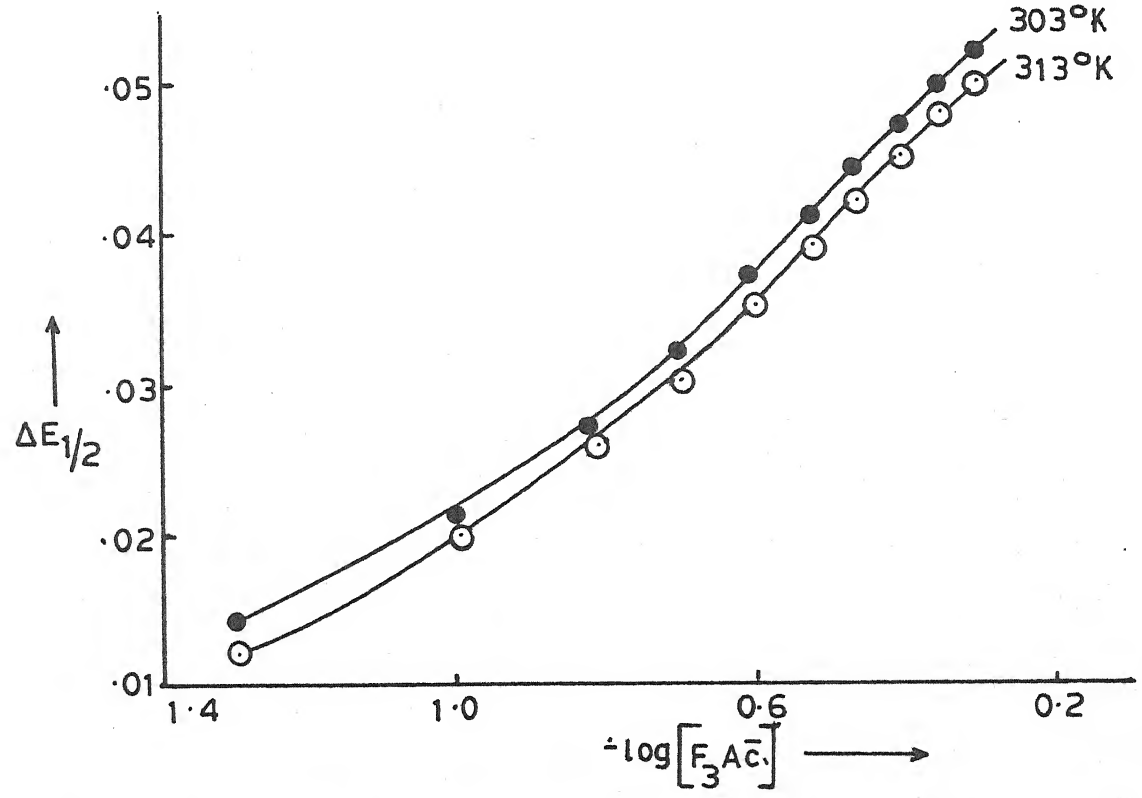

Fig. 3·10 - Plot of $\Delta E_{1/2}$ Vs. $-\log[F_3 Ac.]$; Cu ($F_3 Ac.$) system.

indicate the reduction of Cu difluoroacetate complexes to be reversible and diffusion controlled.

The stability constants were also determined at 313° K. The polarographic data is reported in table 3.08 and the $F_j(X)$ function depicted in figure 3.09. The stability constants so obtained were 21.5 and 131 for 1:1 and 1:2 complexes of Cu(II) with difluoroacetate ions.

It was now possible to compute thermodynamic parameters which are included in table 3.09.

Table 3.09

Copper difluoroacetate system

Temperature (° K)	log β_1	$-\Delta G$ (kj)	$-\Delta H$ (kj)	$-\Delta S$ (kj deg^{-1})x10^3
303	1.4471	8.3957		41.0339
			20.8290	
313	1.3324	7.9854		41.0338

3.3.04 Copper trifluoroacetate system :

(a) Nature of reduction : The reduction of copper trifluoroacetate complexes is reversible involving two electrons. This was inferred from the straight line slopes of plots of $-E_{de}$ vs. $-\log.i/i_d-i$ which were of the order of 30-31 mV and temperature co-efficient of $E_{1/2}$ which was less than 0.3 mV per degree

centigrade. The diffusion controlled nature of reduction was inferred from the temperature co-efficient of i_d (0.4 $\pm$ 0.1 percent per degree) and constancy of ratio of i_d and square root of effective height of mercury column.

(b) Effect of ligand concentration : As the concentration of trifluoroacetate ions increased in test solutions containing 0.9 mM Cu(II) ions, 0.002% gelatin and requisite amount of sodium perchlorate to keep ionic strength constant at 1.0 M at 303° K, the polarographic wave shifted to the more negative side and its height became shorter to show complex formation. The plots of $\Delta E_{1/2}$ vs. -log. $[F_3Ac^-]$ was a curve(figure 3.10) indicating the formation of more than one complex. DeFord and Hume's method yielded the overall stability constant values of 17.5 and 250 for $[Cu\ (F_3Ac.)\ ]^+$ and $[Cu(F_3Ac.)_2]$ complexes respectively. The polarographic data is included in table 3.10 and the $F_j(X)$ functions plotted in figure 3.11.

(c) Effect of temperature : The temperature co-efficient of $E_{1/2}$ and i_d have already indicated that the reduction of Cu trifluoroacetate complexes is reversible and diffusion controlled.

In order to compute thermodynamic parameters ΔG, ΔH and ΔS, the stability constants of the complexes $[Cu\ (F_3Ac.)\ ]^+$ and $[Cu\ (F_3Ac.)_2]$ were computed at 313° K and found to be 15 and 168 respectively. The relevant polarographic data appear in table 3.11 and the $F_j(X)$ functions find place in

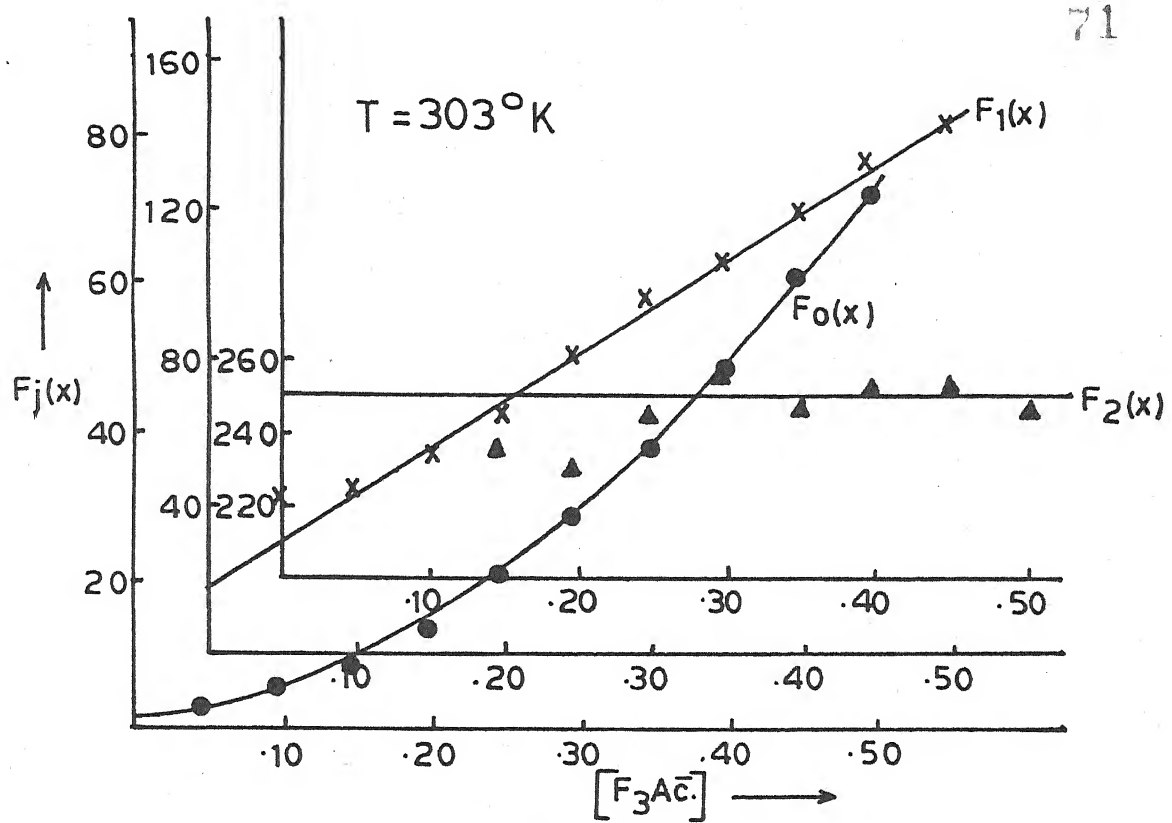

Fig. 3·11 - Plot of $F_j(x)$ Vs. $[F_3 A\bar{c}.]$; $Cu(F_3 A\bar{c}.)$ system.

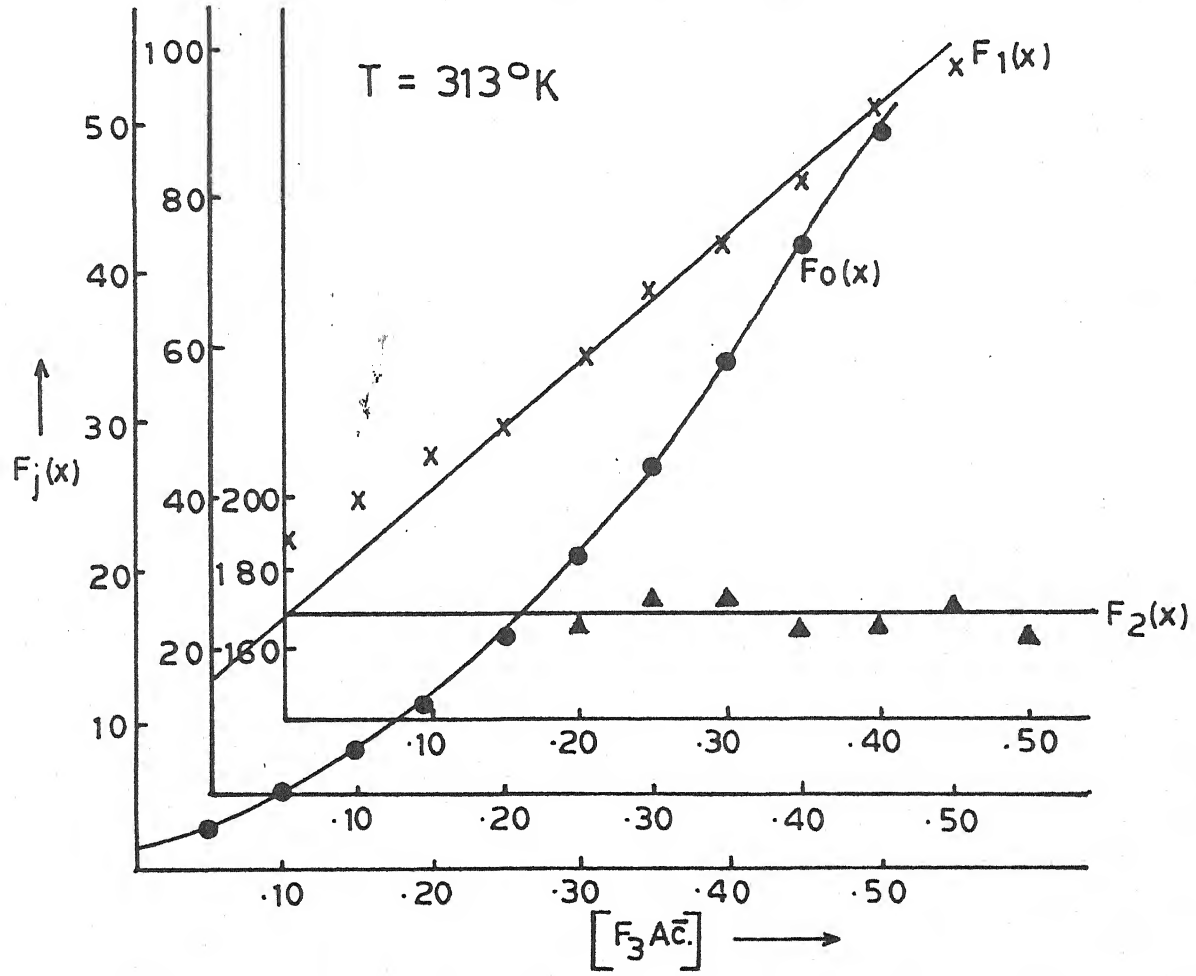

Fig. 3·12 - Plot of $F_j(x)$ Vs. $[F_3 A\bar{c}.]$; $Cu(F_3 A\bar{c}.)$ system.

Table 3.10

Polarographic data for copper trifluoroacetate system

Concn. of Cu^{++} ions = 0.9 mM Ionic strength = 1.0 M ($NaClO_4$)

$E_{1/2}$ of Cu^{++} ions = 0.012 V vs. SCE Temperature = 303° K

Slopes of plots of $-E_{de}$ vs.-log. i/i_d-i = 30-31 mV

$[F_3A\bar{c}.]$ (M)	$\Delta E_{1/2}$ (V)	log. I_M/I_C	$F_0(X)$	$F_1(X)$	$F_2(X)$
0.05	0.014	0.0233	3.08	41.6	-
0.10	0.021	0.0385	5.45	44.5	-
0.15	0.027	0.0575	9.03	53.33	238.0
0.20	0.032	0.0741	13.76	63.8	231.5
0.25	0.037	0.0877	20.82	79.28	247.1
0.30	0.041	0.1055	29.47	94.9	258.0
0.35	0.044	0.1128	37.72	104.85	249.5
0.40	0.047	0.1202	48.28	118.20	251.7
0.45	0.050	0.1202	60.75	132.77	256.1
0.50	0.052	0.1277	72.06	142.0	249.0

$\beta_1 = 17.5$ $\beta_2 = 250$

Table 3.11

Polarographic data for copper trifluoroacetate system

Concn. of Cu^{++} ions = 0.9 mM Ionic strength = 1.0 M ($NaClO_4$)

$E_{1/2}$ of Cu^{++} ions = 0.016 V vs. SCE Temperature = 313° K

Slopes of plots of $-E_{de}$ vs. log. i/i_d-i = 30-31 mV

$[F_3A\bar{c}.]$ (M)	$\Delta E_{1/2}$ (V)	log. I_M/I_C	$F_0(X)$	$F_1(X)$	$F_2(X)$
0.05	0.012	0.0319	2.62	32.4	-
0.10	0.020	0.0460	4.89	38.9	-
0.15	0.026	0.0576	7.85	45.66	-
0.20	0.030	0.0635	10.70	48.50	167.5
0.25	0.035	0.0695	15.72	58.88	175.5
0.30	0.039	0.0725	21.30	67.66	175.5
0.35	0.042	0.0755	26.80	73.71	167.7
0.40	0.045	0.0786	33.71	81.77	166.9
0.45	0.048	0.0817	42.42	92.04	171.1
0.50	0.050	0.0848	49.55	97.10	164.2

$\beta_1 = 15$ $\beta_2 = 168$

figure 3.12. The thermodynamic parameters are included in table 3.12.

Table 3.12

Copper trifluoroacetate system

Temperature (^{o} K)	log β_1	- ΔG (kj)	- ΔH (kj)	- ΔS (kj deg^{-1})x10^{3}
303	1.2430	7.2116		16.3541
			12.1669	
313	1.1760	7.0480		16.3543

3.3.05 Copper monochloroacetate system :

(a) Nature of reduction : From the observations that

(i) the straight line plots of $-E_{de}$ vs. -log. i/i_d-i have slopes of 30-31 mV,

(ii) the temperature co-efficients of $E_{1/2}$ and i_d are 0.1 to 0.3 mV per degree and 0.4 $\pm$ 0.1 percent per degree respectively,

(iii) the plot of i_d against square root of effective height of mercury column is linear, it was inferred that the two electron reduction of Cu(II) monochloroacetate complexes is reversible and entirely diffusion controlled.

(b) Effect of ligand concentration : When test solutions

containing 0.9 mM Cu(II) ions, 0.002% gelatin, increasing amounts of monochloroacetate ions and correspondingly decreasing amounts of sodium perchlorate to keep ionic strength constant at 1.0 M, were polarographed at 303° K, a cathodic shift in $E_{1/2}$ and gradual decrease in i_d was observed to indicate complex formation. As the plot of $\Delta E_{1/2}$ vs. -log. $[ClAc^-]$ was a curve (figure 3.13) indicating stepwise complex formation, the method of DeFord and Hume was employed to determine the stability constants of the complexes so formed. The two complexes formed $[Cu\ (ClAc.)]^+$ and $[Cu\ (ClAc.)_2]$ have overall stability constant values of 51.5 and 306 respectively. The polarographic data and the $F_j(X)$ plots are presented in table 3.13 and figure 3.14.

(b) Effect of temperature : Earlier in this section, the reversible and diffusion controlled nature of reduction of copper monochloroacetate complexes has been established from the temperature co-efficient of half wave potential and diffusion current.

The stability constants of the complexes $[Cu\ (ClAc.)]^+$ and $[Cu\ (ClAc.)_2]$ were redetermined at 313° K and were found to be 37 and 240 respectively. The relevant polarographic data and $F_j(X)$ plots appear in table 3.14 and figure 3.15.

The knowledge of stability constants at two temperatures was used to compute thermodynamic parameters which are presented in table 3.15.

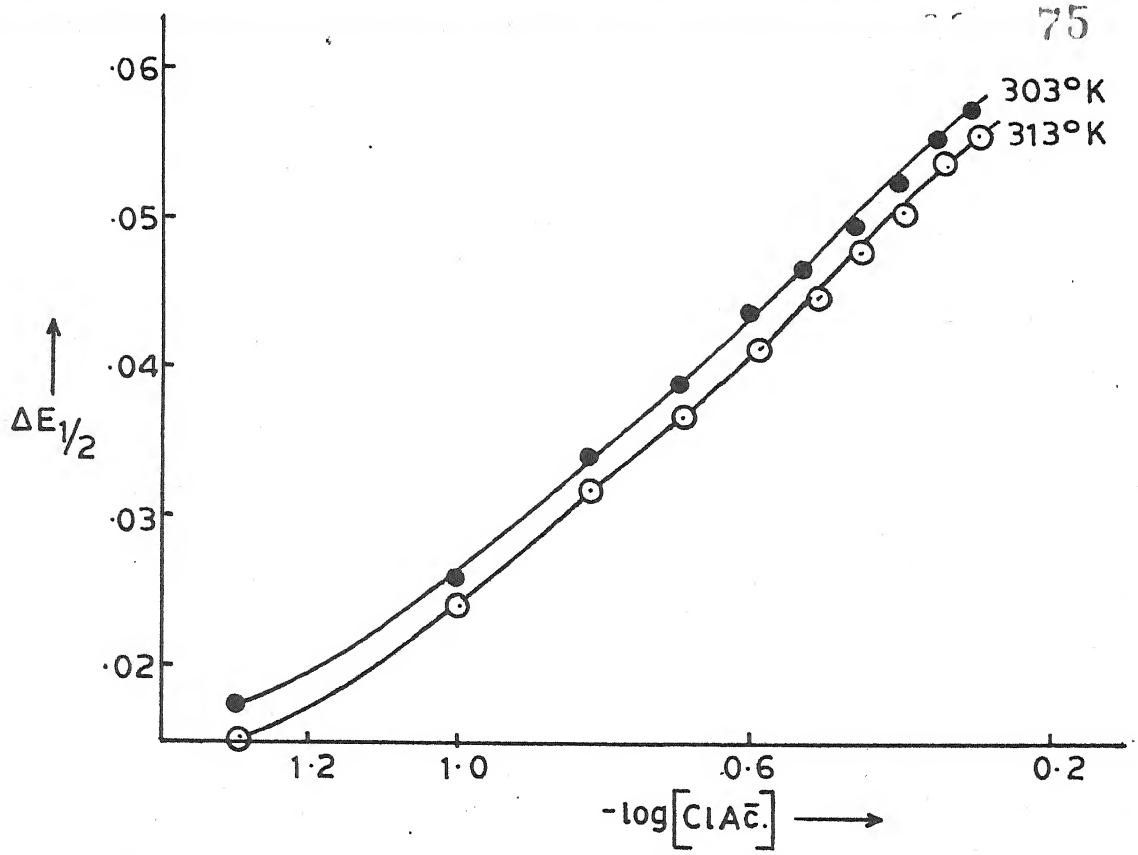

Fig. 3·13 - Plot of $\Delta E_{1/2}$ Vs. $-\log[ClA\bar{c}.]$; Cu(ClAc̄.)system.

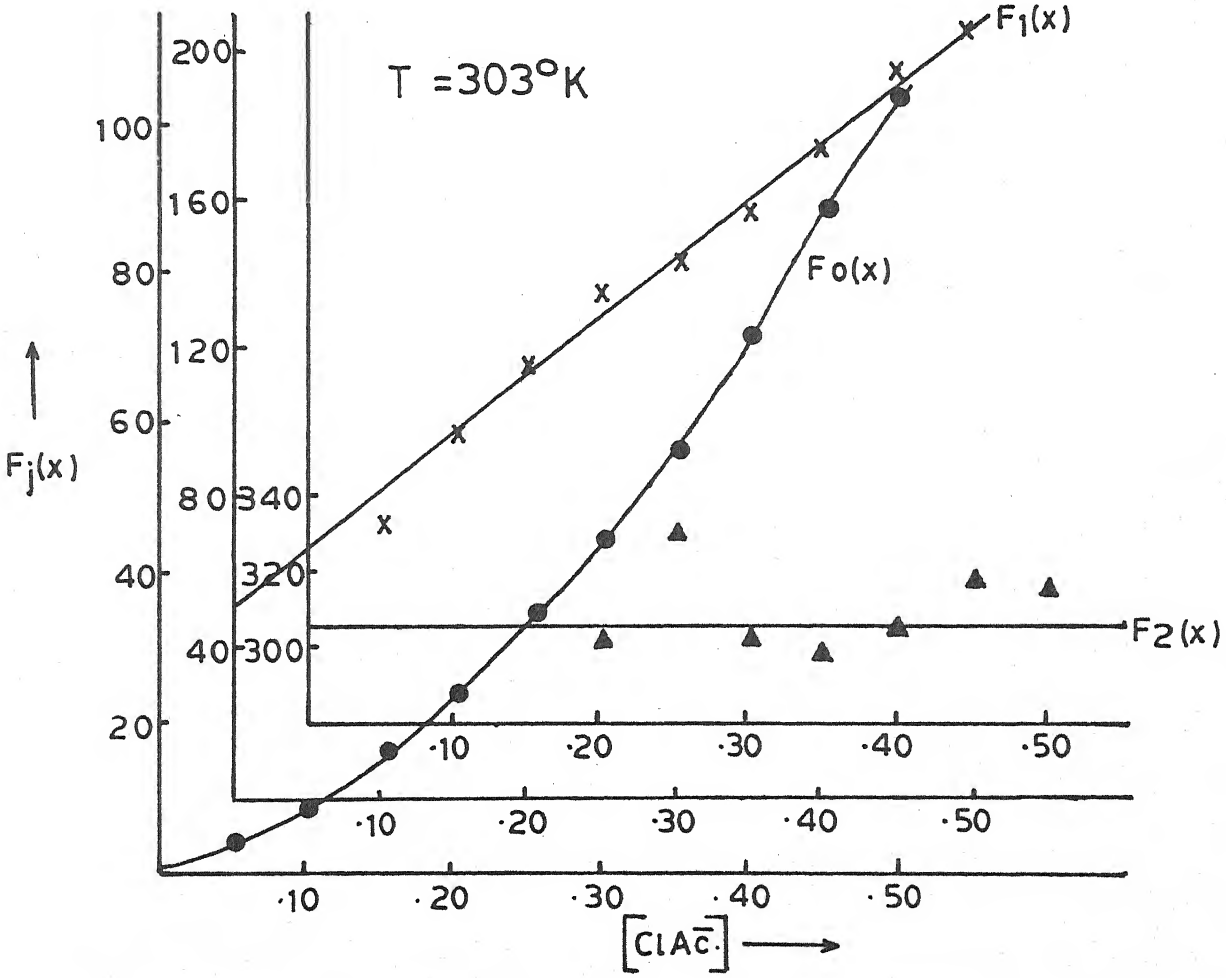

Fig. 3·14 - Plot of $F_j(x)$ Vs. $[ClA\bar{c}.]$; Cu(ClAc̄.)system.

Table 3.13

Polarographic data for copper monochloroacetate system

Concn. of Cu^{++} ions = 0.9 mM Ionic strength = 1.0 M ($NaClO_4$)
$E_{1/2}$ of Cu^{++} ions = 0.012 V vs. SCE Temperature = 303° K
Slopes of plots of $-E_{de}$ vs. -log. i/i_d-i = 30-31 mV

$[ClAc^-]$ (M)	$\Delta E_{1/2}$ (V)	log. I_M/I_C	$F_0(X)$	$F_1(X)$	$F_2(X)$
0.05	0.017	0.0352	3.98	59.6	-
0.10	0.026	0.0539	8.29	72.9	-
0.15	0.34	0.0669	15.77	98.46	313.0
0.20	0.039	0.0735	23.49	112.45	304.7
0.25	0.044	0.0769	34.72	134.88	333.5
0.30	0.047	0.0803	44.08	143.6	307.0
0.35	0.050	0.0837	55.85	156.71	300.6
0.40	0.053	0.0871	70.84	174.6	307.7
0.45	0.056	0.0871	89.15	195.88	320.8
0.50	0.058	0.0871	103.91	205.82	308.6

$\beta_1 = 51.5$ $\beta_2 = 306$

Table 3.14

Polarographic data for copper monochloroacetate system

Concn. of Cu^{++} ions = 0.9 mM Ionic strength = 1.0 M ($NaClO_4$)
$E_{1/2}$ of Cu^{++} ions = 0.016 V vs. SCE Temperature = 313° K
Slopes of plots of $-E_{de}$ vs. -log. i/i_d-i = 30-31 mV

$[ClAc^-]$ (M)	$\Delta E_{1/2}$ (V)	log. I_M/I_C	$F_0(X)$	$F_1(X)$	$F_2(X)$
0.05	0.015	0.0312	3.26	45.2	-
0.10	0.024	0.0479	6.61	56.1	-
0.15	0.032	0.0590	12.29	75.26	255.0
0.20	0.037	0.0677	18.16	85.8	244.0
0.25	0.042	0.0766	26.87	103.4	265.0
0.30	0.045	0.0827	34.03	110.1	243.6
0.35	0.048	0.0888	43.11	120.31	238.0
0.40	0.051	0.0888	53.85	132.12	237.8
0.45	0.054	0.0919	67.75	150.55	252.3
0.50	0.056	0.0919	78.58	155.16	236.3

$\beta_1 = 32$ $\beta_2 = 240$

Table 3.15

Copper monochloroacetate system

Temperature (° K)	log β_1	- ΔG (kj)	-ΔH (kj)	-ΔS (kj deg^{-1})x10^3
303	1.7118	9.9315		53.2861
			26.0772	
313	1.5682	9.3986		53.2862

3.3.06 Copper dichloroacetate system :

(a) Nature of reduction : As the linear plots of $-E_{de}$ vs. -log. i/i_d-i had slopes of 30-31 mV and the temperature co-efficient of $E_{1/2}$ was 0.1 - 0.2 mV per degree, the reduction of Cu(II) in dichloroacetate ions was established to be reversible involving two electrons. That it is diffusion controlled, too, was inferred from the temperature co-efficient of i_d which was of the order of 0.5 $\pm$ 0.1 percent per degree and constancy of ratio of i_d and square root of effective height of mercury column of the DME.

(b) Effect of ligand concentration : As solutions containing increasing concentration of dichloroacetate ions and 0.9 mM Cu(II) ions, 0.002% gelatin and requisite amount of sodium perchlorate to maintain ionic strength at 1.0 M were polarographed at 303° K, a cathodic shift in $E_{1/2}$ and a gradual

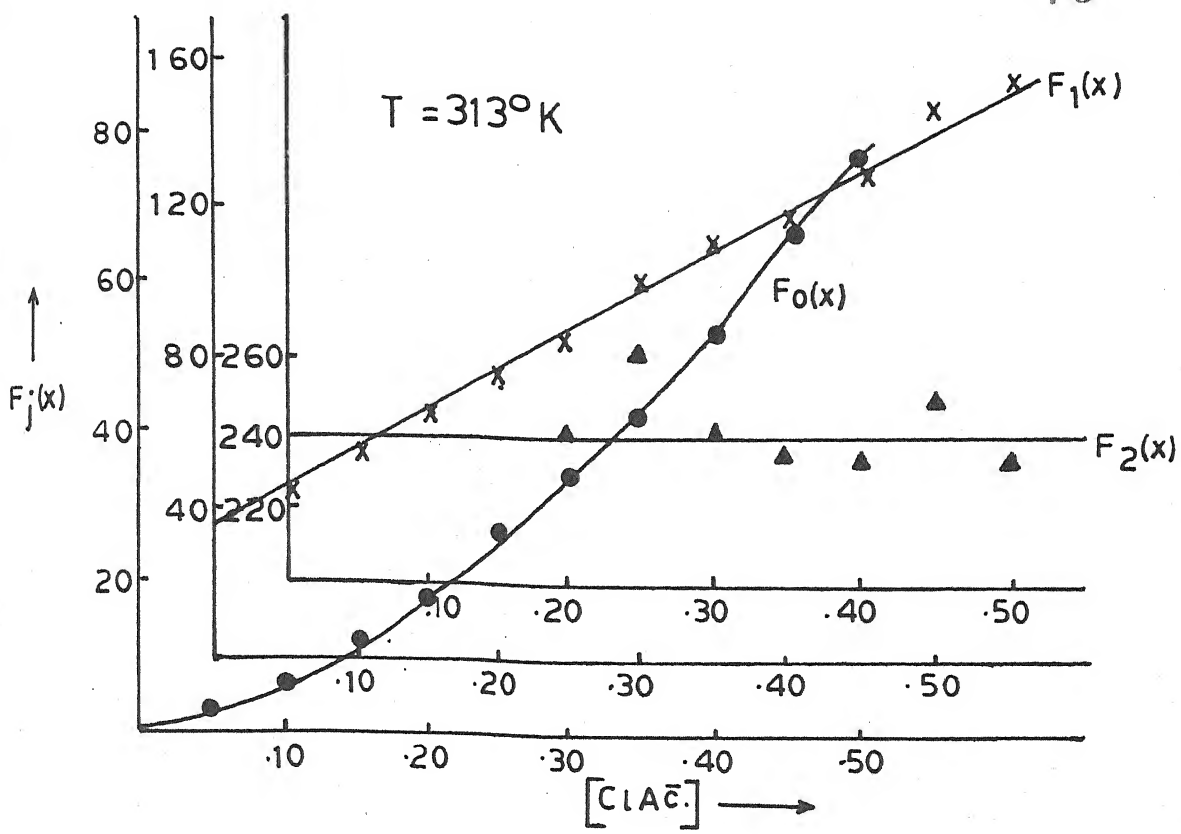

Fig. 3·15 - Plot of $F_j(x)$ Vs. $[ClA\bar{c}.]$; Cu ($ClA\bar{c}.$) system.

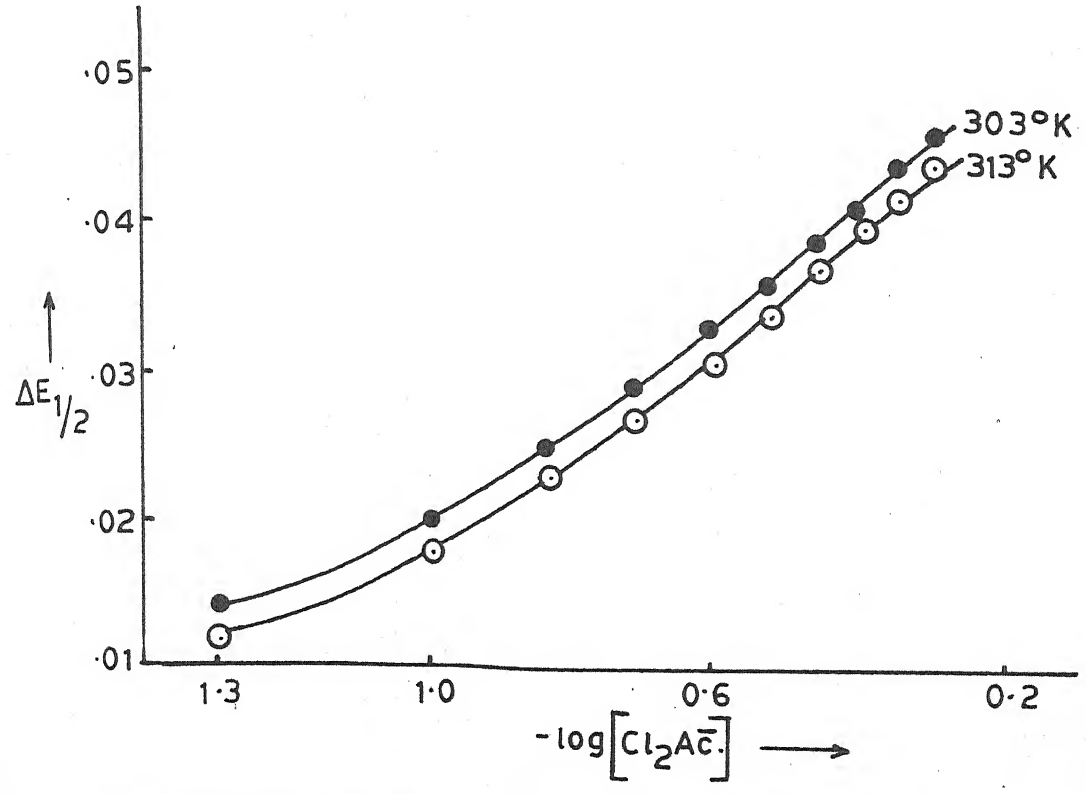

Fig. 3·16 - Plot of $\Delta E_{1/2}$ Vs. $-\log[Cl_2A\bar{c}.]$; Cu ($Cl_2A\bar{c}.$) system.

Table 3.16

Polarographic data for copper dichloroacetate system

Concn. of Cu^{++} ions = 0.9 mM Ionic strength = 1.0 M ($NaClO_4$)

$E_{1/2}$ of Cu^{++} ions = 0.012 V vs. SCE Temperature = 303° K

Slopes of plots of $-E_{de}$ vs. $-\log. i/i_d-i$ = 30-31 mV

$[Cl_2A\bar{c}.]$ (M)	$\Delta E_{1/2}$ (V)	$\log. I_M/I_C$	$F_0(X)$	$F_1(X)$	$F_2(X)$
0.05	0.014	0.0321	3.14	-	-
0.10	0.020	0.0476	5.16	41.6	-
0.15	0.025	0.0604	7.8	45.33	102.2
0.20	0.029	0.0702	10.83	49.15	95.7
0.25	0.033	0.0769	14.95	55.8	103.2
0.30	0.036	0.0837	19.11	60.36	101.2
0.35	0.039	0.0837	24.05	65.85	102.4
0.40	0.041	0.0871	28.25	68.12	95.3
0.45	0.044	0.0906	35.84	77.42	105.3
0.50	0.046	0.0940	42.11	82.22	104.4

$\beta_1 = 30$ $\beta_2 = 102$

Table 3.17

Polarographic data for copper dichloroacetate system

Concn. of Cu^{++} ions = 0.9 mM Ionic strength = 1.0 M ($NaClO_4$)

$E_{1/2}$ of Cu^{++} ions = 0.016 V vs. SCE Temperature = 313° K

Slopes of plots of $-E_{de}$ vs. $-\log. i/i_d-i$ = 30-31 mV

$[Cl_2A\bar{c}.]$ (M)	$\Delta E_{1/2}$ (V)	$\log. I_M/I_C$	$F_0(X)$	$F_1(X)$	$F_2(X)$
0.05	0.012	0.0292	2.6	-	-
0.10	0.018	0.0431	4.19	31.9	79.0
0.15	0.023	0.0547	6.24	34.93	72.8
0.20	0.027	0.0635	8.57	37.85	69.2
0.25	0.031	0.0695	11.69	42.76	75.0
0.30	0.034	0.0755	14.80	46.0	73.3
0.35	0.037	0.0786	18.27	50.37	75.3
0.40	0.040	0.0786	23.28	55.67	79.2
0.45	0.042	0.0817	27.18	58.17	75.9
0.50	0.044	0.0848	31.75	61.50	75.0

$\beta_1 = 24$ $\beta_2 = 74$

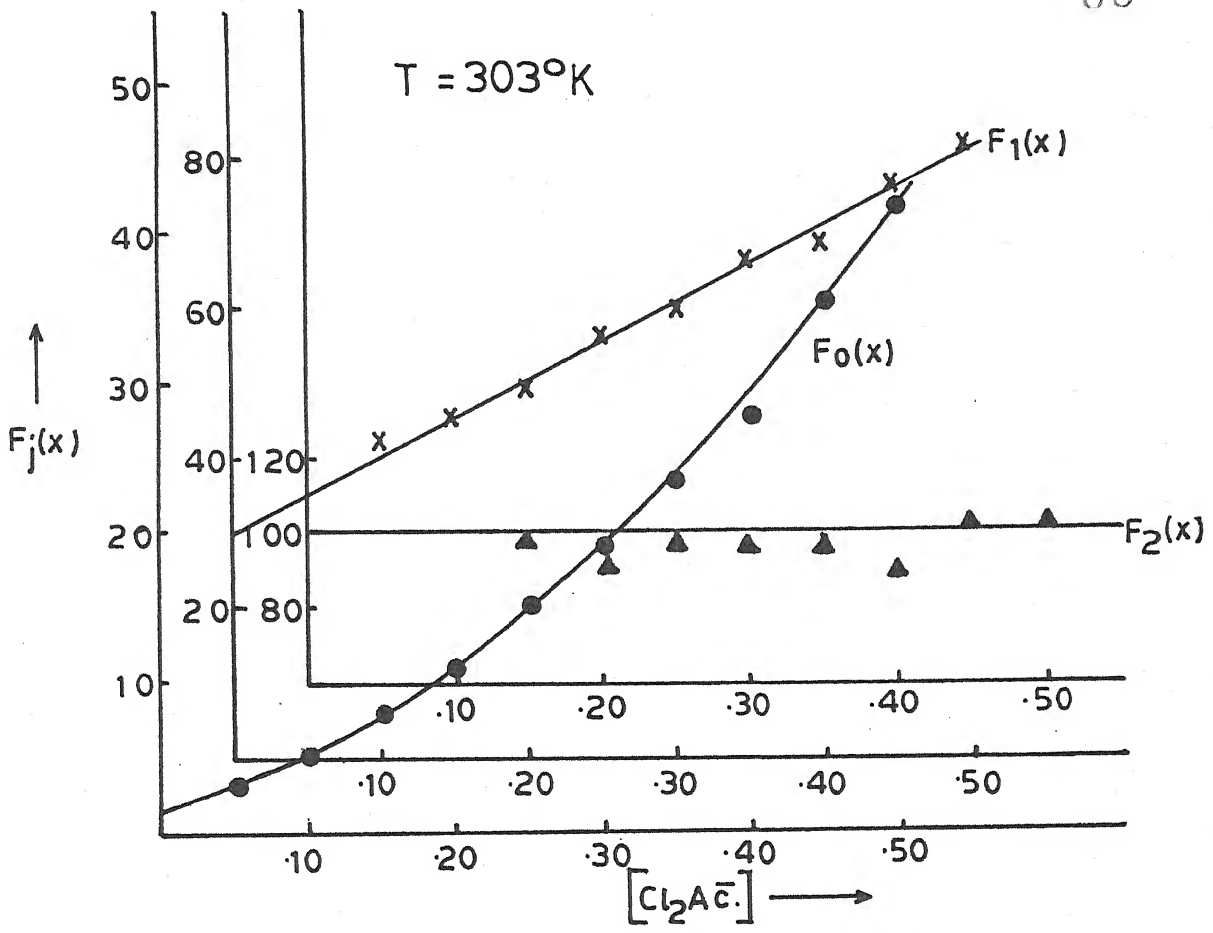

Fig. 3·17 - Plot of $F_j(x)$ Vs. $[Cl_2A\bar{c}.]$; $Cu(Cl_2A\bar{c}.)$ system.

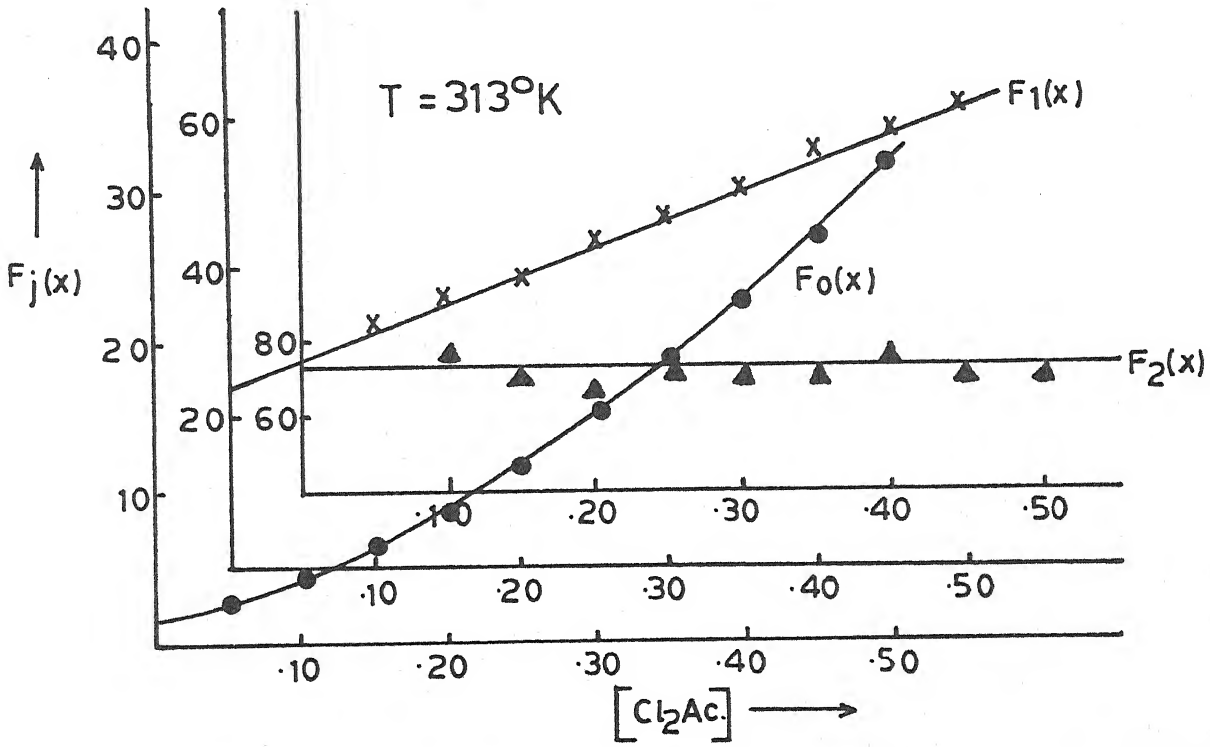

Fig. 3·18 - Plot of $F_j(x)$ Vs. $[Cl_2A\bar{c}.]$; $Cu(Cl_2A\bar{c}.)$ system.

decrease in i_d was observed which indicated complex formation. The plot of $\Delta E_{1/2}$ vs. -log. $[Cl_2A\bar{c}.]$ being curve (figure 3.16) stepwise complex formation was inferred and DeFord and Hume's method applied to compute stability constants which were found to be 30 and 102 for 1:1 and 1:2 complex respectively. The polarographic data and $F_j(X)$ plots appear in table 3.16 and figure 3.17 respectively.

(c) Effect of temperature : The reversibility and diffusion controlled nature of Cu(II) in dichloroacetate ions has already been inferred earlier in this section from the temperature co-efficient of $E_{1/2}$ and i_d.

The stability constants were determined at 313° K and were found to be 24 and 74 for 1:1 and 1:2 complexes respectively. The relevant polarographic data is included in table 3.17 and $F_j(X)$ functions plotted in figure 3.18.

The knowledge of stability constants at two temperatures enabled us to calculate the thermodynamic parameters which find place in table 3.18.

Table 3.18

Copper dichloroacetate system

Temperature (° K)	log β_1	$-\Delta G$ (kj)	$-\Delta H$ (kj)	$-\Delta S$ (kj deg^{-1})x10^3
303	1.4771	8.5698		29.7914
			17.5966	
313	1.3802	8.2719		29.7913

3.3.07 Copper trichloroacetate system :

(a) Nature of reduction : The reduction of Cu(II) in trichloroacetate ions was reversible involving two electrons and was entirely diffusion controlled. This could be inferred from the linear plots of $-E_{de}$ vs. -log. i/i_d-i with slopes of 30-31 mV, temperatures co-efficients of $E_{1/2}$ (0.2 $\pm$ 0.1 mV per degree) and i_d (0.4 $\pm$ 0.1 percent per degree) and linearity of the plot of i_d against $\sqrt{h_{eff.}}$.

(b) Effect of ligand concentration : Polarographic examination of solutions containing 0.9 mM Cu(II) ions 0.002% gelatin, increasing amounts of trichloroacetate ions and decreasing amounts of sodium perchlorate to maintain ionic strength constant at 1.0 M at 303° K exhibited a gradual cathodic shift in $E_{1/2}$ and decrease in i_d. Since the plot of $\Delta E_{1/2}$ vs. -log. $[Cl_3A\bar{c}.]$ (figure 3.19) was a curve, formation of more than one complex was indicated so that method of DeFord and Hume was applied to compute the stability constantswhich were found to be 23.5 (β_1) and 195 (β_2). The relevant polarographic data and $F_j(X)$ plots have been included in table 3.19 and figure 3.20.

(c) Effect of temperature : The magnitude of temperature co-efficient of half wave potential and diffusion current, as already indicated earlier in this section, have confirmed that the reduction of copper trichloroacetate is reversible and entirely diffusion controlled.

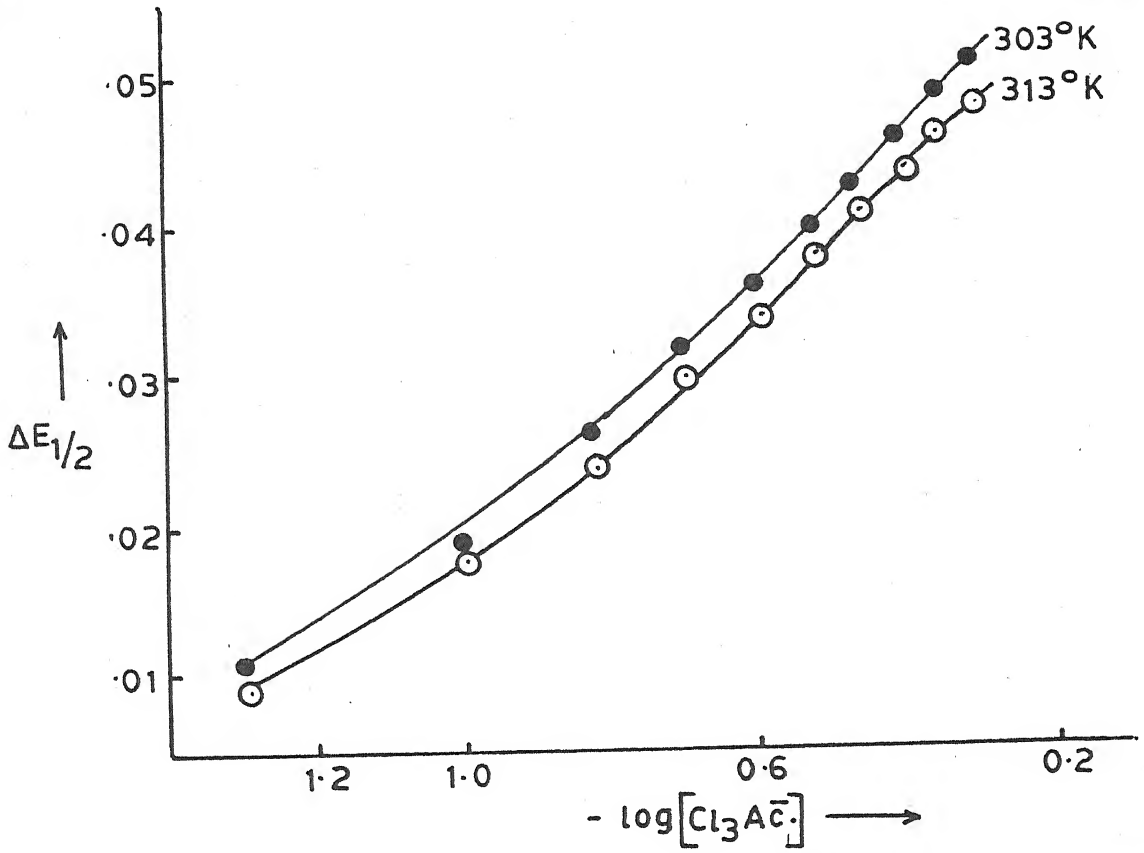

Fig. 3·19 - Plot of $\Delta E_{1/2}$ Vs. $-\log[Cl_3Ac.]$; $Cu(Cl_3Ac.)$ system.

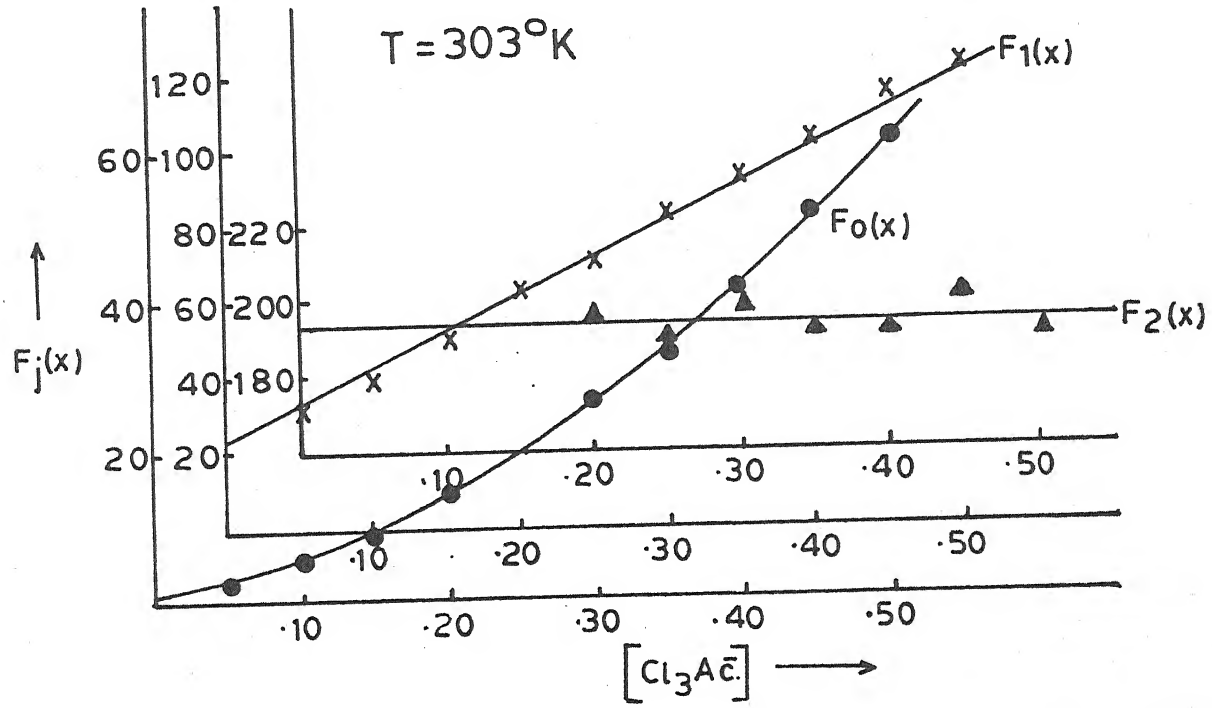

Fig. 3·20 - Plot of $F_j(x)$ Vs. $[Cl_3Ac.]$; $Cu(Cl_3Ac.)$ system.

Table 3.19

Polarographic data for copper trichloroacetate system

Concn. of Cu^{++} ions = 0.9 mM Ionic strength = 1.0 M ($NaClO_4$)

$E_{1/2}$ of Cu^{++} ions = 0.012 V vs. SCE Temperature = 303° K

Slopes of plots of $-E_{de}$ vs. $-\log. i/i_d-i$ = 30-31 mV

$[Cl_3Ac^-]$ (M)	$\Delta E_{1/2}$ (V)	$\log. I_M/I_C$	$F_0(X)$	$F_1(X)$	$F_2(X)$
0.05	0.011	0.0317	2.49	29.8	-
0.10	0.019	0.0469	4.77	37.7	-
0.15	0.026	0.0595	8.40	49.33	-
0.20	0.032	0.0692	13.60	63.0	197.5
0.25	0.036	0.0758	18.77	71.08	193.2
0.30	0.040	0.0859	26.09	83.63	200.4
0.35	0.043	0.0893	33.09	91.68	194.8
0.40	0.046	0.0893	41.65	101.62	195.3
0.45	0.049	0.0927	52.82	115.15	203.6
0.50	0.051	0.0927	61.57	121.14	195.3

$\beta_1 = 23.5$ $\beta_2 = 195$

Table 3.20

Polarographic data for copper trichloroacetate system

Concn. of Cu^{++} ions = 0.9 mM Ionic strength = 1.0 M ($NaClO_4$)

$E_{1/2}$ of Cu^{++} ions = 0.016 V vs. SCE Temperature = 313° K

Slopes of plots of $-E_{de}$ vs. $-\log. i/i_d-i$ = 30-31 mV

$[Cl_3Ac^-]$ (M)	$\Delta E_{1/2}$ (V)	$\log. I_M/I_C$	$F_0(X)$	$F_1(X)$	$F_2(X)$
0.05	0.009	0.0287	2.08	21.6	-
0.10	0.018	0.0451	4.21	32.1	151.0
0.15	0.024	0.0536	6.70	38.0	140.0
0.20	0.030	0.0652	10.74	48.7	158.5
0.25	0.034	0.0741	14.76	55.04	152.1
0.30	0.038	0.0801	20.13	63.76	155.8
0.35	0.041	0.0863	25.50	70.0	151.4
0.40	0.044	0.0894	32.09	77.72	151.8
0.45	0.046	0.0925	37.47	81.08	142.4
0.50	0.048	0.0925	43.48	84.96	135.9

$\beta_1 = 17$ $\beta_2 = 149$

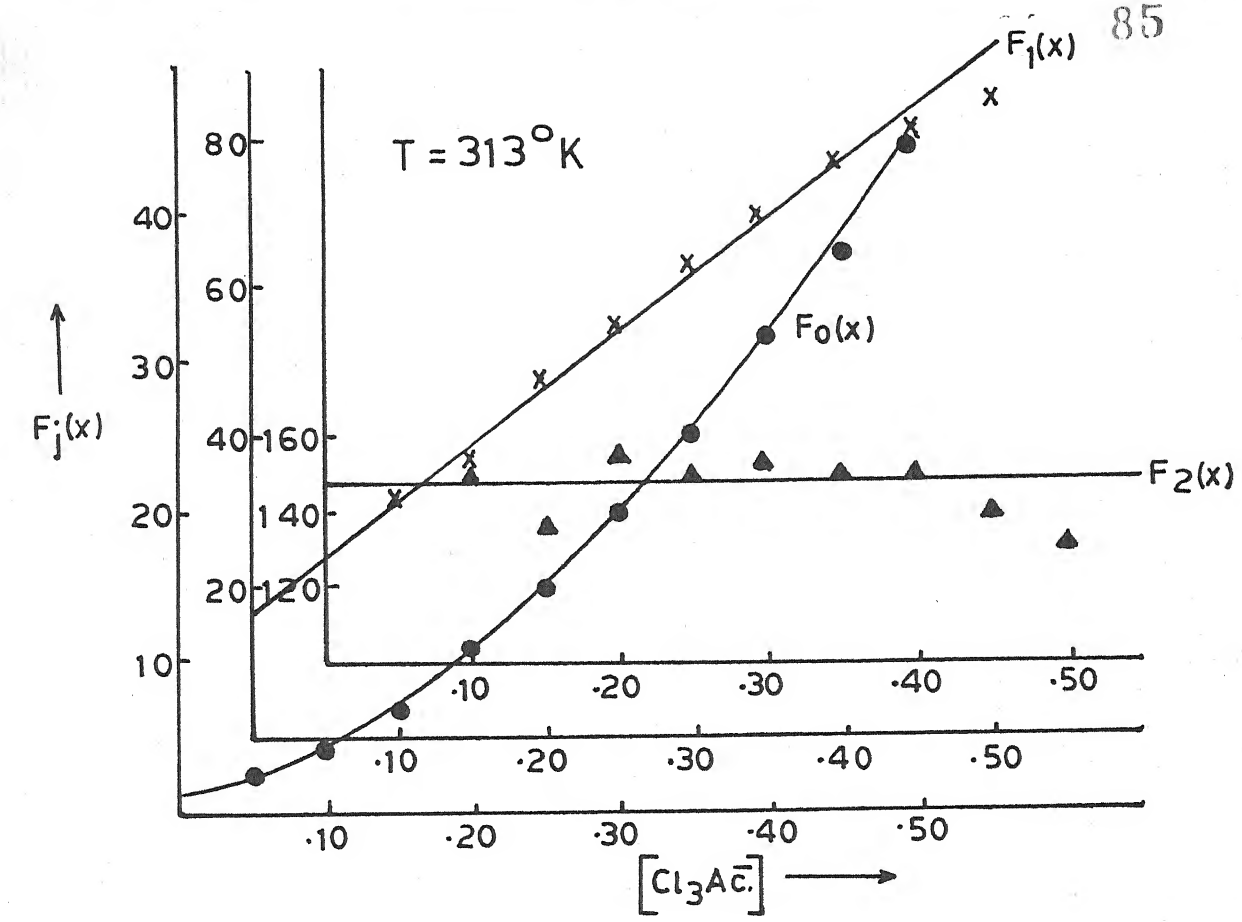

Fig. 3·21 - Plot of $F_j(x)$ Vs. $[Cl_3A\bar{c}.]$; $Cu(Cl_3A\bar{c}.)$ system.

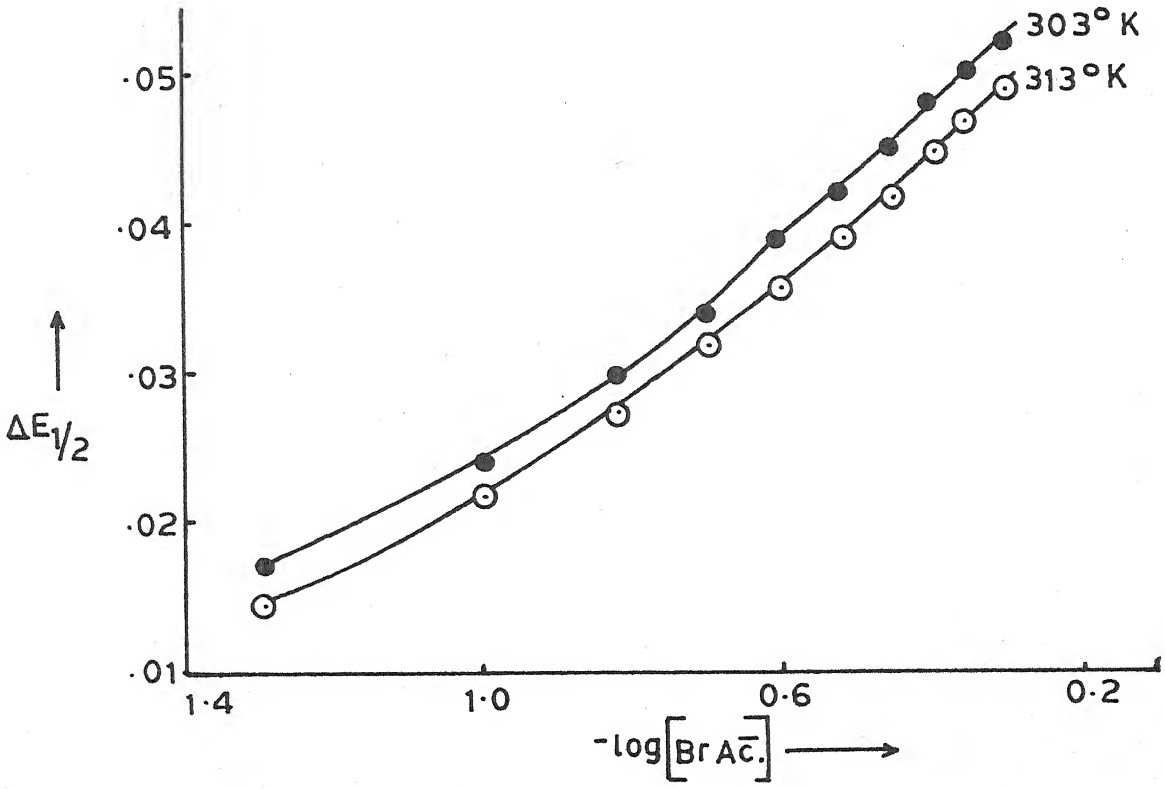

Fig. 3·22 - Plot of $\Delta E_{1/2}$ Vs. $-\log[BrA\bar{c}.]$; $Cu(BrA\bar{c}.)$ system.

It was thought worthwhile to determine the stability constants at 313° K so that thermodynamic parameters could be computed. β_1 and β_2 for the complexes $[Cu\ (Cl_3Ac.)\ ]^+$ and $[Cu\ (Cl_3Ac.)_2]$ were found to be 17 and 149 respectively for which the polarographic data and $F_j(X)$ plots have been presented in table 3.20 and figure 3.21.

Table 3.21 contains the thermodynamic parameters.

Table 3.21

Copper trichloroacetate system

Temperature (° K)	log β_1	$-\Delta G$ (kj)	$-\Delta H$ (kj)	$-\Delta S$ (kj deg^{-1})x10^3
303	1.3710	7.9542		58.0138
			25.5324	
313	1.2304	7.3741		58.0137

3.3.08 Copper monobromoacetate system :

(a) Nature of reduction : The linear plots of $-E_{de}$ vs. $-\log i/i_d-i$ had slopes of 30-31 mV. The temperature co-efficient of $E_{1/2}$ and i_d were found to be 0.3 ± 0.1 mV per degree and 0.5 ± 0.1 percent per degree respectively. The ratio of i_d and $\sqrt{h_{eff.}}$ of mercury column, in each case was constant. These results conclusively indicated that the two electron reversible reduction of Cu(II) in presence of monobromoacetate ions is entirely diffusion controlled.

(b) Effect of ligand concentration : Reduction at DME of test solutions containing increasing amounts of monobromoacetate ions, 0.9 mM Cu(II) ions, 0.002% gelatin and requisite amount of sodium perchlorate to keep ionic strength unchanged at 1.0 M yielded polarograms at 303° K with gradual cathodic shift of $E_{1/2}$ and decrease in diffusion current to indicate complex formation. The plot of $\triangle E_{1/2}$ against -log. $[BrAc^-]$ yielded a curve (Figure 3.22) so that stepwise complex formation was inferred. The application of DeFord and Hume's method lead to calculation of β_1 (42) and β_2 (168) for $[Cu(BrAc.)]^+$ and $[Cu(BrAc.)_2]$ complexes. Table 3.22 and figure 3.23 contain the relevant polarographic data and $F_j(X)$ plots.

(c) Effect of temperature : Earlier in this section, the temperature co-efficient of $E_{1/2}$ and i_d has been used to infer the reversible and diffusion controlled nature of reduction of Cu(II) monobromoacetate complexes.

The stability constants of the monobromoacetate complexes with Cu(II) were determined at another temperature i.e. 313° K and were found to be 35 and 112 for 1:1 and 1:2 metal/ligand ratio complexes. The relevant polarographic data find place in table 3.23 while the $F_j(X)$ plots are depicted in figure 3.24.

The determination of stability constants at two temperatures (303 and 313° K) was utilised to calculate $\triangle G$, $\triangle H$ and $\triangle S$ which are included in table 3.24.

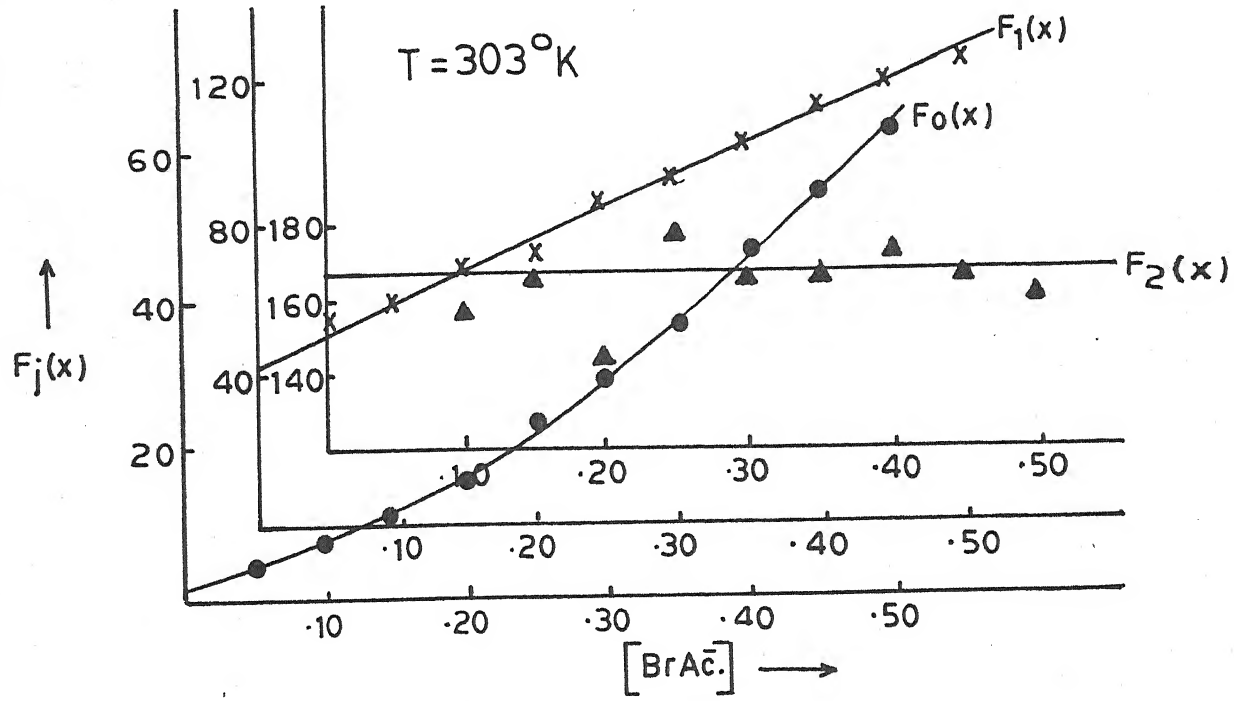

Fig. 3·23 - Plot of $F_j(x)$ Vs. $[BrA\bar{c}.]$; Cu(BrAc̄.) system.

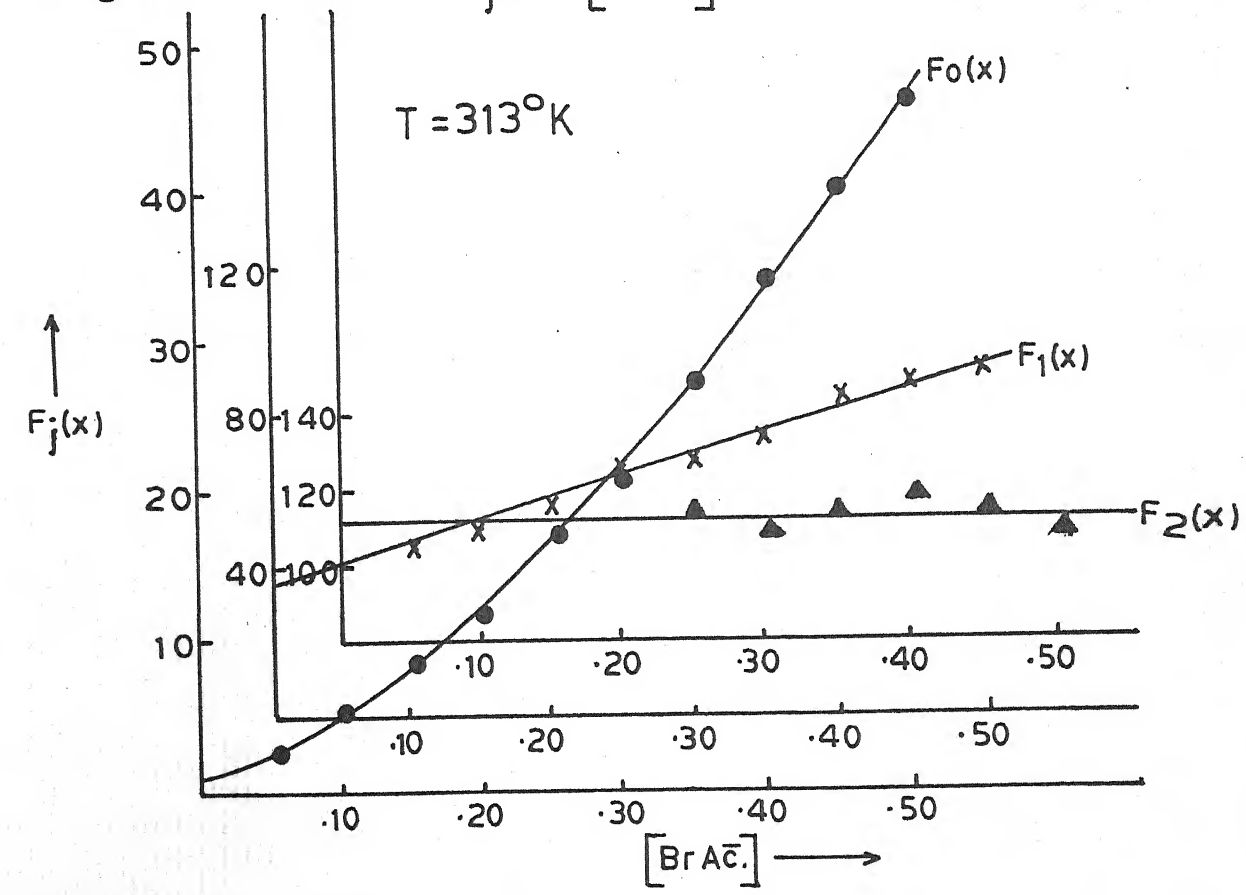

Fig. 3·24 - Plot of $F_j(x)$ Vs. $[BrA\bar{c}.]$; Cu(BrAc̄.) system.

Table 3.22

Polarographic data for copper monobromoacetate system

Concn. of Cu^{++} ions = 0.9 mM Ionic strength = 1.0 M ($NaClO_4$)
$E_{1/2}$ of Cu^{++} ions = 0.012 V vs. SCE Temperature = 303° K
Slopes of plots of $-E_{de}$ vs. -log. i/i_d-i = 30-31 mV

$[BrAc^-]$ (M)	$\Delta E_{1/2}$ (V)	log. I_M/I_C	$F_0(X)$	$F_1(X)$	$F_2(X)$
0.05	0.017	0.0210	3.86	-	-
0.10	0.024	0.0335	6.79	57.9	159.0
0.15	0.030	0.0464	11.07	66.13	167.5
0.20	0.034	0.0529	15.27	71.35	146.7
0.25	0.039	0.0596	22.75	87.0	180.0
0.30	0.042	0.0630	28.85	92.83	169.3
0.35	0.045	0.0664	36.60	101.71	170.5
0.40	0.048	0.0664	46.05	112.62	176.5
0.45	0.050	0.0698	54.10	118.0	168.8
0.50	0.052	0.0698	63.06	124.12	164.2

$\beta_1 = 42$ $\beta_2 = 168$

Table 3.23

Polarographic data for copper monobromoacetate system

Concn. of Cu^{++} ions = 0.9 mM Ionic strength = 1.0 M ($NaClO_4$)
$E_{1/2}$ of Cu^{++} ions = 0.016 V vs. SCE Temperature = 313° K
Slopes of plots of $-E_{de}$ vs. -log. i/i_d-i = 30-31 mV

$[BrAc^-]$ (M)	$\Delta E_{1/2}$ (V)	log. I_M/I_C	$F_0(X)$	$F_1(X)$	$F_2(X)$
0.05	0.014	0.0271	3.0	40.0	-
0.10	0.022	0.0385	5.58	45.8	-
0.15	0.028	0.0504	8.31	48.73	-
0.20	0.032	0.0621	12.37	56.85	-
0.25	0.036	0.0713	17.01	64.0	116.0
0.30	0.039	0.0776	21.55	68.5	111.6
0.35	0.042	0.0839	27.32	75.2	114.8
0.40	0.045	0.0871	34.38	83.45	121.1
0.45	0.047	0.0903	40.17	87.04	115.5
0.50	0.049	0.0903	46.59	91.18	112.3

$\beta_1 = 35$ $\beta_2 = 112$

Table 3.24

Copper monobromoacetate system

Temperature (° K)	log β_1	$-\Delta G$ (kj)	$-\Delta H$ (kj)	$-\Delta S$ (kj deg^{-1})x10^3
303	1.6232	9.4175		16.3858
			14.3824	
313	1.5440	9.2536		16.3859

3.3.09 Copper dibromoacetate system :

(a) Nature of reduction : The linear plots of $-E_{de}$ vs. -log. i/i_d-i had slopes of 30-31 mV. The temperature co-efficients of half wave potential and diffusion current were found to be 0.4 $\pm$ 0.1 mV and 0.5 $\pm$ 0.1 percent per degree respectively. These results conclusively proved that the two electron reversible reduction of Cu(II) in presence of dibromoacetate ions is entirely diffusion controlled.

(b) Effect of ligand concentration : Solutions, containing 0.9 mM Cu(II) ions, 0.002% gelatin, increasing amounts of dibromoacetate ions and correspondingly decreasing amounts of sodium perchlorate to keep ionic strength unchanged at 1.0 M, were polarographed at 303° K. With increasing ligand concentration, a gradual cathodic shift of $E_{1/2}$ and decrease in i_d indicated complex formation. Since the plot of $\Delta E_{1/2}$ vs. -log. $[Br_2A\bar{c}.]$ was a curve (figure 3.25) stepwise complex formation was indicated and therefore

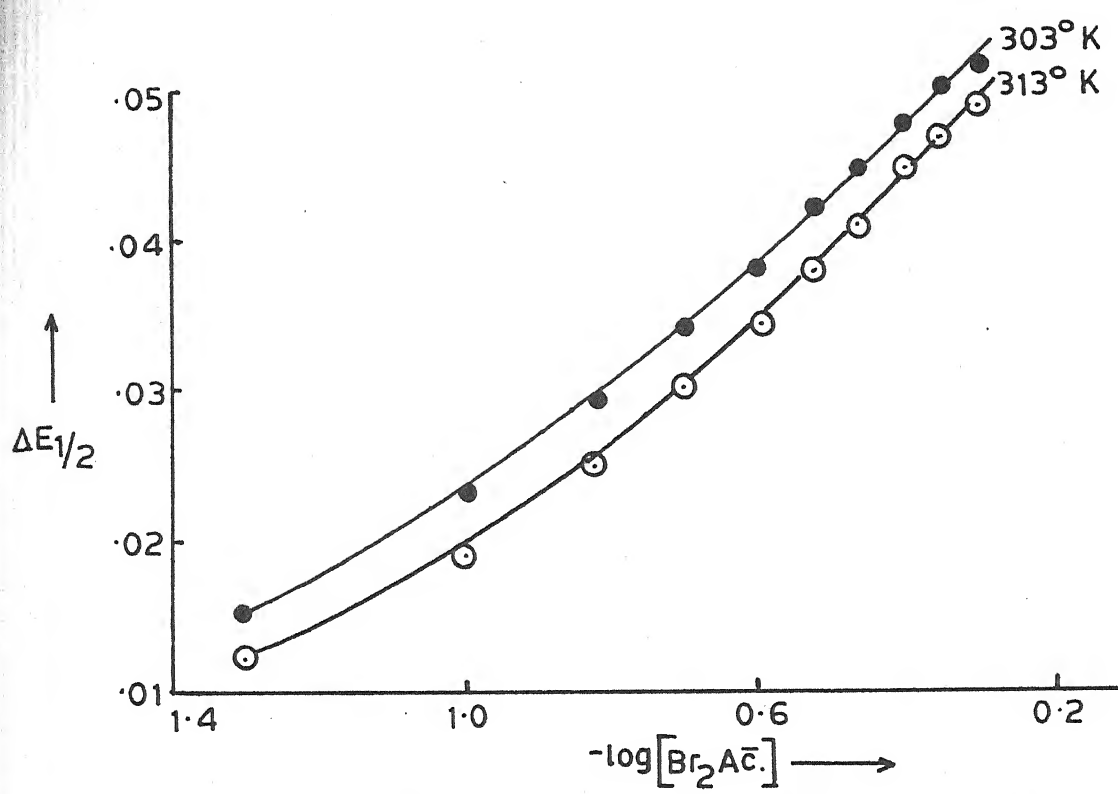

Fig. 3·25 - Plot of $\Delta E_{1/2}$ Vs. $-\log[Br_2Ac^-]$; Cu(Br_2Ac^-) system.

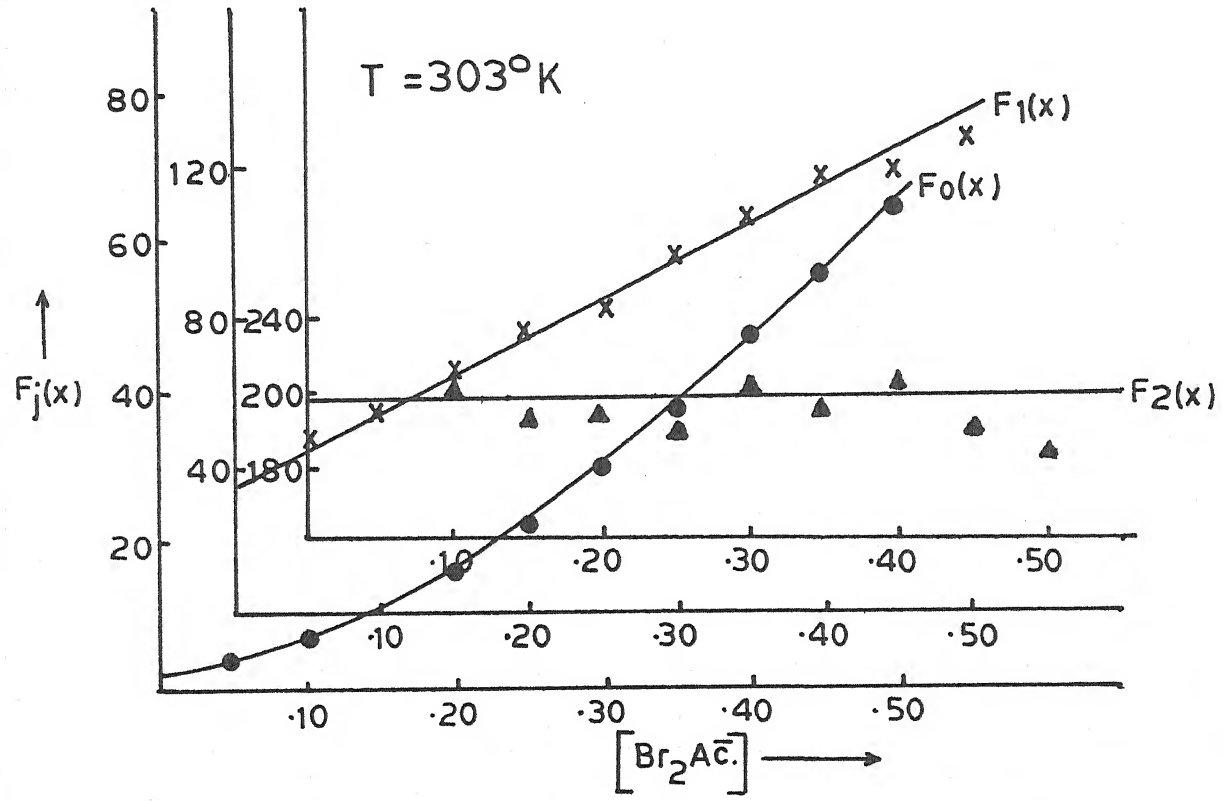

Fig. 3·26 - Plot of $F_j(x)$ Vs. $[Br_2Ac^-]$; Cu(Br_2Ac^-) system.

Table 3.25

Polarographic data for copper dibromoacetate system

Concn. of Cu^{++} ions = 0.9 mM Ionic strength = 1.0 M ($NaClO_4$)
$E_{1/2}$ of Cu^{++} ions = 0.012 V vs. SCE Temperature = 303° K
Slopes of plots of $-E_{de}$ vs. -log. i/i_d-i = 30-31 mV

$[Br_2Ac^-]$ (M)	$\Delta E_{1/2}$ (V)	log. I_M/I_C	$F_0(X)$	$F_1(X)$	$F_2(X)$
0.05	0.015	0.0303	3.38	47.6	-
0.10	0.023	0.0431	6.43	54.30	203.0
0.15	0.029	0.0529	10.41	62.73	191.5
0.20	0.034	0.0630	15.63	73.15	195.7
0.25	0.038	0.0664	21.41	81.64	190.5
0.30	0.042	0.0698	29.31	94.36	201.2
0.35	0.045	0.0733	37.18	103.37	198.2
0.40	0.048	0.0768	47.17	115.42	203.5
0.45	0.050	0.0768	54.98	119.92	191.0
0.50	0.052	0.0768	64.08	126.0	184.0

β_1 = 34 β_2 = 198

Table 3.26

Polarographic data for copper dibromoacetate system

Concn. of Cu^{++} ions = 0.9 mM Ionic strength = 1.0 M ($NaClO_4$)
$E_{1/2}$ of Cu^{++} ions = 0.016 V vs. SCE Temperature = 313° K
Slopes of plots of $-E_{de}$ vs. -log. i/i_d-i = 30-31 mV

$[Br_2Ac^-]$ (M)	$\Delta E_{1/2}$ (V)	log. I_M/I_C	$F_0(X)$	$F_1(X)$	$F_2(X)$
0.05	0.012	0.0330	2.62	32.4	-
0.10	0.019	0.0504	4.59	35.9	-
0.15	0.025	0.0625	7.37	42.46	-
0.20	0.030	0.0718	10.91	49.55	115.2
0.25	0.034	0.0781	14.89	55.56	116.2
0.30	0.038	0.0845	20.33	64.43	126.4
0.35	0.041	0.0877	25.59	70.25	125.0
0.40	0.044	0.0909	32.20	78.0	128.7
0.45	0.047	0.0942	40.22	87.0	134.4
0.50	0.049	0.0942	47.0	92.0	131.0

β_1 = 26.5 β_2 = 126

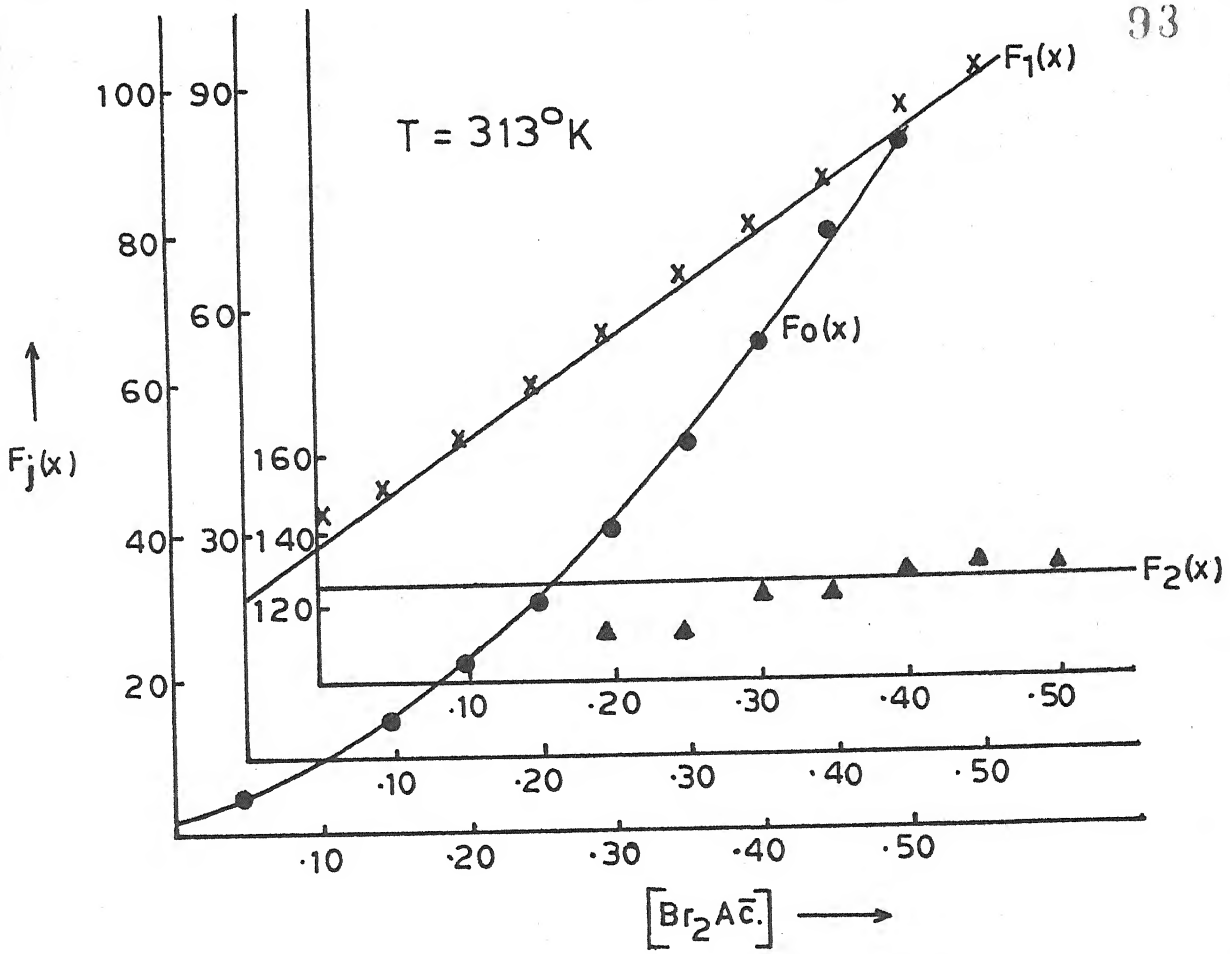

Fig. 3·27 - Plot of $F_j(x)$ Vs. $[Br_2 A\bar{c}.]$; Cu $(Br_2 A\bar{c}.)$ system.

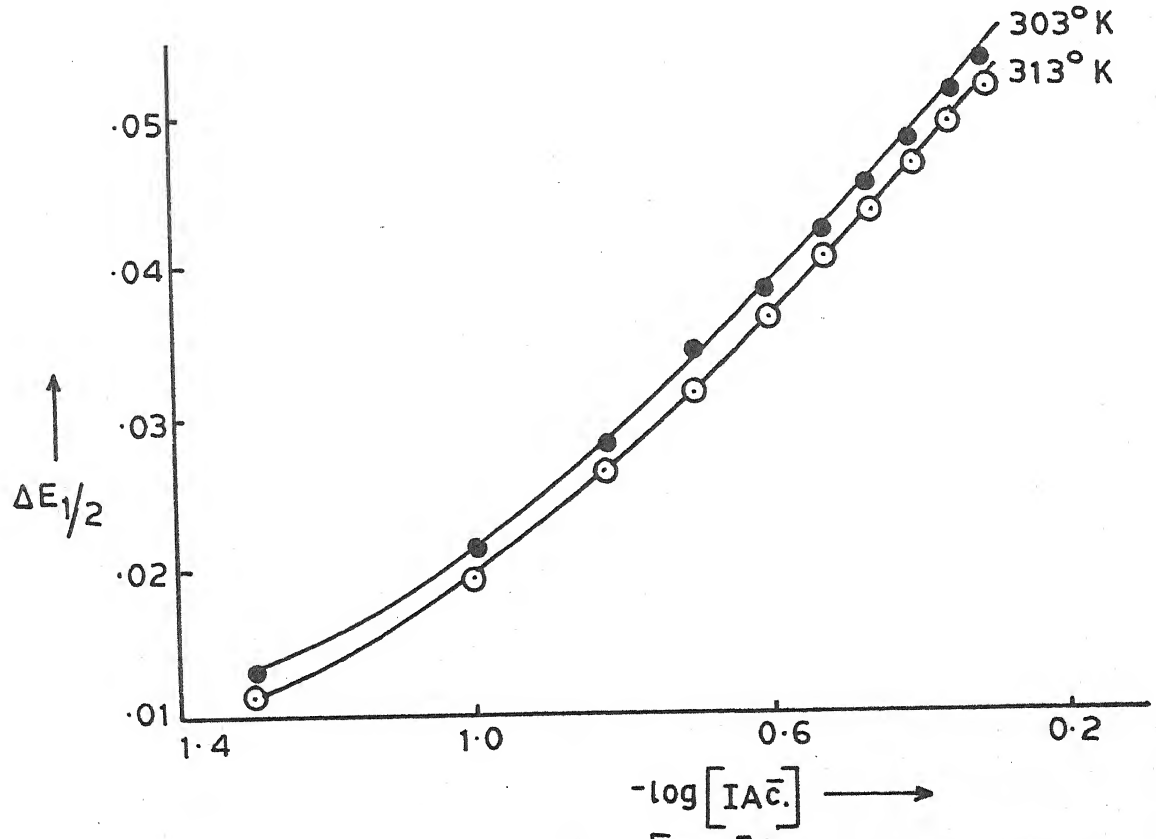

Fig. 3·28 - Plot of $\Delta E_{1/2}$ Vs. $-\log[IA\bar{c}.]$; Cu $(IA\bar{c}.)$ system.

method of DeFord and Hume was used to compute the stability constant of the complexes so formed. The overall stability constants β_1 and β_2 were found to be 34 and 198 respectively. Table 3.25 and figure 3.26 contain the polarographic data and the $F_j(X)$ function plotted against $[Br_2Ac.]$.

(c) Effect of temperature : The temperature co-efficient values of $E_{1/2}$ and i_d have been, earlie r in this section, used to establish the reversible and diffusion controlled character of the reduction of Cu dibromoacetate complexes.

In order to determine the thermodynamic parameters, the stability constants were obtained at 313° K also and were found to be 26.5 and 126 for 1:1 and 1:2 metal/ligand ratio complexes. The relevant polarographic data is available in table 3.26 while the $F_j(X)$ functions are depicted in figure 3.27.

Table 3.27 contains the thermodynamic parameters so obtained.

Table 3.27

Copper dibromoacetate system

Temperature (° K)	log β_1	$-\Delta G$ (kj)	$-\Delta H$ (kj)	$-\Delta S$ (kj deg^{-1})x10^3
303	1.5314	8.8848		35.5244
			19.6487	
313	1.4232	8.5296		35.5242

3.3.10 Copper monoiodoacetate system :

(a) Nature of reduction : The following results, taken together, conclusively prove that the reversible reduction involving two electron transfer of Cu(II) in presence of monoiodoacetate ions is entirely diffusion controlled.

(i) The linear plots of $-E_{de}$ vs. -log. i/i_d-i with slopes of 30-31 mV.

(ii) Temperature co-efficients of $E_{1/2}$ (0.2 $\pm$ 0.1 mV per degree) and i_d (0.5 $\pm$ 0.1 percent per degree).

(iii) Linearity of plots of i_d vs. $\sqrt{h_{eff.}}$.

(b) Effect of ligand concentration : Test solutions consisting of 0.9 mM Cu(II) ions, 0.002% gelatin, increasing amounts of monoiodoacetate ions and correspondingly decreasing amounts of sodium perchlorate to maintain ionic strength were polarographed at 303° K. Complex formation was indicated by a cathodic shift in $E_{1/2}$ and decrease in diffusion current with increase in $[IAc^-]$ concentration. Since the plot of $\Delta E_{1/2}$ vs. -log.$[IAc^-]$ was a curve (figure 3.28), the method of DeFord and Hume was employed to determine the stability constants of the stepwise complexes so formed. The overall stability constant values were found to be 26.5 and 231 for 1:1 and 1:2 metal/ligand ratio complexes. The polarographic data has been presented in table 3.28 and $F_j(X)$ functions depicted in figure 3.29.

(c) Effect of temperature : Earlier in this section, the reversibility and diffusion controlled character of reduction of Cu(II) in monoiodoacetate ions has been established from the temperature co-efficient values of half wave potential and

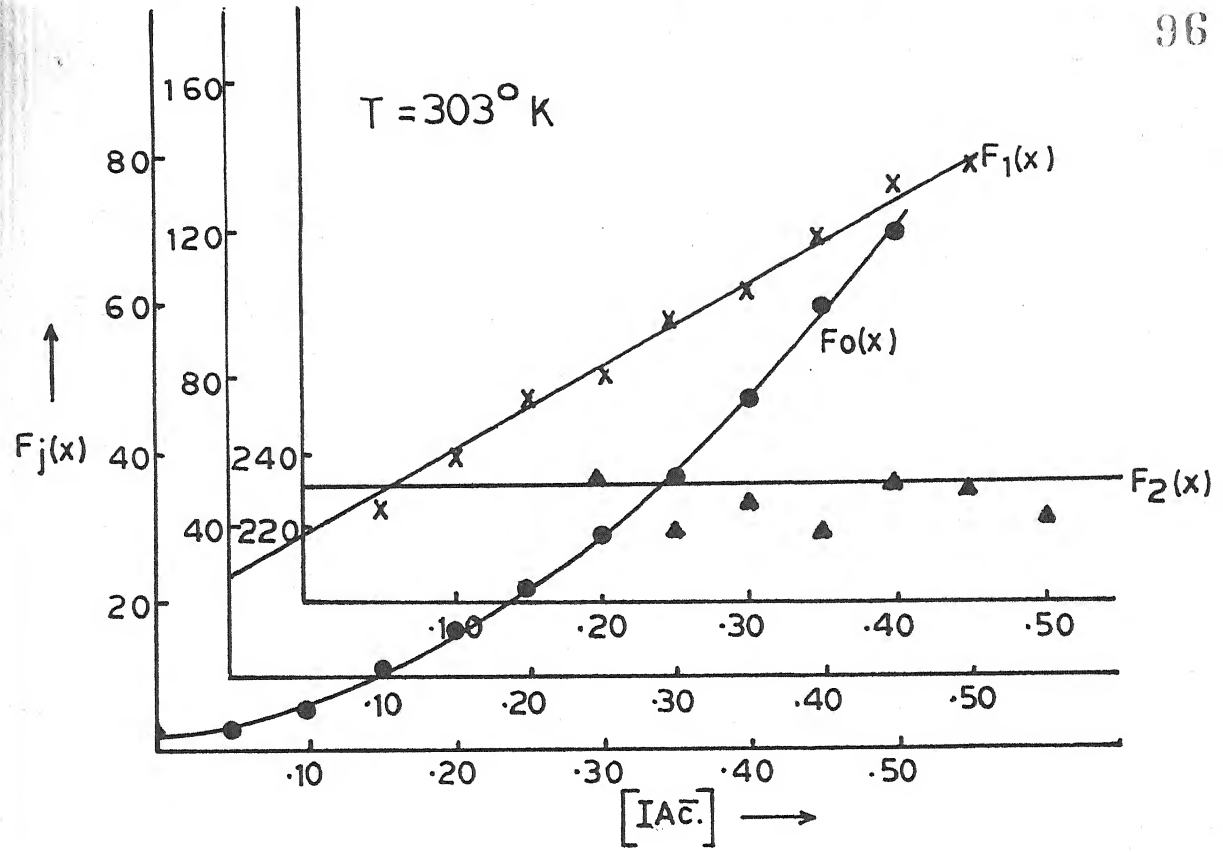

Fig. 3·29 - Plot of $F_j(x)$ Vs. $[IA\bar{c}.]$; Cu(IAc̄.) system.

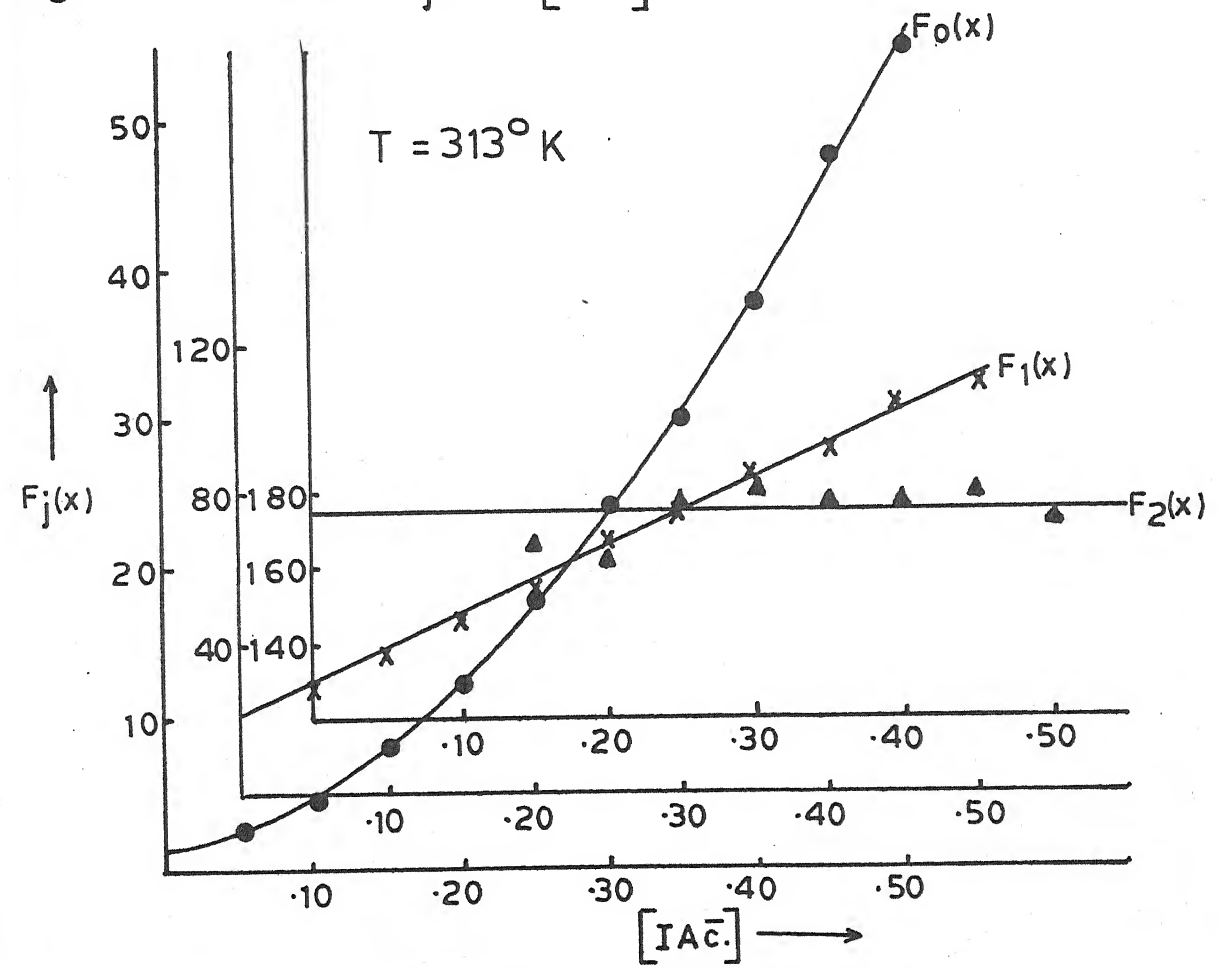

Fig. 3·30 - Plot of $F_j(x)$ Vs. $[IA\bar{c}.]$; Cu(IAc̄.) system.

Table 3.28

Polarographic data for copper monoiodoacetate system

Concn. of Cu^{++} = 0.9 mM Ionic strength = 1.0 M ($NaClO_4$)

$E_{1/2}$ of Cu^{++} ions = 0.012 V vs. SCE Temperature = 303° K

Slopes of plots of $-E_{de}$ vs. -log. i/i_d-i = 30-31 mV

$[IAc^-]$ (M)	$\Delta E_{1/2}$ (V)	log. I_M/I_C	$F_0(X)$	$F_1(X)$	$F_2(X)$
0.05	0.013	0.0345	2.93	38.6	-
0.10	0.021	0.0497	5.60	46.0	-
0.15	0.028	0.0591	9.78	58.53	-
0.20	0.034	0.0655	15.42	73.6	235.5
0.25	0.038	0.0687	21.52	82.08	222.3
0.30	0.042	0.0720	29.46	94.86	227.8
0.35	0.045	0.0753	37.35	103.85	221.0
0.40	0.048	0.0786	47.36	115.9	233.5
0.45	0.051	0.0819	60.06	131.24	232.7
0.50	0.053	0.0819	70.0	138.0	223.0

$\beta_1 = 26.5$ $\beta_2 = 231$

Table 3.29

Polarographic data for copper monoiodoacetate system

Concn. of Cu^{++} ions = 0.9 mM Ionic strength = 1.0 M ($NaClO_4$)

$E_{1/2}$ of Cu^{++} ions = 0.016 V vs. SCE Temperature = 313° K

Slopes of plots of $-E_{de}$ vs. -log. i/i_d-i = 30-31 mV

$[IAc^-]$ (M)	$\Delta E_{1/2}$ (V)	log. I_M/I_C	$F_0(X)$	$F_1(X)$	$F_2(X)$
0.05	0.011	0.0368	2.46	29.2	-
0.10	0.019	0.0536	4.62	36.2	-
0.15	0.026	0.0623	7.93	46.2	168.0
0.20	0.031	0.0741	11.81	54.05	165.2
0.25	0.036	0.0832	17.48	65.92	179.6
0.30	0.040	0.0894	23.85	76.16	183.9
0.35	0.043	0.0956	30.23	83.51	178.6
0.40	0.046	0.0988	38.03	92.5	178.7
0.45	0.049	0.0988	47.51	103.35	183.0
0.50	0.051	0.1019	55.51	109.02	176.0

$\beta_1 = 21$ $\beta_2 = 176$

diffusion current.

The stability constants of the copper monoiodoacetate complexes were also obtained at 313° K. The β_1 and β_2 values so determined are 21 and 176 respectively. The relevant polarographic data and the $F_j(X)$ plots appear in table 3.29 and figure 3.30.

From the knowledge of stability constants at two temperatures, the thermodynamic parameters were computed and are presented in table 3.30.

Table 3.30

Copper monoiodoacetate system

Temperature (° K)	log β_1	$-\Delta G$ (kj)	$-\Delta H$ (kj)	$-\Delta S$ (kj deg^{-1})x10^3
303	1.4232	8.2571		33.2808
			18.3412	
313	1.3222	7.9243		33.2808

3.4 DISCUSSION :

In this chapter the complex forming tendency of Cu(II) with acetate and various halogen substituted acetate ions has been reported.

The study of subject of formation constant of metal complexes presents a field which is large and varied. There are a number of variables associated with the central metal, the ligand, the composition of the solvent and temperature which

complicate the investigations and comparison of results. But if, as many variables as possible are kept constant i.e. only the minimum requisite variations essential for the study are made, it becomes possible to compare and contrast the results in a reasonable and logical manner. It is with these considerations in mind that it has been attempted to study the complexes of various haloacetate ions with Cu(II) under as identical conditions as possible.

Our investigations were however, restricted by the ready hydrolysis of tribromo-, diiodo- and triiodoacetic acids when their sodium salts are prepared. Their tendency to hydrolyse is attributable to the comparatively smaller energy of the carbon-halogen bond and greater intramolecular repulsions (due to larger size of halogens) between the halogen atoms of the haloacetate ion which becomes unstable and hydrolyses to form more stable products. The following data[15] would clarify the situation.

Bond	Bond length (A^{o})	Bond energy (kj)
C-F	1.42	447.7
C-Cl	1.77	326.4
C-Br	1.91	284.5
C-I	2.13	213.4

The non-formation of complexes with metal/ligand ratio greater than 1:2 may attributed to the smaller range (0.00-0.5 M) of ligand concentration taken in our investigations.

A comparative view of stabilities of the various complexes, under investigation, is quite revealing.

System	At 303° K		At 313° K	
	β_1	β_2	β_1	β_2
Cu acetate	80	198	58.5	144
Cu monofluoroacetate	58.5	142	46	96
Cu difluoroacetate	28	194	21.5	131
Cu trifluoroacetate	17.5	250	15	168
Cu monochloroacetate	51.5	306	37	240
Cu dichloroacetate	30	102	24	74
Cu trichloroacetate	23.5	195	17	149
Cu monobromoacetate	42	168	35	112
Cu dibromoacetate	34	198	26.5	126
Cu monoiodoacetate	26.5	231	21	176

A bird's eyeview of the stability constants shows that for each system at a given temperature, K_1 or β_1 is invariably greater that of K_2 or β_2/β_1. There are several reasons for decrease in K_2 as compared to K_1. (a) Statistical factors; (b) increased steric hinderance as the number of ligands increases as they are bulkier than the H_2O molecules they replace; (c) coulombic factors since the ligands are charged.

The statistical factors may be treated in the following way. Suppose, as is almost certainly the case for

Cu(II), the co-ordination number is four. Initially, in the free metal ion $Cu(H_2O)_4^{2+}$, there are four sites for the ligand (L^-) to get attached to, to form $Cu(H_2O)_3L^+$. Now when the second ligand is to enter the co-ordination sphere, there are lesser sites i.e. only three to which it can attach itself. Hence the probability of its getting attached to the metal is lesser than in the case when the first ligand got attached. Thus, the probability of formation of 1:2 complex is less than that for 1:1 complex. As regards the steric hindrance, once $Cu(H_2O)L^+$ has been formed, the second ligand has lesser space available to accomodate itself around the metal ion as each of our ligands is bulkier than replaceable H_2O molecules. Coulombic forces also come into play when the ligands are charged. When the first ligand enters the co-ordination sphere, its uninegative charge experiences attraction from bipositive $Cu(H_2O)_4^{2+}$ ion. However, the second identical ligand is attracted by unipositive $Cu(H_2O)_3L^+$ complex ion. Thus for the second ligand, the attraction to attach to the metal ion is lesser. These three factors combine together to explain why K_1 (which is also called formation constant) is greater than K_2 in all the systems under investigation.

Another important trend emerges from the comparative observation of formation constant data. The formation constant (K_1 or β_1) values for monosubstituted acetate complexes are less than those of non-substituted acetate ion complexes, these for disubstituted acetate ion complexes less than monosubstituted

acetate ion complexes and those of trisubstituted acetate ion complexes are still less than disubstituted acetate ion complexes. This trend holds good for each of the three halogens separately. Thus K_1 values follow the order

$$[Cu(Ac.)]^{+} > [Cu(XAc.)]^{+} > [Cu(X_2Ac.)]^{+} > [Cu(X_3Ac.)]^{+}$$

Where X stands for a halogen.

Two factors appear to be mainly responsible for this trend and are discussed below :

The substitution of a hydrogen atom with halogen in acetic acid changes their complex forming power which depends on the introduced halogen and the number of substituents. The acetate ion of acetic acid has limited co-ordinating power which is further weakend by substitution of halogens as shown below :

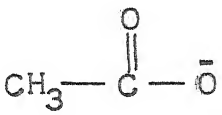

acetate ion

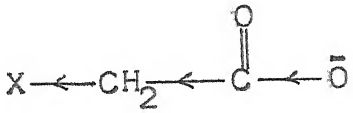

monohaloacetate ion

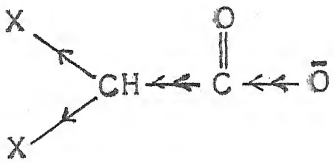

dihaloacetate ion

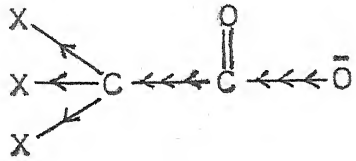

trihaloacetate ion

Due to the high electronegativity of halogen, electron withdrawal as shown above occurs to reduce the basicity of substituted ion as compared to the unsubstituted ion. Consequently the trisubstituted acetate ion is the weakest base while the non-substituted acetate ion is the strongest base. This explains the order of K_1 values referred to earlier. Another factor which contributes towards this trend is the steric hindrance created by successively bulkier mono-, di- and trisubstituted haloacetate ions. Thus for a given halogen, the stability decreases in the order non-, mono-, di- and trihalosubstituted acetate ion complexes with Cu(II). For example, Cu-acetate with a formation constant K_1 of 80 is the strongest while Cu trifluoroacetate with K_1 = 17.5 is the weakest complex for fluorine substituted acetate ions at 303° K.

Another notable trend is discernible in equally halo-substituted acetate complexes with different halogens. Thus the stability constants have the order

(a) $[Cu(FAc.)]^+ > [Cu(ClAc.)]^+ > [Cu(BrAc.)]^+ > [Cu(IAc.)]^+$

(b) $[Cu(F_2Ac.)]^+ < [Cu(Cl_2Ac.)]^+ < [Cu(Br_2Ac.)]^+$

(c) $[Cu(F_3Ac.)]^+ < [Cu(Cl_3Ac.)]^+$

In the trend (a) for monohalosubstituted acetate complexes with Cu(II), the fluorine substituted acetate complex has the maximum stability as it is able to experience minimum

steric hindrance due to its smaller size because fluorine is smallest among the halogens. Iodine being the largest (IAc^-) exerts the maximum steric hindrance. It appears that in monosubstituted haloacetate complexes, the pull of electrons by most electronegative fluorine is more than counterbalanced by the bulk of the ligand to give the above trend.

But in the case of di-, and trisubstituted acetate complexes with Cu(II), the above trend is reversed. This may be explained as follows :

When one halogen replaces a hydrogen atom in acetate ion there is considerable increase in size of the ligand which appears to overweigh the effect due electron withdrawl (maximum for F and minimum for I) by the substituted halogen. Hence the trend (a). But when the second halogen replaces another hydrogen from monohaloacetate ion, there is relatively lower increase in size of the ligand as the (XAc^-) was already bulkier. There are now, however, two halogen atoms to exert electron withdrawl with a consequent decrease in basicity of the (X_2Ac^-) ions. The effect would be more so when three halogen atoms have replaced there hydrogen atoms. In other words, the reduction in basicity by replaced halogen atoms overwhelms the effect due to more bulkier ligands due to increase in size of the substituted halogen Viewed from this angle, the trends (b) and (c) stand explained as electronegativity decreases in the order $F < Cl < Br < I$.

In short the trend (a) is dictated by the size of the ligand while the trends (b) and (c) are determined by the

electronegativity of the substituted halogen which reduces the basic character and hence the co-ordinating ability of the substituted acetate ion.

It has also been observed that the stability constants in each system are lower at the higher temperature. This is due to greater dissociation of the complex at the elevated temperature. It may, however, be noted that the ΔS values for a complex at both the temperatures is almost the same. This is easily explained. Since our ligand in all the systems is a monodentate one, its dissociation does not lead to decrease or increase in number of particles as per the equation

$$\left[Cu(H_2O)_3(XAc.)\right]^{+} + H_2O \rightleftharpoons \left[Cu(H_2O)_4\right]^{++} + (XAc.)^{-}$$

As the number of particles in a system determine its disorder or entropy, there is virtually no difference in ΔS values of a complex at the two temperatures.

We also observe a positive shift in ΔG value of a complex at higher temperature. There is understandable as at higher temperatures, the system becomes less stable resulting in enhancement of its free energy. In general, more stable is a system, lesser is the free energy.

In each system we find that we have obtained a negative value of ΔH i.e. enthalpy. This simply means that the heat content of the system has decreased due to complex formation. This is obviously so because the weaker metal to O (of water molecules) bonds have been replaced by comparatively stronger metal to ligand bonds.

LITERATURE CITED

1. N. Tanaka, Y. Saito and H. Ogino, Bull. Chem. Soc. Jap., 38, 984 (1965).
2. R.S. Kolat and J.E. Powell, Inorg. Chem., 1, 293 (1962).
3. A. Swinarski and J. Wajezakove, Z. Phys. Chem., 223, 345 (1963).
4. D.W. Archer and C.B. Monk, J. Chem. Soc., 3117 (1964).
5. S. Aditga, J. Inorg. Nucl. Chem., 29, 1901 (1967).
6. H. Erlenmeyer, Griesser. B. Prijis and H. Sigel, Helo Chim. Acta., 51, 339 (1968).
7. John Eva, J. Inorg. Nucl. Chem., 43, 325 (1981).
8. R.S. Vidya and S.N. Banerji, Ind. J. Chem., 11, 1201 (1973).
9. S.A. Carrano, K.A. Chen and R.F.O. Malley, Inorg. Chem., 3, 1047 (1964).
10. Milan Melnik, Co-ord. Chem. Rev., 36, 1 (1981).
11. M.M. Emara and N.A. Farid, Egypt J. Chem., 22, 77 (1980).
12. John Eva, Pol. J. Chem., 57, 1119 (1983).
13. D.D. DeFord and D.N. Hume, J. Am. Chem. Soc., 73, 5321 (1951).
14. H. Irving, 'Advances in polarography', Pergamon Press, Oxford, 49 (1960).
15. I.L. Finar, 'Organic Chemistry', Vol. 1, ELBS/Longman, 36-37 (1985).

CHAPTER IV

Pb(II) Complexes with

(a) acetate ion

(b) mono-, di- and trifluoroacetate ions

(c) mono-, di- and trichloroacetate ions

(d) mono- and dibromoacetate ions

(e) monoiodoacetate ion

4.1 INTRODUCTION :

Like Cu(II), Pb(II) has also been found to form fairly stable complexes though less stable than the former in accord with the Mellor and Maley[1] order. Acetate ion is known to form not very stable complexes with Pb(II) as found out by a number of investigators. Thus, Kolat and Powell[2], Archer and Monk[3] and Bannerjea and Singh[4] have studied the lead acetate complexes at the glass electrode and reported the formation of upto 1:2 complex in aqueous medium. Proll and Sutchiffe[5] have studied the complex spectrophotometrically in acetic acid medium.

Halosubstituted acetate ions are expected to be weaker bases than simple acetate ion due to electron withdrawal by more electronegative (than hydrogen) halogens. They form weaker complexes with Pb(II) as found out by a number of researchers. Carrano and coworkers[6] have made polarographic studies of Pb trifluoroacetate system and reported the formation of two successive complexes. The monochloro-, monobromo- and monoiodo acetate complexes of Pb(II) have been explored potentiometrically by Ewa et.al.[7] Klemeneic and Filipowic[8] have investigated the reduction of lead acetate and lead chloroacetate systems at DME and determined the stability constants of the complexes so formed.

The above literature survey reveals that the complexes of Pb(II) with halogen substituted acetate ions have only been studied in parts and meagre data is available on di- and

trisubstituted haloacetate ions with the metal ion. Hence it was thought worthwhile to carry out a systematic study of various fluoro-, chloro-, bromo- and iodo substituted acetate ion complexes with Pb(II) polarographically and determine their formation constants under identical conditions at two different temperatures so that the results are strictly comparable and thermodynamic parameters can be evaluated.

4.2 EXPERIMENTAL :

All chemicals of analy-tical reagent grade purity were used. K & K (USA), Fluka (Swiss), BDH (UK) and Riedel (German) brand halogen substituted acetic acids were used. Their sodium salts were prepared by adding dilute solution of sodium bicarbonate. Care had to taken in handling haloacetic acids as they cause serious burns and blisters on the skin. A semi-micro burette was used to add requisite amounts of their salt solutions to the test solutions.

All solutions were made in conductivity water. Sodium perchlorate at 1.0 M was the supporting electrolyte used. Its concentration was correspondingly reduced with increasing concentration of the ligand to keep ionic strength constant. In each case, the concentration of Pb(II) ions was kept constant at 0.9 mM. 0.002% gelatin in final solutions just sufficed to suppress the maxima observed.

The reduction at DME of each test solution was carried out by placing it in a thermostated H-cell coupled with a saturated calomel electrode. Prior to the polarographic

examination of each test solution, hydrogen gas was passed for atleast ten minutes to remove dissolved oxygen. The potential of the DME was gradually increased and the change in current noted.

The intercepts on the potential axis in the plots of $-E_{de}$ vs. -log. i/i_d-i gave the half wave potential.

The capillary had the following characteristics in 0.1 M sodium perchlorate in the open circuit.

m = 2.43 mg/sec

t = 2.9 sec

$h_{corr.}$ = 53 cms.

The study of the effect of ligand concentration on $E_{1/2}$ and diffusion current was carried out at two temperatures i.e. 30° C and 40° C.

4.3 RESULTS :

4.3.01 Lead acetate system :

(a) Nature of reduction : Polarography of Pb(II) in presence of acetate ions reveals that its reduction proceeds via two electron transfer and is reversible as borne out by the slopes of linear plots of $-E_{de}$ vs. -log. i/i_d-i in the range of 31 ± 1 mV and temperature co-efficient (0.2 mV per degree) of half wave potential.

The diffusion controlled nature of the reduction was inferred from the temperature co-efficient (0.5 ± 0.1 percent per degree) of the diffusion current and linearity of plots of diffusion current against square root of effective height of

mercury column of the DME.

(b) Effect of ligand concentration : Polarographic examination at 303° K of solutions containing 0.9 mM Pb(II) ions, 0.002% gelatin, increasing amounts of acetate ions and correspondingly decreasing concentration of sodium perchlorate to keep ionic strength constant at 1.0 M, revealed that complex formation occurs as there is a gradual cathodic shift in $E_{1/2}$ and a decrease in i_d. Plot of $\Delta E_{1/2}$ vs. -log. $[Ac^-]$ (figure 4.01) is a curve indicating multiple complex formation. Hence the method of DeFord and Hume[9] as improved by Irving[10] was applied to determine the stability of complexes so formed. The formation constants were found to be 77 and 172 for the 1:1 and 1:2 metal/ligand ratio complexes. Polarographic data is included in table 4.01 while the $F_j(X)$ functions are depicted in figure 4.02.

(c) Effect of temperature : Earlier in this section the temperature co-efficients of $E_{1/2}$ and i_d have aided the inference that the reduction of Pb acetate complex is reversible and diffusion controlled.

In order to compute thermodynamic functions ΔG, ΔH, and ΔS, the formation constants were determined at 313° K too and were found to be 60 (β_1) and 142 (β_2). The relevant polarographic data appears in table 4.02 and the $F_j(X)$ plots in figure 4.03.

The thermodynamic functions obtained find place in table 4.03.

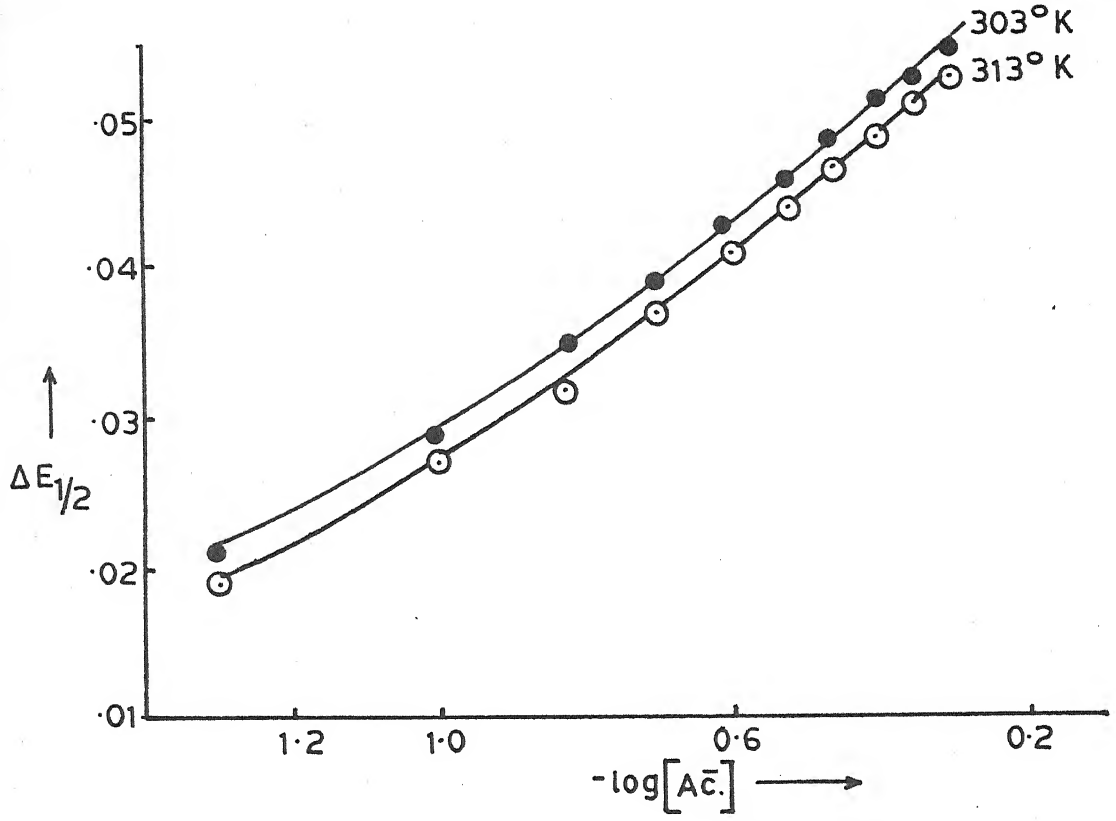

Fig. 4·01 - Plot of $\Delta E_{1/2}$ Vs. $-\log[A\bar{c}.]$; Pb(Ac̄.) system.

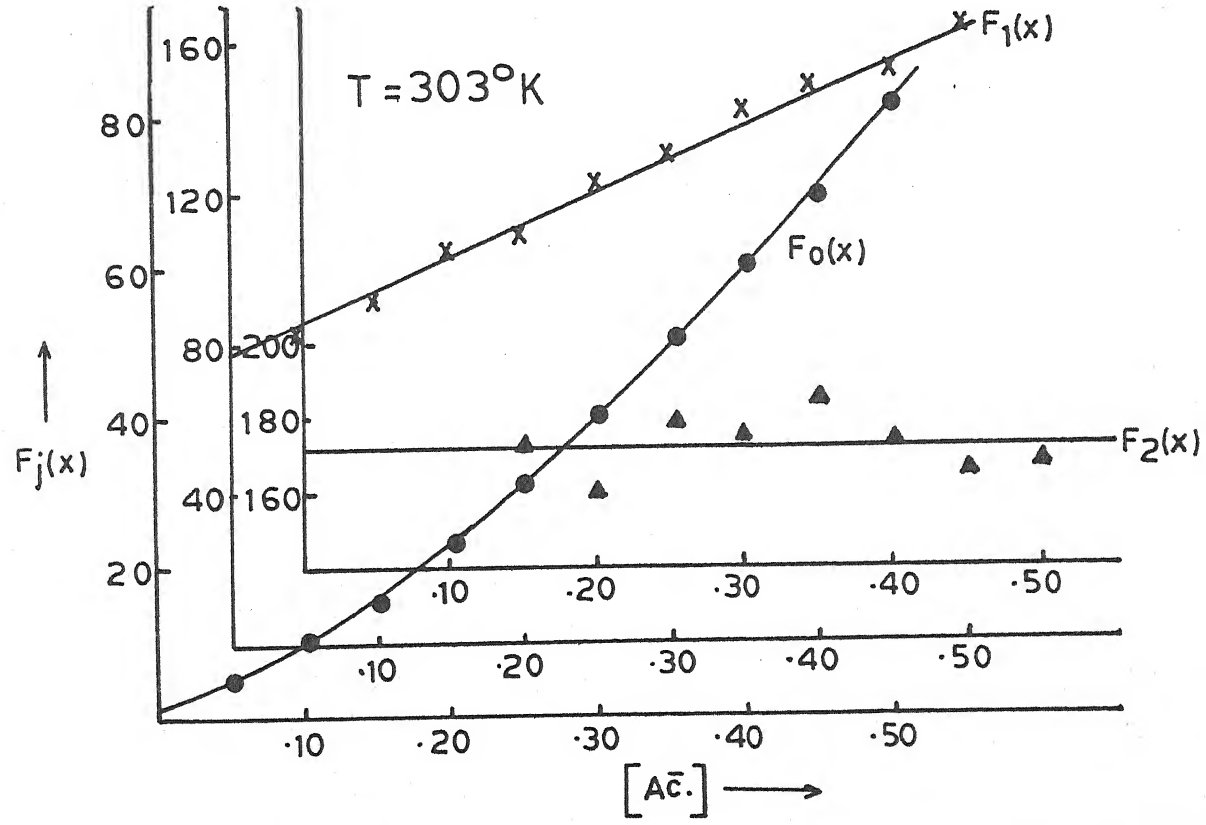

Fig. 4·02 - Plot of $F_j(x)$ Vs. $[A\bar{c}.]$; Pb(Ac̄.) system.

Table 4.01

Polarographic data for Lead acetate system

Concn. of Pb^{++} ions = 0.9 mM Ionic strength = 1.0 M ($NaClO_4$)

$E_{1/2}$ of Pb^{++} ions = -0.401 V vs. SCE Temperature = 303° K

Slopes of plots of $-E_{de}$ vs. -log. i/i_d-i = 30-32 mV

$[\bar{Ac}.]$ (M)	$\Delta E_{1/2}$ (V)	log. I_M/I_C	$F_0(X)$	$F_1(X)$	$F_2(X)$
0.05	0.021	0.0234	5.27	85.4	-
0.10	0.029	0.0388	10.08	90.8	-
0.15	0.035	0.0515	16.43	102.86	172.4
0.20	0.039	0.0612	22.84	109.2	161.0
0.25	0.043	0.0679	31.50	122.0	180.0
0.30	0.046	0.0712	39.95	129.83	176.1
0.35	0.049	0.0746	50.66	141.88	185.3
0.40	0.051	0.0780	59.52	146.3	173.2
0.45	0.053	0.0814	69.27	151.71	166.0
0.50	0.055	0.0814	81.50	161.0	168.0

$\beta_1 = 77$ $\beta_2 = 72$

Table 4.02

Polarographic data for Lead acetate system

Concn. of Pb^{++} ions = 0.9 mM Ionic strength = 1.0 M ($NaClO_4$)

$E_{1/2}$ of Pb^{++} ions = -0.397 V vs. SCE Temperature = 313° K

Slopes of plots of $-E_{de}$ vs. -log. i/i_d-i = 30-32 mV

$[\bar{Ac}.]$ (M)	$\Delta E_{1/2}$ (V)	log. I_M/I_C	$F_0(X)$	$F_1(X)$	$F_2(X)$
0.05	0.019	0.0403	4.49	69.8	-
0.10	0.027	0.0547	8.39	73.9	-
0.15	0.032	0.0665	12.50	76.66	-
0.20	0.037	0.0755	18.49	87.45	135.2
0.25	0.041	0.0817	25.24	96.96	147.8
0.30	0.044	0.0880	31.98	103.26	144.2
0.35	0.047	0.0943	40.54	112.97	151.3
0.40	0.049	0.0975	47.37	115.92	139.8
0.45	0.051	0.0975	54.95	119.88	133.0
0.50	0.053	0.1007	64.21	126.42	132.8

$\beta_1 = 60$ $\beta_2 = 142$

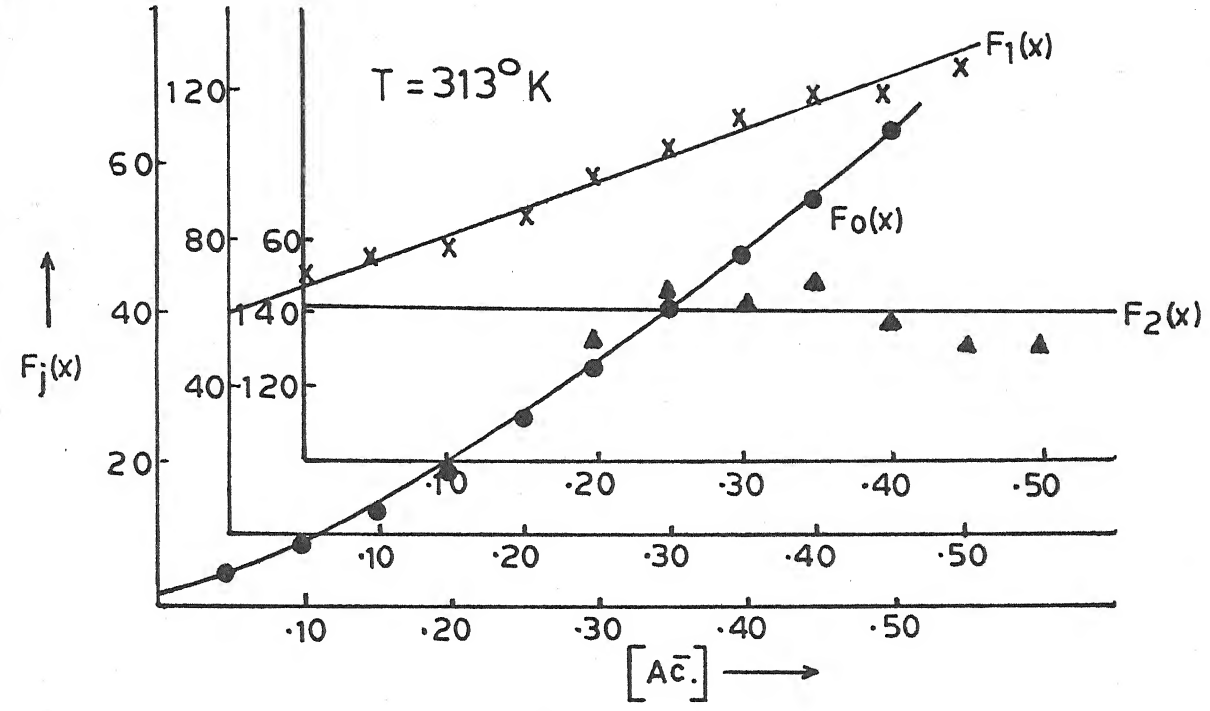

Fig. 4·03 - Plot of $F_j(x)$ Vs. $[A\bar{c}.]$; Pb ($A\bar{c}.$) system.

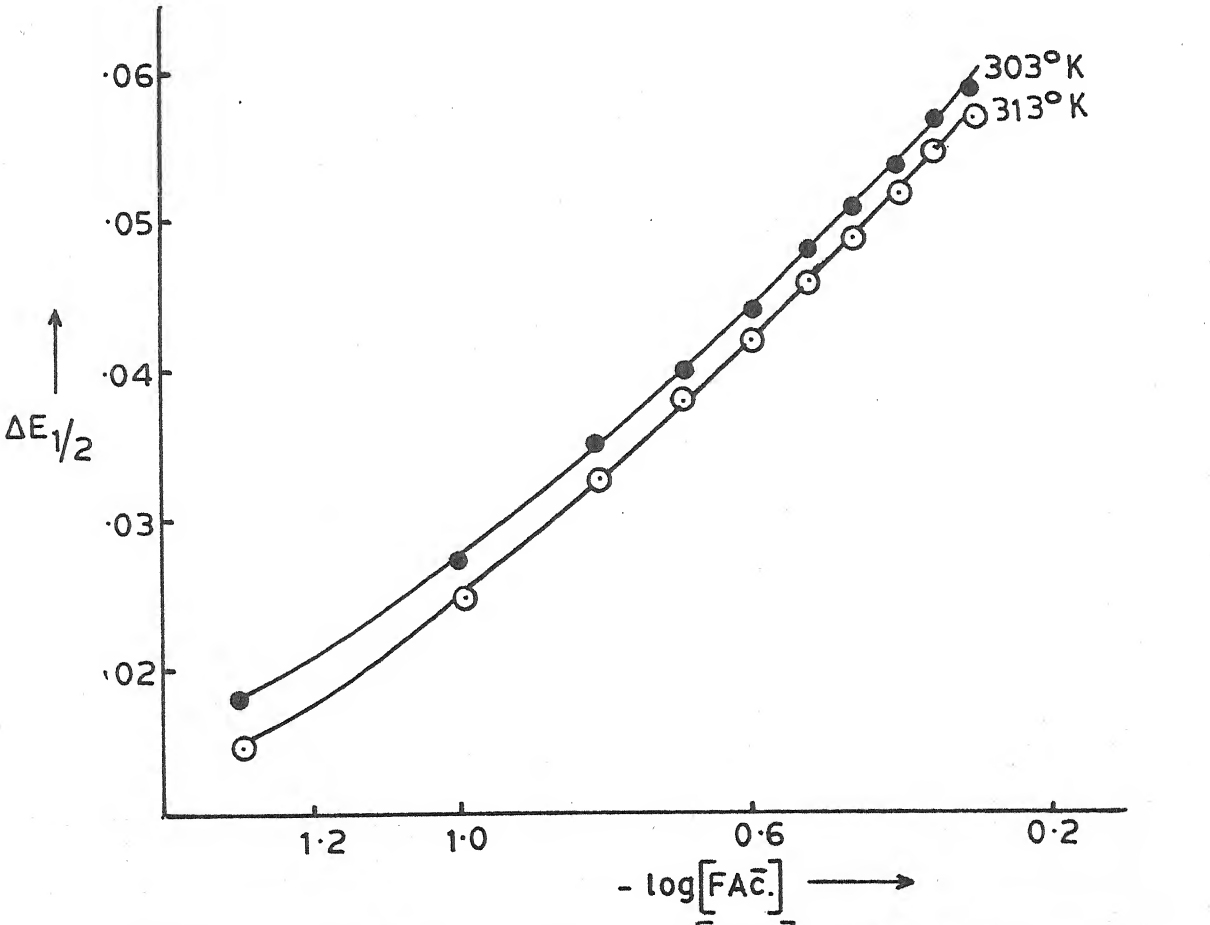

Fig. 4·04 - Plot of $\Delta E_{1/2}$ Vs. $-\log[FA\bar{c}.]$; Pb($FA\bar{c}.$) system.

Table 4.03

Lead acetate system

Temperature (° K)	log β_1	-ΔG (kj)	-ΔH (kj)	-ΔS (kj deg^{-1})x10^3
303	1.8864	10.9445		28.7864
			19.6668	
313	1.7781	10.6566		28.7865

4.3.02 Lead monofluoroacetate system :

(a) Nature of reduction : The linearity of plots $-E_{de}$ vs. $-\log.i/i_d-i$ with slopes of 30-32 mV and the temperature co-efficient (0.3 $\pm$ 0.1 mV per degree) of $E_{1/2}$ coupled with temperature co-efficient of i_d (0.6 percent per degree) and constancy of ratio of i_d and square root of effective height of mercury column conclusively indicated that the two electron reversible reduction of Pb(II) in monofluoroacetate ions is entirely diffusion controlled.

(b) Effect of ligand concentration : Solutions containing 0.9 mM Pb(II) ions, 0.002% gelatin, increasing concentration of monofluoroacetate ions ($F\bar{A}c.$) and decreasing amounts of sodium perchlorate for maintaining ionic strength at 1.0 M, when polarographed at 303° K, showed a shift in half wave potential to the more negative side and a decrease in diffusion current to indicate complex formation between Pb(II) and ($F\bar{A}c.$) ions. Since

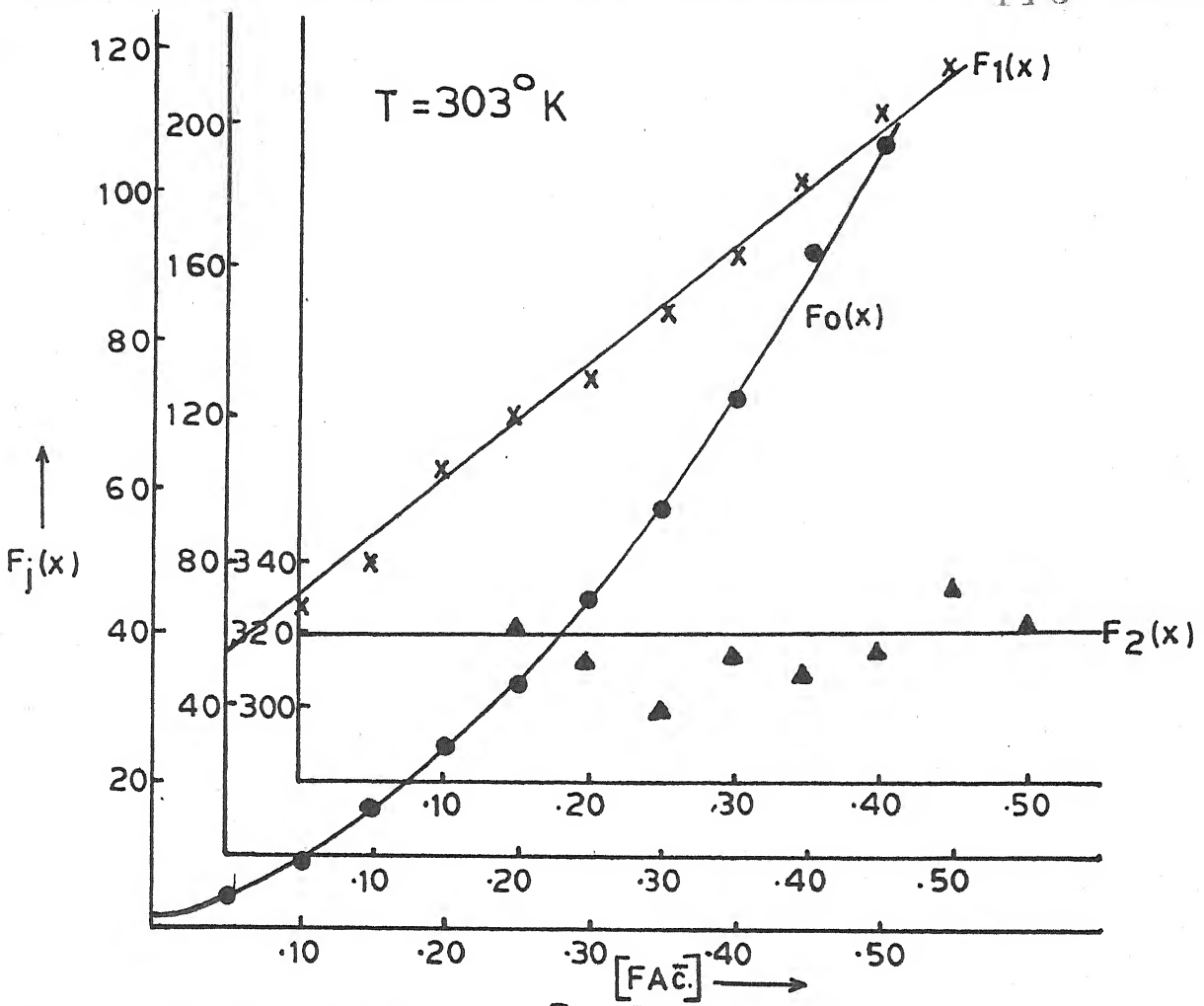

Fig. 4·05 - Plot of $F_j(x)$ Vs. $[FA\bar{c}.]$; Pb(FAc̄.) system.

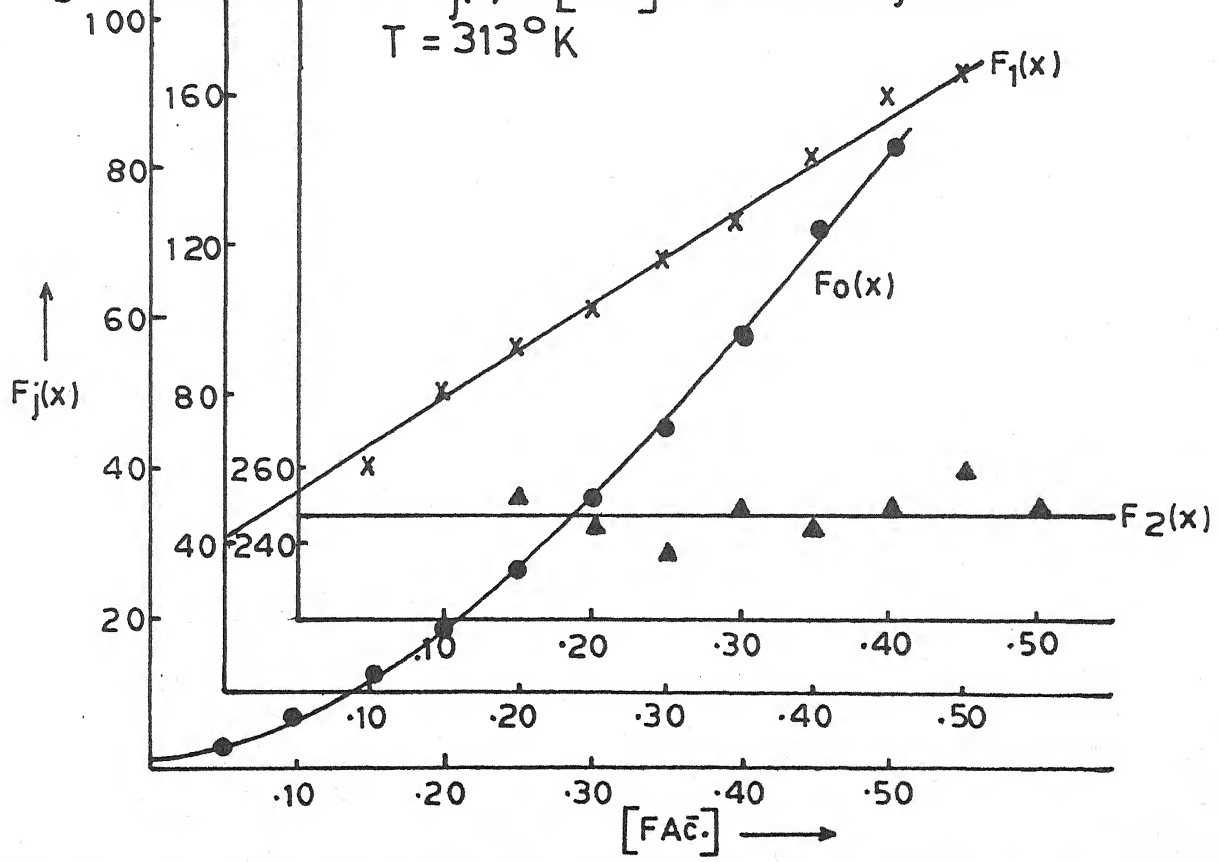

Fig. 4·06 - Plot of $F_j(x)$ Vs. $[FA\bar{c}.]$; Pb(FAc̄.) system.

Table 4.04

Polarographic data for Lead monofluoroacetate system

Concn. of Pb^{++} ions = 0.9 mM Ionic strength = 1.0 M ($NaClO_4$)

$E_{1/2}$ of Pb^{++} ions = -0.401 V vs. SCE Temperature = 303° K

Slopes of plots of $-E_{de}$ vs. -log. i/i_d-i = 30-32 mV

$[F\bar{A}c.]$ (M)	$\Delta E_{1/2}$ (V)	log. I_M/I_C	$F_0(X)$	$F_1(X)$	$F_2(X)$
0.05	0.018	0.0321	4.27	65.3	-
0.10	0.027	0.0445	8.76	77.6	-
0.15	0.037	0.0539	16.53	103.53	323.5
0.20	0.040	0.0604	24.61	118.05	315.4
0.25	0.044	0.636	33.66	130.64	302.5
0.30	0.048	0.0669	46.10	150.33	317.7
0.35	0.051	0.0702	58.46	164.17	311.9
0.40	0.054	0.0735	74.13	182.82	319.5
0.45	0.057	0.0769	94.01	206.66	337.0
0.50	0.059	0.0769	109.57	217.14	324.3

$\beta_1 = 55$ $\beta_2 = 320$

Table 4.05

Polarographic data for Lead monofluoroacetate system

Concn. of Pb^{++} ions = 0.9 mM Ionic strength = 1.0 M ($NaClO_4$)

$E_{1/2}$ of Pb^{++} ions = -0.397 V vs. SCE Temperature = 313° K

Slopes of plots of $-E_{de}$ vs. -log. i/i_d-i = 30-32 mV

$[F\bar{A}c.]$ (M)	$\Delta E_{1/2}$ (V)	log. I_M/I_C	$F_0(X)$	$F_1(X)$	$F_2(X)$
0.05	0.015	0.0283	3.24	44.8	-
0.10	0.025	0.0418	7.03	60.3	-
0.15	0.033	0.0530	13.05	80.33	255.0
0.20	0.038	0.0615	19.29	91.45	247.0
0.25	0.042	0.0702	26.47	101.88	239.5
0.30	0.046	0.0761	36.10	117.0	250.0
0.35	0.049	0.0821	45.73	127.8	245.0
0.40	0.052	0.0882	57.92	142.3	250.7
0.45	0.055	0.0913	72.87	159.71	261.5
0.50	0.057	0.0913	84.52	167.04	250.0

$\beta_1 = 42$ $\beta_2 = 248$

the plot (figure 4.04) of $\Delta E_{1/2}$ vs. -log.[$FA\bar{c}$.] is a curve indicating stepwise complex formation, DeFord and Hume's method was used to compute the stability constants of the complexes so formed. The overall stability constant values β_1 and β_2 were found to be 55 and 320 respectively. The polarographic data and $F_j(X)$ functions appear in table 4.04 and figure 4.05.

(c) Effect of temperature : The temperature co-efficients of half wave potential and diffusion current have earlier in this section, been used to infer the reversibility and diffusion controlled character of reduction of the lead monofluoroacetate complexes.

The stability constants of the complexes were determined at 313° K too and were found to be 42 (β_1) and 248 (β_2). The relevant polarographic data and $F_j(X)$ plots have been presented in table 4.05 and figure 4.06.

From the knowledge of stability constants at two temperatures, the thermodynamic functions were computed and have been included in table 4.06.

Table 4.06

Lead monofluoroacetate system

Temperature (° K)	log β_1	$-\Delta G$ (kj)	$-\Delta H$ (kj)	$-\Delta S$ (kj deg^{-1})x10^3
303	1.7403	10.0968		36.8584
			21.2649	
313	1.6232	9.7282		36.8584

4.3.03 Lead difluoroacetate system :

(a) Nature of reduction : The reduction of Pb(II) in presence of difluoroacetate ions was inferred to be reversible with two electron transfer and also diffusion controlled from the following observations.

(i) The straight line plots of $-E_{de}$ vs. -log. i/i_d-i have slopes of 31 ± 1 mV.

(ii) Temperature co-efficient values for $E_{1/2}$ and i_d were 0.3 ± 0.1 mV per degree and 0.5 ± 0.1 percent per degree.

(iii) The constancy of ratio of i_d and $\sqrt{h_{eff.}}$.

(b) Effect of ligand concentration : Complex formation between Pb(II) ions and difluoroacetate ions was indicated by the cathodic shift in half wave potential and decrease in diffusion current when solutions containing 0.9 mM Pb(II) ions, 0.002% gelatin, increasing (F_2Ac^-) ion concentration and correspondingly decreasing $NaClO_4$ concentration were polarographed at 303° K. The non-linearity of the plot (figure 4.07) of $-\Delta E_{1/2}$ vs. $-\log.[F_2Ac^-]$ lead us to conclude multiple complex formation so that DeFord and Hume's improved method could be conveniently used to determine the overall formation constants of complexes so formed. The β_1 and β_2 for lead difluoroacetate complexes were found to be 18.5 and 128 respectively. The relevant polarographic data find place in table 4.07 while the $F_j(X)$ functions are depicted in figure 4.08.

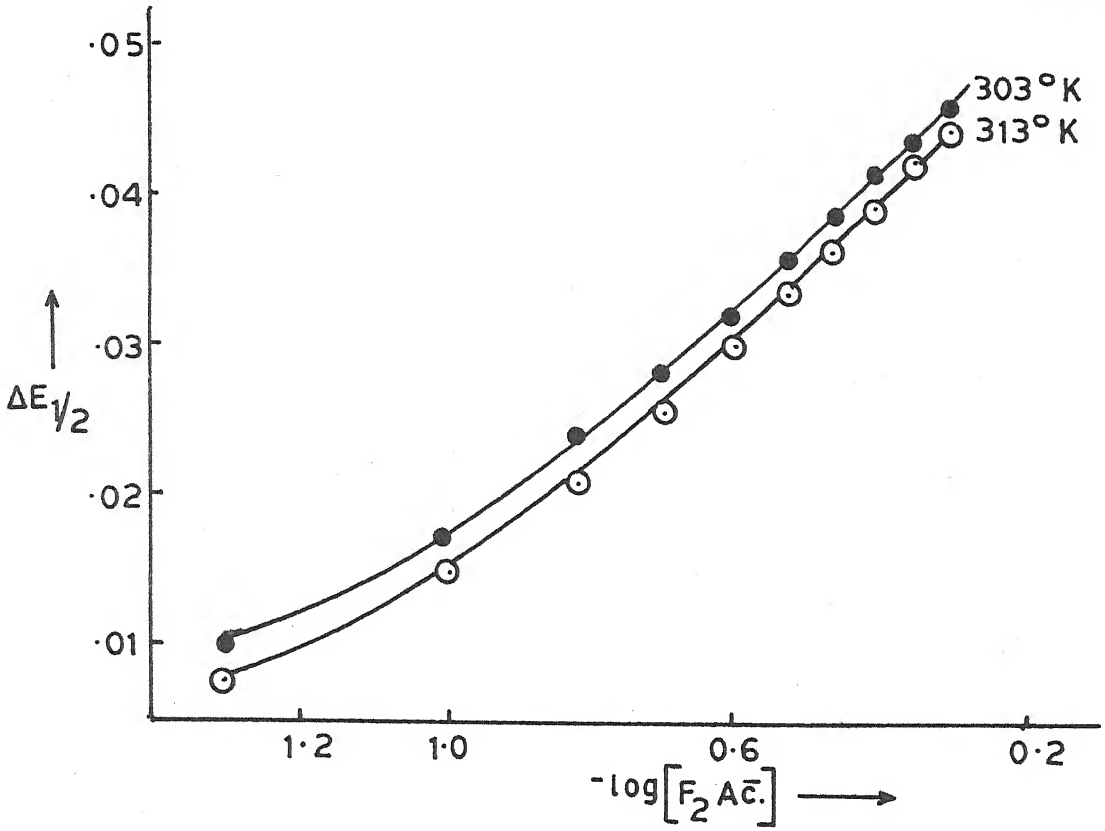

Fig. 4·07 - Plot of $\Delta E_{1/2}$ Vs. $-\log[F_2Ac.]$; $Pb(F_2Ac.)$ system.

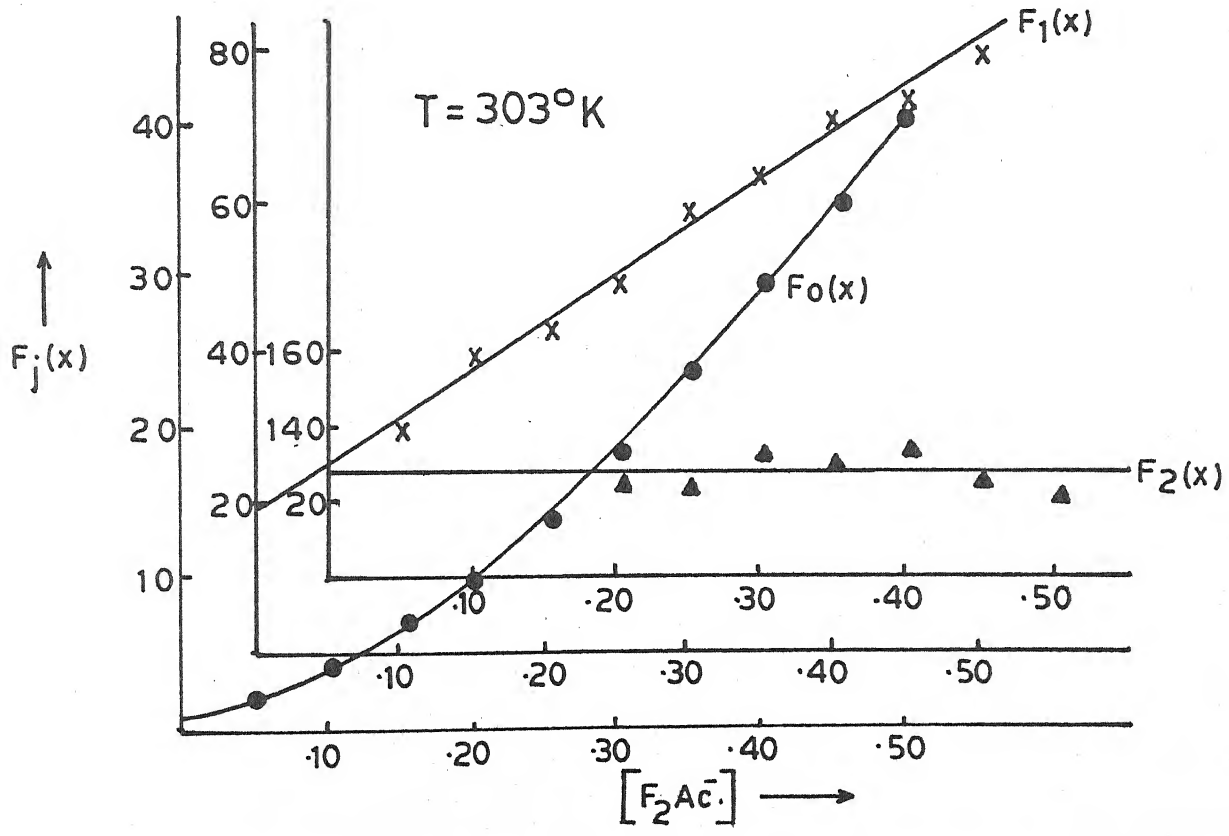

Fig. 4·08 - Plot of $F_{j(x)}$ Vs. $[F_2Ac.]$; $Pb(F_2Ac.)$ system.

Table 4.07

Polarographic data for Lead filuoroacetate system

Concn. of Pb^{++} ions = 0.9 mM Ionic strength = 1.0 M ($NaClO_4$)
$E_{1/2}$ of Pb^{++} ions = -0.401 V vs. SCE Temperature = 303° K
Slopes of plots of $-E_{de}$ vs. $-\log. i/i_d-i$ = 30-32 mV

$[F_2Ac^-]$ (M)	$\Delta E_{1/2}$ (V)	$\log. I_M/I_C$	$F_0(X)$	$F_1(X)$	$F_2(X)$
0.05	0.010	0.0241	2.27	25.4	-
0.10	0.017	0.0367	4.0	30.0	-
0.15	0.024	0.0496	7.04	40.26	-
0.20	0.028	0.0596	9.79	43.95	127.2
0.25	0.032	0.0664	13.52	50.08	126.0
0.30	0.036	0.0733	18.66	58.86	134.5
0.35	0.039	0.0768	23.67	64.77	132.2
0.40	0.042	0.0803	30.03	72.57	135.2
0.45	0.044	0.0803	35.0	75.55	126.7
0.50	0.046	0.0839	41.13	80.26	123.5

β_1 = 18.5 β_2 = 128

Table 4.08

Polarographic data for Lead difluoroacetate system

Concn. of Pb^{++} ions = 0.9 mM Ionic strength = 1.0 M ($NaClO_4$)
$E_{1/2}$ of Pb^{++} ions = -0.397 V vs. SCE Temperature = 313° K
Slopes of plot of $-E_{de}$ vs. $-\log. i/i_d-i$ = 30-32 mV

$[F_2Ac^-]$ (M)	$\Delta E_{1/2}$ (V)	$\log. I_M/I_C$	$F_0(X)$	$F_1(X)$	$F_2(X)$
0.05	0.008	0.0356	1.96	19.2	114.0
0.10	0.015	0.0531	3.52	24.3	108.0
0.15	0.021	0.0651	5.51	30.06	110.4
0.20	0.026	0.0713	8.10	35.5	110.0
0.25	0.031	0.0807	11.99	43.96	121.8
0.30	0.034	0.0871	15.20	47.33	112.7
0.35	0.037	0.0936	19.28	52.22	110.7
0.40	0.040	0.0969	24.27	58.17	111.7
0.45	0.043	0.1002	30.54	65.64	115.8
0.50	0.045	0.1002	35.43	68.86	110.3

β_1 = 13.5 β_2 = 110

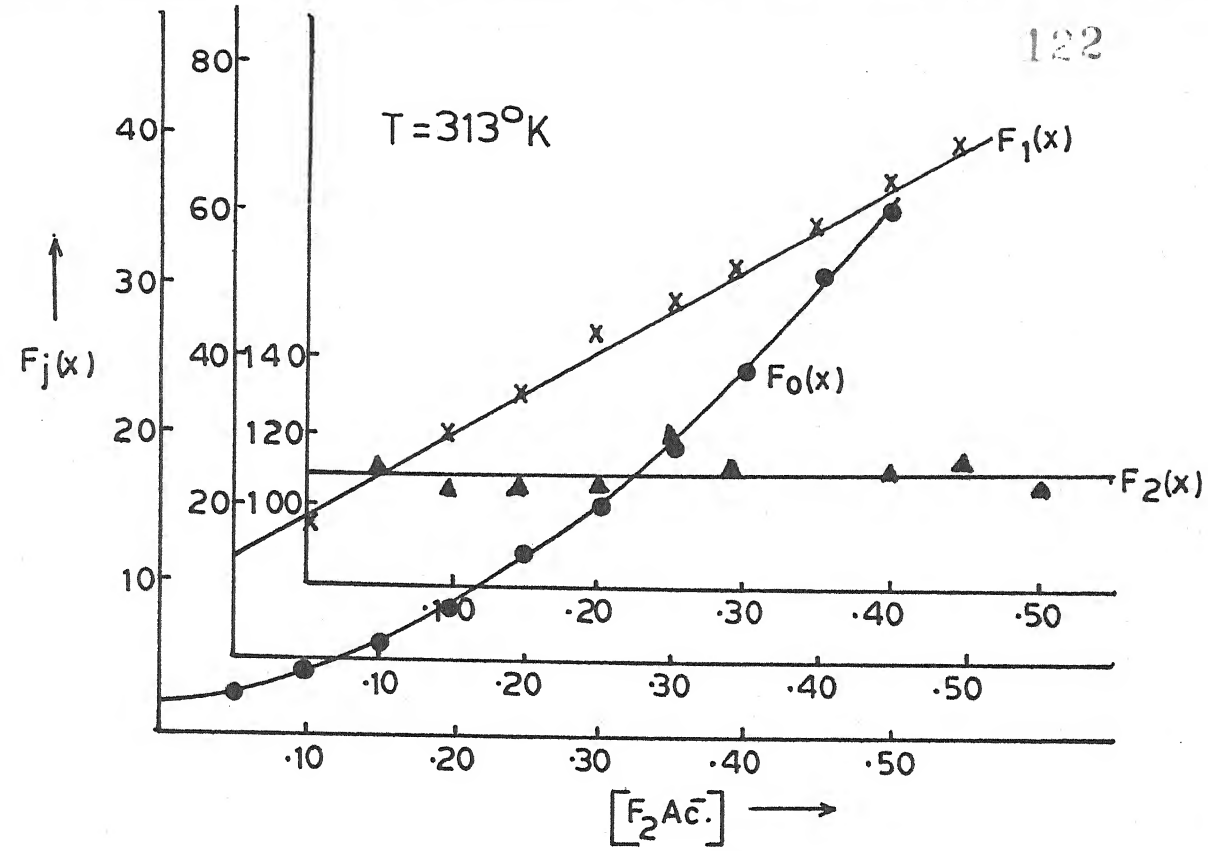

Fig. 4·09 - Plot of $F_j(x)$ Vs. $[F_3Ac^-]$; Pb(F_3Ac.) system.

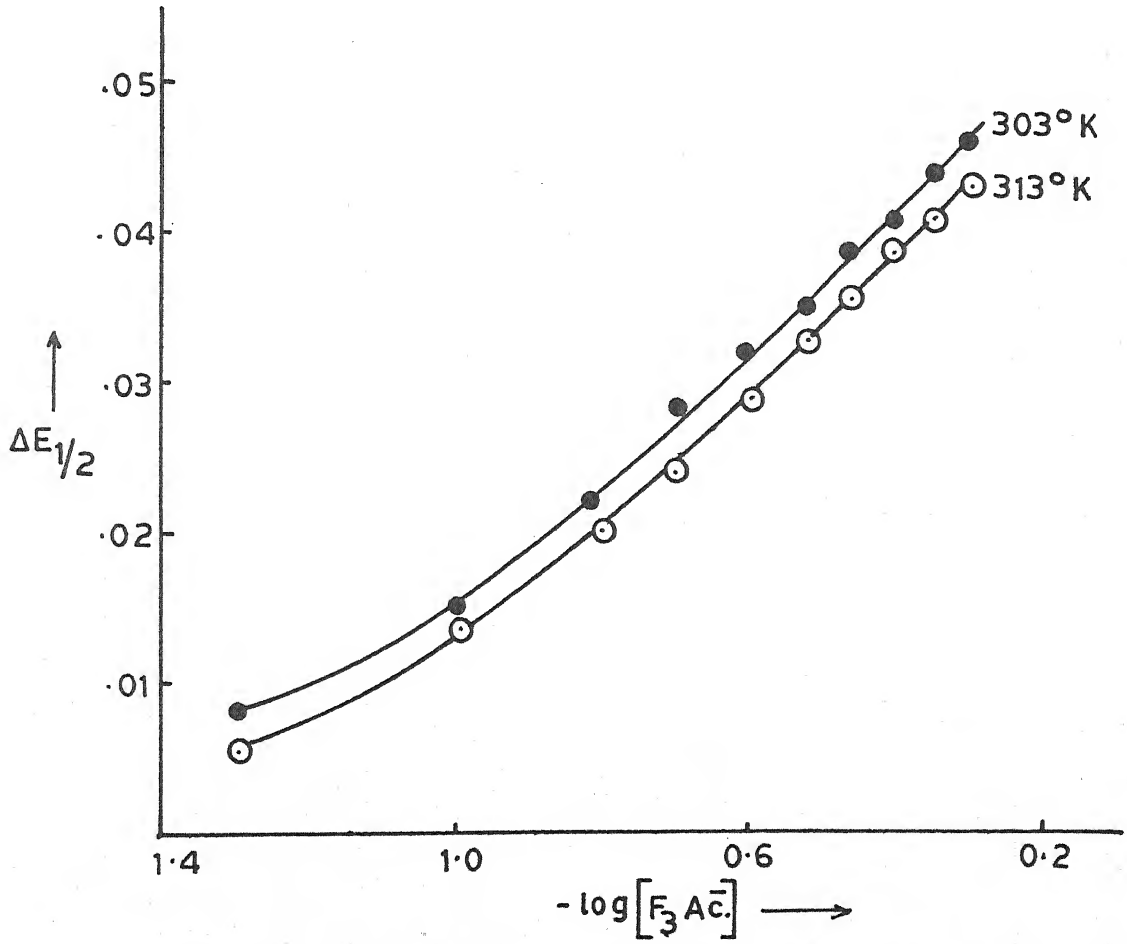

Fig. 4·10 - Plot of $\Delta E_{1/2}$ Vs. $-\log[F_3Ac^-]$; Pb(F_3Ac^-) system.

(c) Effect of temperature : The temperature co-efficients of $E_{1/2}$ and i_d have already been used earlier in this section to aid establish reversibility and diffusion controlled character of reduction at DME of Pb(II) in presence of difluoroacetate ions.

The knowledge of stability constants enables us to evaluate thermodynamic parameters. Hence the stability constants were determined at 313° K also and were found to be 13.5 and 110 respectively for $\left[Pb\ (F_2Ac.)\right]^+$ and $\left[Pb\ (F_2Ac.)_2\right]$ complexes. Table 4.08 contains the relevant polarographic data while figure 4.09 depicts the $F_j(X)$ functions.

The thermodynamic functions find place in table 4.09.

Table 4.09

Lead difluoroacetate system

Temperature (° K)	log β_1	$-\Delta G$ (kj)	$-\Delta H$ (kj)	$-\Delta S$ (kj deg^{-1})x10^3
303	1.2671	7.3514		57.7257
			24.8423	
313	1.1303	6.7741		57.7258

4.3.04 Lead trifluoroacetate system :

(a) Nature of reduction : It was found that the linear plots of $-E_{de}$ vs. $-\log. i/i_d-i$ have slopes of 31 ± 1 mV, temperature co-efficients of half wave potential and diffusion current are 0.3 ± 0.1 mV per degree and 0.6 ± 0.1 percent per degree and the

plots of diffusion current against square root of effective height of mercury column are linear for the reduction at DME of Pb(II) in presence of trifluoroacetate ions. These results conclusively established that the two electron reversible reduction is totally diffusion controlled.

(b) Effect of ligand concentration : A cathodic shift in $E_{1/2}$ coupled with decrease in diffusion current when solutions containing 0.9 mM Pb(II) ions, 0.002% gelatin, increasing amounts of $(F_3A\bar{c}.)$ ions and correspondingly decreasing amounts of sodium perchlorate (for μ = 1.0 M) were reduced at the DME at 303° K indicated complex formation between Pb(II) and $(F_3A\bar{c}.)$ ions. The plots of $\Delta E_{1/2}$ vs. -log. $[F_3A\bar{c}.]$ were curves (figure 4.10) leading us to conclude multiple complex formation and apply DeFord and Hume's method to determine overall formation constants which were found to be 16 and 146 for 1:1 and 1:2 metal/ligand ratio complexes. Table 4.10 and figure 4.11 represent the requisite polarographic data and $F_j(X)$ plots.

(c) Effect of temperature : Earlier in this section, the temperature co-efficients of $E_{1/2}$ and i_d have been utilized to establish the reversibility and diffusion controlled behaviour of reduction of Pb(II) ions in presence of trifluoroacetate ions.

In order to compute ΔG, ΔH and ΔS, it was thought worthwhile to determine formation constants at another temperature i.e. 313° K. The formation constant values for the two complexes were found to be β_1 = 12 and β_2 = 100. The relevant polarographic data and $F_j(X)$ have been presented in table 4.11

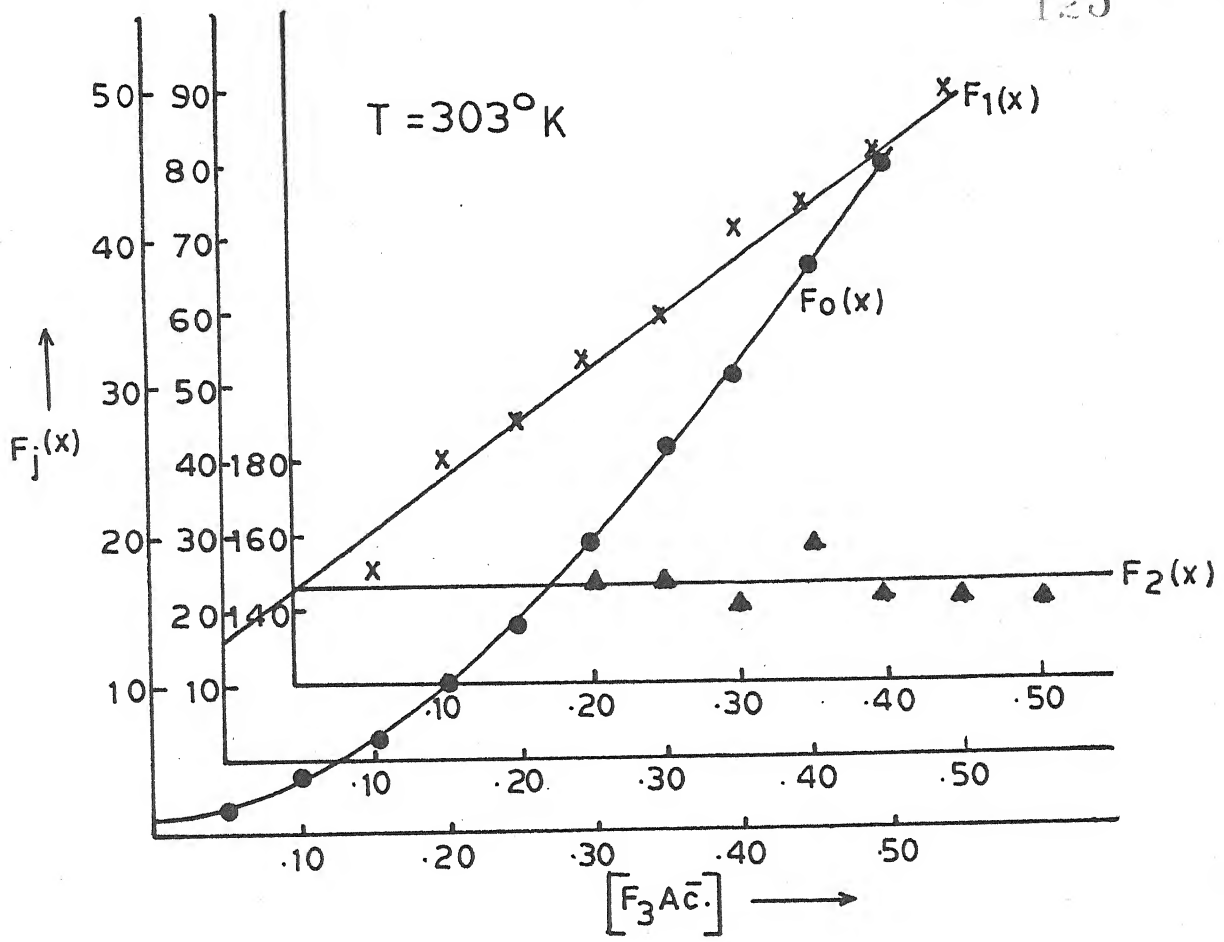

Fig. 4·11 - Plot of $F_j(x)$ Vs. $[F_3A\bar{c}.]$; Pb $(F_3A\bar{c}.)$ system.

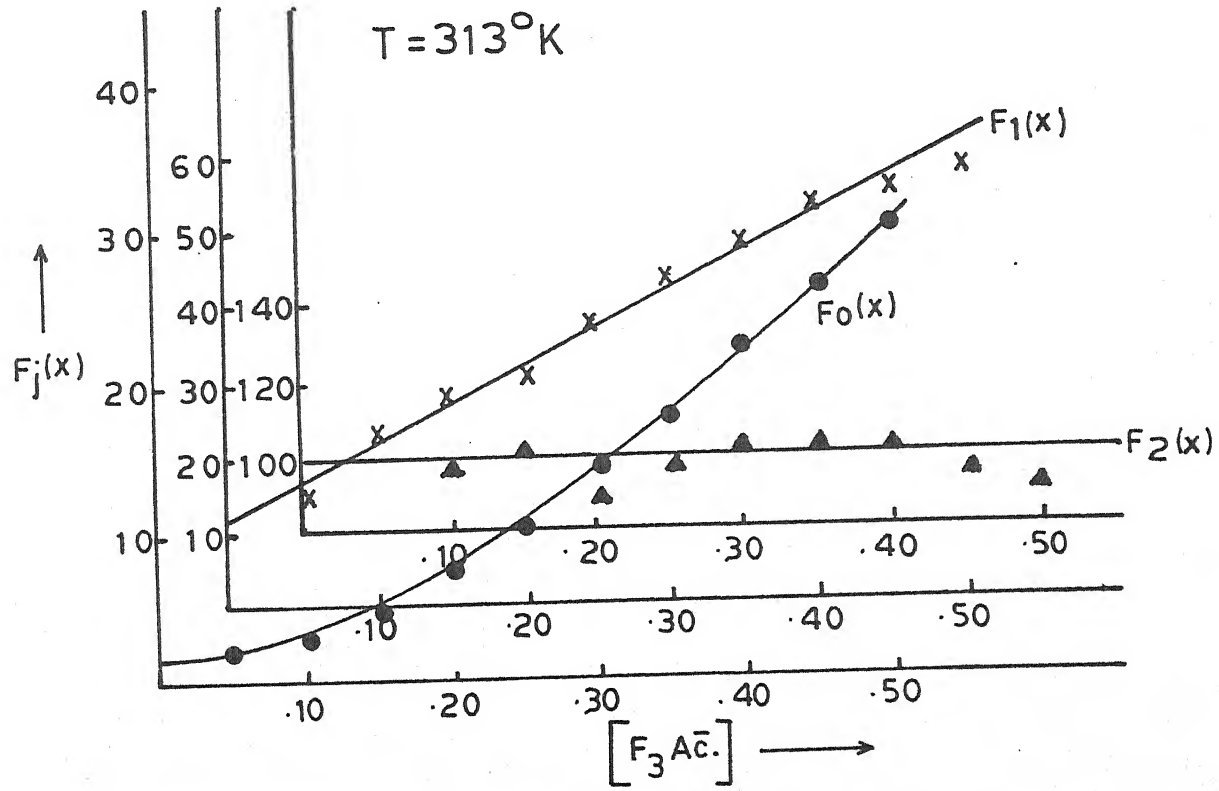

Fig. 4·12 - Plot of $F_j(x)$ Vs. $[F_3A\bar{c}.]$; Pb $(F_3A\bar{c}.)$ system.

Table 4.10

Polarographic data for Lead trifluoroacetate system

Concn. of Pb^{++} ions = 0.9 mM Ionic strength = 1.0 M ($NaClO_4$)

$E_{1/2}$ of Pb^{++} ions = -0.401 V vs. SCE Temperature = 303° K

Slopes of plots of $-E_{de}$ vs. $-\log. i/i_d-i$ = 30-31 mV

$[F_3Ac^-]$ (M)	$\Delta E_{1/2}$ (V)	$\log. I_M/I_C$	$F_0(X)$	$F_1(X)$	$F_2(X)$
0.05	0.008	0.0263	1.96	19.2	-
0.10	0.015	0.0448	3.48	24.8	-
0.15	0.022	0.0543	6.12	40.73	-
0.20	0.028	0.0741	10.12	45.6	148.0
0.25	0.032	0.0877	14.20	52.8	147.2
0.30	0.035	0.1091	18.77	59.23	144.1
0.35	0.039	0.1202	26.16	71.88	159.6
0.40	0.041	0.1239	30.75	74.37	145.8
0.45	0.044	0.1239	38.7	81.55	145.6
0.50	0.046	0.1277	45.50	89.0	146.0

$\beta_1 = 16$ $\beta_2 = 146$

Table 4.11

Polarographic data for Lead trifluoroacetate system

Concn. of Pb^{++} ions = 0.9 mM Ionic strength = 1.0 M ($NaClO_4$)

$E_{1/2}$ of Pb^{++} ions = -0.397 V vs. SCE Temperature = 313° K

Slopes of plots of $-E_{de}$ vs. $-\log. i/i_d-i$ = 30-32 mV

$[F_3Ac^-]$ (M)	$\Delta E_{1/2}$ (V)	$\log. I_M/I_C$	$F_0(X)$	$F_1(X)$	$F_2(X)$
0.05	0.006	0.0347	1.69	13.8	-
0.10	0.014	0.0517	3.18	21.8	98.0
0.15	0.020	0.0635	5.10	27.3	102.0
0.20	0.024	0.0725	7.0	30.0	90.0
0.25	0.029	0.0786	10.29	37.16	100.6
0.30	0.033	0.0817	13.94	43.13	103.7
0.35	0.036	0.0848	17.54	47.25	100.7
0.40	0.039	0.0880	22.07	52.67	101.6
0.45	0.041	0.0911	25.79	55.08	95.7
0.50	0.043	0.0911	29.92	55.84	91.7

$\beta_1 = 12$ $\beta_2 = 100$

and figure 4.12 while the thermodynamic functions appear in table 4.12.

Table 4.12

Lead trifluoroacetate system

Temperature (° K)	log β_1	- ΔG (kj)	- ΔH (kj)	- ΔS (kj deg^{-1})x10^3
303	1.2041	6.9860		51.8019
			22.6820	
313	1.0792	6.4681		51.8015

4.3.05 Lead monochloroacetate system :

(a) Nature of reduction : The plots of $-E_{de}$ vs. -log. i/i_d-i were straight lines with slopes of 31 $\pm$ 1 mV. The temperature co-efficient values for $E_{1/2}$ and i_d were 0.2 mV per degree and 0.4 $\pm$ 0.1 percent per degree respectively and the ratio $i_d/\sqrt{h_{eff.}}$ was constant in each case for the reduction at DME of Pb(II) in monochloroacetate ions. Hence the reduction must be reversible, involve a two electron transfer process and must also be totally diffusion controlled.

(b) Effect of ligand concentration : Polarography at 303° K of solutions consisting of 0.9 mM Pb(II) ions, 0.002% gelatin, gradually increasing concentrations of ($ClAc^-$) ions, correspondingly decreasing amounts of sodium perchlorate (for μ = 1.0 M) revealed a cathodic shift in $E_{1/2}$ coupled with decrease in i_d to indicate complex formation between Pb(II) and ($ClAc^-$) ions. The

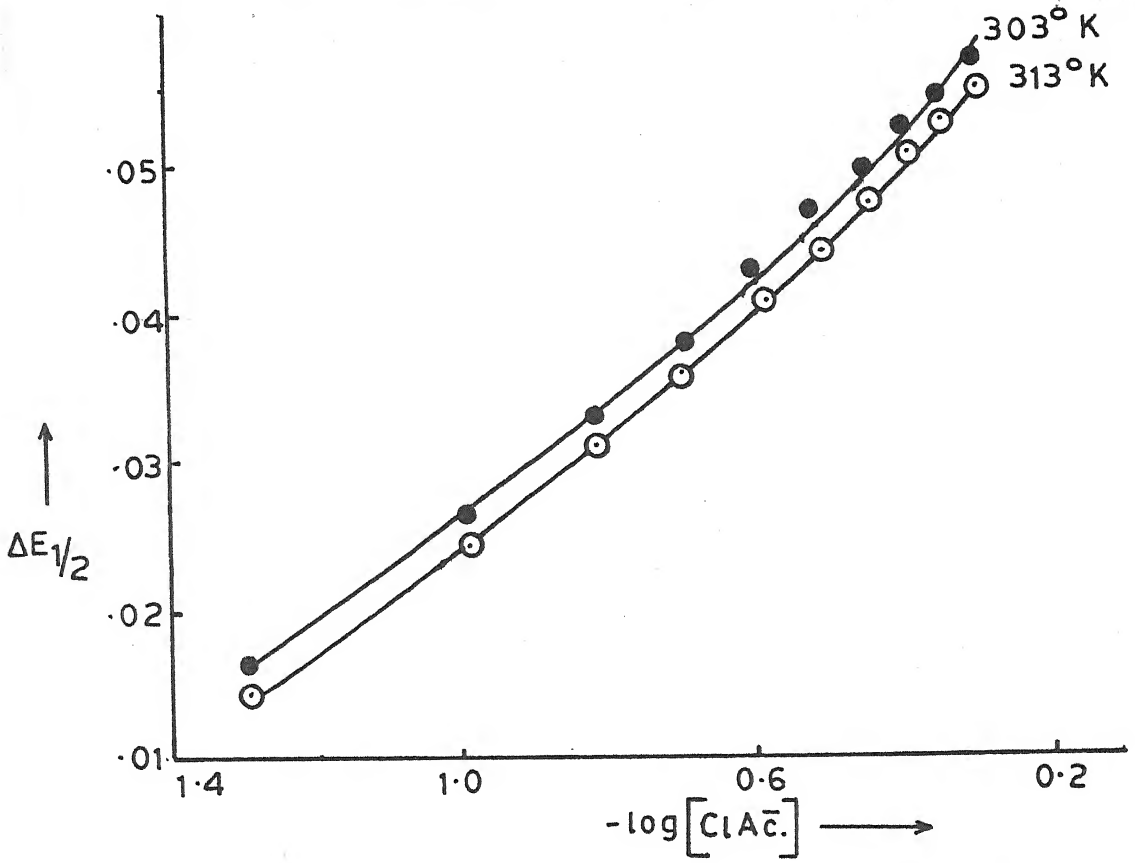

Fig. 4·13 - Plot of $\Delta E_{1/2}$ Vs. $-\log[ClA\bar{c}.]$; Pb(ClAc̄.) system.

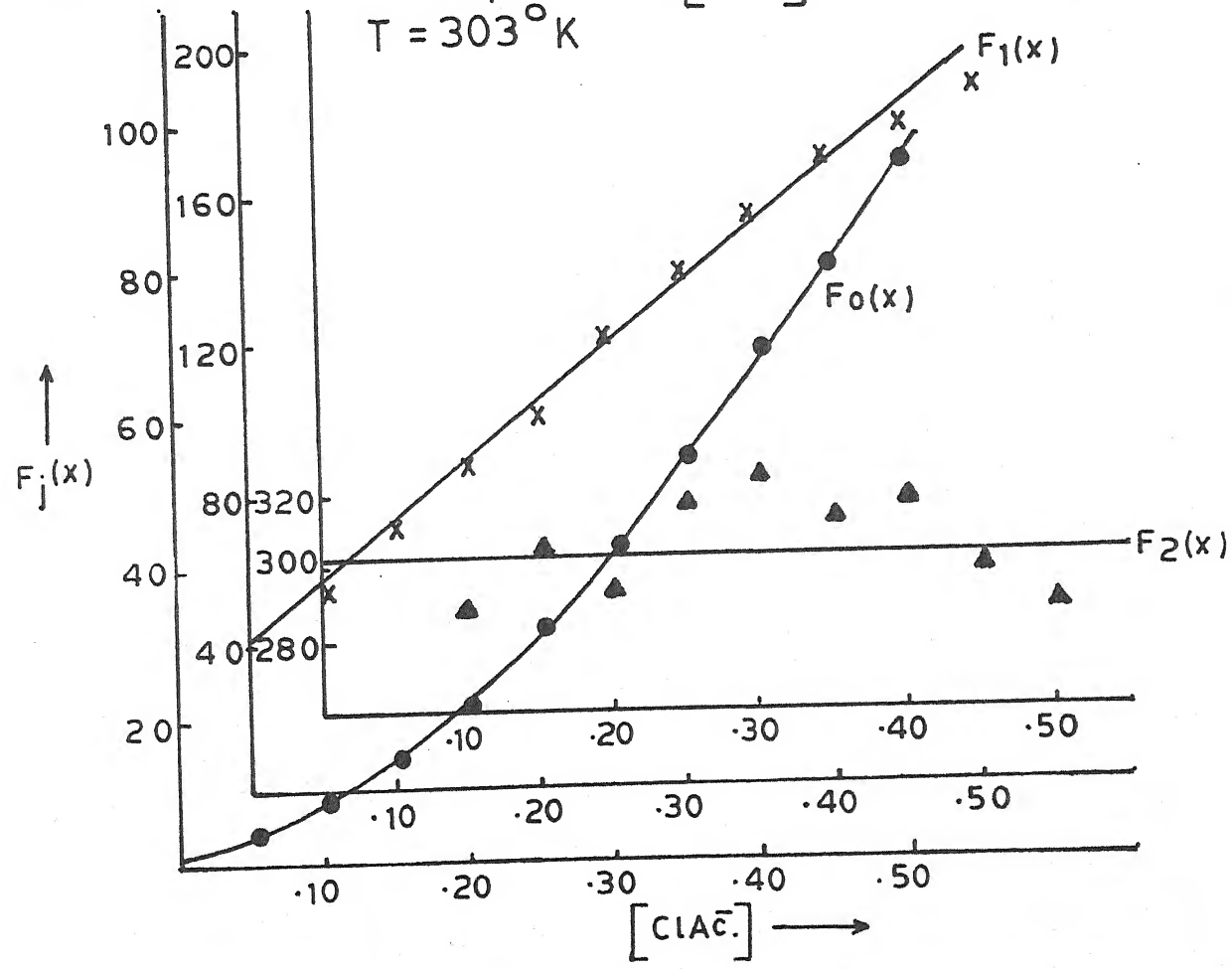

Fig. 4·14 - Plot of $F_j(x)$ Vs. $[ClA\bar{c}.]$; Pb(ClAc̄.) system.

Table 4.13

Polarographic data for Lead monochloroacetate system

Concn. of Pb^{++} ions = 0.9 mM Ionic strength = 1.0 M ($NaClO_4$)

$E_{1/2}$ of Pb^{++} ions = -0.401 V vs. SCE Temperature = 303° K

Slopes of plots of $-E_{de}$ vs. $-\log. i/i_d - i$ = 30-32 mV

$[ClAc^-]$ (M)	$\Delta E_{1/2}$ (V)	$\log. I_M/I_C$	$F_0(X)$	$F_1(X)$	$F_2(X)$
0.05	0.016	0.0228	3.59	51.8	-
0.10	0.026	0.0377	7.99	69.9	289.0
0.15	0.033	0.0501	14.05	87.0	306.0
0.20	0.038	0.0564	20.92	99.6	293.0
0.25	0.043	0.0627	31.13	120.52	318.0
0.30	0.047	0.0660	42.61	138.66	325.0
0.35	0.050	0.0692	54.03	151.42	315.5
0.40	0.053	0.0725	68.50	168.75	319.4
0.45	0.055	0.0758	80.45	176.55	301.2
0.50	0.057	0.0758	93.77	185.54	289.0

$\beta_1 = 41$ $\beta_2 = 302$

Table 4.14

Polarographic data for Lead monochloroacetate system

Concn. of Pb^{++} ions = 0.9 mM Ionic strength = 1.0 M ($NaClO_4$)

$E_{1/2}$ of Pb^{++} ions = -0.397 V vs. SCE Temperature = 313° K

Slopes of plots of $-E_{de}$ vs. $-\log. i/i_d - i$ = 30-32 mV

$[ClAc^-]$ (M)	$\Delta E_{1/2}$ (V)	$\log. I_M/I_C$	$F_0(X)$	$F_1(X)$	$F_2(X)$
0.05	0.014	0.0258	2.99	29.8	-
0.10	0.024	0.0421	6.53	55.3	238.0
0.15	0.031	0.0562	11.33	68.86	249.0
0.20	0.036	0.0677	16.87	79.35	239.0
0.25	0.041	0.0766	24.94	95.76	257.0
0.30	0.045	0.0827	34.03	110.10	262.0
0.35	0.048	0.0950	43.73	122.08	258.8
0.40	0.051	0.0950	54.63	134.07	256.4
0.45	0.053	0.0950	63.36	138.57	237.9
0.50	0.055	0.0981	74.03	146.07	229.1

$\beta_1 = 31.5$ $\beta_2 = 238$

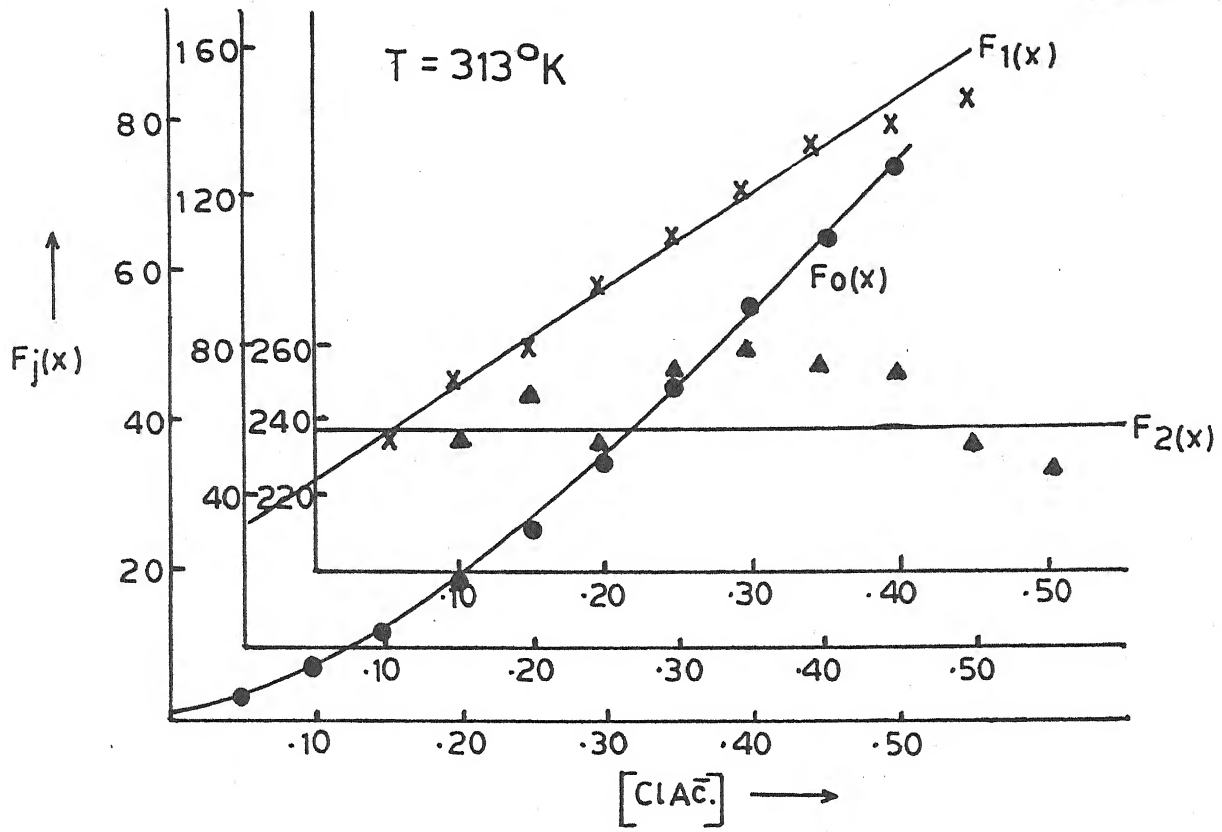

Fig. 4·15 -Plot of $F_{j(x)}$ Vs. $[ClA\bar{c}.]$; Pb(ClAc̄.)system.

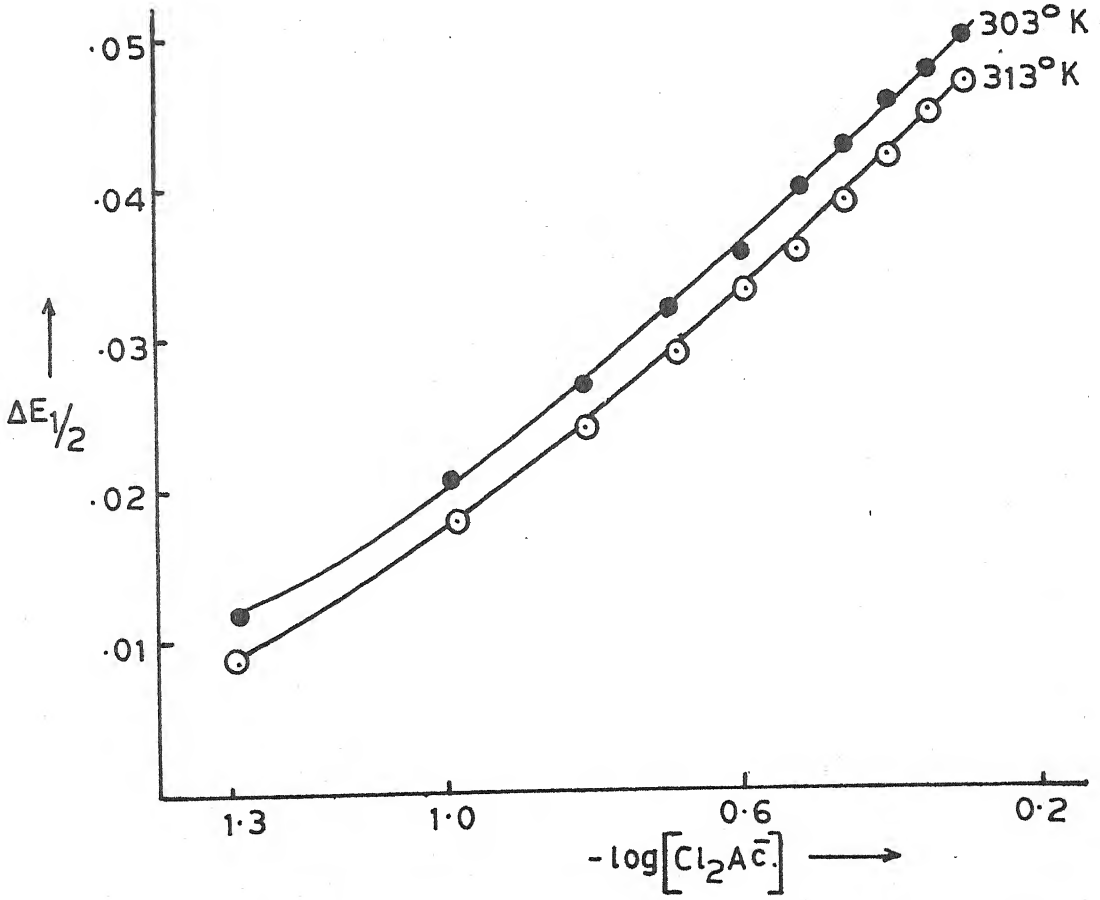

Fig. 4·16 - Plot of $\Delta E_{1/2}$ Vs. $-\log[Cl_2A\bar{c}.]$; Pb($Cl_2A\bar{c}.$)system.

curved nature (figure 4.13) of plot of $\Delta E_{1/2}$ vs. log. $[ClAc^-]$ induced us to use DeFord and Hume's method to calculate overall formation constants as multiple complex formation was indicated. Two successive complexes had β_1 and β_2 values of 41 and 302 respectively. The polarographic data and $F_j(X)$ plots are presented in table 4.13 and figure 4.14.

(c) Effect of temperature : The temperature co-efficients of $E_{1/2}$ and i_d have conveniently been used earlier in this section to help infer the reversible diffusion controlled character of reduction of Pb(II) in presence monochloroacetate ions.

The knowledge of formation constants at two temperatures enables us to compute ΔG, ΔH and ΔS. Hence the experiment (b) was repeated at 313° K. The overall formation constant values were found to be 31.5 and 238 respectively for $[Pb(ClAc.)]^+$ and $[Pb(ClAc.)_2]$ complexes. The relevant polarographic data, $F_j(X)$ plots and thermodynamic functions are available in table 4.14, figure 4.15 and table 4.15 respectively.

Table 4.15

Lead monochloroacetate system

Temperature (° K)	log β_1	- ΔG (kj)	- ΔH (kj)	- ΔS (kj deg^{-1})x10^3
303	1.6127	9.3565		37.6171
			20.7545	
313	1.4983	8.9797		37.6191

4.3.06 Lead dichloroacetate system :

(a) Nature of reduction : The reversibility involving two electron transfer and diffusion controlled nature of reduction of Pb(II) ion in dichloroacetate medium could be inferred from :

(i) Linear plots of $-E_{de}$ vs. -log. i/i_d-i with slopes of 30-32 mV.

(ii) Temperature co-efficients of $E_{1/2}$ (0.3 mV per degree) and i_d (0.6 $\pm$ 0.1 percent per degree).

(iii) Constancy of ratio $i_d/\sqrt{h_{eff.}}$.

(b) Effect of ligand concentration : When solutions consisting of 0.9 mM Pb(II) ions, 0.002% gelatin, increasing concentrations of $(Cl_2A\bar{c}.)$ ions and correspondingly decreasing amounts of sodium perchlorate to maintain ionic strength constant at 1.0 M were polarographed at 303° K, a cathodic shift in $E_{1/2}$ coupled with a decrease in i_d was observed to enable us to infer complex formation. The plot of $\Delta E_{1/2}$ vs. -log. $[Cl_2A\bar{c}.]$ being a curve (figure 4.16), DeFord and Hume's method was applied to compute the stability constants which were found to be 26 and 164 for 1:1 and 1:2 complexes respectively. The relevant polarographic data appear in table 4.16 while the $F_j(X)$ plots find place in figure 4.17.

(c) Effect of temperature : Earlier in this section, the reversible and diffusion controlled character has been inferred from the values of temperature co-efficients of half wave potential and diffusion current.

The procedure reported in (b) was repeated at 313° K to

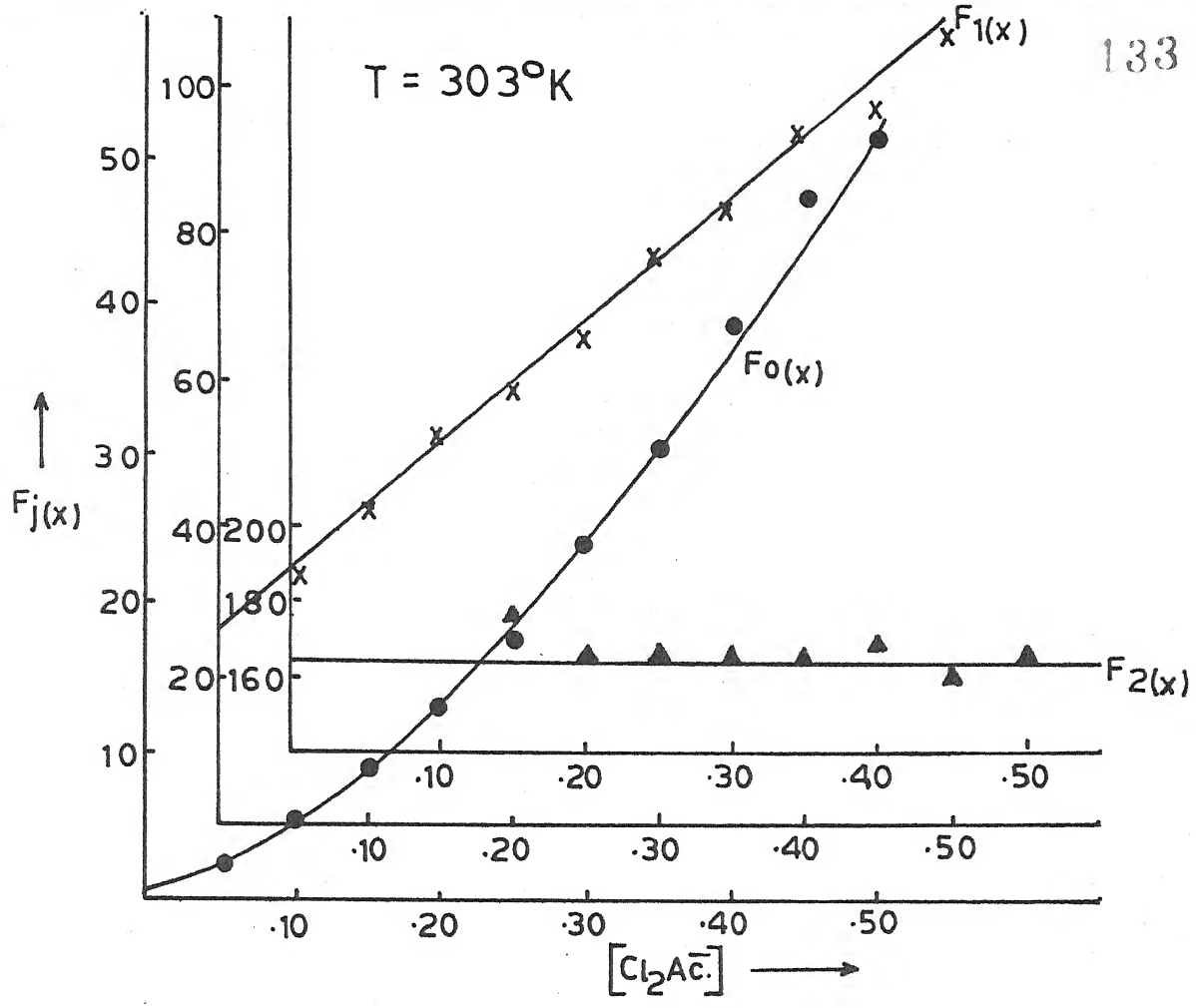

Fig. 4·17 - Plot of $F_{j(x)}$ Vs. $[Cl_2A\bar{c}.]$; $Pb(Cl_2A\bar{c}.)$ system.

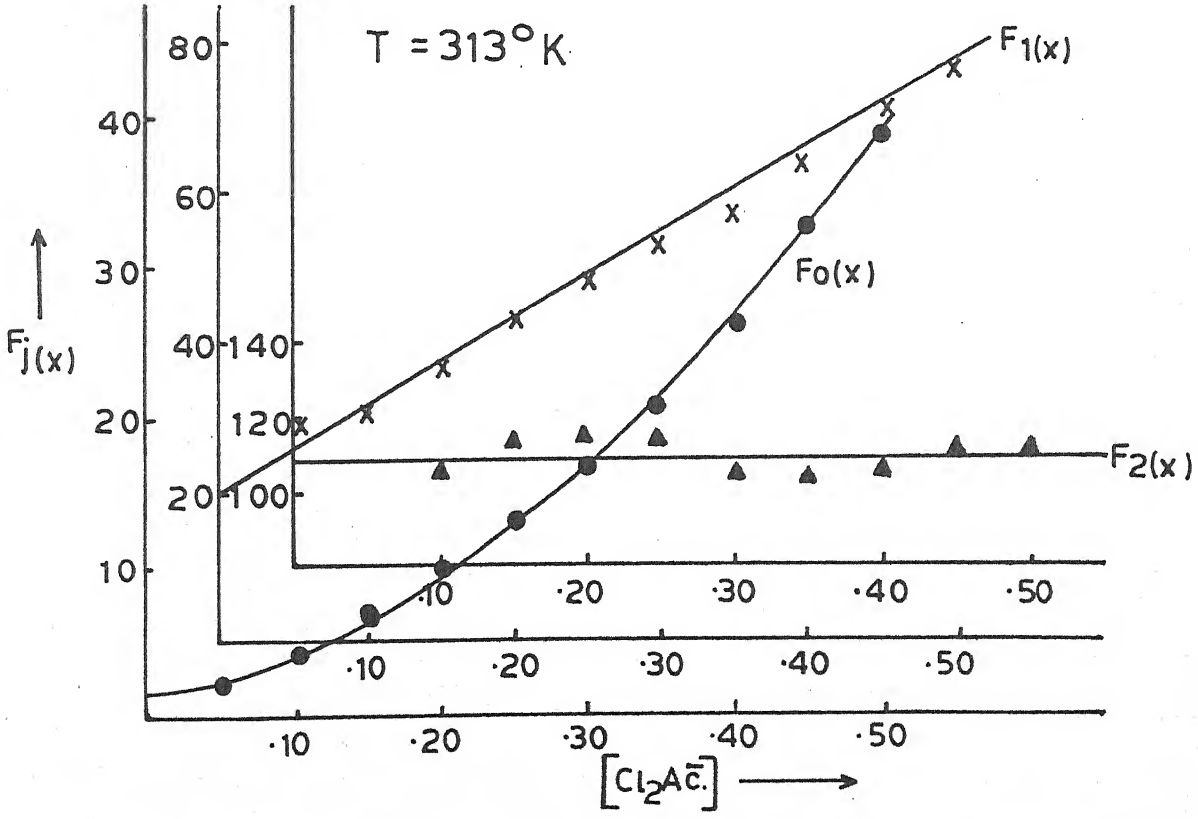

Fig. 4·18 - Plot of $F_{j(x)}$ Vs. $[Cl_2A\bar{c}.]$; $Pb(Cl_2A\bar{c}.)$ system.

Table 4.16

Polarographic data for Lead dichloroacetate system

Concn. of Pb^{++} ions = 0.9 mM Ionic strength = 1.0 M ($NaClO_4$)

$E_{1/2}$ of Pb^{++} ions = -0.401 V vs. SCE Temperature = 303° K

Slopes of plots of $-E_{de}$ vs. -log. i/i_d-i = 30-32 mV

$[Cl_2Ac^-]$ (M)	$\Delta E_{1/2}$ (V)	log. I_M/I_C	$F_0(X)$	$F_1(X)$	$F_2(X)$
0.05	0.012	0.0241	2.65	33.0	-
0.10	0.021	0.0367	5.43	44.3	-
0.15	0.027	0.0496	8.86	52.4	176.0
0.20	0.032	0.0496	13.0	60.0	170.0
0.25	0.036	0.0496	17.54	66.16	166.4
0.30	0.040	0.0496	24.0	76.66	168.8
0.35	0.043	0.0529	30.44	84.1	165.7
0.40	0.046	0.0529	38.6	94.0	170.0
0.45	0.048	0.0563	44.99	97.77	159.5
0.50	0.050	0.0563	52.44	108.8	165.6

$\beta_1 = 26$ $\beta_2 = 164$

Table 4.17

Polarographic data for Lead dichloroacetate system

Concn. of Pb^{++} ions = 0.9 mM Ionic strength = 1.0 M ($NaClO_4$)

$E_{1/2}$ of Pb^{++} ions = -0.397 V vs. SCE Temperature = 313° K

Slopes of plots of $-E_{de}$ vs. -log. i/i_d-i = 30-31 mV

$[Cl_2Ac^-]$ (M)	$\Delta E_{1/2}$ (V)	log. I_M/I_C	$F_0(X)$	$F_1(X)$	$F_2(X)$
0.05	0.009	0.0217	2.04	20.8	-
0.10	0.018	0.0358	4.12	31.2	110.0
0.15	0.024	0.0475	6.61	37.4	116.0
0.20	0.029	0.0534	9.71	43.55	117.7
0.25	0.033	0.0595	13.25	49.0	116.0
0.30	0.036	0.0626	16.66	52.2	107.3
0.35	0.037	0.0656	20.97	57.05	105.8
0.40	0.042	0.0688	26.38	63.45	108.6
0.45	0.045	0.0718	33.19	71.53	114.5
0.50	0.047	0.0749	38.77	75.54	111.0

$\beta_1 = 20$ $\beta_2 = 108$

determine the formation constants β_1 and β_2 which were 20 and 108 respectively. The concerned $F_j(X)$ data have been presented in table 4.17 and figure 4.18.

Table 4.18 contains the thermodynamic parameters obtained from the knowledge of formation constants at the two temperatures.

Table 4.18

Lead dichloroacetate system

Temperature (° K)	log β_1	- ΔG (kj)	- ΔH (kj)	- ΔS (kj deg^{-1})x10^3
303	1.4149	8.2089		41.1712
			20.6838	
313	1.3010	7.7972		41.1712

4.3.07 Lead trichloroacetate system :

(a) Nature of reduction : Well defined diffusion controlled polarographic waves involving reversible two electron transfer process were obtained as obvious from the following observations :

(i) the plot of $-E_{de}$ vs. -log. i/i_d-i were linear with slopes of 30-31 mV,

(ii) the temperature co-efficients of $E_{1/2}$ and i_d were 0.2 ± 0.1 mV per degree and 0.5 ± 0.1 percent per degree respectively,

(iii) the plot of i_d vs. $\sqrt{h_{eff.}}$ was linear.

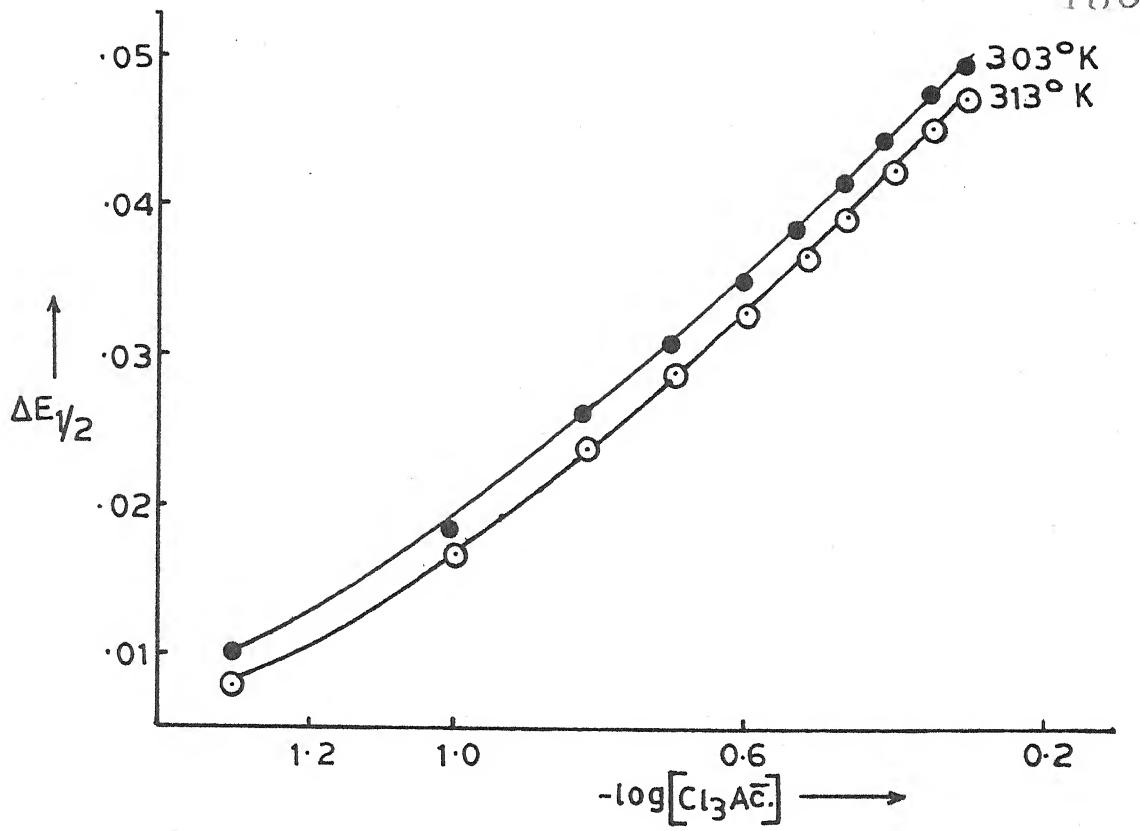

Fig. 4·19 - Plot of $\Delta E_{1/2}$ Vs. $-\log[Cl_3A\bar{c}.]$; $Pb(Cl_3A\bar{c}.)$ system.

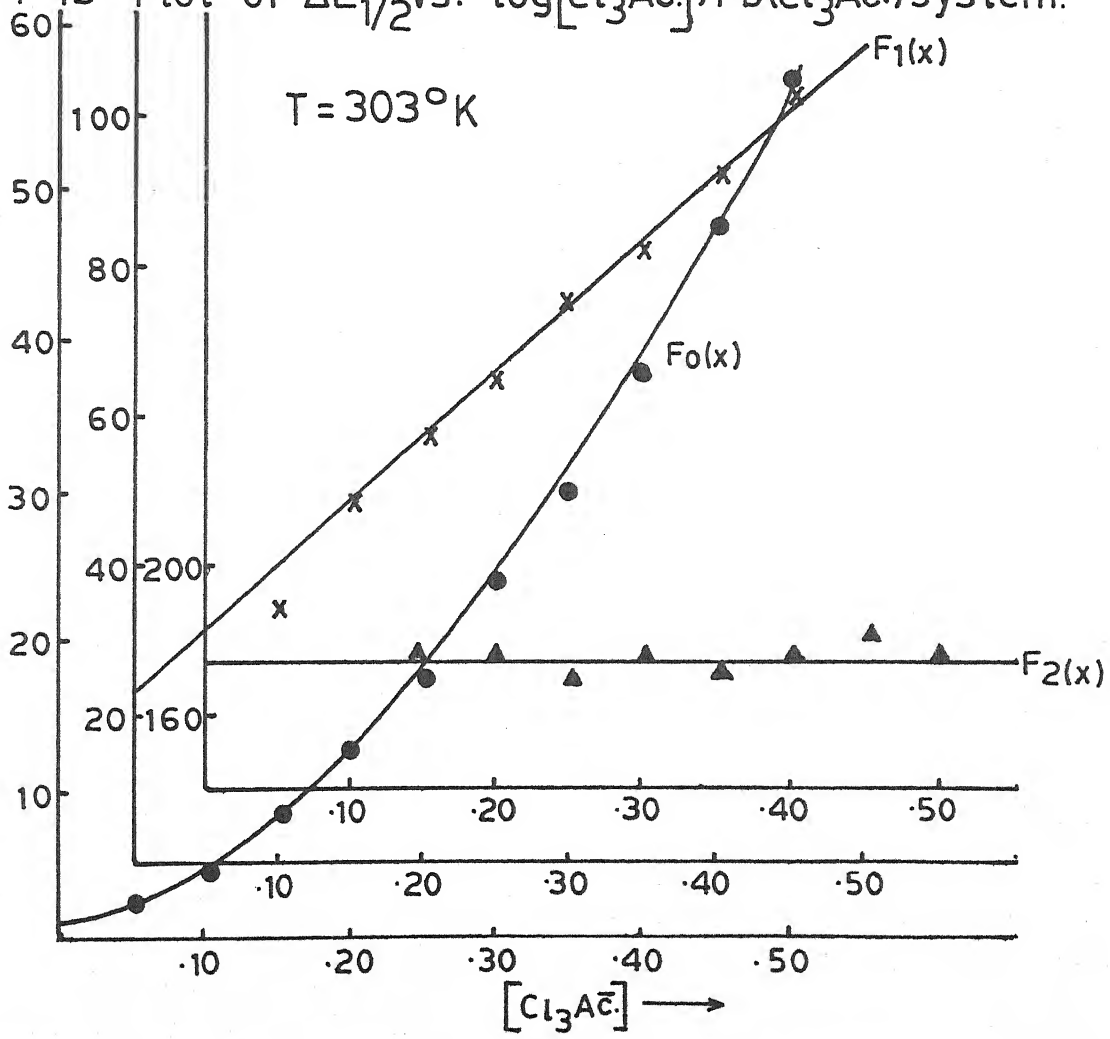

Fig. 4·20 - Plot of $F_j(x)$ Vs. $[Cl_3A\bar{c}.]$; $Pb(Cl_3A\bar{c}.)$ system.

Table 4.19

Polarographic data for Lead trichloroacetate system

Concn. of Pb^{++} ions = 0.9 mM Ionic strength = 1.0 M ($NaClO_4$)

$E_{1/2}$ of Pb^{++} ions = -0.401 V vs. SCE Temperature = 303° K

Slopes of plots of $-E_{de}$ vs. -log. i/i_d-i = 30-31 mV

$[Cl_3A\bar{c}.]$ (M)	$\Delta E_{1/2}$ (V)	log. I_M/I_C	$F_0(X)$	$F_1(X)$	$F_2(X)$
0.05	0.010	0.0287	2.29	25.8	-
0.10	0.018	0.0469	4.42	34.2	-
0.15	0.026	0.0595	8.40	49.33	178.0
0.20	0.031	0.692	12.6	58.0	177.5
0.25	0.035	0.0758	17.38	65.52	172.0
0.30	0.039	0.0791	23.80	76.0	178.0
0.35	0.042	0.0825	30.18	83.37	173.9
0.40	0.045	0.0859	38.27	93.17	176.6
0.45	0.048	0.0859	48.16	104.8	182.9
0.50	0.050	0.0859	56.14	110.28	175.6

$\beta_1 = 225$ $\beta_2 = 74$

Table 4.20

Polarographic data for Lead trichloroacetate system

Concn. of Pb^{++} ions = 0.9 mM Ionic strength = 1.0 M ($NaClO_4$)

$E_{1/2}$ of Pb^{++} ions = -0.397 V vs. SCE Temperature = 313° K

Slopes of plots of $-E_{de}$ vs. -log. i/i_d-i = 30-31 mV

$[Cl_3A\bar{c}.]$ (M)	$\Delta E_{1/2}$ (V)	log. I_M/I_C	$F_0(X)$	$F_1(X)$	$F_2(X)$
0.05	0.008	0.0314	1.94	18.8	-
0.10	0.017	0.0480	3.93	29.3	-
0.15	0.024	0.0565	6.75	38.33	145.0
0.20	0.029	0.0682	10.04	45.2	143.0
0.25	0.033	0.0771	13.80	51.2	138.8
0.30	0.037	0.0832	18.82	59.4	143.0
0.35	0.040	0.0894	23.85	65.28	139.4
0.40	0.043	0.0925	30.0	72.5	140.0
0.45	0.046	0.0925	37.49	81.08	143.5
0.50	0.048	0.0956	43.79	85.58	138.2

$\beta_1 = 16.5$ $\beta_2 = 140$

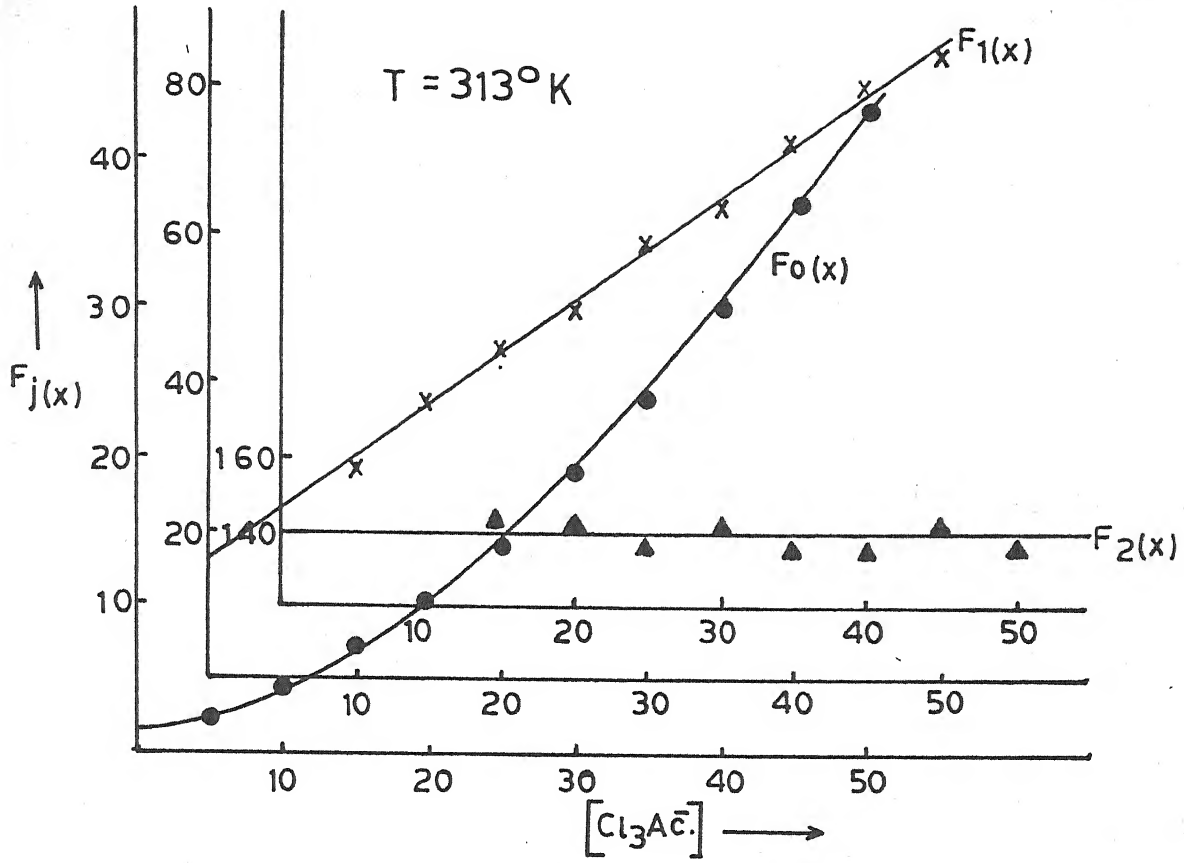

Fig. 4·21 - Plot of $F_{j(x)}$ Vs. $[Cl_3Ac.]$; $Pb(Cl_3Ac.)$ system.

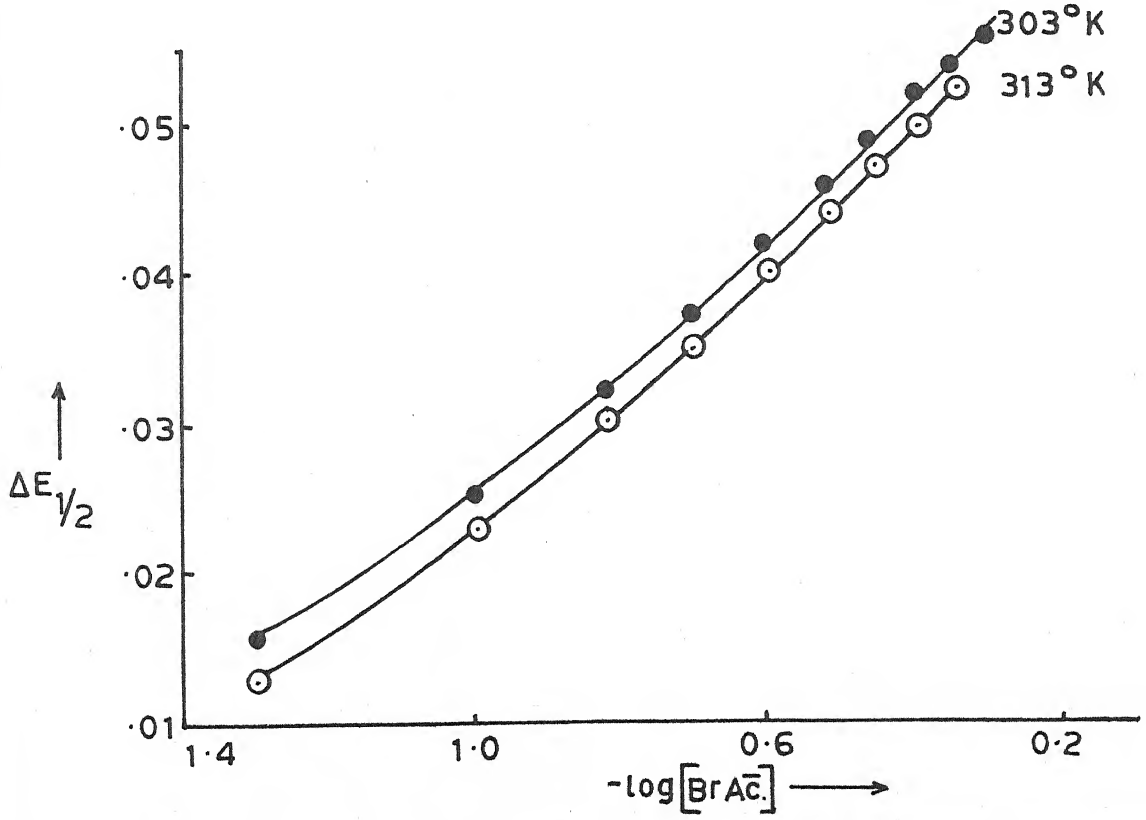

Fig. 4·22 - Plot of $\Delta E_{1/2}$ Vs. $-\log[BrAc.]$; $Pb(BrAc.)$ system.

(b) Effect of ligand concentration : The shift of $E_{1/2}$ towards the more negative side along with decrease in i_d when solutions consisting of 0.9 mM Pb(II) ions, 0.002% gelating, increasing ($Cl_3A\bar{c}$.) concentration and decreasing sodium perchlorate (to maintain μ = 1.0 M) were polarographed at 303° K ~~to~~ indicated complex formation. The successive nature of complex formation was inferred from the plot of $\Delta E_{1/2}$ vs. -log. $[Cl_3A\bar{c}.]$ which was a curve (figure 4.19). Hence the method of DeFord and Hume, when applied, gave the overall formation constant values β_1 and β_2 to be 22.5 and 174. The polarographic data and the $F_j(X)$ plots are presented in table 4.19 and figure 4.20.

(c) Effect of temperature : The temperature co-efficient values of $E_{1/2}$ and i_d have been, earlier in this section, aided in establishing the reversibility and diffusion controlled behaviour of reduction of Pb(II) in presence of trichloroacetate ions.

The previous experiment of effect of ligand concentration on $E_{1/2}$ and i_d was repeated at 313° K to obtain formation constant values of 16.5 and 140 for 1:1 and 1:2 metal/ligand ratio complexes. The polarographic data and the $F_j(X)$ plots appear in table 4.20 and figure 4.21.

The ΔG, ΔH and ΔS values calculated from effect of temperature on formation constants are included in table 4.21.

Table 4.21

Lead trichloroacetate system

Temperature (° K)	log β_1	- ΔG (kj)	- ΔH (kj)	- ΔS (kj deg^{-1}) x 10^3
303	1.3521	7.8446		54.8393
			24.4609	
313	1.2174	7.2962		54.8392

4.3.08 Lead monobromoacetate system :

(a) Nature of reduction : The observations that the linear plots of $-E_{de}$ vs. -log. i/i_d-i had slopes of 30-32 mV, the temperature co-efficients of $E_{1/2}$ and i_d were 0.2 $\pm$ 0.1 mV per degree and 0.5 $\pm$ 0.1 percent per degree and the plots of i_d vs. $\sqrt{h_{eff.}}$ were also linear combined together to conclusively prove that two electron reversible reduction of Pb(II) in presence of monobromoacetate ions is diffusion controlled.

(b) Effect of ligand concentration : As the concentration of monobromoacetate ions is increased in solutions containing 0.9 mM Pb(II) ions, 0.002% gelatin and decreasing amounts of sodium perchlorate to maintain ionic strength at 1.0 M and reduced at DME at 303° K, there was complex formation as evident from cathodic shift in $E_{1/2}$ and decrease in i_d. The curved nature of plot of $\Delta E_{1/2}$ vs. -log. $[BrAc^-]$ (figure 3.20) indicating successive complex formation enabled us to apply the method of DeFord and Hume for determination of formation constants which were found to be 39.5 and 294 for $[Pb(BrAc.)]^+$ and $[Pb(BrAc.)_2]$ complexes respectively. The polarographic data and $F_j(X)$ functions find place in table 4.22 and figure 4.23.

(c) Effect of temperature : The effect of temperature on $E_{1/2}$ and i_d has been described earlier in this section whereby the reversibility and diffusion controlled nature of reduction of Pb(II) in presence of monobromoacetate ions was inferred.

The effect of ligand concentration on $E_{1/2}$ and i_d was

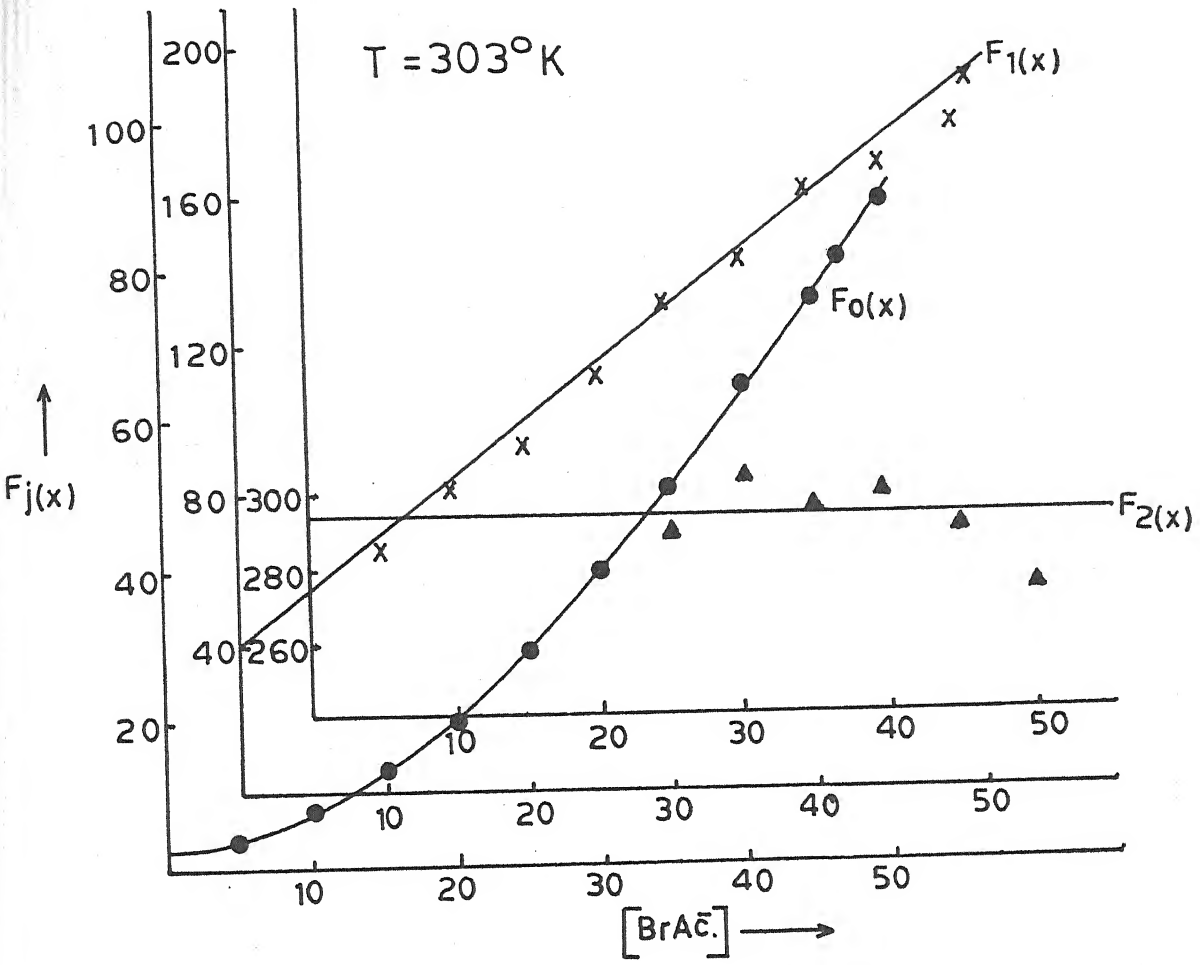

Fig. 4·23 - Plot of $F_{j(x)}$ Vs. $[BrA\bar{c}.]$; Pb(BrAc̄.) system.

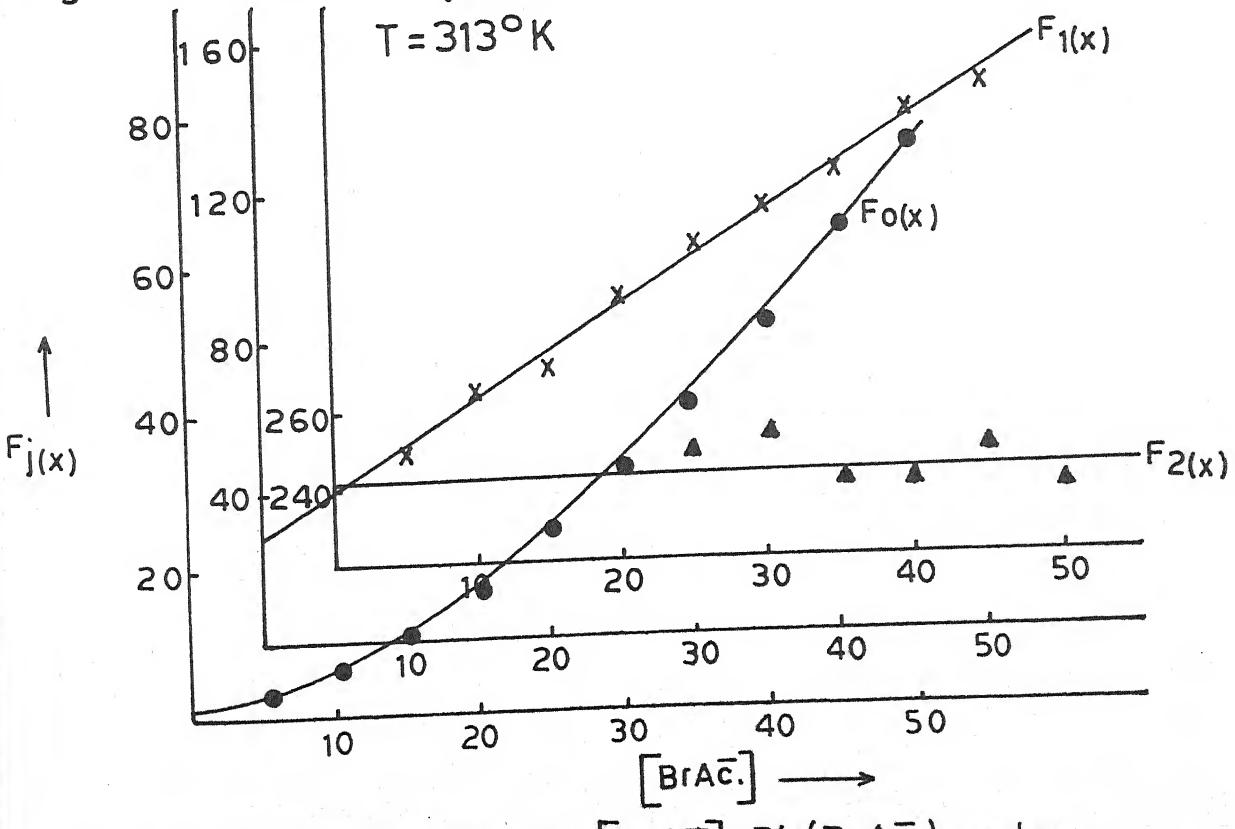

Fig. 4·24 - Plot of $F_{j(x)}$ Vs. $[BrA\bar{c}.]$; Pb(BrAc̄.) system.

Table 4.22

Polarographic data for Lead monobromoacetate system

Concn. of Pb^{++} ions = 0.9 mM Ionic strength = 1.0 M ($NaClO_4$)

$E_{1/2}$ of Pb^{++} ions = -0.401 V vs. SCE Temperature = 303° K

Slopes of plots of $-E_{de}$ vs. -log. i/i_d-i = 30-32 mV

$[BrAc^-]$ (M)	$\Delta E_{1/2}$ (V)	log. I_M/I_C	$F_0(X)$	$F_1(X)$	$F_2(X)$
0.05	0.016	0.0319	3.66	53.2	-
0.10	0.025	0.0442	7.51	65.1	-
0.15	0.032	0.0536	13.12	80.8	-
0.20	0.037	0.0599	19.53	92.65	-
0.25	0.042	0.0664	29.08	112.32	291.3
0.30	0.046	0.0763	40.42	131.4	306.3
0.35	0.049	0.0797	51.26	143.6	297.4
0.40	0.052	0.0831	65.32	160.8	303.2
0.45	0.054	0.0865	76.37	167.5	284.4
0.50	0.056	0.0899	89.73	177.5	275.9

β_1 = 39.5 β_2 = 294

Table 4.23

Polarographic data for Lead monobromoacetate system

Concn. of Pb^{++} ions = 0.9 mM Ionic strength = 1.0 M ($NaClO_4$)

$E_{1/2}$ of Pb^{++} ions = -0.397 V vs. SCE Temperature = 313° K

Slopes of plots of $-E_{de}$ vs. -log. i/i_d-i = 30-31 mV

$[BrAc^-]$ (M)	$\Delta E_{1/2}$ (V)	log. I_M/I_C	$F_0(X)$	$F_1(X)$	$F_2(X)$
0.05	0.013	0.0285	2.80	36.0	-
0.10	0.023	0.0449	6.10	51.0	-
0.15	0.030	0.0590	10.59	63.93	-
0.20	0.035	0.0707	15.77	73.85	-
0.25	0.040	0.0857	23.65	90.6	250.4
0.30	0.044	0.0919	32.27	104.23	254.1
0.35	0.047	0.0950	40.61	113.17	243.3
0.40	0.050	0.0981	51.08	125.2	243.0
0.45	0.053	0.1013	64.29	140.6	250.2
0.50	0.055	0.1045	75.10	148.2	240.4

β_1 = 28 β_2 = 242

also investigated at 313° K to compute the stability constants which were 28 and 242 for 1:1 and 1:2 complexes. Table 4.23 and figure 4.24 contain the polarographic data and $F_j(X)$ plots.

The thermodynamic functions obtained by utilising formation constants at two temperatures appear in table 4.24.

Table 4.24

Lead monobromoacetate system

Temperature (° K)	log β_1	- ΔG (kj)	- ΔH (kj)	- ΔS (kj deg^{-1})x10^3
303	1.5965	9.2625		58.9700
			27.13.04	
313	1.4471	8.6728		58.9699

4.309 Lead dibromoacetate system :

(a) Nature of reduction : Well defined polarograms obtained for the reduction of Pb(II) in presence of dibromoacetate ions revealed that

(i) straight line plots of $-E_{de}$ vs. -log. i/i_d-i have slopes of 31 $\pm$ 1 mV,

(ii) one degree rise in temperature changed the $E_{1/2}$ by 0.2 - 0.3 mV and i_d by 0.5 $\pm$ 0.1 percent,

(iii) plot of i_d vs. $\sqrt{h_{eff.}}$ is linear.

Hence it could be concluded that the reduction is reversible, involves two electrons and is totally diffusion controlled.

(b) Effect of ligand concentration : Half wave potential showed a gradual cathodic shift and i_d decreased as concentration of dibromoacetate ions was increased for polarography of solutions containing 0.9 mM Pb(II) ions, 0.002% gelatin and decreasing amounts of $NaClO_4$ to keep ionic strength constant at 1.0 M indicating complex formation between Pb(II) and $(Br_2A\bar{c}.)$ ions. The plot (figure 4.25) of $\Delta E_{1/2}$ vs. -log. $[Br_2A\bar{c}.]$ was a curve. Thus, there was multiple complex formation and method of DeFord and Hume could be used to evaluate overall formation constants. The β_1 and β_2 so obtained were 33.5 and 232. Table 4.25 and figure 4.26 depict the polarographic data and $F_j(X)$ functions.

(c) Effect of temperature : Change in $E_{1/2}$ and i_d per degree rise in temperature has, earlier in this section, been used to infer the reversibility and diffusion controlled character of reduction of Pb(II) in presence of dibromoacetate ions.

In order to determine thermodynamic functions the formation constants were determined at another temperature i.e. 313° K. The β_1 and β_2 values were found to be 25 and 180. The polarographic data, $F_j(X)$ functions and thermodynamic parameters are presented in table 4.26, figure 4.27 and table 4.27 respectively.

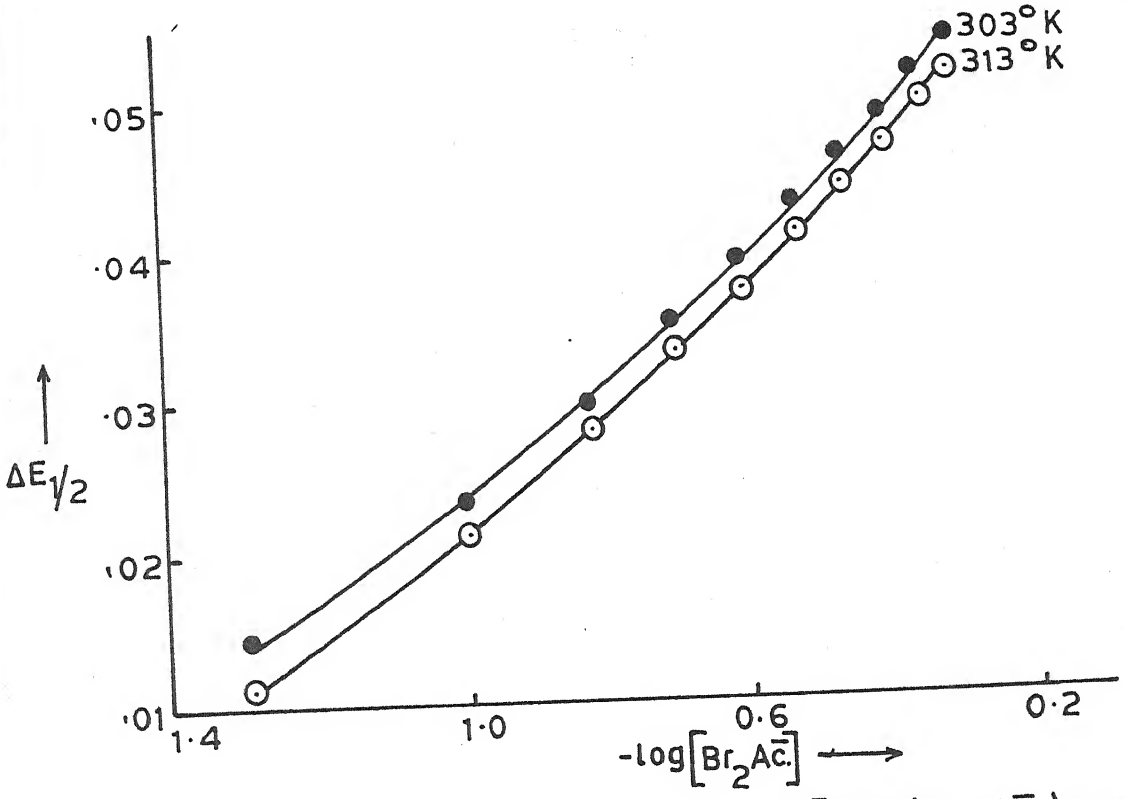

Fig. 4·25 -Plot of $\Delta E_{1/2}$ Vs. $-\log[Br_2 Ac.]$; $Pb(Br_2 Ac.)$ system.

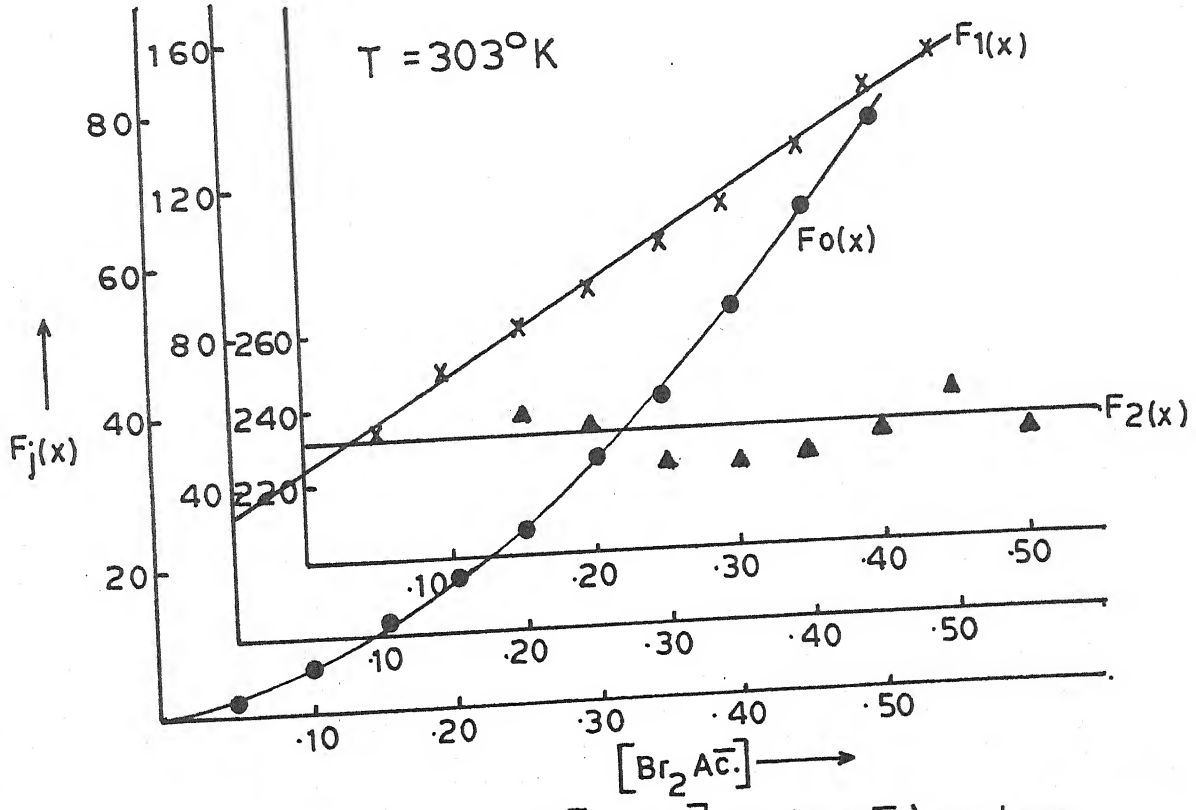

Fig. 4·26 - Plot of $F_{j(x)}$ Vs. $[Br_2 Ac.]$; $Pb(Br_2 Ac.)$ system.

Table 4.25

Polarographic data for Lead dibromoacetate system

Concn. of Pb^{++} ions = 0.9 mM Ionic strength = 1.0 M ($NaClO_4$)
$E_{1/2}$ of Pb^{++} ions = -0.401 V vs. SCE Temperature = 303° K
Slopes of plots of $-E_{de}$ vs. -log. i/i_d-i = 30-32 mV

$[Br_2A\bar{c}.]$ (M)	$\Delta E_{1/2}$ (V)	log. I_M/I_C	$F_0(X)$	$F_1(X)$	$F_2(X)$
0.05	0.014	0.0315	3.14	42.8	-
0.10	0.023	0.0466	6.48	54.8	-
0.15	0.030	0.0591	11.43	69.53	240.2
0.20	0.035	0.0687	17.13	80.65	235.7
0.25	0.039	0.0753	23.55	90.2	226.8
0.30	0.043	0.0786	32.23	104.1	226.3
0.35	0.046	0.0819	40.69	113.4	228.3
0.40	0.049	0.0853	51.94	127.35	234.6
0.45	0.052	0.0853	65.36	142.97	243.2
0.50	0.054	0.0853	76.17	150.34	233.7

β_1 = 33.5 β_2 = 232

Table 4.26

Polarographic data for Lead dibromoacetate system

Concn. of Pb^{++} ions = 0.9 mM Ionic strength = 1.0 M ($NaClO_4$)
$E_{1/2}$ of Pb^{++} ions = -0.397 V vs. SCE Temperature = 313° K
Slopes of plots of $-E_{de}$ vs. -log. i/i_d-i = 30-31 mV

$[Br_2A\bar{c}.]$ (M)	$\Delta E_{1/2}$ (V)	log. I_M/I_C	$F_0(X)$	$F_1(X)$	$F_2(X)$
0.05	0.011	0.0341	2.44	28.8	-
0.10	0.021	0.0480	5.30	43.0	180.0
0.15	0.028	0.0594	9.14	54.26	195.0
0.20	0.033	0.0682	13.51	62.55	187.7
0.25	0.037	0.0741	18.43	69.72	178.8
0.30	0.041	0.0801	25.15	80.5	185.0
0.35	0.044	0.0863	31.86	88.17	180.5
0.40	0.047	0.0894	40.08	97.7	181.8
0.45	0.050	0.0925	50.43	109.84	188.7
0.50	0.052	0.0925	58.49	114.98	180.0

β_1 = 25 β_2 = 180

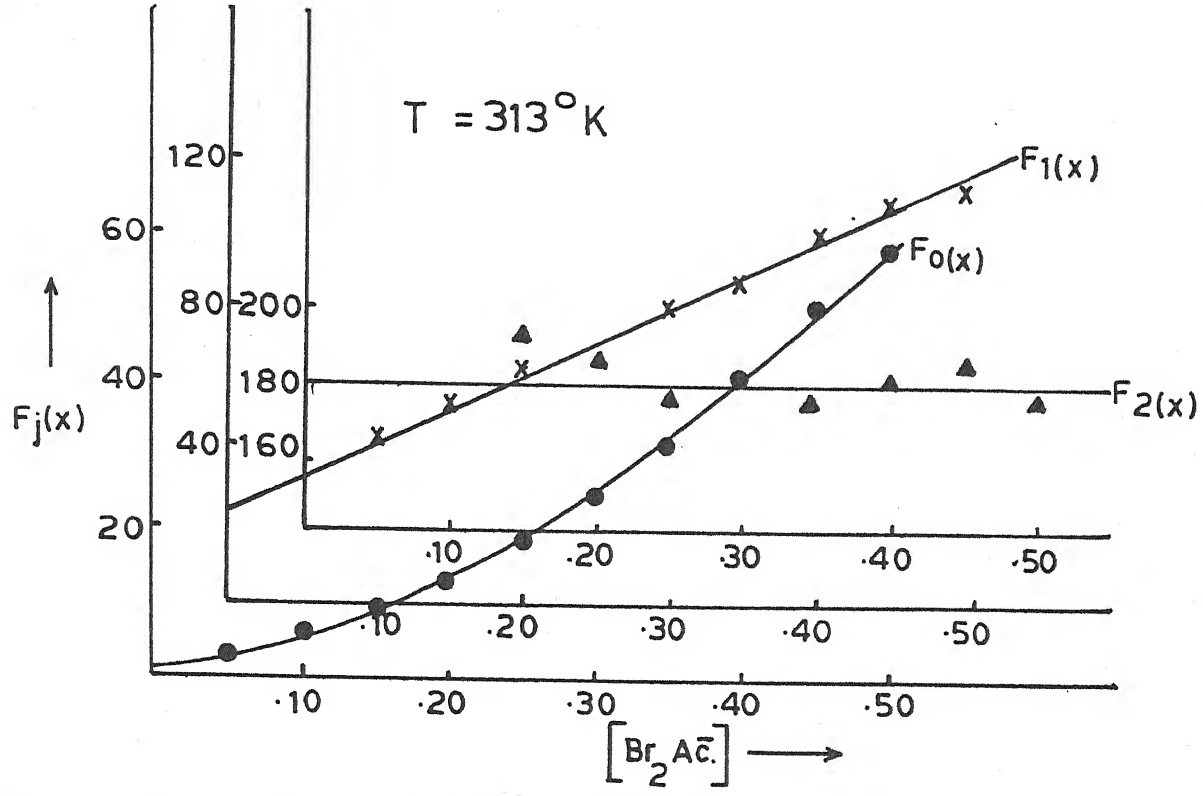

Fig. 4·27 - Plot of $F_j(x)$ Vs. $[Br_2 Ac.]$; Pb(Br_2 Ac.) system.

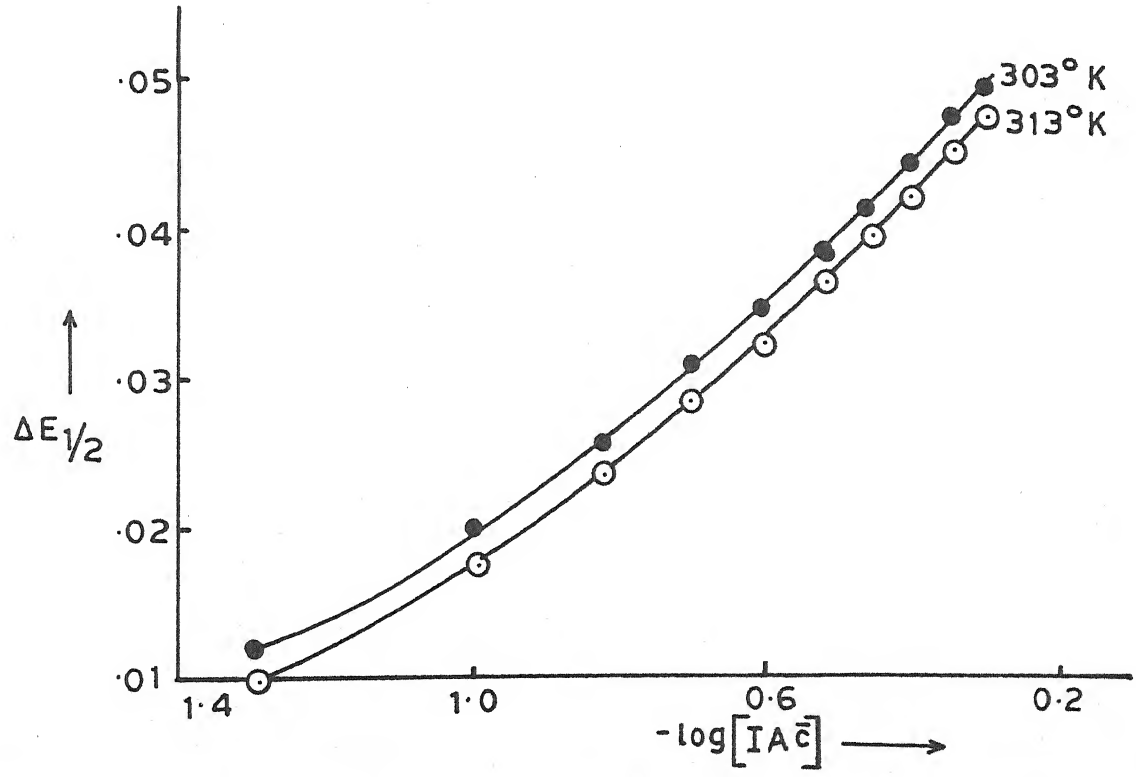

Fig. 4·28 - Plot of $\Delta E_{1/2}$ Vs. $-\log[IAc.]$; Pb(IAc.) system.

Table 4.27

Lead dibromoacetate system

Temperature (° K)	log β_1	- ΔG (kj)	- ΔH (kj)	- ΔS (kj deg^{-1})x10^3
303	1.5250	8.8477		46.9739
			23.0808	
313	1.3979	8.3779		46.9741

4.3.10 Lead monoiodoacetate system :

(a) Nature of reduction : That the reduction of Pb(II) in presence of monoiodoacetate ions, is reversible, involves two electrons and is diffusion controlled was inferred from the following observations.

(i) The plot of $-E_{de}$ vs. -log. i/i_d-i are straight lines with slopes of 31 $\pm$ 1 mV.

(ii) For every degree rise in temperature $E_{1/2}$ changes by 0.2 $\pm$ 0.1 mV and i_d by 0.5 $\pm$ 0.1 percent.

(iii) The ratio $i_d/\sqrt{h_{eff.}}$ is constant.

(b) Effect of ligand concentration : The gradual cathodic shift in half wave potential and decrease in diffusion current when solutions containing 0.9 mM Pb(II) ions, 0.002% gelatin, increasing concentration of monoiodoacetate ions and corresponding decreasing amounts of sodium perchlorate to maintain ionic strength at 1.0 M were polarographed at 303° K, definitely

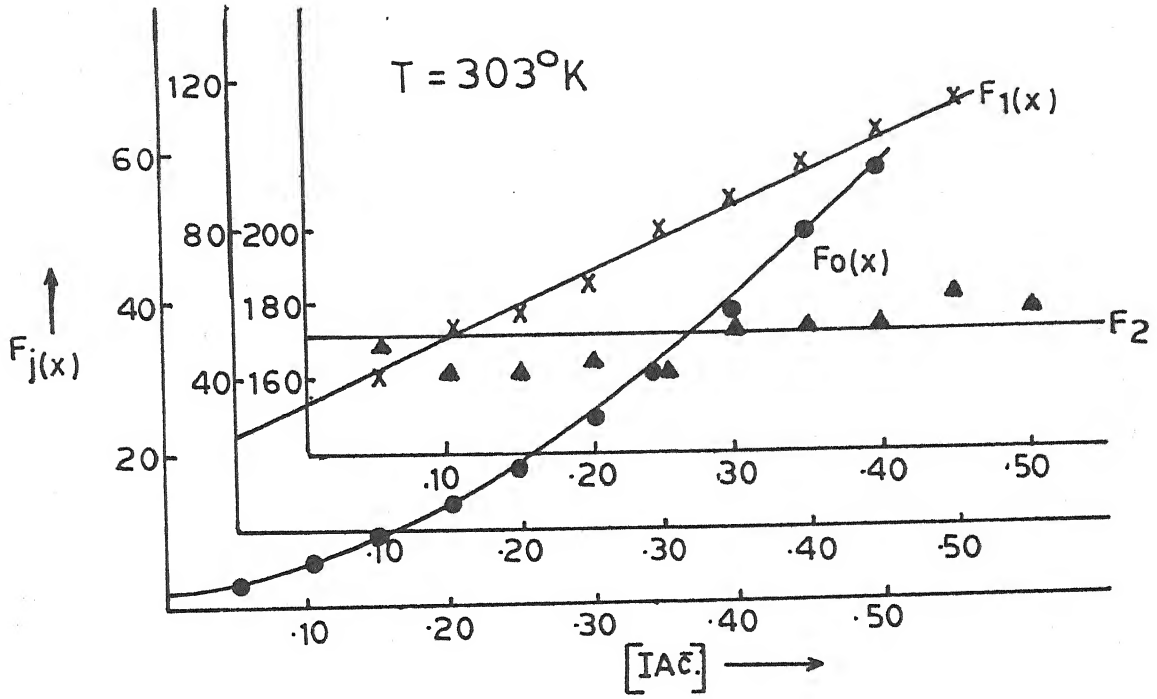

Fig. 4·29 - Plot of $F_{j(x)}$ Vs. $[IA\bar{c}.]$; Pb(IAc̄.) system.

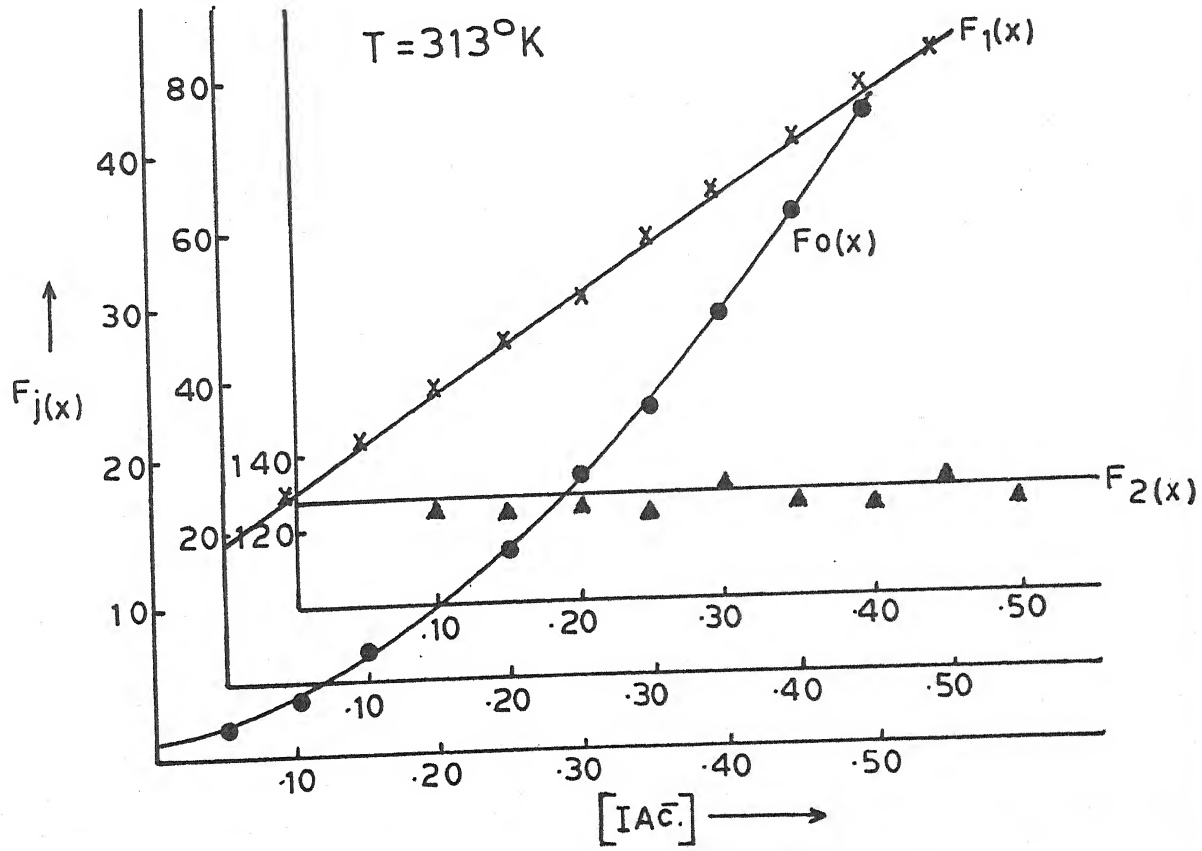

Fig. 4·30 - Plot of $F_{j(x)}$ Vs. $[IA\bar{c}.]$; Pb(IAc̄.) system.

Table 4.28

Polarographic data for Lead monoiodoacetate system

Concn. of Pb^{++} ions = 0.9 mM Ionic strength = 1.0 M ($NaClO_4$)

$E_{1/2}$ of Pb^{++} ions = -0.401 V vs. SCE Temperature = 303° K

Slopes of plots of $-E_{de}$ vs. $-\log. i/i_d-i$ = 30-32 mV

$[IAc^-]$ (M)	$\Delta E_{1/2}$ (V)	$\log. I_M/I_C$	$F_0(X)$	$F_1(X)$	$F_2(X)$
0.05	0.012	0.0299	2.68	33.6	172.0
0.10	0.020	0.0457	5.14	41.4	164.0
0.15	0.026	0.0621	8.45	49.66	164.4
0.20	0.031	0.0722	12.67	58.45	167.2
0.25	0.035	0.0791	17.52	66.08	164.3
0.30	0.039	0.0861	24.18	77.25	174.2
0.35	0.042	0.0969	31.19	86.22	175.0
0.40	0.045	0.0769	39.25	95.4	176.0
0.45	0.048	0.1005	49.25	108.3	185.0
0.50	0.050	0.1005	58.65	115.3	180.6

β_1 = 25 β_2 = 180

Table 4.29

Polarographic data for Lead monoiodoacetate system

Concn. of Pb^{++} ions = 0.9 mM Ionic strength = 1.0 M ($NaClO_4$)

$E_{1/2}$ of Pb^{++} ions = -0.397 V vs. SCE Temperature = 313° K

Slopes of plots of $-E_{de}$ vs. $-\log. i/i_d-i$ = 30-31 mV

$[IAc^-]$ (M)	$\Delta E_{1/2}$ (V)	$\log. I_M/I_C$	$F_0(X)$	$F_1(X)$	$F_2(X)$
0.05	0.010	0.0266	2.23	24.6	-
0.10	0.018	0.0434	4.19	31.9	129.0
0.15	0.024	0.0550	6.72	38.1	127.3
0.20	0.029	0.0639	9.95	44.75	128.7
0.25	0.033	0.0699	13.57	50.28	125.1
0.30	0.037	0.0760	18.52	58.4	131.3
0.35	0.040	0.0791	23.30	63.71	127.7
0.40	0.043	0.0822	29.31	70.77	129.4
0.45	0.046	0.0822	36.61	79.13	133.6
0.50	0.048	0.0854	42.78	83.56	129.1

β_1 = 19 β_2 = 128

indicated complex formation. Successive complex formation was inferred from the curved plot of $\Delta E_{1/2}$ vs. -log. $[IAc^-]$ (figure 4.28) and the method of DeFord and Hume applied to determine overall formation constants β_1 (25) and β_2 (172). The polarographic data and $F_j(X)$ functions appear in table 4.28 and figure 4.29.

(c) Effect of temperature : The temperature co-efficient of $E_{1/2}$ and i_d have been used, earlier in this section, to help establish the diffusion controlled reversible character of reduction of Pb(II) in presence of monoiodoacetate ions.

The effect of ligand concentration on $E_{1/2}$ and i_d was re-investigated at another temperature i.e. 313° K and formation constants β_1 (19) and β_2 (128) computed. Table 4.29 and figure 4.30 present the polarographic data and $F_j(x)$ functions.

From the effect of temperature on formation constant (β_1), thermodynamic functions ΔG, ΔH and ΔS were calculated and are presented in table 4.30.

Table 4.30

Lead monoiodoacetate system

Temperature (° K)	log β_1	- ΔG (kj)	- ΔH (kj)	- ΔS (kj deg^{-1})x10^3
303	1.3979	8.1103		44.6729
			21.6462	
313	1.2787	7.6635		44.6731

4.4 DISCUSSION :

The subject of stability constants or also called formation constants of metal complexes is indeed a large and varied one. The many variables associated with central metal ion and the ligand in addition to variables that arise due composition of the solvent and temperature serve to greatly complicate the subject. The only reasonable approach to the study of stability is to maintain as many variables constant as possible and then examine a small area of the subject. Only then would it be possible for us to compare and contrast the formation constants of the various systems under investigation. This is exactly what we have endeavoured in our present studies.

Our investigations on complexes of tribromo acetic acid, diiodoacetic acid and triiodoacetic acid could not be carried out due to their ready hydrolysis when their sodium salts are prepared. Their hydrolysis may be attributed to the lower carbon - halogen bond strength and greater intramolecular repulsions between larger halogen atoms rendering them unstable to form products of greater stability. This would be obvious from the following data[11].

Bond	Bond length (A^{o})	Bond energy (kj)
C - F	1.42	447.7
C - Cl	1.77	326.4
C - Br	1.91	284.5
C - I	2.13	213.4

Lead(II) does not form particularly strong complexes with the halosubstituted acids. A comparative view of the stability constants is given below :

System	At 303° K		At 313° K	
	β_1	β_2	β_1	β_2
Pb acetate	77	172	60	142
Pb monofluoroacetate	55	320	42	243
Pb difluoroacetate	18.5	128	13.5	110
Pb trifluoroacetate	16	146	12.0	100
Pb monochloroacetate	41	302	31.5	238
Pb dichloroacetate	26	164	20	108
Pb trichloroacetate	22.5	174	16.5	140
Pb monobromoacetate	39.5	274	28	242
Pb dibromoacetate	33.5	232	25	180
Pb monoiodoacetate	25	172	19	128

It may be noticed that in each case not more than two stepwise complexes are formed. Perhaps, more complexes would have formed if our ligand concentration range had been wider than 0.00 to 0.50 M.

It may also be noted that at a given temperature $K_2 (\beta_2/\beta_1)$ is invariably less than K_1 or β_1. The decrease in K_2 as compared to K_1 may be attributed to the following factors :

(a) Statistical factors : Pb(II) has a maximum co-ordination

number of six. Initially in the free metal ion $Pb(H_2O)_6^{2+}$, there are six sites for the ligand L^- to get co-ordinated to form $Pb(H_2O)_5L^+$ 1:1 metal ligand ratio complex. Now when the second ligand has to enter the co-ordination sphere, there are lesser sites i.e. only five to which it can attach itself. Hence the probability, statistically speaking, of the second ligand entering the co-ordination sphere is less than that when the first ligand was to enter. Thus 1:2 complex is less likely to form than the 1:1 complex.

(b) Steric hindrance : Once 1:1 complex has been formed, there is lesser space available around the central metal to accomodate the second ligand, as the replaced first ligand is bulkier than the water molecules initially occupying the co-ordination sphere.

(c) Coulombic factors : When the first uninegative ligand enters the co-ordination sphere to form $[Pb(H_2O)_5L]^+$ from $[Pb(H_2O)_6]^{++}$ experience certain attractive force. There is lesser attraction for the second incoming uninegative ligand as compared to the first ligand because the 1:1 complex now has only a unipositive charge on it as compared to the free metal which is bipositive.

All these factors combine together to explain why K_1, in each case, is greater than K_2.

The comparative observation of the formation constant data reveals another trend. The first formation constant values for monosubstituted acetate ion complexes are less than those of non-substituted acetate ion complexes, those for the disubstituted acid complexes are less than those of the

monosubstituted acid complex, and the trisubstituted haloacid complexes are still less stable than the disubstituted haloacid complexes. Thus the K_1 values follow the trend

$$[PbAc.]^{+} > [Pb(XAc.)]^{+} > [Pb(X_2Ac.)]^{+} > [Pb(X_3Ac.)]^{+}$$

where X stands for a given halogen.

Two factors are mainly responsible for the trend.

The substitution of a hydrogen atom by a halogen in acetic acid alters the basicity of the acetate ions depending upon the halogen introduced and the number of substitutions. The acetate ions have low basicity and hence limited co-ordinating ability which is further weakened by halogen substitution.

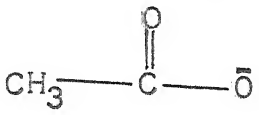

acetate ion

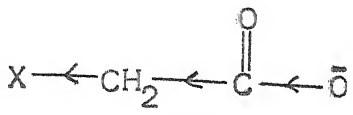

monohaloacetate ion

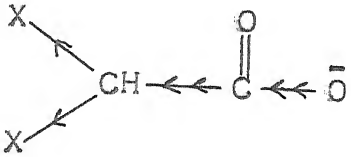

dihaloacetate ion

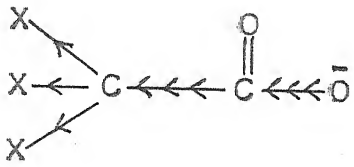

trihaloacetate ion

The high electronegativity of the halogen atom exerts a strong inductive effect, thereby reducing the basic character

of the parent ion.

The larger the number of halogen atoms, the stronger is the inductive effect and consequently weaker is the basicity of the parent acetate ion. Obviously the trisubstituted acetate ion is the weakest base while the non-substituted acetate ion is the strongest.

Another factor which is responsible for the trend is that the successively bulkier mono-, di- and tri-halosubstituted haloacetate ions experience gradually greater steric hindrance in entering the co-ordination sphere. Hence the order of stability $[Pb(Ac.)]^+ = 77 > [Pb(FAc.)]^+ = 55 > [Pb(F_2Ac.)]^+ = 18.5 > [Pb(F_3Ac.)]^+ = 16$, and so for each of the halogen at a given temperature (303° K in this case).

The survey of stability constant values also discloses the following trends :

(a) $[Pb(FAc.)]^+ > [Pb(ClAc.)]^+ > [Pb(BrAc.)]^+ > [Pb(IAc.)]^+$

(b) $[Pb(F_2Ac.)]^+ < [Pb(Cl_2Ac.)]^+ < [Pb(Br_2Ac.)]^+$

(c) $[Pb(F_3Ac.)]^+ < [Pb(Cl_3Ac.)]^+$

Inspite of the stronger inductive effect, the monofluoroacetate complex of Pb(II) has more stability than than the remaining monohaloacetate complex as $(FA\bar{c}.)$ experiences minimum steric hindrance due to its smaller size since the substituted halogen is the smallest among the halogens. Iodine,

on the other hand, being the largest has the bulkiest (IAc^-) ion. It appears that in monohaloacetate complexes, the inductive effect due to greater electronegativity is more than counter-balanced by the smaller bulk of the ligand to yield the trend (a).

However, for the di- and trihaloacetate complexes, this trend is reversed. This reversal of trend is easily explained.

Single halogen substitution of hydrogen atom in acetate ion results in a considerable increase in the size of the ligand which overweighs the inductive effect (maximum for F and minimum for I) explaining the trend (a). However, when second halogen replaces hydrogen atom in the monohaloacetate ion, there is relatively smaller increase in size of the ligand as (XAc^-) was already quite bulkie r while the inductive effect gets doubled. This effect is more pronounced when three halogen atoms have substituted in acetate ion. Consequently the basicity of (X_2Ac^-) and (X_3Ac^-) is much less. Now the inductive effect overwhelms the effect due to bulkier ligands due to the increase in size of the substituted halogen atom. It is in this context that the trends (b) and (c) appear to be logical for the electronegativity decreases in the order F > Cl > Br > I and halogen size decreases in the reverse order.

In other words, the size of the ligand governs the trend (a) while inductive effect governs the trends (b) and (c).

It is also noted that the stability constant β_1 for each system is less at the higher temperature. It is due to the

greater dissociation of the complex when the temperature is raised. It may however, be noted that ΔS values of 1:1 complexes at the two temperatures exhibit little change. This is also easily explained. In each case, our ligand is monodentate one and hence its dissociation at the elevated temperature does not result in increase or decrease in number of particles. Thus,

$$\left[Pb(H_2O)_5 \quad (XAc.)\right]^{+} + H_2O \rightleftharpoons \left[Pb(H_2O)_6\right]^{++} + (XAc.)^{-}$$

As the number of particles in a system determines its degree of disorder or entropy, there is virtually no change in entropy when the temperature is raised.

The positive shift in ΔG at higher temperatures is understandable in view of the lesser stability resulting in enhancement of its free energy.

In each system we have observed that the ΔH values are negative. This has been taken to mean that the heat content of the system has decreased due to complex formation in which weaker metal to water bonds have been replaced by stronger metal to ligand bonds.

LITERATURE CITED

1. D.P. Mellor and L.E. Maley, Nature, 159, 370 (1947).
2. R.S. Kolat and J.E. Powell, Inorg. Chem., 1, 293 (1962).
3. D.W. Archer and C.B. Monk, J. Chem. Soc., 3117 (1964).
4. D. Bannerjea and I.P. Singh, Z. Anorg. Chem., 381, 225 (1964).
5. P.J. Proll and L.H. Sutchiffe, Trerns. Faraday. Soc., 57, 1078 (1961).
6. S.A. Carrano, K.A. Chem and R.F. O'Malley, Inorg. Chem., 3, 1047 (1964).
7. Kulig Ewer, Czakis Sulikowska and W. Ryszard, Rev. Roum. Chim., 25, 1177 (1980).
8. V. Klemencis and Filipovic, Croat. Chem. Acta, 31, 3 (1959).
9. D.D. DeFord and D.N. Hume, J. Am. Chem. Soc., 73, 5321 (1951).
10. H. Irving, 'Advances in Polarography', Pergamon Press, Oxford, 49 (1960).
11. I.L. Finar, 'Organic Chemistry', Vol. 1, ELBS/Longman, 36-37 (1985).

CHAPTER V

Zn(II) complexes with

(a) acetate ion

(b) mono-, di- and trifluoroacetate ions

(c) mono-, di- and trichloroacetate ions

(d) mono- and dibromoacetate ions

(e) monoiodoacetate ion

5.1 INTRODUCTION :

Zn(II) does not form particularly strong complexes which are weaker than those of Cu(II) and Pb(II) in accord with the Mellor and Maley order[1]. The reduction of Zn acetate complex at DME was studied by Matsuda and coworkers[2] who found the logarithm of stability constant of 1:1 complex that is formed to be 0.96. Kolat and Powel[3], Archer and Monk[4] and Griesser, Prijs and Siegel[5] carried out potentiometric studies on the Zinc acetate system and reported the formation of fairly weak complexes. Arora and Mahajan[6] have made polarographic investigations into Zn(II) complexes with ligands containing one or more acetate groups.

Halosubstituted acetate ions are considerably weaker ligands than simple acetate ion due to withdrawal of electrons by comparatively more electronegative (than hydrogen) halogen atoms from the co-ordination site to reduce their basic character. Zn(II) complexes with acetic and chloroacetic acids have been explored by Van Doorne and Hannink[7]. The studies on formation of mixed carboxylato complexes of Zn(II) have been carried out by Khokhlora et.al[8] by the pH metric method. Earlier on, Zinc monochloroacetate complexes were studied by Liberti and co-workers[9] at a quinhydrone electrode to report the possibility of stepwise complex formation up to 1:4 complexes.

However, no serious attempt has been made to study Zn(II) complexes systematically with various halosubstituted acetic acids in order to explore the effect of electron withdrawal

by steric hindrance due to substituted halogens. It is in this context that it was thought worthwhile to make polarographic examination of Zinc haloacetate complexes under identical conditions at two different temperatures to study the above effects and compute the thermodynamic parameters viz. ΔG, ΔH and ΔS.

5.2 EXPERIMENTAL :

All chemicals of analy-tical reagent grade purity were used. Halosubstituted acetic acids manufactured by K & K (USA), Fluka (Swiss), BDH (UK) and Riedel (German) were used. Their sodium salts were prepared by adding a dilute solution of sodium bicarbonate. Care had to be taken in handling the haloacetic acids as they cause serious burns and blisters on the skin. A semimicro burette was used to add requisite amounts of their salt solution to the test solutions.

All solutions were made in double distilled conductivity water. Sodium perchlorate at 1.0 M was the supporting electrolyte used. With increasing concentration of the ligand, its concentration was correspondingly reduced to maintain the ionic strength. In each case the concentration of Zn(II) ions was kept constant at 0.9 mM. 0.002% gelatin, in final solutions, was just sufficient to suppress the maxima observed.

The polarography of each test solution was carried out by placing it in a thermostated H-cell coupled with a saturated calomel electrode. Prior to the polarographic examination of each solution, hydrogen gas was passed for about ten minutes to remove dissolved oxygen. The potential of DME was gradually

increased and the change in current noted.

The intercept on the potential axis in the plot of $-E_{de}$ vs. -log. i/i_d-i gave the half wave potential.

The capillary had the following characteristics in 0.1 M sodium perchlorate in the open circuit.

m = 2.43 mg/sec

t = 2.9 sec

$h_{corr.}$ = 53 cms.

Investigations on effect of ligand concentration on half wave potential and diffusion current were effected at two temperatures i.e. 303° and 313° K.

5.3 RESULTS :

(a) Nature of reduction : That Zn(II) reduces reversibly with two electron transfer and diffusion control in presence of acetate ions could be deduced from the following observations :

(i) The linear conventional log. plots had slopes of 31-32 mV.

(ii) The change in $E_{1/2}$ and i_d per degree rise in temperature was 0.3 $\pm$ 0.1 mV and 0.6 $\pm$ 0.1 percent.

(iii) The linearity of plot of i_d vs. square root of effective height of mercury column of the DME.

(b) Effect of ligand concentration : Well defined polarographic waves at 303° K of solutions containing 0.9 mM Zn(II) ions, 0.002% gelatin, increasing concentrations of acetate ions and requisite amounts of sodium perchlorate to keep ionic strength at 1.0 M shifted towards more negative side and had decreased heights

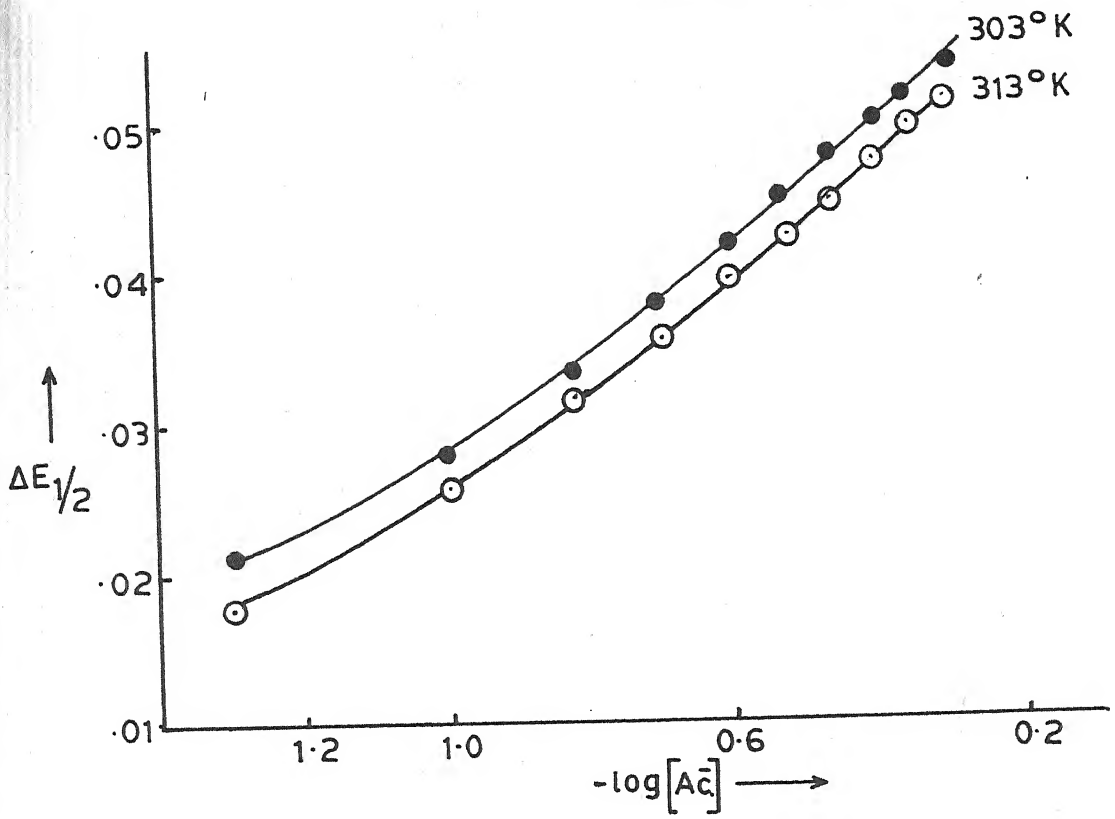

Fig.5·01-Plot of $\Delta E_{1/2}$ Vs. $-\log[Ac.]$; Zn(Ac.) system.

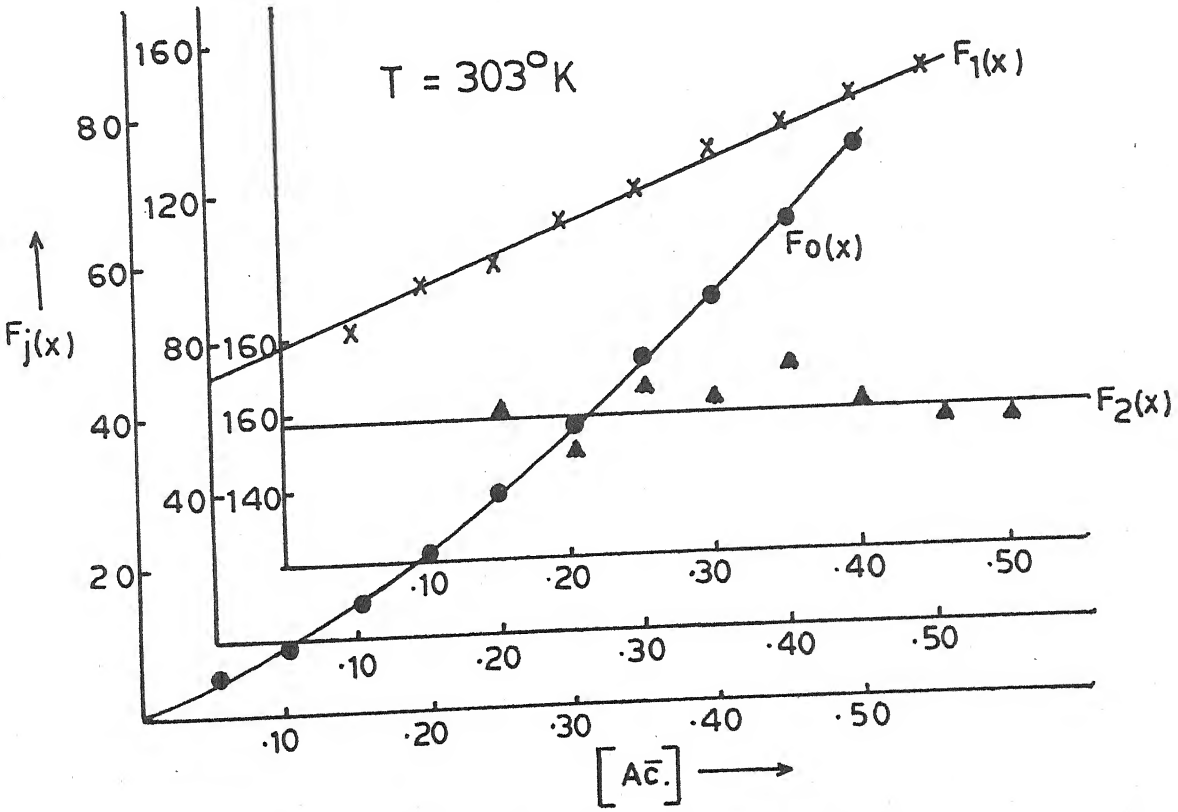

Fig.5·02-Plot of $F_{j(x)}$ Vs. $[Ac.]$; Zn(Ac.) system.

Table 5.01

Polarographic data for Zinc acetate system

Concn. of Zn^{++} ions = 0.9 mM Ionic strength = 1.0 M ($NaClO_4$)

$E_{1/2}$ of Zn^{++} ions = -0.998 V vs. SCE Temperature = 303° K

Slopes of plots of $-E_{de}$ vs. $-\log. i/i_d - i$ = 31-32 mV

$[\bar{Ac}.]$ (M)	$\Delta E_{1/2}$ (V)	$\log. I_M/I_C$	$F_0(X)$	$F_1(X)$	$F_2(X)$
0.05	0.021	0.0263	5.3	-	-
0.10	0.028	0.0385	9.33	83.0	-
0.15	0.034	0.0511	15.21	94.73	161.5
0.20	0.038	0.0608	21.13	100.65	150.7
0.25	0.042	0.0674	29.15	112.6	168.4
0.30	0.045	0.0704	36.96	119.86	164.5
0.35	0.048	0.0741	46.87	131.05	173.0
0.40	0.050	0.0774	55.06	135.15	161.6
0.45	0.052	0.0808	64.68	141.55	157.8
0.50	0.054	0.0808	75.39	148.78	156.6

β_1 = 70.5 β_2 = 158

Table 5.02

Polarographic data for Zinc acetate system

Concn. of Zn^{++} ions = 0.9 mM Ionic strength = 1.0 M ($NaClO_4$)

$E_{1/2}$ of Zn^{++} ions = -0.991 V vs. SCE Temperature = 313° K

Slopes of plots of $-E_{de}$ vs. $-\log. i/i_d - i$ = 31-32 mV

$[\bar{Ac}.]$ (M)	$\Delta E_{1/2}$ (V)	$\log. I_M/I_C$	$F_0(X)$	$F_1(X)$	$F_2(X)$
0.05	0.018	0.0375	4.14	62.8	-
0.10	0.026	0.0517	7.74	67.4	-
0.15	0.032	0.0635	12.41	76.0	120.0
0.20	0.036	0.0725	17.05	80.25	111.2
0.25	0.040	0.0786	23.27	89.08	124.3
0.30	0.043	0.0848	29.48	94.93	123.1
0.35	0.045	0.0913	34.70	96.28	109.4
0.40	0.048	0.0943	43.66	106.65	121.6
0.45	0.050	0.0975	51.02	111.15	118.1
0.50	0.052	0.0975	59.17	116.37	116.7

β_1 = 58 β_2 = 120

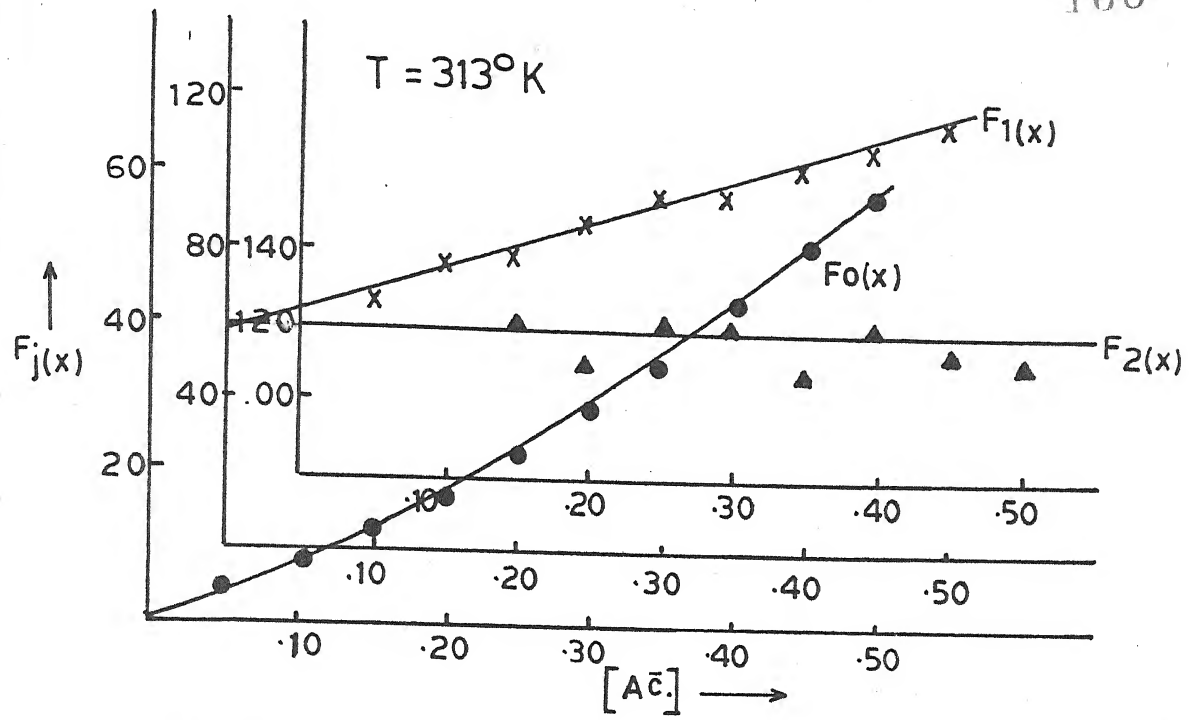

Fig. 5·03 - Plot of $F_{j(x)}$ Vs. $[A\bar{c}.]$; Zn(Ac̄.) system.

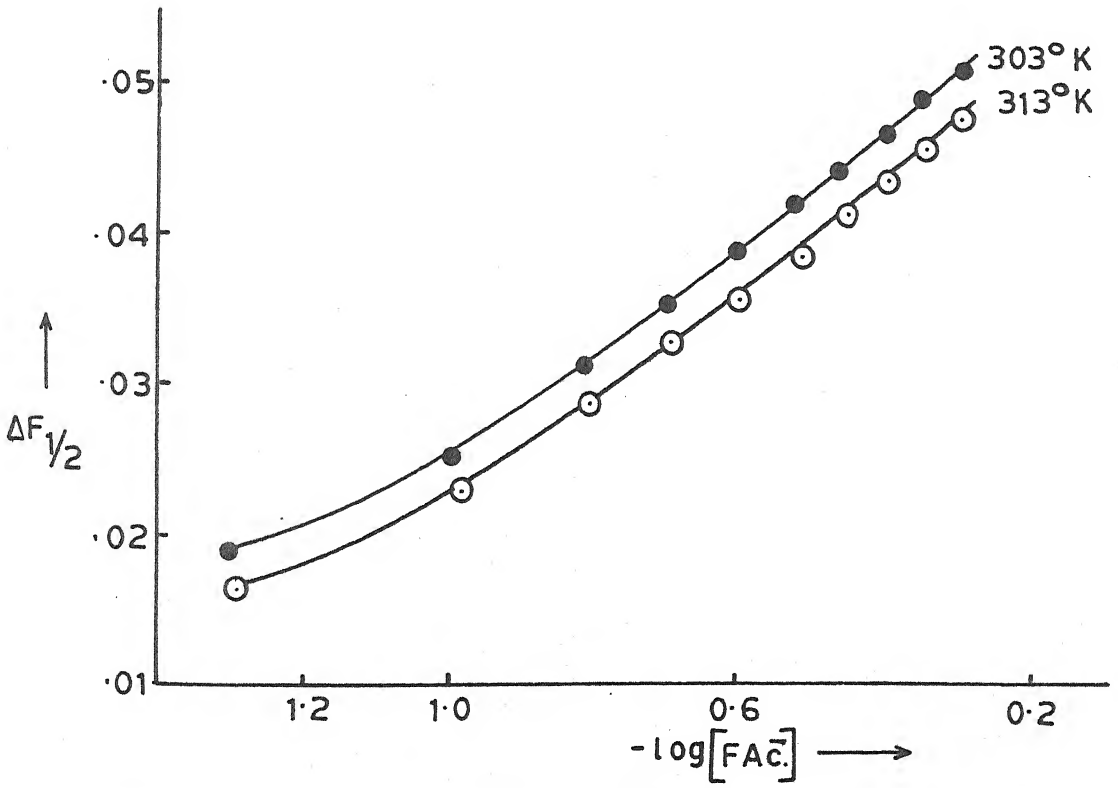

Fig. 5·04 - Plot of $\Delta E_{1/2}$ Vs. $-\log[FA\bar{c}.]$; Zn(FAc̄.) system.

with increasing ligand concentration indicating complex formation The plot of $\Delta E_{1/2}$ vs. -log $[\bar{Ac}.]$ being a curve (figure 5.01) stepwise complex formation was inferred leading to the applicatio of method of DeFord and Hume[10] as improved by Irving[11] to compute the formation constants of the complexes which were found to be 70.5 and 158 respectively for $[Zn(Ac.)]^+$ and $[Zn(Ac.)_2]$ complexes ~~respectively~~. The polarographic data and the $F_j(X)$ functions are presented in table 5.01 and figure 5.02.

(c) Effect of temperature : Changes in $E_{1/2}$ and i_d per degree rise in temperature have been conveniently used earlier in this section to show that the reduction of Zinc acetate complex is reversible and diffusion controlled.

The experiment of effect of ligand concentration on $E_{1/2}$ and i_d was repeated at 313° K to compute the stepwise overal formation constants which were found to be 58 and 120 for 1:1 and 1:2 complexes. The relevant polarographic data and $F_j(X)$ function are included in table 5.02 and figure 5.03.

The thermodynamic variables ΔG, ΔH and ΔS were calculated from the knowledge of formation constants at two temperatures. Table 5.03 presents these functions.

Table 5.03

Zinc acetate system

Temperature (° K)	log β_1	- ΔG (kj)	- ΔH (kj)	- ΔS (kj deg^{-1})x10^3
303	1.8481	10.7222	15.3811	15.3759
313	1.7634	10.5685		15.3757

5.3.02 Zinc monofluoroacetate system :

(a) Nature of reduction : The straight line nature of the conventional log. plots, the temperature coefficients of $E_{1/2}$ and i_d (0.2 ± 0.1 mV per degree and 0.6 ± 1 percent per degree) coupled with the linearity of diffusion current against square root of effective height of mercury column, conclusively established that the reduction of Zn(II) in presence of monofluoroacetate ions is reversible, involves two electrons and is diffusion controlled.

(b) Effect of ligand concentration : Half wave potential shifted towards the cathodic direction and diffusion current decreased with increasing ligand concentration when solutions containing 0.9 mM Zn(II) ions, 0.002% gelatin and requisite amount of sodium perchlorate to maintain ionic strength at 1.0 M were polarographed at 303° K to indicate complex formation. The curved nature of the plot of $\Delta E_{1/2}$ vs. -log. $[FAc^-]$ (figure 5.04) made us use the method of DeFord and Hume as successive complex formation had occurred. The formation constants so obtained for 1:1 and 1:2 complexes were 54 and 132 as shown by the polarographic data in table 5.04 and figure 5.05.

(c) Effect of temperature : The reversibility and diffusion managed nature of reduction of Zn(II) in presence of monofluoroacetate ions has already been, earlier in this section, inferred with the aid of temperature coefficient of $E_{1/2}$ and i_d.

In order to compute thermodynamic parameters ΔG, ΔH and ΔS, the formation constants were determined at another

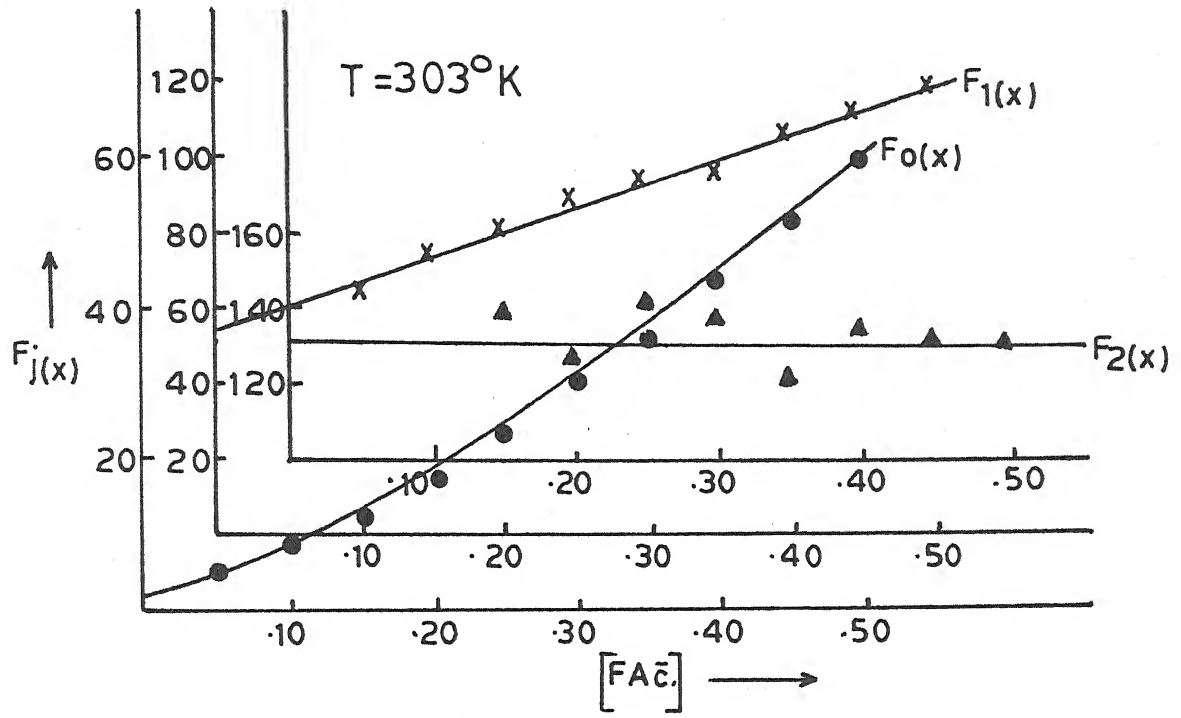

Fig.5·05 - Plot of $F_{j(x)}$ Vs. $[FA\bar{c}.]$; Zn(FAc̄.)system.

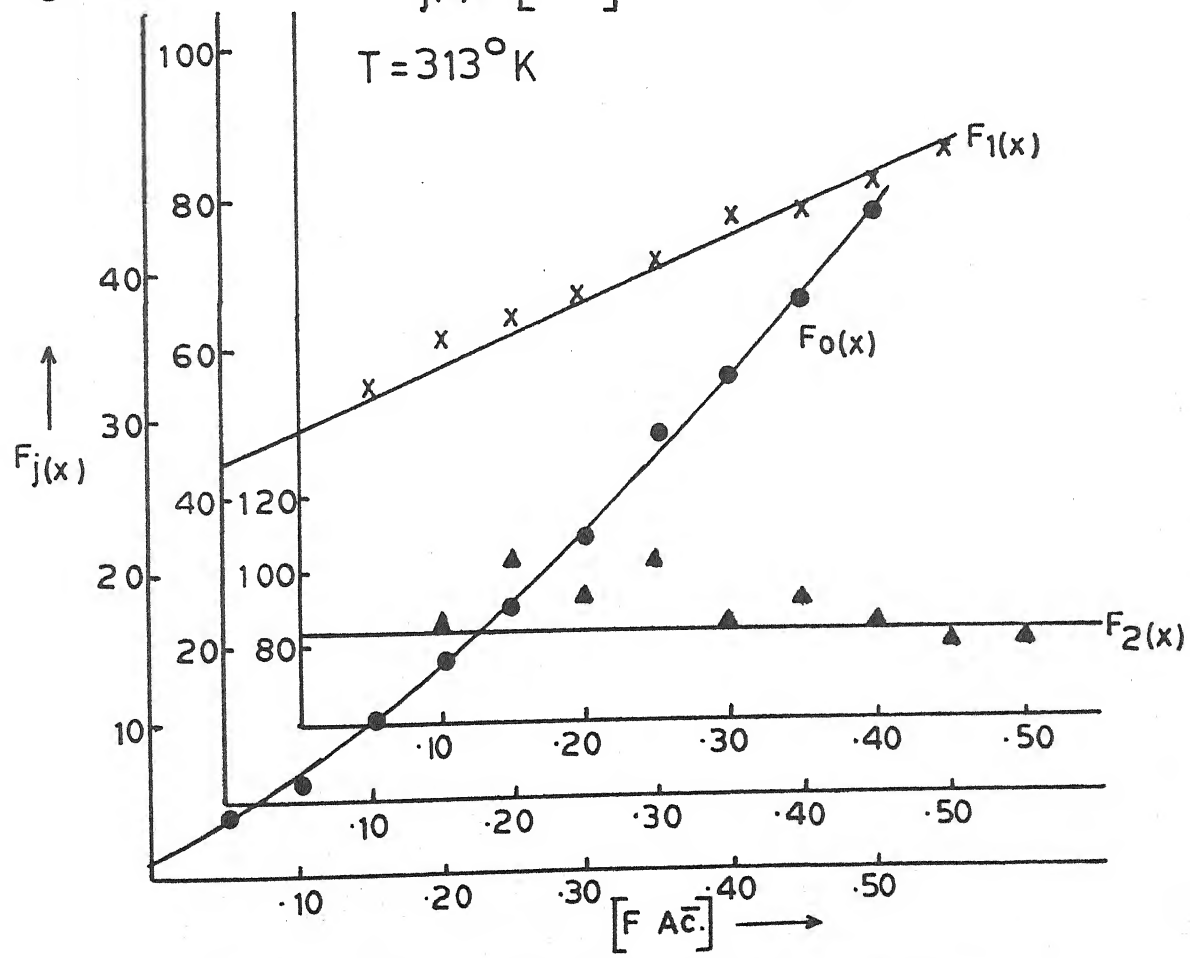

Fig.5·06 - Plot of $F_{j(x)}$ Vs. $[FA\bar{c}.]$; Zn(FAc̄.)system.

Table 5.04

Polarographic data for Zinc monofluoroacetate system

Concn. of Zn^{++} ions = 0.9 mM Ionic strength = 1.0 M ($NaClO_4$)

$E_{1/2}$ of Zn^{++} ions = -0.998 V vs. SCE Temperature = 303° K

Slopes of plots of $-E_{de}$ vs. -log. i/i_d-i = 31.32 mV

$[F\bar{A}c.]$ (M)	$\Delta E_{1/2}$ (V)	log. I_M/I_C	$F_0(X)$	$F_1(X)$	$F_2(X)$
0.05	0.019	0.0326	4.62	-	-
0.10	0.025	0.0451	7.53	65.3	-
0.15	0.031	0.0599	12.28	75.2	141.3
0.20	0.035	0.0676	17.07	80.35	131.7
0.25	0.039	0.0746	23.55	90.2	144.8
0.30	0.042	0.0780	29.87	96.23	140.7
0.35	0.044	0.0818	35.09	97.4	124.0
0.40	0.047	0.0845	44.51	108.77	136.9
0.45	0.049	0.0884	52.30	114.06	133.4
0.50	0.051	0.0884	60.96	119.92	131.8

β_1 = 54 β_2 = 132

Table 5.05

Polarographic data for Zinc monofluoroacetate system

Concn. of Zn^{++} ions = 0.9 mM Ionic strength = 1.0 M ($NaClO_4$)

$E_{1/2}$ of Zn^{++} ions = -0.991 V vs. SCE Temperature = 313° K

Slopes of plots of $-E_{de}$ vs. -log. i/i_d-i = 31-32 mV

$[F\bar{A}c.]$ (M)	$\Delta E_{1/2}$ (V)	log. I_M/I_C	$F_0(X)$	$F_1(X)$	$F_2(X)$
0.05	0.017	0.0489	3.94	-	-
0.10	0.023	0.0635	6.37	53.7	87.0
0.15	0.029	0.0725	10.15	61.0	106.6
0.20	0.033	0.0786	13.84	64.2	96.0
0.25	0.036	0.0848	17.54	66.16	105.8
0.30	0.039	0.0911	22.24	70.8	86.0
0.35	0.042	0.0975	28.8	77.6	93.2
0.40	0.044	0.0975	21.70	79.25	85.6
0.45	0.046	0.1007	38.21	82.68	83.4
0.50	0.048	0.1007	44.31	86.62	83.2

β_1 = 45 β_2 = 84

temperature i.e. 313° K and were found to be 45 and 84 for 1:1 and 1:2 metal/ligand ratio complexes. The relevant polarographic data, $F_j(X)$ plots and thermodynamic parameters have been presented in table 5.05, figure 5.06 and table 5.06 respectively.

Table 5.06

Zinc monofluoroacetate system

Temperature (° K)	log β_1	- G (kj)	- H (kj)	- S (kj deg^{-1})x10^3
303	1.7323	10.0504		14.2369
			14.3642	
313	1.6532	9.9080		14.2370

5.3.03 Zinc difluoroacetate system :

(a) Nature of reduction : That the reduction of Zn(II) in presence of difluoroacetate ions is reversible involving two electrons and is diffusion controlled could be deduced from the following observations.

(i) Linearity of plots of $-E_{de}$ vs. -log. i/i_d-i with slopes of 31-32 mV.

(ii) Temperature coefficient values of $E_{1/2}$ and i_d which were 0.2-0.3 mV per degree and 0.6 $\pm$ 0.1 percent per degree respectively.

(iii) Constancy of the ratio $i_d/\sqrt{h_{eff.}}$.

(b) Effect of ligand concentration : When solutions containing

0.9 mM Zn(II) ions, 0.002% gelatin, increasing ($F_2A\bar{c}.$) ion concentration and decreasing $NaClO_4$ concentration (for μ= 1.0 M) were polarographed at 303° K, a gradual shift in $E_{1/2}$ to the more negative side coupled with decrease in i_d gave evidence of complex formation between Zn(II) and ($F_2Ac.$) ions. Formation of more than one complex was inferred from the plot of $\Delta E_{1/2}$ vs. -log. $[F_2A\bar{c}.]$ which was a curve (figure 5.07). The method of DeFord and Hume could, therefore, be applied to compute the overall stability constants which were 15.5 and 100 respectively for $[Zn(F_2Ac.)]^+$ and $[Zn(F_2Ac.)_2]$ complexes. The polarographic data and $F_j(X)$ functions appear in table 5.07 and figure 5.08.

(c) Effect of temperature : Earlier in this section, the reversible and diffusion controlled behaviour of Zn(II) in presence of ($F_2A\bar{c}.$) ions has been established from the temperature co-efficient of $E_{1/2}$ and i_d.

The procedure (b) was repeated at 313° K and the stability constant values so obtained are 12.5 and 80 for 1:1 and 1:2 complexes. The relevant polarographic data and $F_j(X)$ plots are presented in table 5.08 and figure 5.09.

The knowledge of stability constants at two temperatures was used to compute thermodynamic functions which are given in table 5.09.

PTO

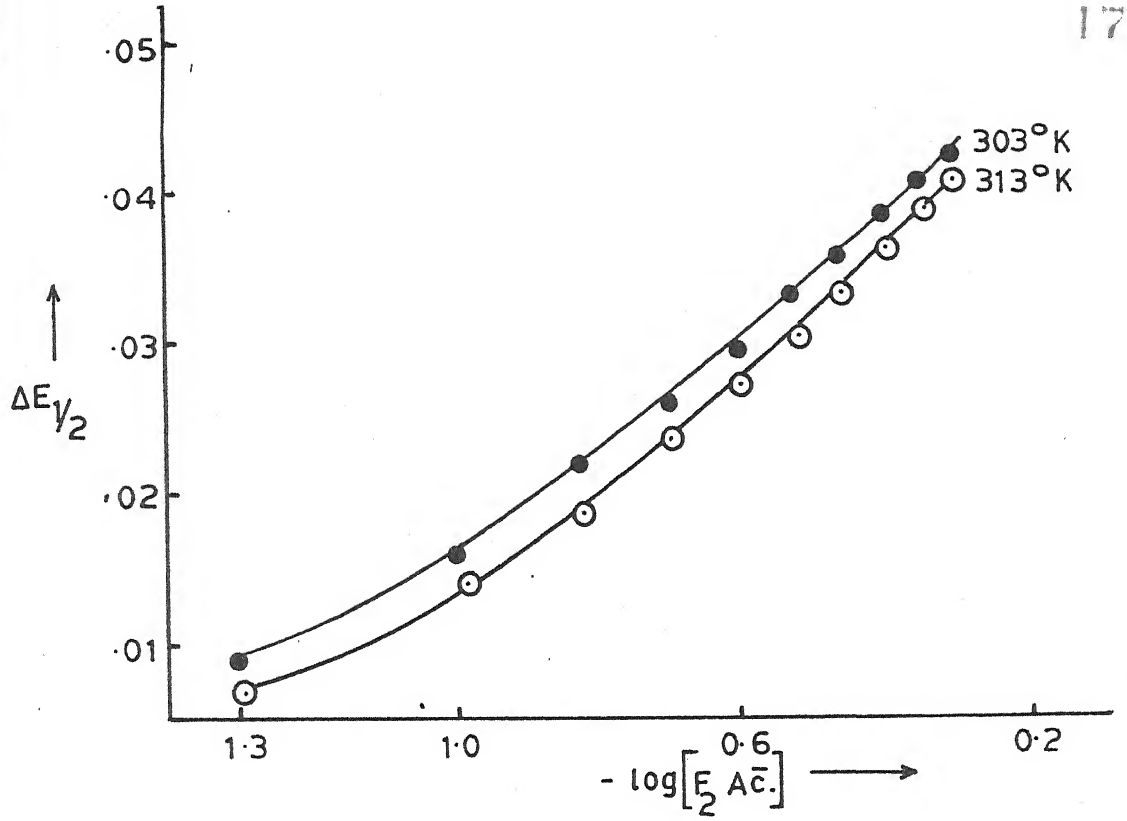

Fig. 5·07 - Plot of $\Delta E_{1/2}$ Vs. $-\log[F_2 A\bar{c}.]$; $Zn(F_2 A\bar{c}.)$ system.

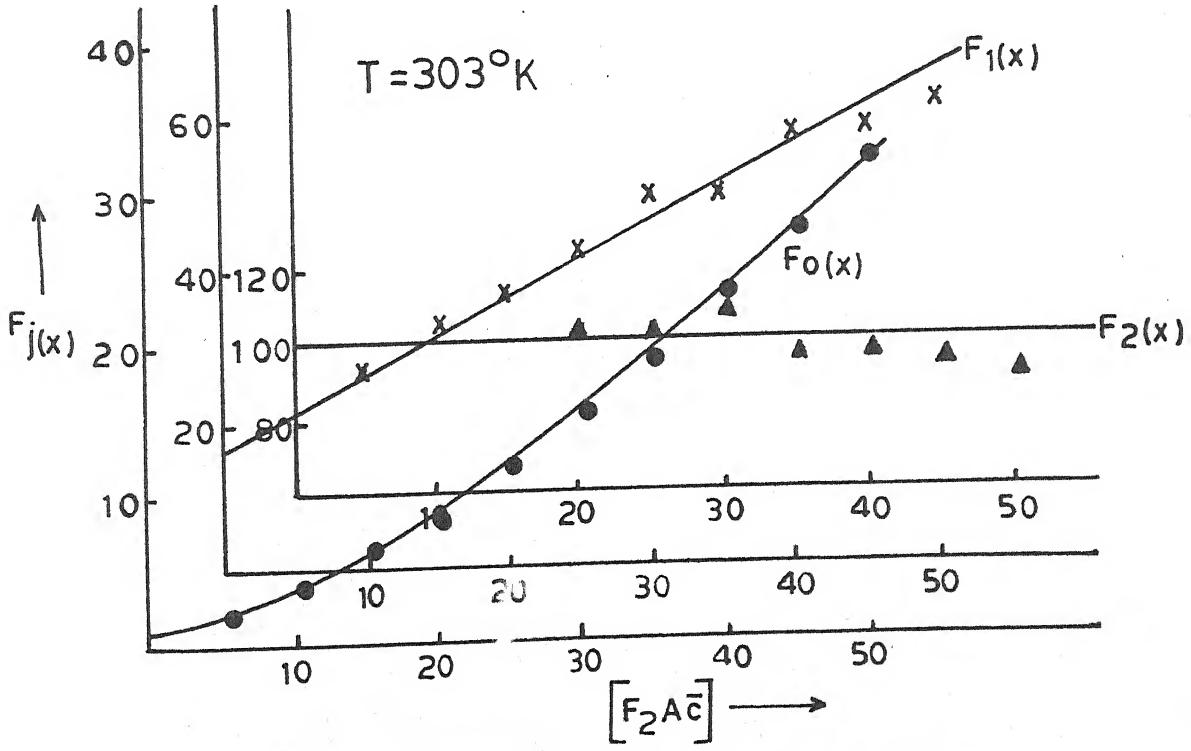

Fig. 5·08 - Plot of $F_{j(x)}$ Vs. $[F_2 A\bar{c}.]$; $Zn(F_2 A\bar{c}.)$ system.

Table 5.07

Polarographic data for Zinc difluoroacetate system

Concn. of Zn^{++} ions = 0.9 mM Ionic strength = 1.0 M ($NaClO_4$)

$E_{1/2}$ of Zn^{++} ions = -0.998 V vs. SCE Temperature = 303° K

Slopes of plots of $-E_{de}$ vs. -log. i/i_d-i = 31-32 mV

$[F_2Ac^-]$ (M)	$\Delta E_{1/2}$ (V)	log. I_M/I_C	$F_0(X)$	$F_1(X)$	$F_2(X)$
0.05	0.009	0.0179	2.07	21.4	-
0.10	0.016	0.0303	3.65	26.5	-
0.15	0.022	0.431	5.95	33.0	-
0.20	0.026	0.0529	8.27	36.35	104.2
0.25	0.030	0.0596	11.42	41.68	104.7
0.30	0.034	0.0630	15.63	48.76	110.9
0.35	0.036	0.0698	18.51	50.0	98.6
0.40	0.039	0.0698	23.29	55.72	100.5
0.45	0.041	0.0733	27.37	58.6	95.8
0.50	0.043	0.0733	31.90	61.8	92.6

β_1 = 15.5 β_2 = 100

Table 5.08

Polarographic data for Zinc difluoroacetate system

Concn. of Zn^{++} ions = 0.9 mM Ionic strength = 1.0 M ($NaClO_4$)

$E_{1/2}$ of Zn^{++} ions = -0.991 V vs. SCE Temperature = 313° K

Slopes of plots of $-E_{de}$ vs. -log. i/i_d-i = 31-32 mV

$[F_2Ac^-]$ (M)	$\Delta E_{1/2}$ (V)	log. I_M/I_C	$F_0(X)$	$F_1(X)$	$F_2(X)$
0.05	0.007	0.0327	1.81	16.2	-
0.10	0.014	0.0472	3.14	21.4	-
0.15	0.019	0.0561	4.65	24.33	78.8
0.20	0.024	0.0651	6.88	29.4	84.5
0.25	0.028	0.0713	9.39	33.56	84.2
0.30	0.031	0.0776	11.91	36.36	79.5
0.35	0.034	0.0807	14.98	39.94	78.4
0.40	0.037	0.0839	18.85	44.62	80.3
0.45	0.040	0.0839	22.88	48.62	80.2
0.50	0.042	0.0871	27.52	53.0	81.0

β_1 = 12.5 β_2 = 80

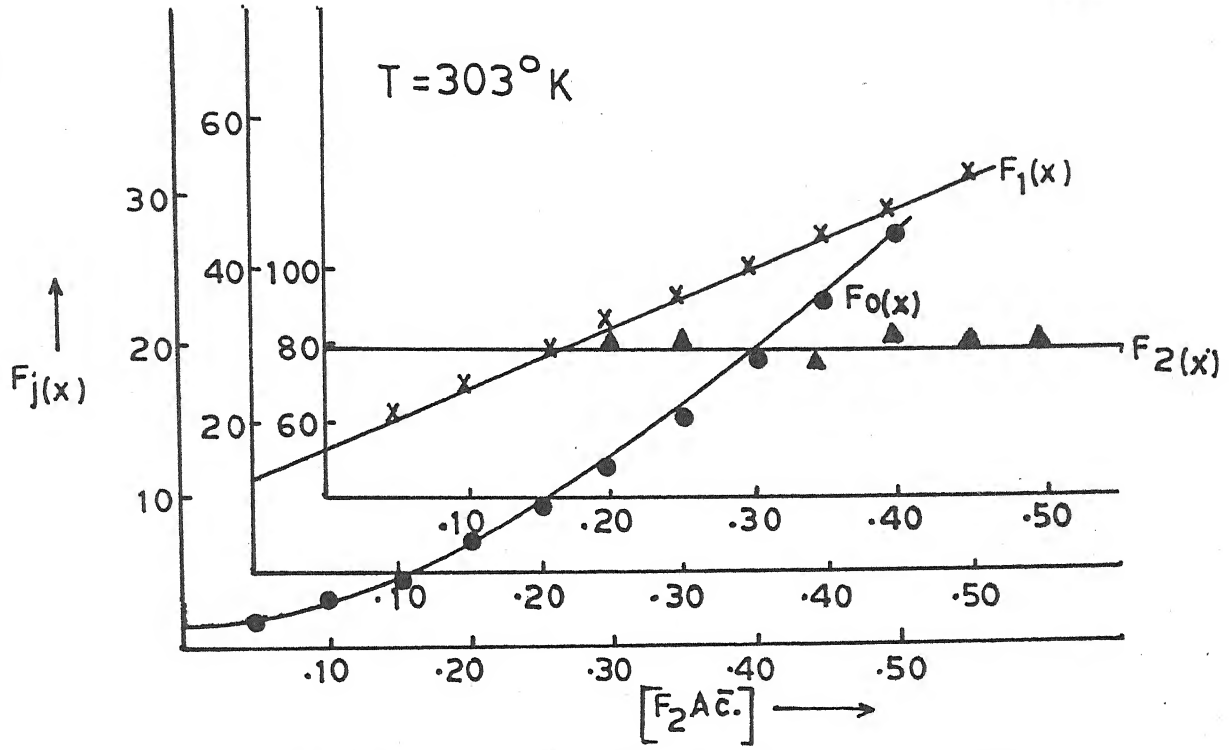

Fig. 5·09 - Plot of $F_{j(x)}$ Vs. $[F_2 A\bar{c}.]$; Zn($F_2 A\bar{c}.$) system.

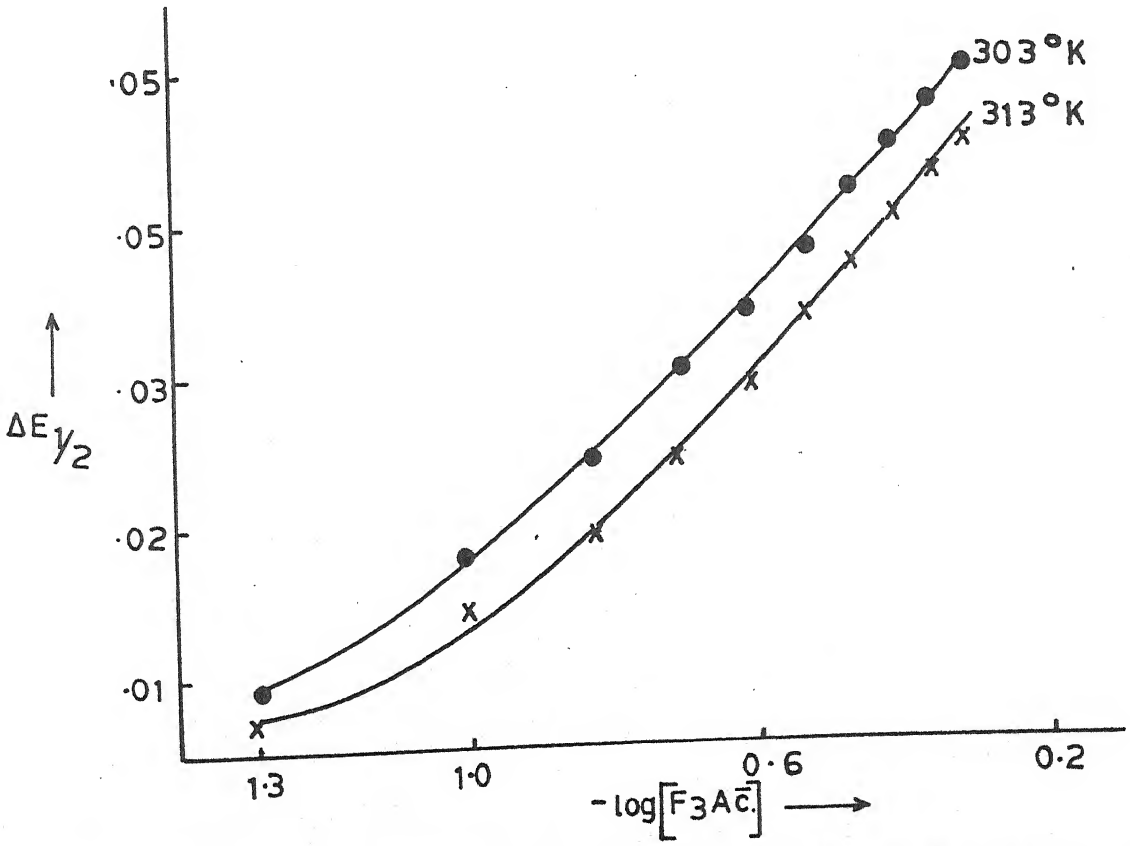

Fig. 5·10 - Plot of $F_{j(x)}$ Vs. $-\log[F_3 A\bar{c}.]$; Zn($F_3 A\bar{c}.$) system.

Table 5.09

Zinc difluoroacetate system

Temperature (° K)	log β_1	- ΔG (kj)	- ΔH (kj)	- ΔS (kj deg^{-1})x10^3
303	1.1903	6.9058		33.1854
			16.9610	
313	1.0969	6.5740		33.1854

5.3.04 Zinc trifluoroacetate system :

(a) Nature of reduction : The following observations conclusively indicated that the two electron reversible reduction of Zn(II) in trifluoroacetate ions is totally diffusion controlled.

(i) Plots of $-E_{de}$ vs. -log. i/i_d-i were linear with slopes of 31-32 mV.

(ii) Per degree rise in temperature $E_{1/2}$ changed by 0.2 ± 0.1 mV and i_d by 0.6 ± 1 %.

(iii) The ratio $i_d/\sqrt{h_{eff.}}$ was constant.

(b) Effect of ligand concentration : Complex formation between Zn(II) and $(F_3A\bar{c}.)$ was inferred from the cathodic shift in $E_{1/2}$ and decrease in i_d when solutions containing 0.9 mM Zn(II) ions, 0.002% gelatin, increasing concentration of $(F_3A\bar{c}.)$ ions and correspondingly decreasing amounts of $NaClO_4$ were polarographed at 303° K. The plot of $\Delta E_{1/2}$ vs. -log. $[F_3A\bar{c}.]$ was curve (figure 5.10) leading us to apply DeFord and Hume's method to

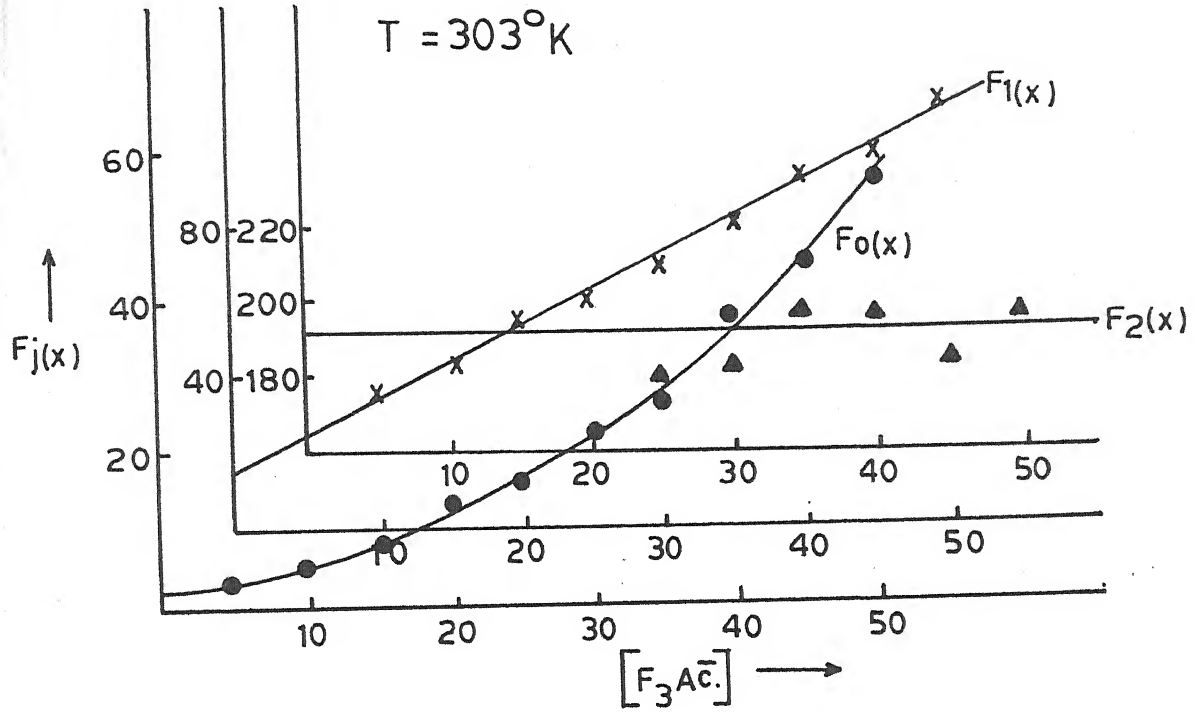

Fig. 5·11 - Plot of $F_{j(x)}$ Vs. $[F_3A\bar{c}.]$; $Zn(F_3A\bar{c}.)$ system.

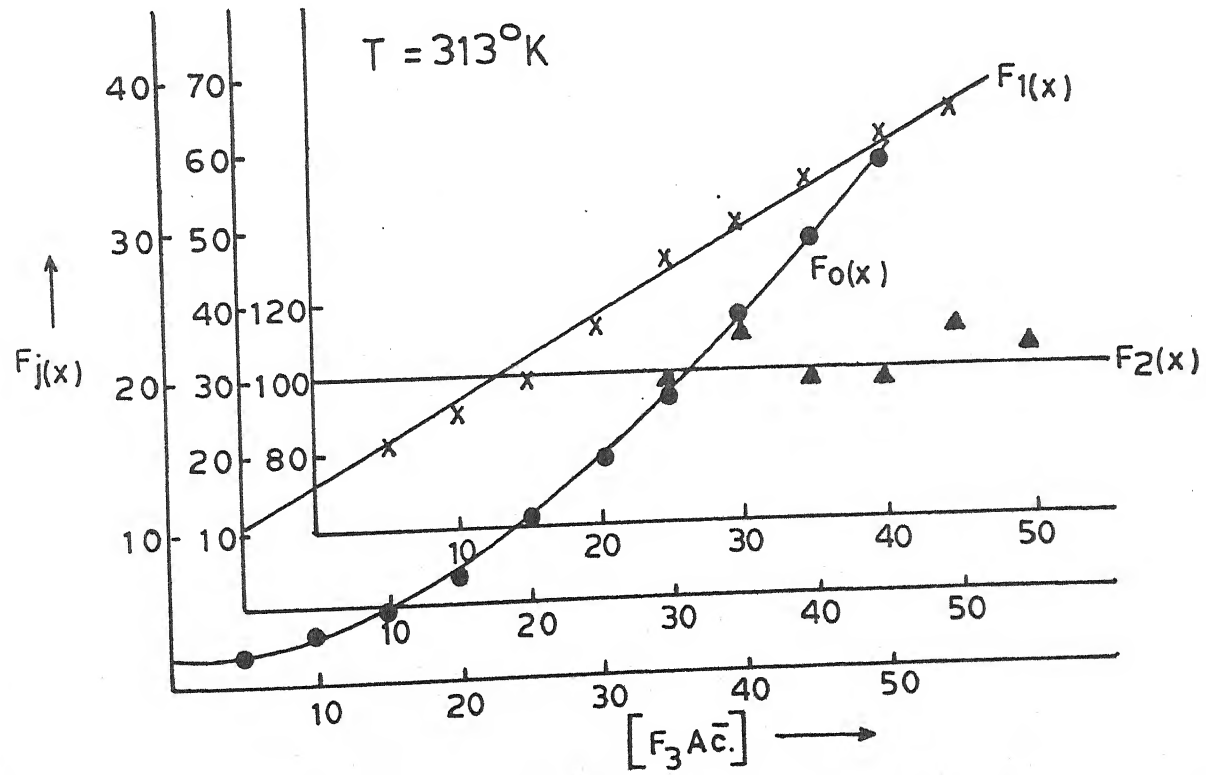

Fig. 5·12 - Plot of $F_{j(x)}$ Vs. $[F_3A\bar{c}.]$; $Zn(F_3A\bar{c}.)$ system.

Table 5.10

Polarographic data for Zinc trifluoroacetate system

Concn. of Zn^{++} ions = 0.9 mM Ionic strength = 1.0 M ($NaClO_4$)

$E_{1/2}$ of Zn^{++} ions = -0.998 V vs. SCE Temperature = 303° K

Slopes of plots of $-E_{de}$ vs. -log. i/i_d-i = 31-32 mV

$[F_3A\bar{c}.]$ (M)	$\Delta E_{1/2}$ (V)	log. I_M/I_C	$F_0(X)$	$F_1(X)$	$F_2(X)$
0.05	0.009	0.0324	2.14	22.8	-
0.10	0.018	0.0448	4.40	34.0	-
0.15	0.024	0.0575	7.17	41.13	-
0.20	0.030	0.0674	11.62	53.10	193.0
0.25	0.034	0.0741	16.03	60.12	182.5
0.30	0.038	0.0808	22.13	70.43	186.4
0.35	0.042	0.0877	30.55	84.42	199.7
0.40	0.045	0.0912	38.75	94.35	199.6
0.45	0.047	0.0947	45.93	98.95	187.6
0.50	0.050	0.0983	57.77	113.54	198.0

β_1 = 14.5 β_2 = 192

Table 5.11

Polarographic data for Zinc trifluoroacetate system

Concn. of Zn^{++} ions = 0.9 mM Ionic strength = 1.0 M ($NaClO_4$)

$E_{1/2}$ of Zn^{++} ions = -0.991 V vs. SCE Temperature = 313° K

Slopes of plots of $-E_{de}$ vs. -log. i/i_d-i = 31-32 mV

$F_3A\bar{c}.$ (M)	$E_{1/2}$ (V)	log. I_M/I_C	$F_0(X)$	$F_1(X)$	$F_2(X)$
0.05	0.006	0.0264	1.78	15.6	-
0.10	0.014	0.0403	3.09	20.9	-
0.15	0.019	0.0517	4.60	24.0	-
0.20	0.024	0.0576	6.76	28.8	-
0.25	0.029	0.0605	9.87	35.48	99.9
0.30	0.034	0.0635	14.40	44.6	113.6
0.35	0.037	0.0667	18.1	48.85	109.6
0.40	0.040	0.0695	22.78	54.45	109.9
0.45	0.043	0.0725	28.66	61.46	113.2
0.50	0.045	0.0755	33.48	64.96	108.9

$_1$ = 10.5 $_2$ = 100

compute stability constants of successively formed complexes. The values of β_1 and β_2 were 14.5 and 192 for which the polarographic data has been included in table 5.10 and figure 5.11.

(c) Effect of temperature : Effect of per degree rise in temperature on $E_{1/2}$ and i_d has been used earlier in this section to help infer the reversibility and diffusion controlled nature of reduction of Zn(II) trifluoroacetate system.

Investigations at 313° K on effect of ligand concentration on $E_{1/2}$ and i_d lead us to compute the formation constants at this temperature. The β_1 and β_2 values so obtained are 10.5 and 100. The relevant polarographic data and $F_j(X)$ functions appear in table 5.11 and figure 5.12.

The thermodynamic functions computed from the knowledge of stability constants at the two temperatures are given in table 5.12.

Table 5.12

Zinc trifluoroacetate system

Temperature (° K)	log β_1	- ΔG (kj)	- ΔH (kj)	- ΔS (kj deg^{-1})x10^3
303	1.1613	6.7376		61.7891
			25.4597	
313	1.0211	6.1197		61.7891

5.3.05 Zinc monochloroacetate system :

(a) Nature of reduction : The slopes of linear conventional log. plots (31-32 mV), temperature co-efficients of $E_{1/2}$ (0.3 mV per degree) and i_d (0.6 ± 0.1 percent per degree) along with proportionality of i_d with square root of effective height of mercury column of the DME convincingly indicated that Zn(II) reduces reversibily with two electron transfer and diffusion control in presence of monochloroacetate ions.

(b) Effect of ligand concentration : The $E_{1/2}$ shifted towards the more negative direction and i_d decreased when solutions containing 0.9 mM Zn(II) ions, 0.002% gelatin and increasing ligand concentration with decreasing concentration of sodium perchlorate (for μ = 1.0 M) were polarographed at 303° K. It indicated complex formation. Since the plot of $\Delta E_{1/2}$ vs. -log. $[ClAc^-]$ is a curve (figure 5.13) stepwise complex formation was inferred and the method of DeFord and Hume used to evaluate the stability constants which were 36.5 and 114 for 1:1 and 1:2 complexes. The related data and $F_j(X)$ curves are given in table 5.13 and figure 5.14.

(c) Effect of temperature : The effect of temperature on $E_{1/2}$ and i_d has already been used earlier in this section to aid establish the reversibility and diffusion controlled nature of reduction of Zn(II) in presence of monochloroacetate ions.

The formation constants were determined at 313° K also and were found to be 27 and 72 respectively for 1:1 and 1:2 complexes. The relevant polarographic data and the $F_j(X)$

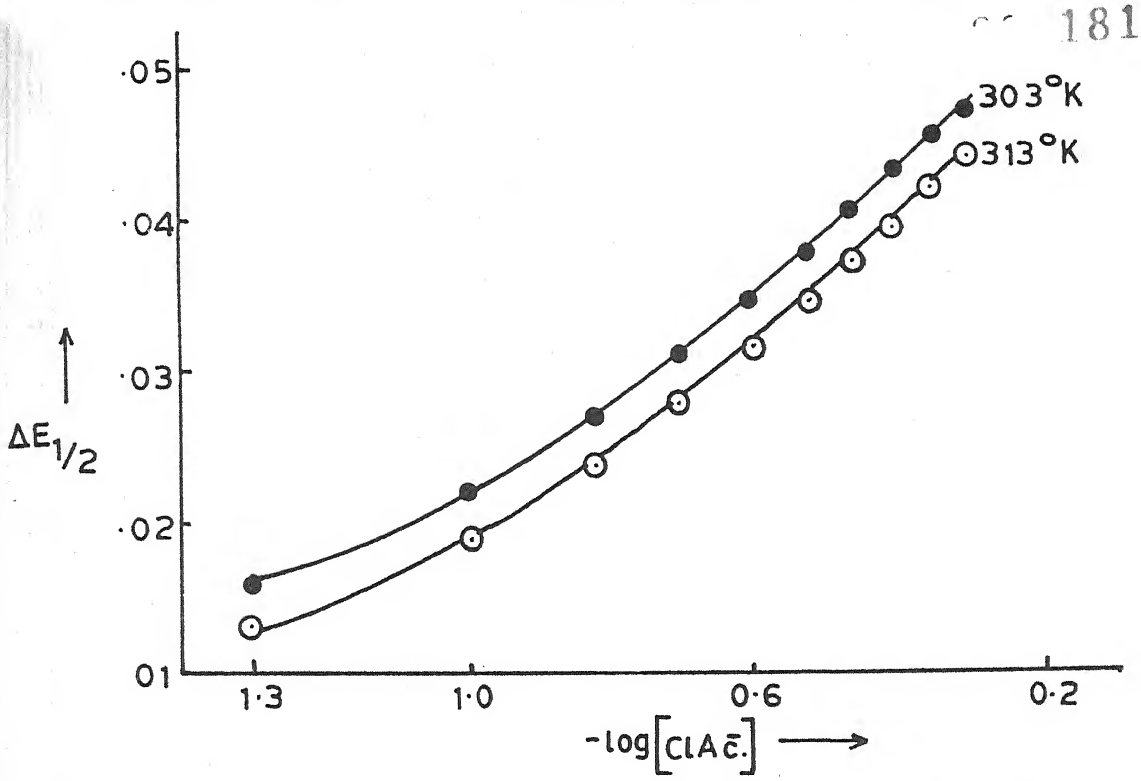

Fig. 5·13 - Plot of $F_{j(x)}$ Vs. $-\log[ClA\bar{c}.]$; Zn(ClAc̄.)system.

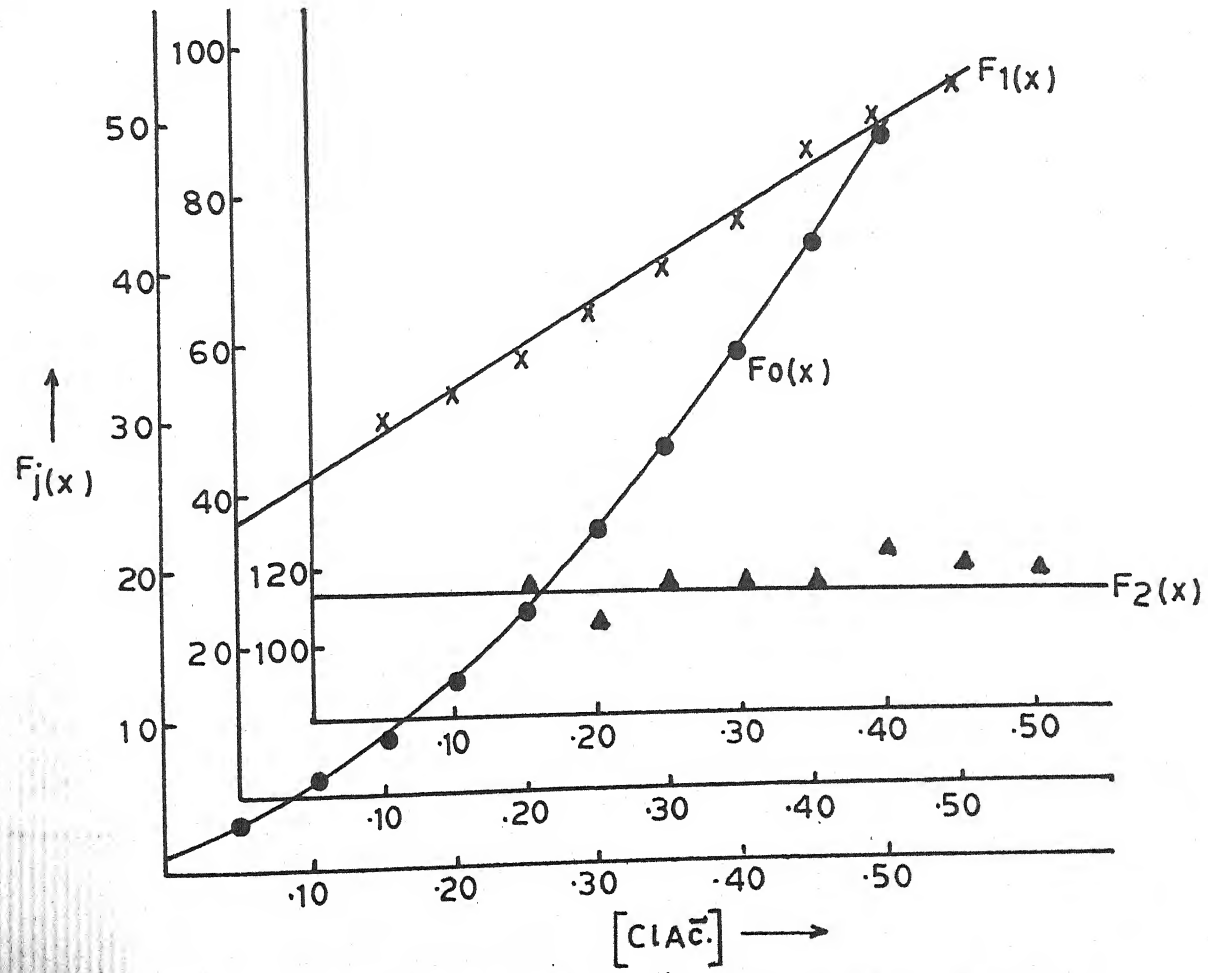

Fig. 5·14 - Plot of $F_{j(x)}$ Vs. $[ClA\bar{c}.]$; Zn(ClAc̄.)system

Table 5.13

Polarographic data for Zinc monochloroacetate system

Concn. of Zn^{++} ions = 0.9 mM Ionic strength = 1.0 M ($NaClO_4$)

$E_{1/2}$ of Zn^{++} ions = -0.998 V vs. SCE Temperature = 303° K

Slopes of plots of $-E_{de}$ vs. $-\log. i/i_d-i$ = 31-32 mV

$[ClAc^-]$ (M)	$\Delta E_{1/2}$ (V)	$\log. I_M/I_C$	$F_0(X)$	$F_1(X)$	$F_2(X)$
0.05	0.016	0.0295	3.64	-	-
0.10	0.022	0.0451	5.98	49.8	-
0.15	0.027	0.0579	9.04	53.6	114.0
0.20	0.031	0.0679	12.56	57.8	106.5
0.25	0.035	0.0746	17.33	65.32	115.3
0.30	0.038	0.0814	22.16	70.53	113.4
0.35	0.041	0.0814	27.88	76.8	115.1
0.40	0.044	0.0849	35.37	85.92	123.5
0.45	0.046	0.0884	41.56	90.13	119.2
0.50	0.048	0.0884	48.44	94.88	116.7

β_1 = 36.5 β_2 = 114

Table 5.14

Polarographic data for Zinc monochloroacetate system

Concn. of Zn^{++} ions = 0.9 mM Ionic strength = 1.0 M ($NaClO_4$)

$E_{1/2}$ of Zn^{++} ions = -0.991 V vs. SCE Temperature = 313° K

Slopes of plots of $-E_{de}$ vs. $-\log. i/i_d-i$ = 31-32 mV

$[ClAc^-]$ (M)	$\Delta E_{1/2}$ (V)	$\log. I_M/I_C$	$F_0(X)$	$F_1(X)$	$F_2(X)$
0.05	0.013	0.0266	2.78	-	-
0.10	0.019	0.0406	4.49	34.9	79.0
0.15	0.024	0.0521	6.68	37.86	72.4
0.20	0.028	0.0609	9.17	40.85	69.2
0.25	0.032	0.0669	12.51	46.04	76.1
0.30	0.035	0.0730	15.85	49.5	75.0
0.35	0.038	0.0760	19.94	54.11	77.4
0.40	0.040	0.0760	23.13	55.32	70.8
0.45	0.043	0.0791	29.10	62.44	78.7
0.50	0.045	0.0791	33.75	65.50	77.0

β_1 = 27 β_2 = 72

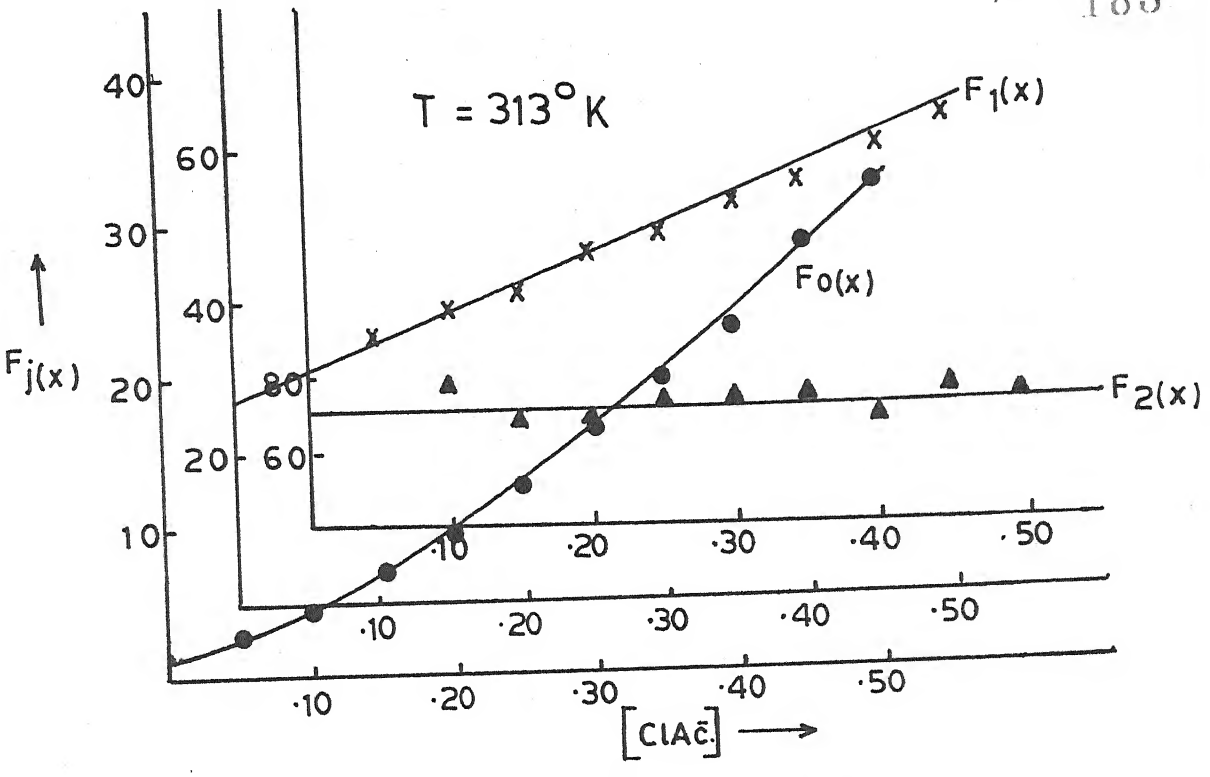

Fig. 5·15 - Plot of $F_{j(x)}$ Vs. $[ClA\bar{c}.]$; Zn(ClAc̄.)system.

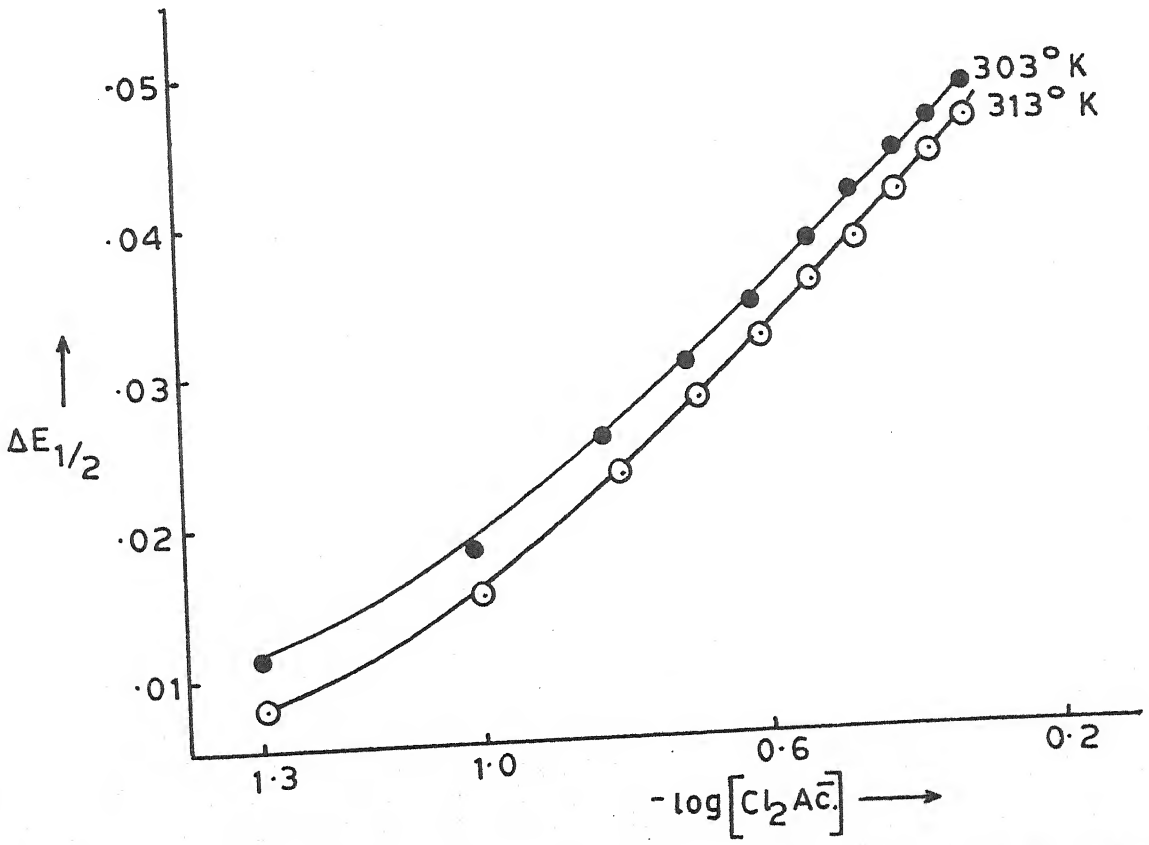

Fig. 5·16 - Plot of $\Delta E_{1/2}$ Vs. $-\log[Cl_2A\bar{c}.]$; Zn(Cl_2Ac̄.)system.

plots are given in table 5.14 and figure 5.15.

The thermodynamic parameters calculated from the knowledge of stability constants at two temperatures are presented in table 5.15.

Table 5.15

Zinc monochloroacetate system

Temperature (° K)	log β_1	- ΔG (kj)	- ΔH (kj)	- ΔS (kj deg^{-1})x10^3
303	1.5622	9.0635		48.5393
			23.7709	
313	1.4313	8.5781		48.5392

5.3.06 Zinc dichloroacetate system :

(a) Nature of reduction : The reduction of Zn(II) in presence of dichloroacetate ions in reversible involving two electrons and is fully diffusion controlled. These conclusions could be deduced from the following observations :

(i) Plots of $-E_{de}$ vs. $-\log. i/i_d-i$ are straight lines with slopes of 31-32 mV.

(ii) Temperature co-efficients of $E_{1/2}$ and i_d are 0.2-0.3 mV per degree and 0.6 $\pm$ 0.1 percent per degree.

(iii) Plots of i_d vs. $\sqrt{h_{eff.}}$ are straight lines.

(b) Effect of ligand concentration : When solutions containing 0.9 mM Zn(II) ions, 0.002% gelatin, increasing concentrations of

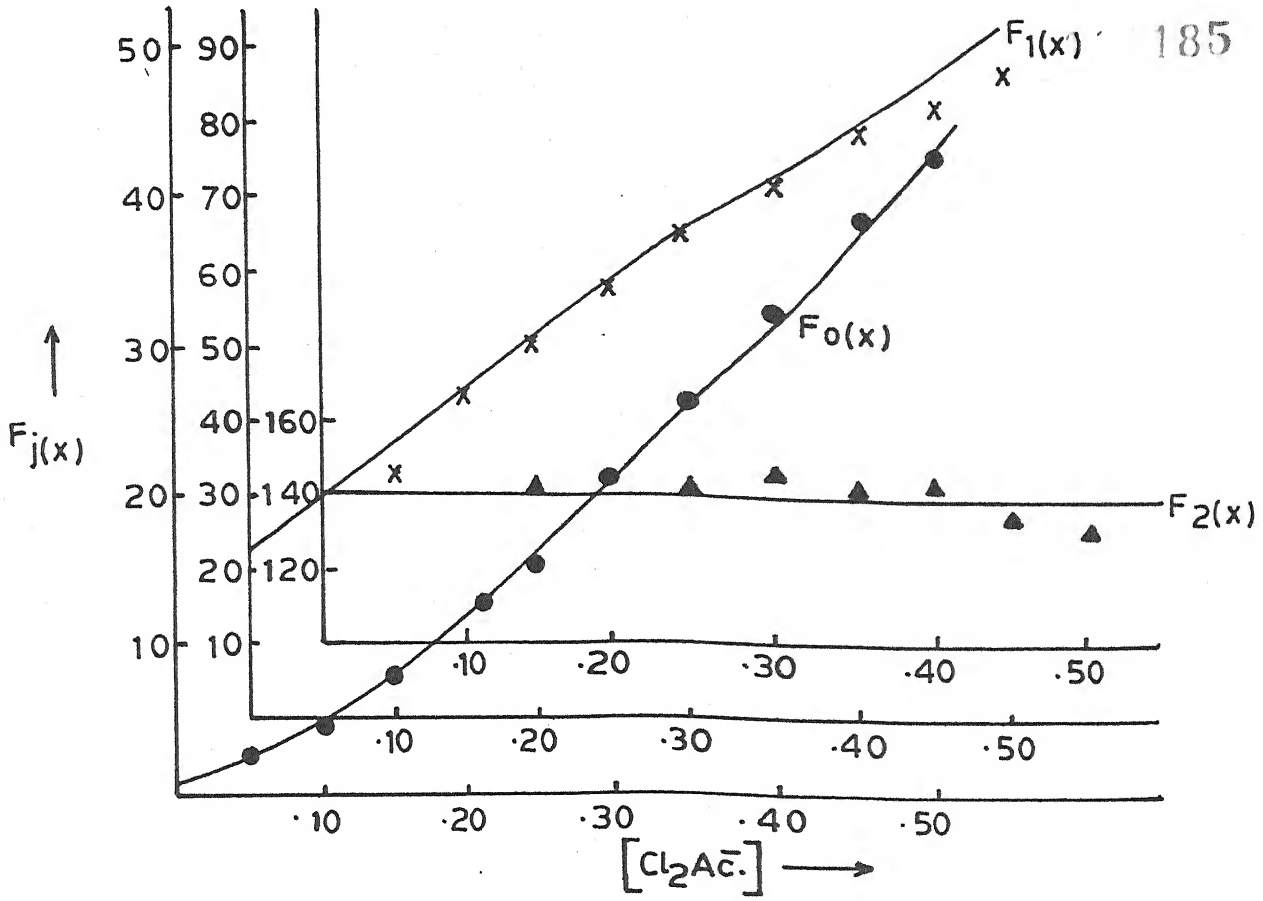

Fig. 5·17 - Plot of $F_{j(x)}$ Vs. $[Cl_2Ac^-]$; $Zn(Cl_2Ac^-)$ system.

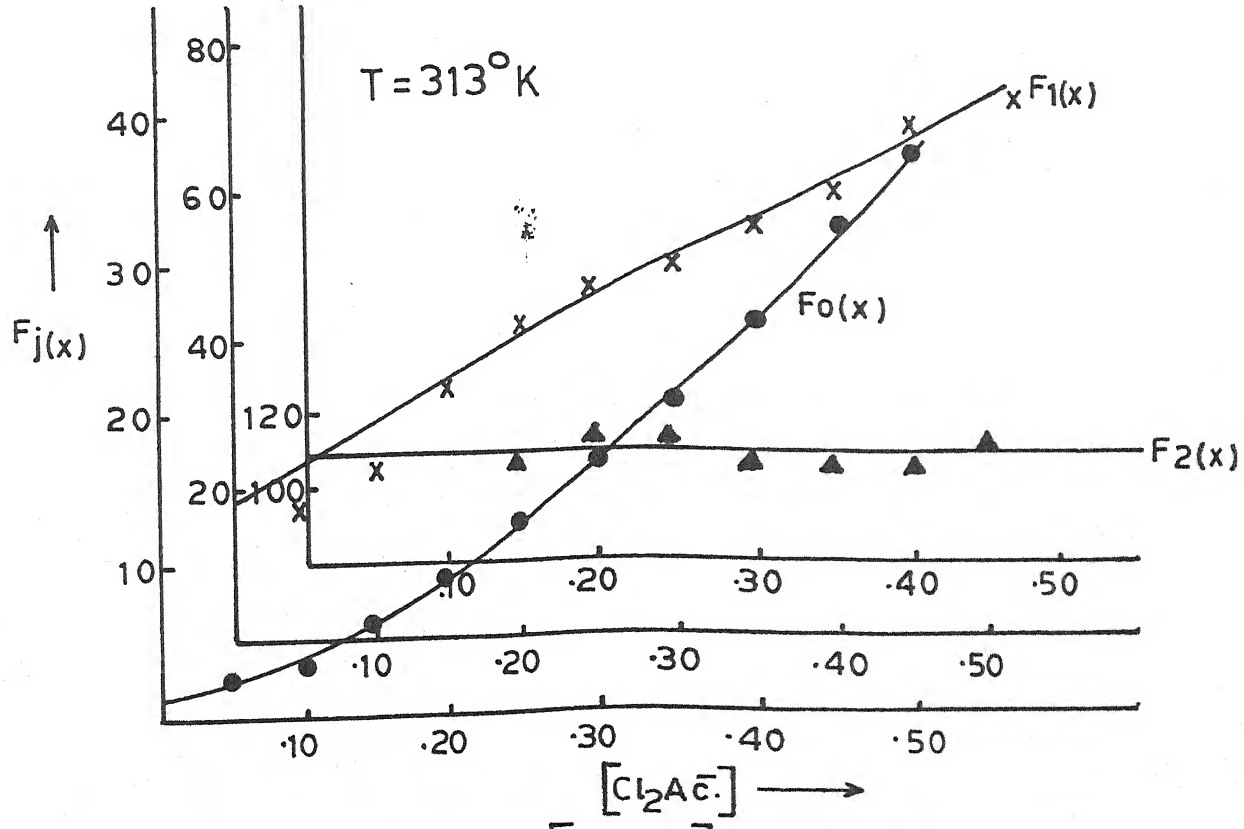

Fig. 5·18 - Plot of $F_{j(x)}$ Vs. $[Cl_2Ac^-]$; $Zn(Cl_2Ac^-)$ system.

Table 5.16

Polarographic data for Zinc dichloroacetate system

Concn. of Zn^{++} ions = 0.9 mM Ionic strength = 1.0 M ($NaClO_4$)

$E_{1/2}$ of Zn^{++} ions = -0.998 V vs. SCE Temperature = 303° K

Slopes of plots of $-E_{de}$ vs. -log. i/i_d-i = 31-32 mV

$[Cl_2Ac^-]$ (M)	$\Delta E_{1/2}$ (V)	log. I_M/I_C	$F_0(X)$	$F_1(X)$	$F_2(X)$
0.05	0.011	0.0272	2.47	29.4	-
0.10	0.018	0.0399	4.35	33.5	-
0.15	0.025	0.0464	7.55	43.66	140.6
0.20	0.030	0.0529	17.24	51.2	143.5
0.25	0.034	0.0563	15.39	57.56	140.2
0.30	0.038	0.0563	21.07	66.66	147.2
0.35	0.041	0.0596	26.52	72.91	144.0
0.40	0.044	0.0596	33.37	80.92	146.0
0.45	0.046	0.0630	39.20	84.88	138.6
0.50	0.048	0.0630	45.69	89.38	133.7

$\beta_1 = 22.5$ $\beta_2 = 142$

Table 5.17

Polarographic data for Zinc dichloroacetate system

Concn. of Zn^{++} ions = 0.9 mM Ionic strength = 1.0 M ($NaClO_4$)

$E_{1/2}$ of Zn^{++} ions = -0.991 V vs. SCE Temperature = 313° K

Slopes of plots of $-E_{de}$ vs. -log. i/i_d-i = 31-32 mV

$[Cl_2Ac^-]$ (M)	$\Delta E_{1/2}$ (V)	log. I_M/I_C	$F_0(X)$	$F_1(X)$	$F_2(X)$
0.05	0.008	0.0245	1.91	18.2	-
0.10	0.015	0.0416	3.34	23.4	-
0.15	0.023	0.564	6.26	35.06	110.4
0.20	0.028	0.0686	9.34	41.7	116.0
0.25	0.032	0.0781	12.84	47.36	115.4
0.30	0.035	0.0845	16.38	51.26	109.2
0.35	0.038	0.0909	20.64	56.11	107.4
0.40	0.041	0.0942	25.98	62.45	109.9
0.45	0.044	0.0975	32.70	70.44	115.4
0.50	0.046	0.1009	38.22	74.44	111.9

$\beta_1 = 18.5$ $\beta_2 = 110$

dichloroacetate ions (ionic strength constant at 1.0 M) were reduced at the DME at 303° K, gradual cathodic shift in $E_{1/2}$ and decrease in i_d indicated complex formation between Zn(II) and (Cl_2Ac^-) ions. The plot of $\Delta E_{1/2}$ vs. $-\log.[Cl_2Ac^-]$ being a curve (figure 5.16), the method of DeFord and Hume could be used to calculate stability constants of the successively formed complexes The β_1 and β_2 were found to be 22.5 and 142 for which the polarographic data and $F_j(X)$ plots are included in table 5.16 and figure 5.17.

(c) Effect of temperature : There is a 0.2 - 0.3 mV shift in $E_{1/2}$ and 0.6 $\pm$ 0.1 percent increase in i_d per degree rise in temperatur

The experiment (b) was repeated at 313° K to obtain the formation constants 18.5 and 110 for $[Zn(Cl_2Ac.)]^+$ and $[Zn(Cl_2Ac.)_2]$ complexes for which the polarographic data and $F_j(X)$ functions are presented in table 5.17 and figure 5.18.

Table 5.18 presents the thermodynamic functions calculated from the knowledge of stability constants at the two temperatures.

Table 5.18

Zinc dichloroacetate system

Temperature (° K)	log β_1	- ΔG (kj)	- ΔH (kj)	- ΔS (kj deg^{-1})x10^3
303	1.3521	7.8446		25.0528
			15.4356	
313	1.2671	7.5940		25.0530

5.3.07 Zinc trichloroacetate system :

(a) Nature of reduction : The linearity of the conventional log. plots with slopes of 31-32 mV, temperature co-efficients of $E_{1/2}$ (0.2 ± 0.1 mV per degree) and i_d (0.6 ± 0.1 % per degree) coupled with the proportionality of i_d with square root of effective height of mercury column of the DME helped us deduce the reversibility with two electron transfer process and diffusion controlled character of reduction of Zn(II) in trichloroacetate ions.

(b) Effect of ligand concentration : Reduction at DME at 303° K revealed a gradual cathodic shift in $E_{1/2}$ and decrease in i_d with increasing trichloroacetate ion concentration in solutions also containing 0.9 mM Zn(II) ions, 0.002% gelatin and requisite amount of $NaClO_4$ (for ionic strength of 1.0 M). This was indicative of complex formation between Zn(II) and (Cl_2Ac^-) ions. The curved nature (figure 5.19) of the plot of $\Delta E_{1/2}$ vs. $-\log.[Cl_3Ac^-]$ indicated multiple complex formation and DeFord and Hume's method was applicable to compute successive overall formation constants which were found to be 19 and 114 for $[Zn(Cl_3Ac.)]^+$ and $[Zn(Cl_3Ac.)_2]$ complexes. The relevant polarographic data appear in table 5.19 and the $F_j(X)$ functions find place in figure 5.20.

(c) Effect of temperature : The temperature co-efficients of half wave potential and diffusion current were found to be 0.2 ± 0.1 mV per degree and 0.6 ± 0.1 percent per degree.

In order to evaluate ΔG, ΔH and ΔS, the formation

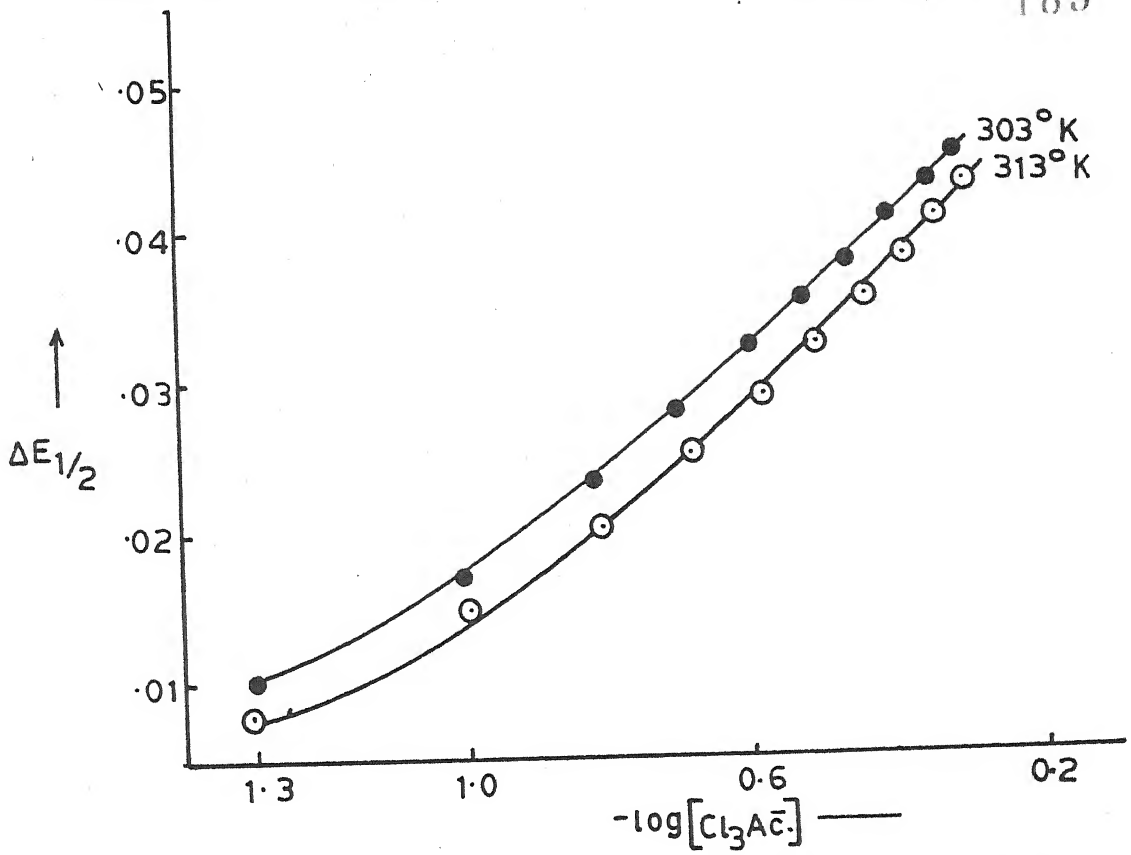

Fig. 5·19 - Plot of $\Delta E_{1/2}$ Vs. $-\log[Cl_3A\bar{c}.]$; $Zn(Cl_3A\bar{c}.)$ system.

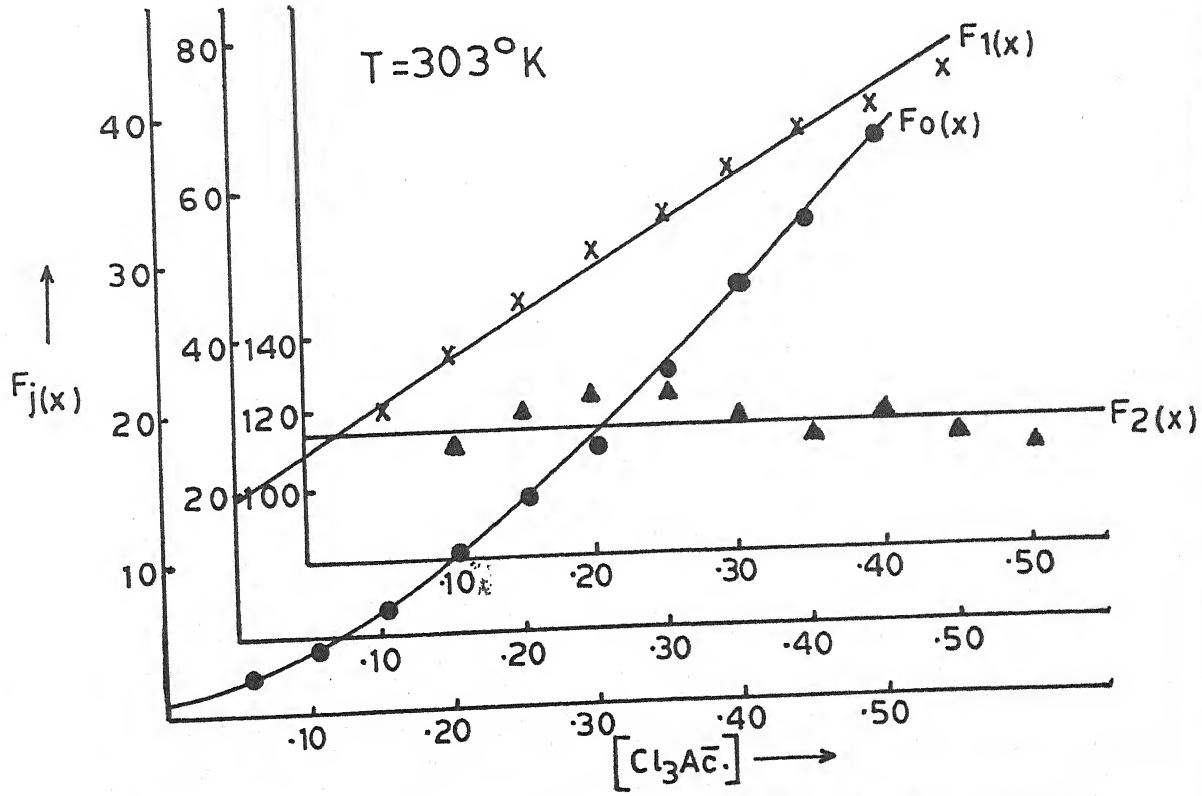

Fig. 5·20 - Plot of $F_{j(x)}$ Vs. $[Cl_3A\bar{c}.]$; $Zn(Cl_3A\bar{c}.)$ system.

Table 5.19

Polarographic data for Zinc trichloroacetate system

Concn. of Zn^{++} ions = 0.9 mM Ionic strength = 1.0 M ($NaClO_4$)

$E_{1/2}$ of Zn^{++} ions = -0.998 V vs. SCE Temperature = 303° K

Slopes of plots of $-E_{de}$ vs. -log. i/i_d-i = 31-32 mV

$[Cl_3Ac^-]$ (M)	$\Delta E_{1/2}$ (V)	log. I_M/I_C	$F_0(X)$	$F_1(X)$	$F_2(X)$
0.05	0.010	0.0272	2.29	25.8	-
0.10	0.014	0.0399	4.03	30.3	113.0
0.15	0.023	0.0529	6.57	37.13	120.8
0.20	0.028	0.0630	9.87	44.35	126.7
0.25	0.032	0.0698	13.62	50.48	125.9
0.30	0.035	0.0733	17.28	54.26	117.5
0.35	0.038	0.0733	21.75	59.28	115.0
0.40	0.041	0.0768	27.59	66.47	119.1
0.45	0.043	0.0768	32.16	69.24	111.6
0.50	0.045	0.0768	37.48	72.96	107.9

$\beta_1 = 19$ $\beta_2 = 114$

Table 5.20

Polarographic data for Zinc trichloroacetate system

Concn. of Zn^{++} ions = 0.9 mM Ionic strength = 1.0 M ($NaClO_4$)

$E_{1/2}$ of Zn^{++} ions = -0.991 V vs. SCE Temperature = 313° K

Slopes of plots of $-E_{de}$ vs. -log. i/i_d-i = 31-32 mV

$[Cl_3Ac^-]$ (M)	$\Delta E_{1/2}$ (V)	log. I_M/I_C	$F_0(X)$	$F_1(X)$	$F_2(X)$
0.05	0.008	0.0358	1.96	19.2	104.0
0.10	0.015	0.0504	3.41	24.1	101.0
0.15	0.021	0.0625	5.48	29.86	105.7
0.20	0.026	0.0718	8.11	35.55	107.7
0.25	0.030	0.0781	11.07	40.28	105.1
0.30	0.034	0.0845	15.11	47.03	110.0
0.35	0.037	0.0845	18.88	51.08	105.9
0.40	0.040	0.0877	23.76	56.9	107.2
0.45	0.042	0.0877	27.56	59.02	100.0
0.50	0.044	0.0909	32.20	62.4	96.8

$\beta_1 = 14$ $\beta_2 = 104$

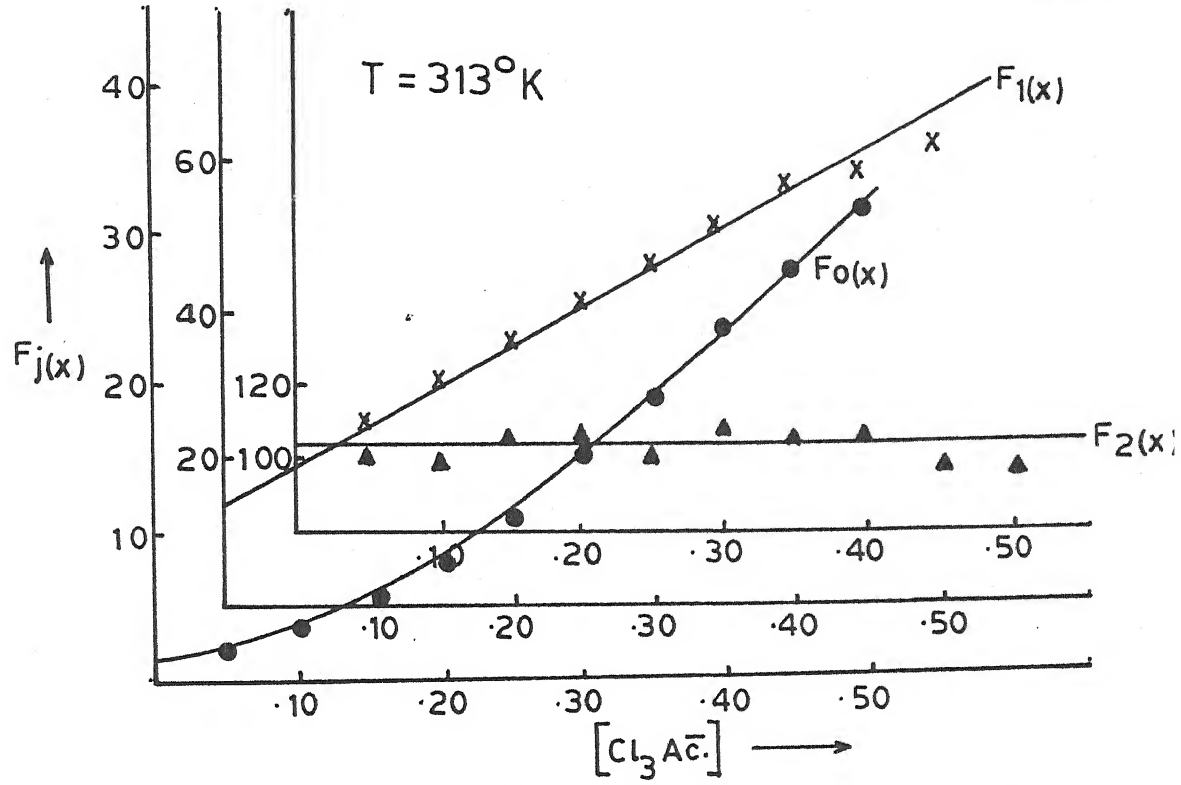

Fig. 5·21 - Plot of $F_{j(x)}$ Vs. $[Cl_3A\bar{c}.]$; Zn ($Cl_3A\bar{c}.$) system.

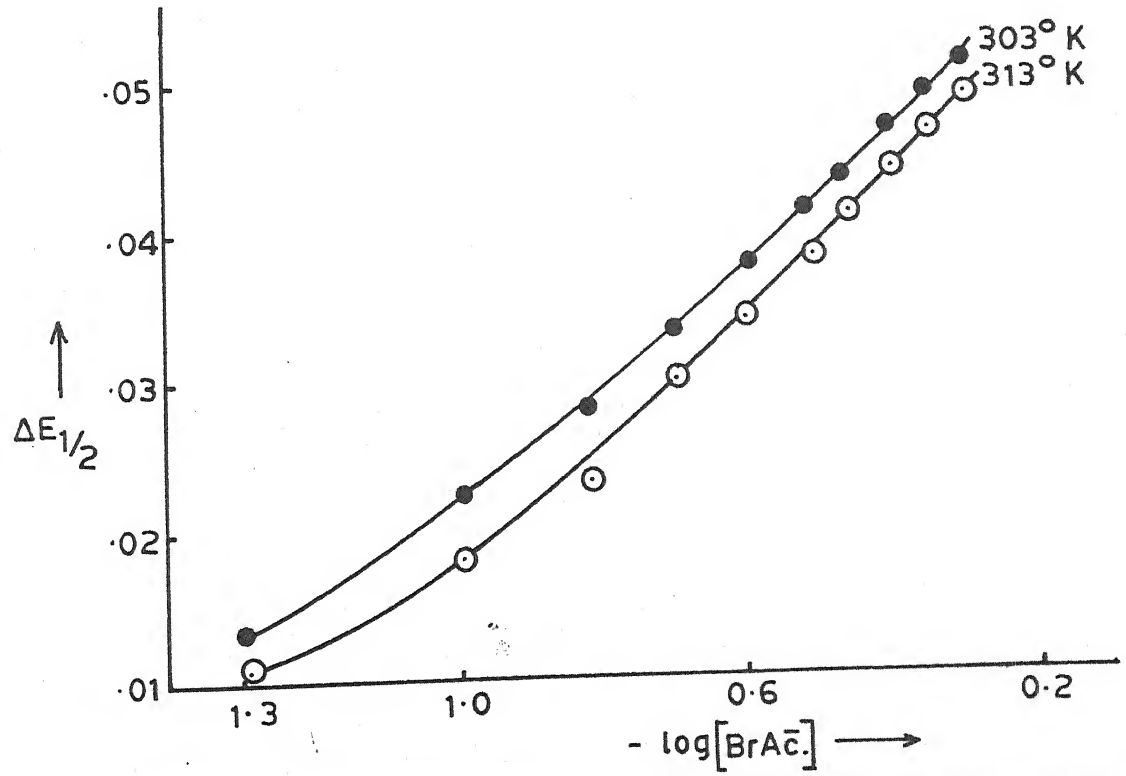

Fig. 5·22 - Plot of $\Delta E_{1/2}$ Vs. $-\log[Br A\bar{c}.]$; Zn($Br A\bar{c}.$) system.

constants were determined again at 313° K and were found to be 14 and 104 for 1:1 and 1:2 respectively. The relevant polarographic data, $F_j(X)$ plots and thermodynamic functions are included in table 5.20, figure 5.21 and table 5.21 respectively.

Table 5.21

Zinc trichloroacetate system

Temperature (° K)	log β_1	- G (kj)	- H (kj)	- S (kj deg^{-1})x10^3
303	1.2787	7.4187		54.9864
			24.0796	
313	1.1461	6.8688		54.9865

5.3.08 Zinc monobromoacetate system :

(a) **Nature of reduction** : Zn(II) reduces reversibly with two electron transfer and with diffusion control in presence of monobromoacetate ions as inferred from the linearity of plots of $-E_{de}$ vs. $-\log. i/i_d-i$, with slopes of 31-32 mV, temperature co-efficient values of $E_{1/2}$ (0.2 - 0.3 mV per degree) and i_d (0.6 $\pm$ 0.1 percent per degree) coupled with proportionality of i_d with the square root of h_{eff}.

(b) Effect of ligand concentration : Polarographic investigations at 303° K of solutions containing 0.9 mM Zn(II) ions, 0.002% gelatin, increasing amounts of monobromoacetate ions and requisite amounts of sodium perchlorate to maintain μ = 1.0 M

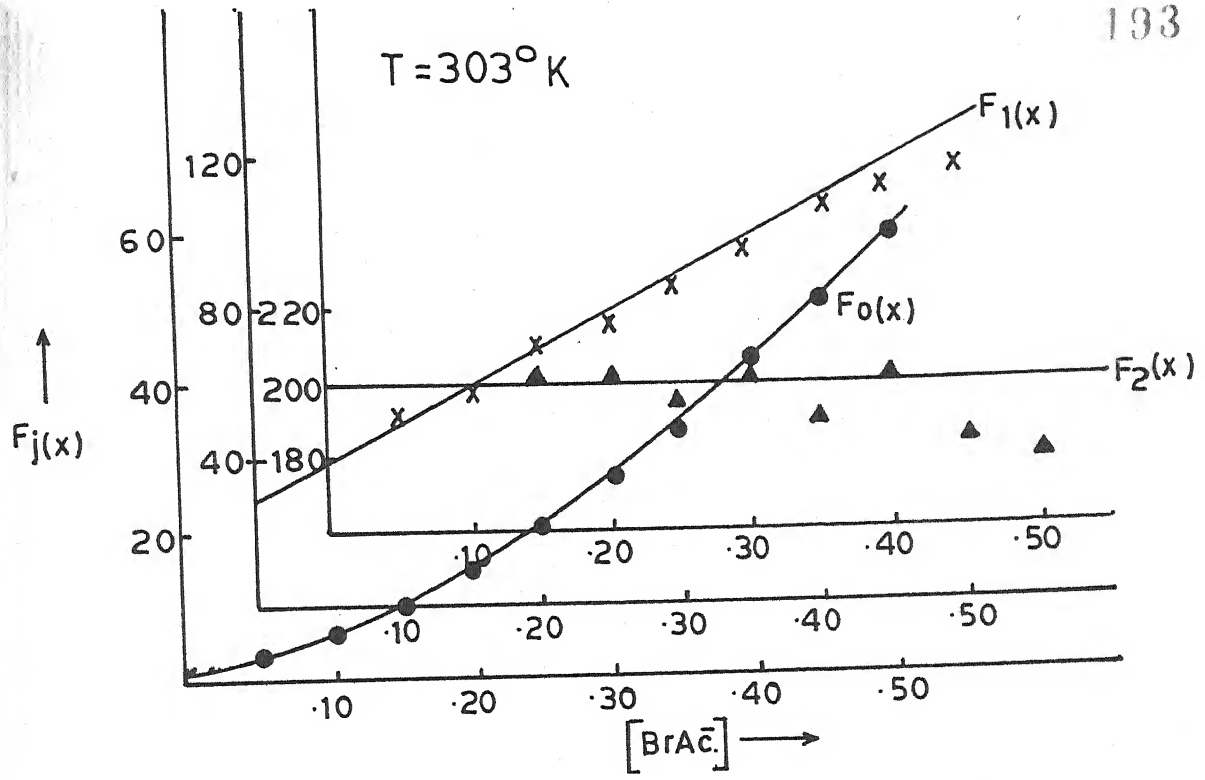

Fig. 5·23 - Plot of $F_{j(x)}$ Vs. $[BrA\bar{c}.]$; Zn(BrAc̄.)system.

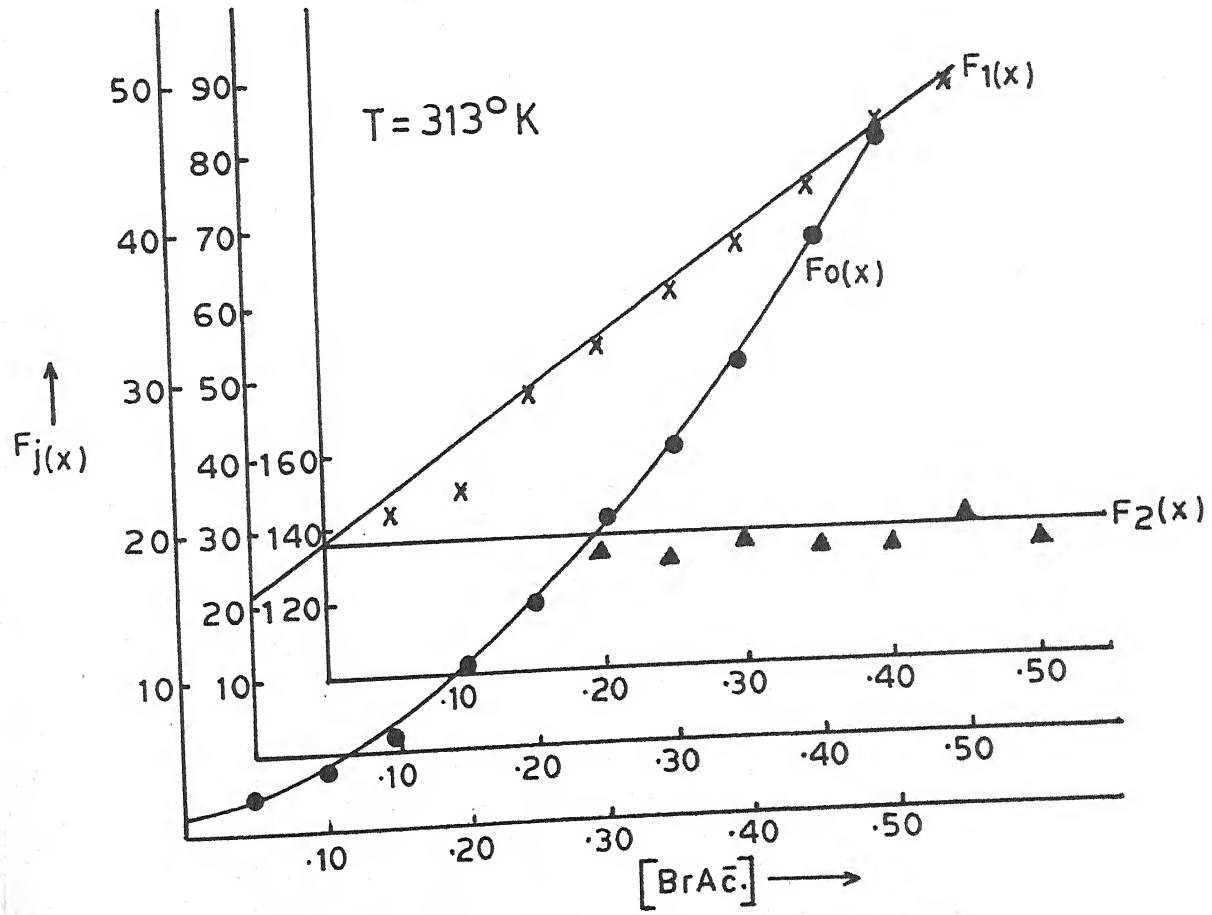

Fig. 5·24 - Plot of $F_{j(x)}$ Vs. $[BrA\bar{c}.]$; Zn(BrAc̄.)system.

Table 5.22

Polarographic data for Zinc monobromobacetate system

Concn. of Zn^{++} ions = 0.9 mM Ionic strength = 1.0 M ($NaClO_4$)
$E_{1/2}$ of Zn^{++} ions = -0.998 V vs. SCE Temperature = 303° K
Slopes of plots of $-E_{de}$ vs. $-\log. i/i_d-i$ = 31-32 mV

$[BrAc^-]$ (M)	$\Delta E_{1/2}$ (V)	$\log. I_M/I_C$	$F_0(X)$	$F_1(X)$	$F_2(X)$
0.05	0.013	0.0335	2.92	38.4	-
0.10	0.022	0.0464	6.0	50.0	-
0.15	0.028	0.0596	9.79	58.6	204.0
0.20	0.033	0.0698	14.71	68.55	202.7
0.25	0.037	0.0768	20.31	77.24	196.9
0.30	0.041	0.0803	27.81	89.36	204.5
0.35	0.043	0.0803	34.42	95.48	192.8
0.40	0.047	0.0839	44.40	108.5	201.2
0.45	0.049	0.0839	51.76	112.84	188.5
0.50	0.051	0.0839	60.33	118.66	181.3

$\beta_1 = 28$ $\beta_2 = 200$

Table 5.23

Polarographic data for Zinc monobroboacetate system

Concn. of Zn^{++} ions = 0.9 mM Ionic strength = 1.0 M ($NaClO_4$)
$E_{1/2}$ of Zn^{++} ions = -0.991 V vs. SCE Temperature = 313° K
Slopes of potential of $-E_{de}$ vs. $-\log. i/i_d-i$ = 31-32 mV

$[BrAc^-]$ (M)	$\Delta E_{1/2}$ (V)	$\log. I_M/I_C$	$F_0(X)$	$F_1(X)$	$F_2(X)$
0.05	0.011	0.0273	2.40	28.0	-
0.10	0.018	0.0416	4.18	31.8	-
0.15	0.023	0.0534	6.22	34.8	-
0.20	0.030	0.0595	10.60	48.0	135.0
0.25	0.034	0.0656	14.47	53.88	131.5
0.30	0.038	0.0718	19.75	62.5	138.3
0.35	0.041	0.0749	24.85	68.14	134.6
0.40	0.044	0.0749	31.04	75.1	135.2
0.45	0.047	0.0781	39.66	84.44	140.9
0.50	0.049	0.0813	45.63	89.26	136.5

$\beta_1 = 21$ $\beta_2 = 136$

revealed cathodic shift in $E_{1/2}$ and decrease in i_d to show complex formation between Zn(II) and ($BrAc^-$.) ions which took place in a stepwise fashion as evident from the curved plot (figure 5.22) of $\Delta E_{1/2}$ vs. -log.[$BrAc^-$.]. The stability constants obtained by applying DeFord and Hume's method are 28 and 200 respectively for 1:1 and 1:2 metal/ligand ratio complexes. Table 5.22 contains the relevant polarographic data while figure 5.23 depicts the $F_j(X)$ plots.

(c) Effect of temperature : The $E_{1/2}$ changes by 0.2-0.3 mV and i_d by 0.6 $\pm$ 0.1 percent per degree rise in temperature.

The effect of ligand concentration on $E_{1/2}$ and i_d was reinvestigated at 313° K to obtain overall stability constant values of 21 and 136 for $[Zn(BrAc.)]^+$ and $[Zn(BrAc.)_2]$ complexes for which the polarographic data and $F_j(X)$ functions have been presented in table 5.23 and figure 5.24.

Table 5.24 contains the thermodynamic functions evaluated from the two sets of stability constants.

Table 5.24

Zinc monobromoacetate system

Temperature (° K)	log β_1	- ΔG (kj)	- ΔH (kj)	- ΔS (kj deg^{-1})x10^3
303	1.4471	8.3957		47.1471
			22.6813	
313	1.3222	7.9253		47.1470

5.3.09 Zinc dibromoacetate system :

(a) Nature of reduction : The reduction at DME of Zn(II) ions in presence of dibromoacetate ions is reversible, involving two electrons and is diffusion controlled as inferred from the following results :

(i) Straight line plots of $-E_{de}$ vs. -log. i/i_d-i with slopes of 31-32 mV.

(ii) Change of $E_{1/2}$ by 0.2-0.3 mV and i_d by 0.6 $\pm$ 0.1 % per degree rise in temperature.

(iii) Constancy of the ratio of i_d and $\sqrt{h_{eff.}}$.

(b) Effect of ligand concentration : Solutions containing 0.9 mM Zn(II) ions, 0.002% gelatin, increasing dibromoacetate ion concentration and decreasing sodium perchlorate to maintain ionic strength at 1.0 M when polarographed at 303° K revealed a cathodic shift in $E_{1/2}$ and a decrease in i_d to indicate complex formation between Zn(II) and ($Br_2A\bar{c}.$) ions. The plot of $\Delta E_{1/2}$ vs. -log. $[Br_2A\bar{c}.]$ was a curve (figure 5.25) revealing multiple complex formation. The application of method of DeFord and Hume gave the values of overall stability constants as 25 and 206 for 1:1 and 1:2 metal/ligand ratio complexes. The polarographic data and $F_j(X)$ functions appear in table 5.25 and figure 5.26.

(c) Effect of temperature : The temperature co-efficients of half wave potential and diffusion current were found to be 0.2 - 0.3 mV per degree and 0.6 $\pm$ 0.1% per degree respectively.

The experiment (b) was repeated at 313° K to obtain 18.5 and 162 as the β_1 and β_2 values for which the polarographic

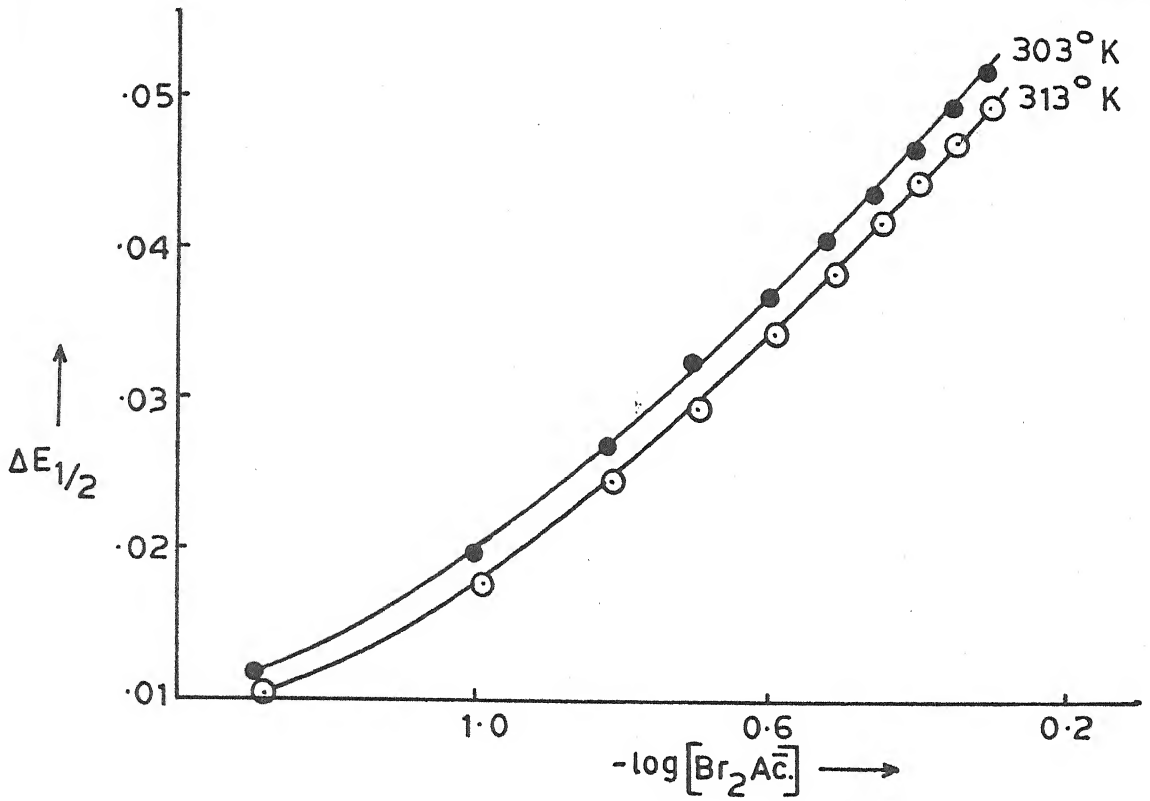

Fig. 5·25 - Plot of $\Delta E_{1/2}$ Vs. $-\log[Br_2 A\bar{c}.]$; Zn ($Br_2 A\bar{c}.$) system.

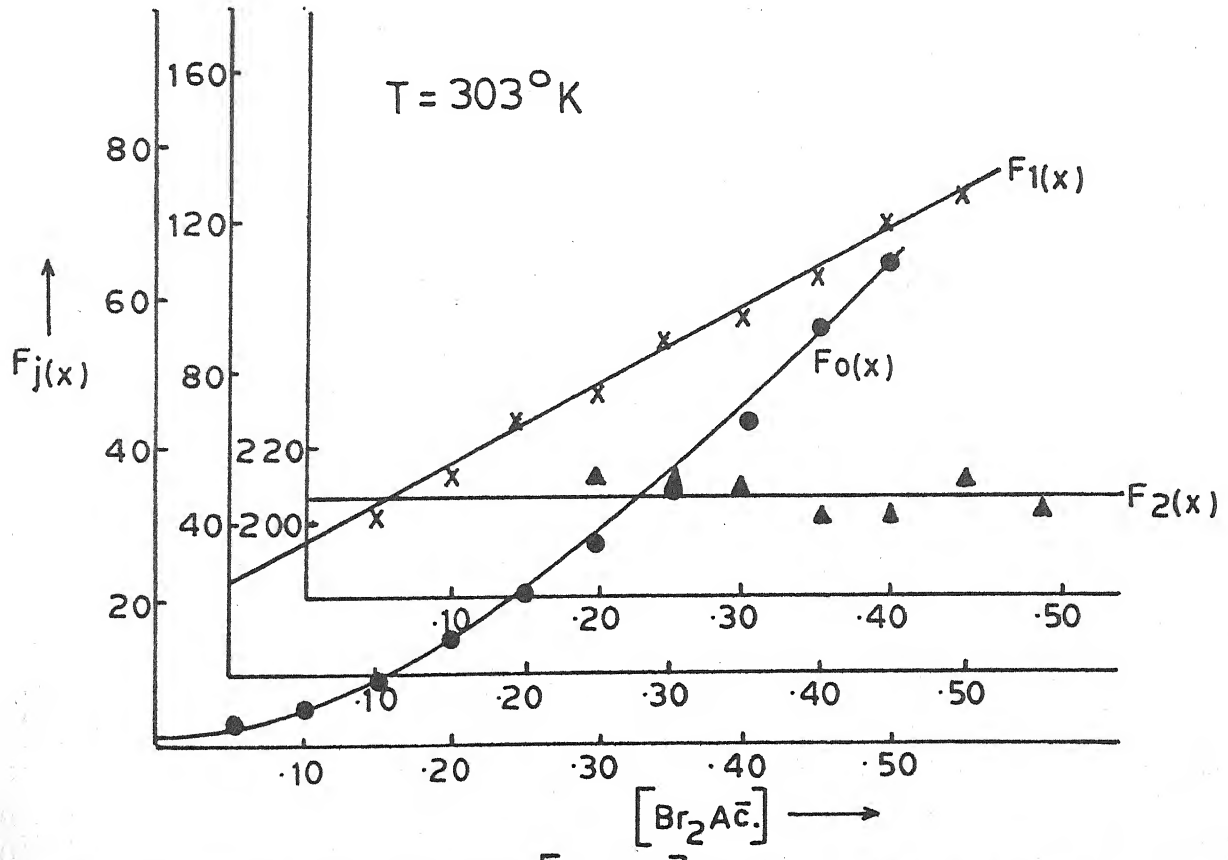

Fig. 5·26 - Plot of $F_{j(x)}$ Vs. $[Br_2 A\bar{c}.]$ Zn ($Br_2 A\bar{c}.$) system.

Table 5.25

Polarographic data for Zinc dibromoacetate system

Concn. of Zn^{++} ions = 0.9 mM Ionic strength = 1.0 M ($NaClO_4$)

$E_{1/2}$ of Zn^{++} = -0.998 V vs. SCE Temperature = 303° K

Slopes of plots of $-E_{de}$ vs. $-\log. i/i_d-i$ = 31-32 mV

$[Br_2Ac^-]$ (M)	$\Delta E_{1/2}$ (V)	$\log. I_M/I_C$	$F_0(X)$	$F_1(X)$	$F_2(X)$
0.05	0.012	0.0347	2.71	34.2	-
0.10	0.020	0.0501	5.19	41.9	-
0.15	0.027	0.0595	9.09	53.8	-
0.20	0.033	0.0660	14.58	67.9	214.5
0.25	0.037	0.0692	19.96	75.84	203.3
0.30	0.041	0.0725	27.32	87.73	209.1
0.35	0.044	0.0758	34.64	96.11	203.1
0.40	0.047	0.0791	43.92	107.3	205.7
0.45	0.050	0.0825	55.70	121.55	214.5
0.50	0.052	0.0825	64.92	127.84	205.6

$\beta_1 = 25$ $\beta_2 = 206$

Table 5.26

Polarographic data for Zinc dibromoacetate system

Concn. of Zn^{++} ions = 0.9 mM Ionic strength = 1.0 M ($NaClO_4$)

$E_{1/2}$ of Zn^{++} = -0.991 V vs. SCE Temperature = 313° K

Slopes of plots of $-E_{de}$ vs. $-\log. i/i_d-i$ = 31-32 mV

$[Br_2Ac^-]$ (M)	$\Delta E_{1/2}$ (V)	$\log. I_M/I_C$	$F_0(X)$	$F_1(X)$	$F_2(X)$
0.05	0.010	0.0260	2.22	24.4	-
0.10	0.018	0.0424	4.18	31.8	-
0.15	0.025	0.0565	7.27	41.8	155.0
0.20	0.030	0.0682	10.82	49.1	153.0
0.25	0.035	0.0771	16.0	60.0	166.0
0.30	0.039	0.0832	21.83	69.0	168.3
0.35	0.042	0.0894	27.66	76.17	164.7
0.40	0.045	0.0925	34.81	84.52	165.0
0.45	0.048	0.0956	43.79	95.0	170.0
0.50	0.050	0.0988	51.17	100.34	163.6

$\beta_1 = 18.5$ $\beta_2 = 162$

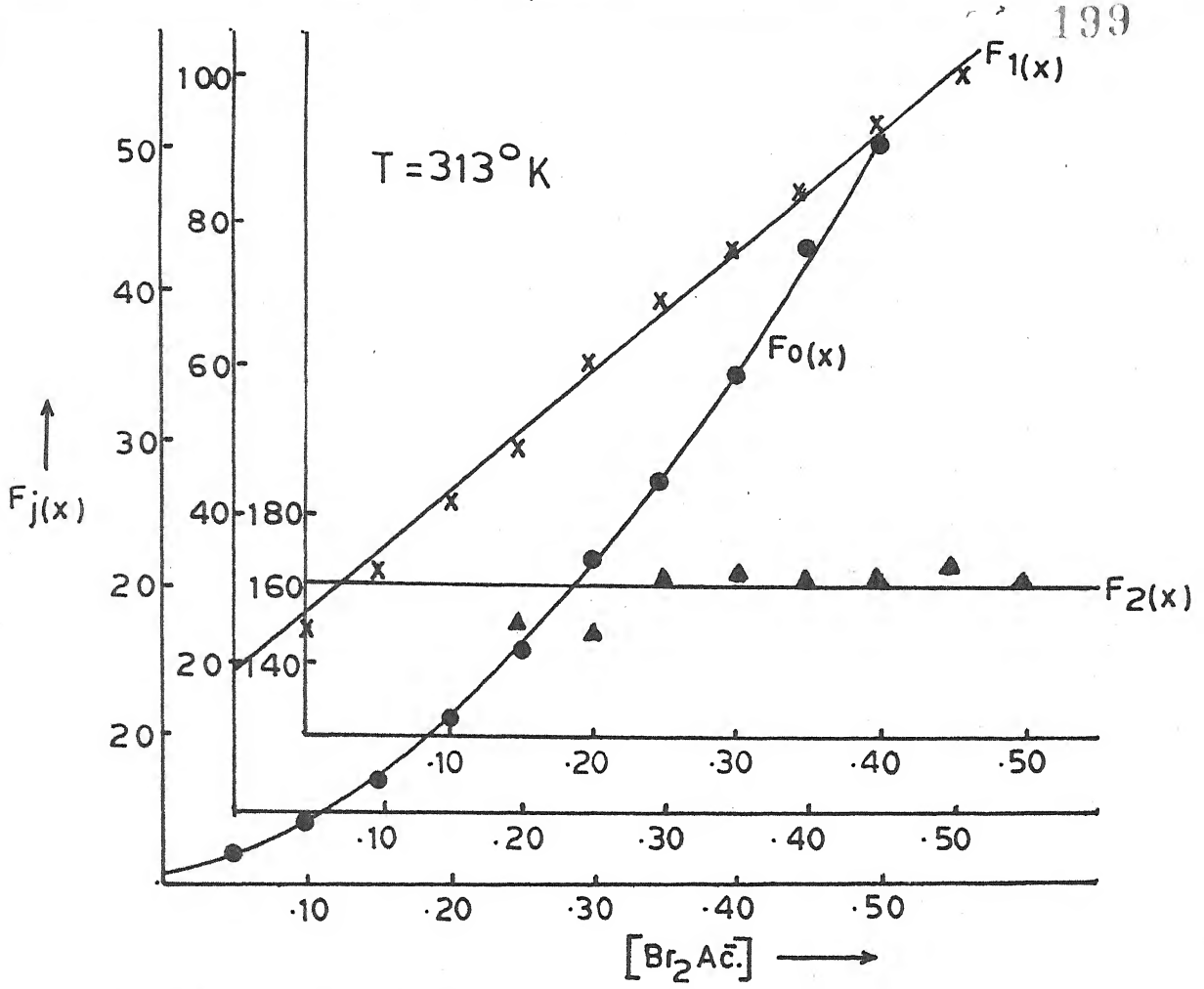

Fig. 5·27 - Plot of $F_{j(x)}$ Vs. $[Br_2 A\bar{c}.]$; Zn($Br_2 A\bar{c}.$) system.

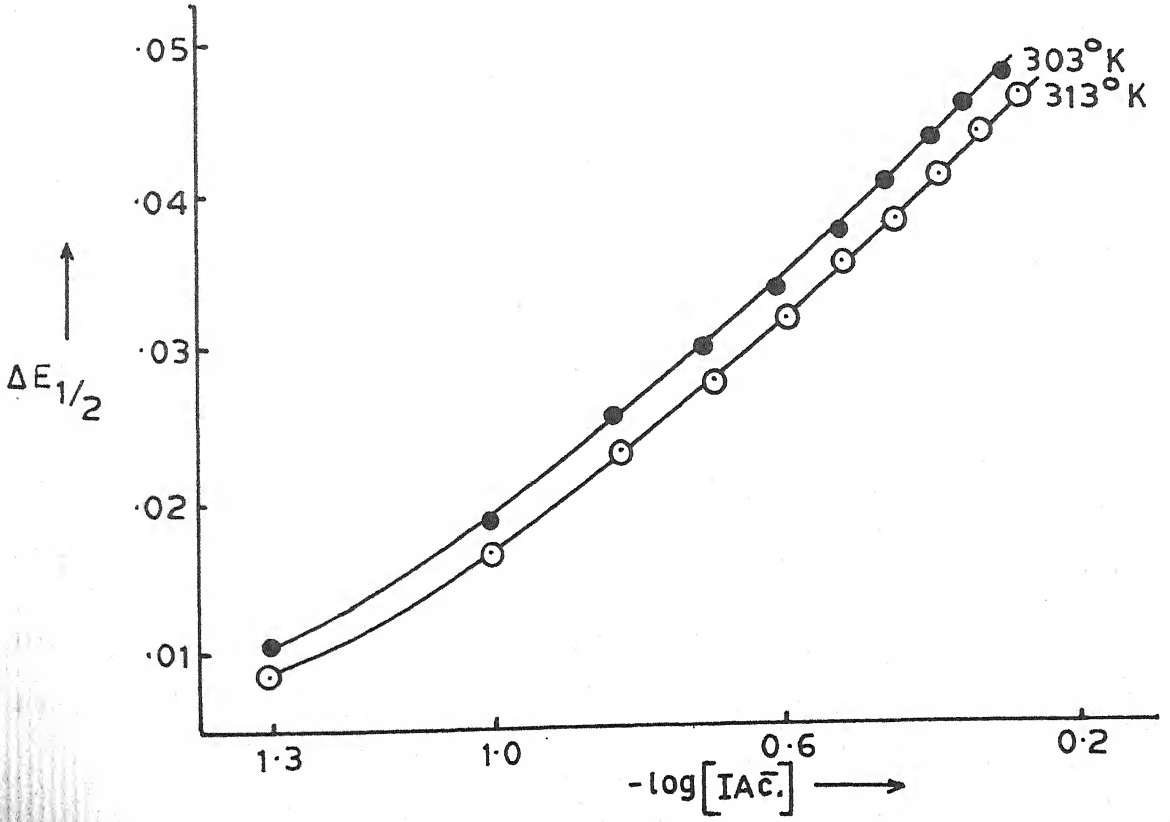

Fig. 5·28 - Plot of $\Delta E_{1/2}$ Vs. $-\log[IA\bar{c}.]$ Zn($IA\bar{c}.$) system.

data has been included in table 5.26 and $F_j(X)$ functions drawn in figure 5.27.

Table 5.27 contains the ΔG, ΔH and ΔS values computed from two sets of β_1 values.

Table 5.27

Zinc dibromoacetate system

Temperature (° K)	log β_1	- ΔG (kj)	- ΔH (kj)	- ΔS (kj deg^{-1})x10^3
303	1.3979	8.1103		51.6250
			23.7527	
313	1.2671	7.5940		51.6252

5.3.10 Zinc monoiodoacetate system :

(a) Nature of reduction : The linearity of conventional log plots with slopes of 31-32 mV, temperature co-efficients of $E_{1/2}$ (0.2 $\pm$ 0.1 mV per degree) and i_d (0.6 $\pm$ 0.1% per degree) coupled with direct proportionality of diffusion current with square root of effective height of mercury column lead us to the conclusion that the reduction of Zn(II) in monoiodoacetate ions is reversible, involves two electrons and is solely diffusion controlled.

(b) Effect of ligand concentration : Half wave potential exhibited a cathodic shift and diffusion current decreased when solutions containing 0.9 mM Zn(II) ions, 0.002% gelatin, increasing

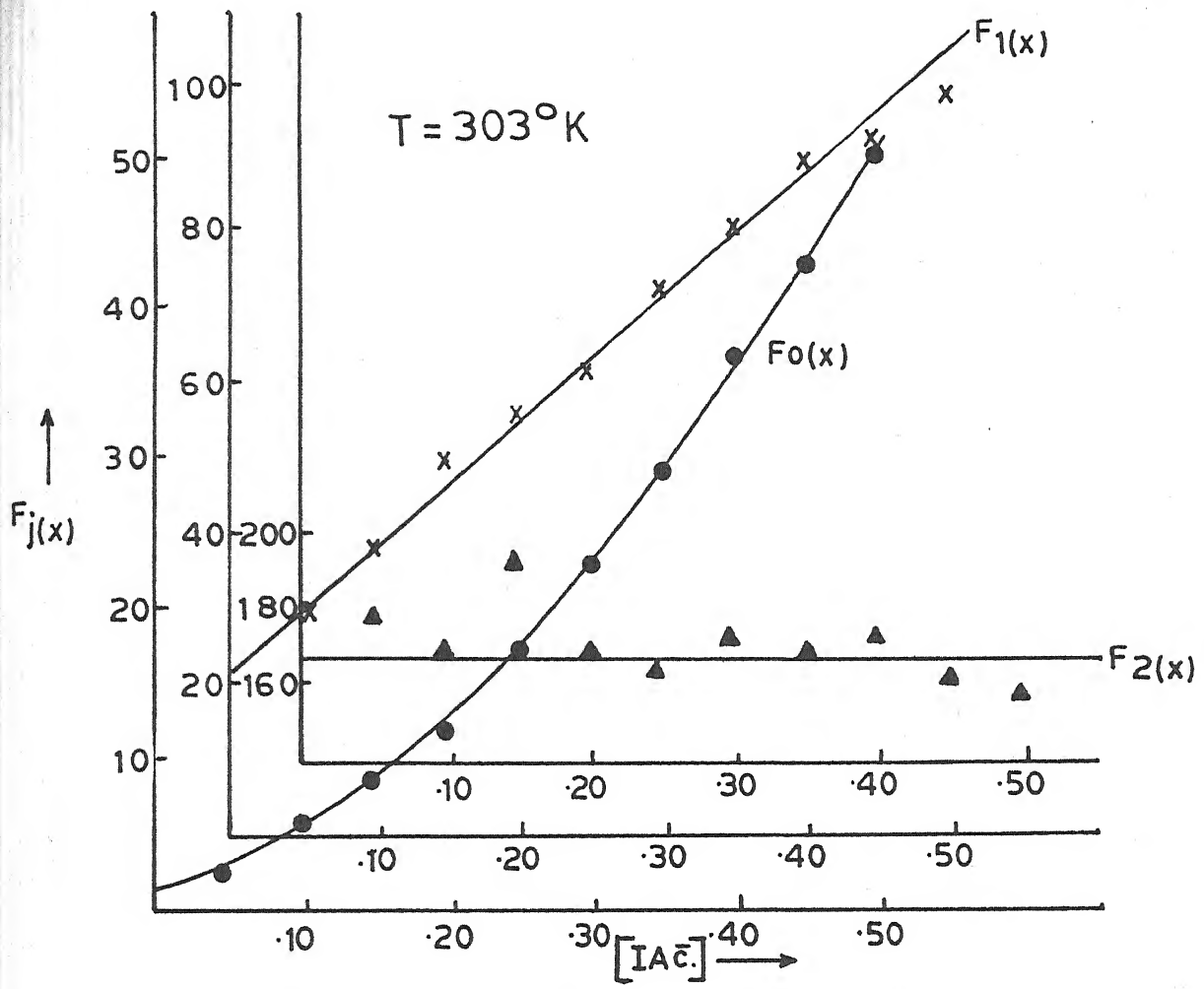

Fig. 5·29 - Plot of $F_{j(x)}$ Vs. $[IA\bar{c}.]$; Zn(IAc̄.)system.

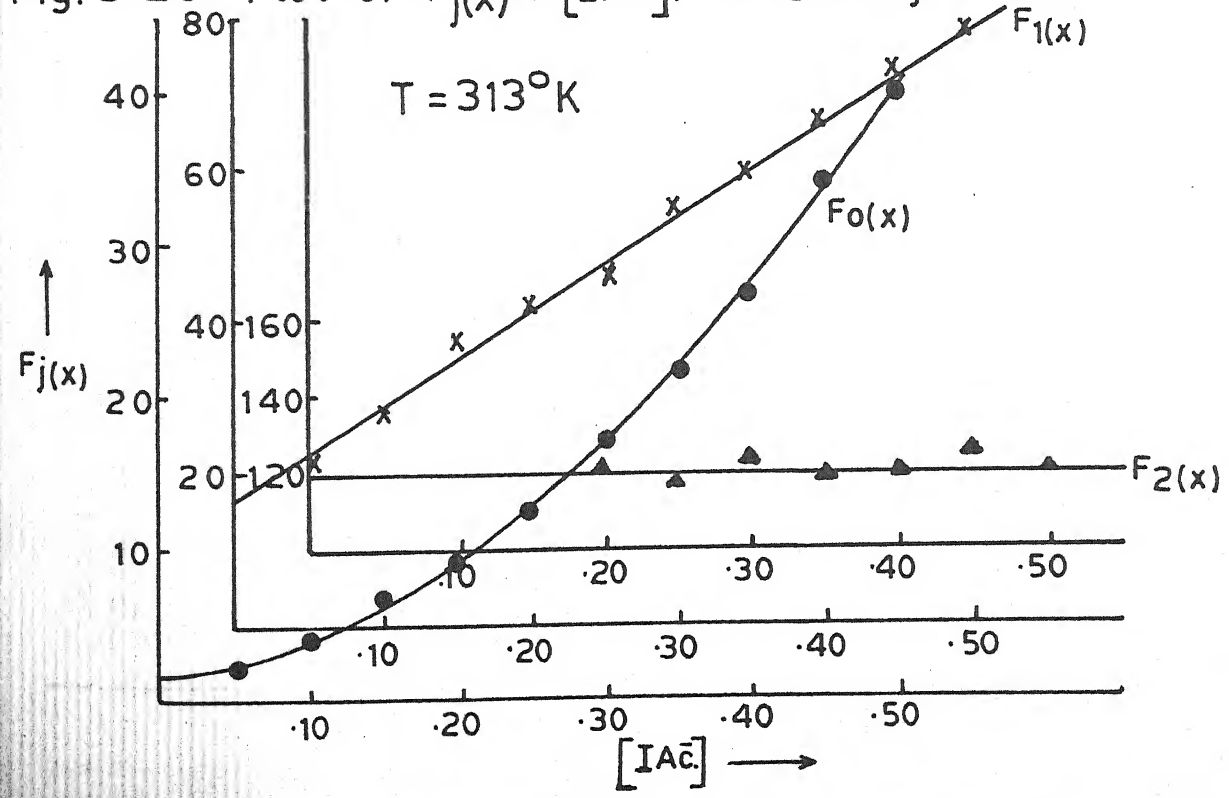

Fig. 5·30 - Plot of $F_{j(x)}$ Vs. $[IA\bar{c}.]$; Zn(IAc̄.)system.

Table 5.28

Polarographic data for Zinc monoiodoacetate system

Concn. of Zn^{++} ions = 0.9 mM Ionic strength = 1.0 M ($NaClO_4$)
$E_{1/2}$ of Zn^{++} ions = -0.998 V vs. SCE Temperature = 303° K
Slopes of plots of $-E_{de}$ vs. -log. i/i_d-i = 31-32 mV

$[I\bar{A}c.]$ (M)	$\Delta E_{1/2}$ (V)	log. I_M/I_C	$F_0(X)$	$F_1(X)$	$F_2(X)$
0.05	0.011	0.0324	2.50	30.0	180.0
0.10	0.019	0.0511	4.82	38.2	172.0
0.15	0.026	0.0674	8.55	50.33	195.5
0.20	0.030	0.0808	11.99	54.95	169.7
0.25	0.034	0.0912	16.68	62.72	166.8
0.30	0.038	0.0983	23.04	73.46	174.8
0.35	0.041	0.1005	29.47	81.34	172.4
0.40	0.044	0.1091	37.40	91.0	175.0
0.45	0.046	0.1091	43.59	94.64	163.6
0.50	0.048	0.1128	51.28	100.5	159.0

$\beta_1 = 21$ $\beta_2 = 168$

Table 5.29

Polarographic data for Zinc monoiodoacetate system

Concn. of Zn^{++} ions = 0.9 mM Ionic strength = 1.0 M ($NaClO_4$)
$E_{1/2}$ of Zn^{++} ions = -0.991 V vs. SCE Temperature = 313° K
Slopes of plots of $-E_{de}$ vs. -log. i/i_d-i = 31-32 mV

$[I\bar{A}c.]$ (M)	$\Delta E_{1/2}$ (V)	log. I_M/I_C	$F_0(X)$	$F_1(X)$	$F_2(X)$
0.05	0.009	0.0288	2.08	21.6	-
0.10	0.017	0.0454	3.91	29.1	-
0.15	0.024	0.0569	6.75	38.33	-
0.20	0.028	0.0656	9.27	41.35	124.5
0.25	0.032	0.0716	12.65	46.6	120.4
0.30	0.036	0.0776	17.25	54.16	125.5
0.35	0.039	0.0776	21.55	58.71	120.6
0.40	0.042	0.0807	27.12	65.3	122.0
0.45	0.045	0.0837	34.11	73.57	126.8
0.50	0.047	0.0868	39.84	77.68	122.3

$\beta_1 = 16.5$ $\beta_2 = 120$

amounts of monoiodoacetate ions and decreasing amounts of sodium perchlorate (for μ = 1.0 M) were reduced at DME at 303° K to indicate complex formation between Zn(II) and monoiodoacetate ions. Having inferred multiple complex formation from the plot of $\Delta E_{1/2}$ vs. -log. $[IAc^-]$ which was a curve (figure 5.28), the method DeFord and Hume yielded 21 and 168 as the β_1 and β_2 values for which the polarographic data and $F_j(X)$ functions are included in table 5.28 and figure 5.29.

(b) Effect of temperature : The temperature co-efficient values of $E_{1/2}$ and i_d are of the order 0.2 $\pm$ 0.1 mV per degree and 0.6 $\pm$ 0.1 percent per degree respectively.

The stability constants were determined at another temperature i.e. 313° K and were found to be 16.5 and 120 respectively for $[Zn(IAc.)]^+$ and $[Zn(IAc.)_2]$ complexes. The polarographic data and $F_j(X)$ functions are presented in table 5.29 and figure 5.30.

The thermodynamic parameters calculated from the knowledge of stability constants at two temperatures are reported in table 5.30.

Table 5.30

Zinc monoiodoacetate system

Temperature (° K)	log β_1	- ΔG (kj)	- ΔH (kj)	- ΔS (kj deg^{-1})x10^3
303	1.3222	7.6711	19.0312	37.492
313	1.2174	7.2962		37.492

5.4 DISCUSSION :

The study of stability constants of metal complexes offers vast and varied possibilities. There are so many variables associated with the phenomenon of complex formation even when investigated by a single method, that it has become a complicated field. One and the only reasonable approach to the study of formation constants would involve keeping as many variables constant as possible. Under these circumstances it would be logical to compare and contrast the formation constants so as to evaluate the effect of a limited number of other factors. With these considerations in view, it has been attempted to investigate the effect of halogen substitution on the co-ordinating ability of the acetate ion. We have attempted to carry out our studies under as identical conditions as possible.

It was not possible for us to undertake the study of Zn(II) complexes with tribromoacetate, diiodoacetate and triiodoacetate ions due to their ready hydrolysability when preparing their sodium salts even by mild alkalies. The hydrolysis of only three of the halosubstituted acetate ions may be attributed to their lower carbon-halogen bond energy coupled with greater intramolecular halogen repulsions making them unstable and susceptible to easy hydrolysis even at the room temperature. A glance at the bond strengths[12], noted underneath, would clarify the situation.

Bond	Bond energy (kj)	Bond length (A^{o})
C - F	447.7	1.42
C - Cl	326.4	1.77
C - Br	284.5	1.91
C - I	213.4	2.13

That the Zn(II) does not form particularly strong complexes with the remaining haloacetate ions is obvious from the following review of the formation constant data.

System	At 303° K		At 313° K	
	β_1	β_2	β_1	β_2
Zinc acetate	70.5	158	58	120
Zinc monofluoroacetate	54	132	45	84
Zinc difluoroacetate	15.5	100	12.5	80
Zinc trifluoroacetate	14.5	192	10.5	100
Zinc monochloroacetate	36.5	114	27	72
Zinc dichloroacetate	22.5	142	18.5	110
Zinc trichloroacetate	19	114	14	104
Zinc monobromoacetate	28	200	21	136
Zinc dibromoacetate	25	206	18.5	162
Zinc monoiodoacetate	21	168	16.5	120

In the ligand concentration range under investigation (0.0 to 0.5 M) only two complexes i.e. 1:1 and 1:2 are formed

to the exclusion of higher complexes.

Expectedly, the K_2 value (β_2/β_1) in each and every case is less than the K_1 or the β_1 value. Such a situation can be explained on the basis of statistical, steric and coulombic considerations which are narrated below :

Zinc(II) can have a maximum co-ordination number of six in which the free metal ion $[Zn(H_2O)_6]^{2+}$ has six co-ordination sites available for the entry of the first ligand L^- to form $[Zn(H_2O)_5L]^+$. For the entry of the second ligand, the availability of co-ordination sites becomes less i.e. five. Thus, stastically speaking, the probability of formation of 1:2 complex is less than that of 1:1 complex.

Once the 1:1 complex $[Zn(H_2O)_5L]^+$ has formed, there is lesser space available around the central metal to accomodate bigger than water molecule ligand ion than was the case prior to entry of the first ligand ion into the co-ordination sphere.

Finally, electrostatic attraction for the entry of second uninegative ligand is less for the unco-ordinated metal ion is bipositive while the monoco-ordinated metal ion is unipositive.

Thus these three factors jointly explain the lesser value of K_2 compared to that of K_1.

While taking a look at the formation constant data, one cannot fail to observe that stability constants for a given halogen, substituted acid complexes with Zn(II) have the

207

following trend :

$$[Zn(Ac.)]^{+} > [Zn(XAc.)]^{+} > [Zn(X_2Ac.)]^{+} > [Zn(X_3Ac.)]^{+}$$

Two factors are mainly responsible for this trend.

(a) Inductive effect : When a halogen atom replaces a hydrogen atom from an acetate ion, its basic character undergoes a decrease; the extent of which depends upon the halogen introduced. Due to inductive effect the greatest decrease in basicity would be effected by F and the least by I. larger number of halogen atoms introduced in the acetate ion also have a similar but more pronounced effect as shown below :

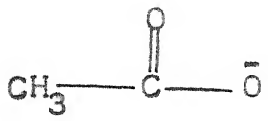

acetate ion

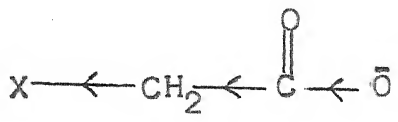

monohaloacetate ion

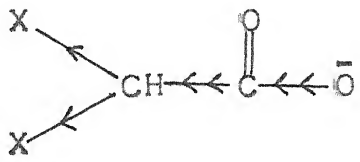

dihaloacetate ion

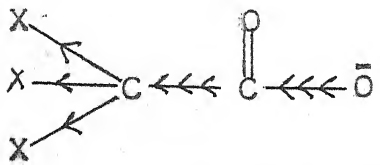

trihaloacetate ion

The higher electronegativity of the replaced halogen

exerts a strong inductive effect to reduce the basicity of the parent ion. This effect is correspondingly greater when two and three halogen atoms enter the acetate ion. Thus $(X_3A\bar{c}.)$ is the weakest base while simple $(A\bar{c}.)$ is the strongest.

(b) Steric factors : The successively bulkier $(XA\bar{c}.)$, $(X_2A\bar{c}.)$ and $(X_3A\bar{c}.)$ ions find greater steric hindrance in entering the co-ordination sphere to form the corresponding complex.

The above two factors combine together to yield the trend (e.g. for chloroacetate complexes).

$[Zn(Ac.)]^+ = 70.5 > [Zn(ClAc.)]^+ = 36.57 > [Zn(Cl_2Ac.)]^+ = 22.5 > [Zn(Cl_3Ac.)]^+ = 19$ at 303° K.

Some other important trends are found to emerge from the survey of the stability constant data. The β_1 values have the order.

(a) $[Zn(FAc.)]^+ > [Zn(ClAc.)]^+ > [Zn(BrAc.)]^+ > [Zn(IAc.)]^+$

(b) $[Zn(F_2Ac.)]^+ < [Zn(Cl_2Ac.)]^+ < [Zn(Br_2Ac.)]^+$

(c) $[Zn(F_3Ac.)]^+ < [Zn(Cl_3Ac.)]^+$

Ignoring the number of substituted halogens trends (b) and (c) are exactly reverse of trend (a).

What is paradoxical in trend (a) is that inspite of the stronger inductive effect of more electronegative halogen,

its complex is more stable for the monohaloacetate complexes only. This is because more electronegative halogen substituted acetate ion is smaller in size (because of the smaller size of the halogen) and hence experiences less steric hindrance in entering the co-ordination sphere. It appears that the lesser steric hindrance prevails over the stronger inductive effect only for single halogen substituted acetate ions to yield the trend (a).

Relatively speaking, single halogen substitution in acetate ion results in a considerably greater enhancement in the size of the parent acetate ion than in the case of double and triple halogen substitution in the parent monohalo and dihaloacetate ions. Simultaneously the inductive effect is doubled and tripled. Thus, while there is no matching increase in size from $(XA\bar{c}.)$ to $(X_3A\bar{c}.)$ via $(X_2A\bar{c}.)$ ion inspite of increase in ~~size~~ number of substituted halogens, the inductive effect is tripled, consequently the inductive effect overwhelms the effect due to bulkier ligand ions. This way, the trend (b) and (c) get explained because the electronegativity follows the order F > Cl > Br > I.

One may, therefore, conclude that the size of the ligand governs the trend (a) while inductive effect is responsible for the trends (b) and (c).

The lesser value of β_1 at the elevated temperature is due to the greater dissociation and hence lesser formation of the complex. At first glance, almost no change in ΔS values

its complex is more stable for the monohaloacetate complexes only. This is because more electronegative halogen substituted acetate ion is smaller in size (because of the smaller size of the halogen) and hence experiences less steric hindrance in entering the co-ordination sphere. It appears that the lesser steric hindrance prevails over the stronger inductive effect only for single halogen substituted acetate ions to yield the trend (a).

Relatively speaking, single halogen substitution in acetate ion results in a considerably greater enhancement in the size of the parent acetate ion than in the case of double and triple halogen substitution in the parent monohalo and dihaloacetate ions. Simultaneously the inductive effect is doubled and tripled. Thus, while there is no matching increase in size from $(XA\bar{c}.)$ to $(X_3A\bar{c}.)$ via $(X_2A\bar{c}.)$ ion inspite of increase in ~~size~~ number of substituted halogens, the inductive effect is tripled, consequently the inductive effect overwhelms the effect due to bulkier ligand ions. This way, the trend (b) and (c) get explained because the electronegativity follows the order F > Cl > Br > I.

One may, therefore, conclude that the size of the ligand governs the trend (a) while inductive effect is responsible for the trends (b) and (c).

The lesser value of β_1 at the elevated temperature is due to the greater dissociation and hence lesser formation of the complex. At first glance, almost no change in ΔS values

at the two temperatures may look surprising. This is not difficult to explain. In each system, the dissociation of the complex does not result in change in number of available particles as the ligand invariably is a monodentate one. Thus, in the dissociation :

$$\left[Zn(H_2O)_5(XAc.)\right]^{+} + H_2O \rightleftharpoons \left[Zn(H_2O)_6\right]^{+} + (XAc.)^{-}$$

there is no change in number of particles i.e. disorder or entropy of the system. This is why there is virtually no change in entropy of a complex when the temperature is raised.

There is no mystery in the positive shift in ΔG at the higher temperature. When the temperature is raised, the complex becomes less stable and hence possesses greater free energy.

Since in the formation of complexes, the less stable Zn(II) - H_2O bond is replaced by more stable Zn-(XAc^{-}.) bond, we have obtained a negative value of enthalpy in each case. Obviously, the heat content of complex is less than that of free metal ion.

LITERATURE CITED

1. D.P. Mellor and L.E. Maley, Nature, 159, 370 (1947).
2. H. Matsuda, Y. Ayabe and K. Adachi, Z. Electrochem, 67, 503 (1963).
3. R.S. Kolat and J.E. Powell, Inorg. Chem., 1, 293 (1962).
4. D.W. Archer and C.B. Monk, J. Chem. Soc., 3117 (1964).
5. R. Gäiesser, B. Psijs and H. Sigel, Inorg. Nucl. Chem. Letters, 4, 443 (1968).
6. N.K. Arora and A.V. Mahajan, J. Inst. Chem. (India), 56, 76 (1984).
7. W. Van Doorne and M. Hannink, Synth. React. Inorg. Metal - Org. Chem., 11, 15 (1981).
8. A.I. Khokhlora, A.M. Robov and V.A. Fedorov, Neorg. Khim., 26, 258 (1981).
9. A. Liberti, P. Curro and G. Calabro, Ricerca Sci., 33, 36 (1963).
10. D.D. DeFord and D.N. Hume, J.Am.Chem.Soc., 73, 5321 (1951).
11. H. Irving, 'Advances in Polarography', Pergamon Press, Oxford, 49 (1960).
12. I.L. Finar, 'Organic Chemistry', Vol. 1, ELBS/Longman, 36-37 (1985).

CHAPTER VI

Cd(II) complexes with

(a) acetate ion

(b) mono-, di- and trifluoroacetate ions

(c) mono-, di- and trichloroacetate ions

(d) mono- and dibromoacetate ions

(e) monoiodoacetate ion

6.1 INTRODUCTION :

Among the four metals studied, Cd(II) forms the weakest complexes being less stable than those of Cu(II), Pb(II) and Zn(II) in that order to strictly follow the Mellor and Maley[1] order of stability of metal complexes with mono-dentate ligands. Kolat and Powel[2], Archer and Monk[3] and Goban[4], have studied Cd(II) acetate complexes potentiometrically to report the formation of maximum of two complexes in each case. Calorimetric studies on the complex have been made by Gerding[5] who has determined the stability constants at ionic strengths varying between 0.25 to 2.00 M of sodium perchlorate. Cd(II) acetate system has also been studied polarographically by Tanaka et.al[6] to determine the formation constants at 15°, 25° and 35° centigrade.

Expectedly, the haloacetate complexes with Cd(II) should be weaker than those of simple acetate ion due to electron withdrawal from co-ordination site of substituted acetate ion by more electronegative halogen which has substituted itself. Goel and Jha[7] have isolated and characterised Cd trifluoroacetate complex from spectral data while Khokhlora et.al[8] have studied the mixed carboxaloto complexes of Cd(II) potentiometrically. Although a few other references[9-10] are available on Cd acetate complexes, there is a lack of relevant literature on the complexes of various halosubstituted acetic acids with the metal ions.

It is this silence of literature which has impelled us

to carry out a systematic investigations on Cd haloacetate complexes by studying their reduction at DME at two different temperatures but under identical conditions to study the effect of different halogen substitution on co-ordinating behaviour of acetate ion and determine the formation constants as well as thermodynamic functions ΔG, ΔH and ΔS.

6.2 EXPERIMENTAL :

All reagents used were of analytical grade purity. Halosubstituted acetic acids manufactured by K & K (USA), Fluka (Swiss), BDH (UK) and Riedel (German) were used. Their sodium salts were prepared by adding a dilute solution of sodium bicarbonate. One had to be careful in handling the haloacetic acids as they cause serious burns and blisters on the skin. A semi-micro burette was used to add requisite amounts of their sodium salt solutions to test solutions.

All solutions were made in double distilled conductivity water. Sodium perchlorate at 1.0 M was the supporting electrolyte used. With increasing ligand concentration, its concentration was correspondingly reduced to maintain a constant ionic strength. In each case 0.002% gelatin, in final solutions, just sufficed to suppress the maxima observed.

Each solution was polarographed by placing it in a thermostated H-cell coupled with a saturated calomel electrode. Hydrogen gas was passed for about ten minutes through each test solution to remove dissolved oxygen prior to its polarographic examination. The potential of the DME was increased gradually and

change in current noted.

The intercepts on the potential axis in the plot of $-E_{de}$ vs. -log. i/i_d-i yielded the half wave potentials.

The capillary of the DME had the following characteristics in 0.1 M sodium perchlorate in the open circuit.

m = 2.43 mg/sec

t = 2.9 sec

$h_{corr.}$ = 53 cms.

Investigations on the effect of ligand concentration on half wave potential and diffusion current were effected at two temperatures viz. 303° and 313° K.

6.3 RESULTS :

6.3.01 Cadmium acetate system :

(a) Nature of reduction : The reversibility involving two electron transfer process and diffusion controlled character of reduction of Cd(II) in acetate ions is deduced from the linearity of plots of $-E_{de}$ vs. -log. i/i_d-i with slopes of 29-30 mV, temperature co-efficient values of half wave potential (0.2-0.3 mV per degree) and diffusion current (0.5 $\pm$ 0.1% per degree) and the direct proportionality of diffusion current with the square root of effective height of mercury column of the DME.

(b) Effect of ligand concentration : The well defined polarographic waves of reduction at 303° K of solutions containing 0.9 mM (Cd(II) ions, 0.002% gelatin, increasing amounts of acetate ions and correspondingly decreasing amounts of sodium perchlorate

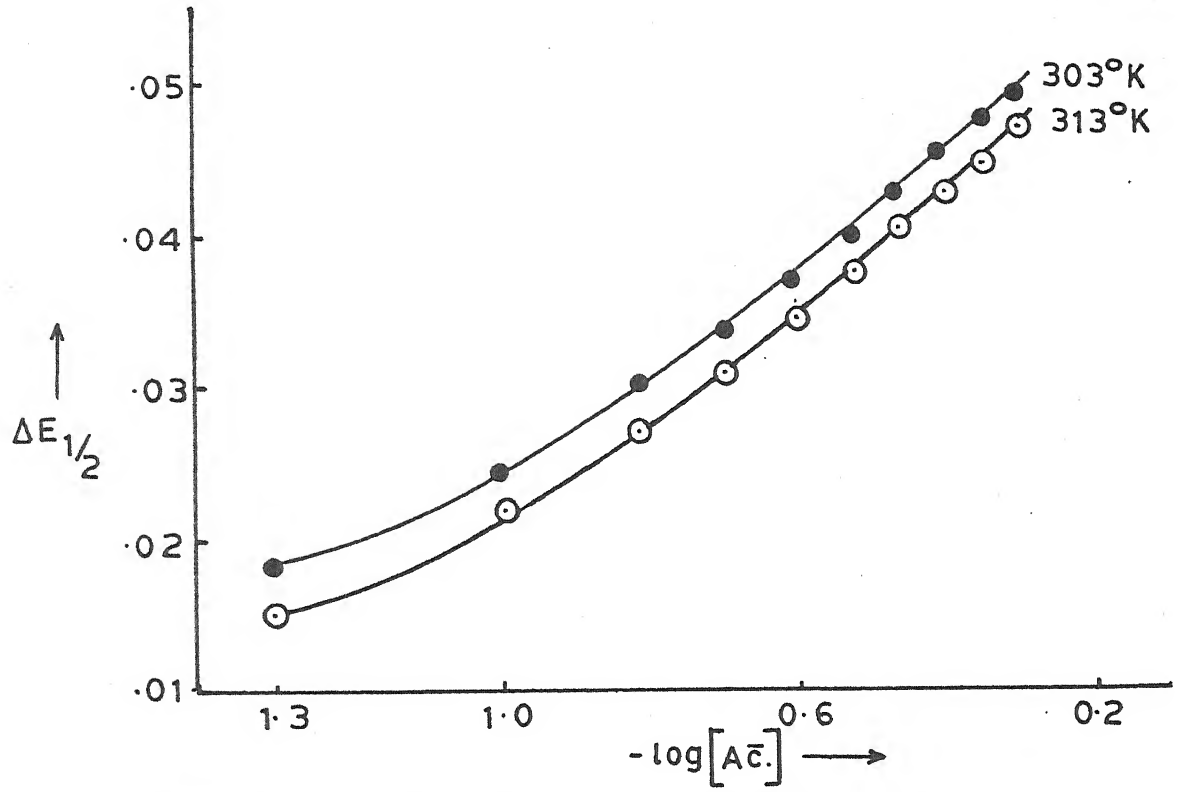

Fig. 6·01 - Plot of $\Delta E_{1/2}$ Vs. $-\log[A\bar{c}.]$; Cd ($A\bar{c}.$) system.

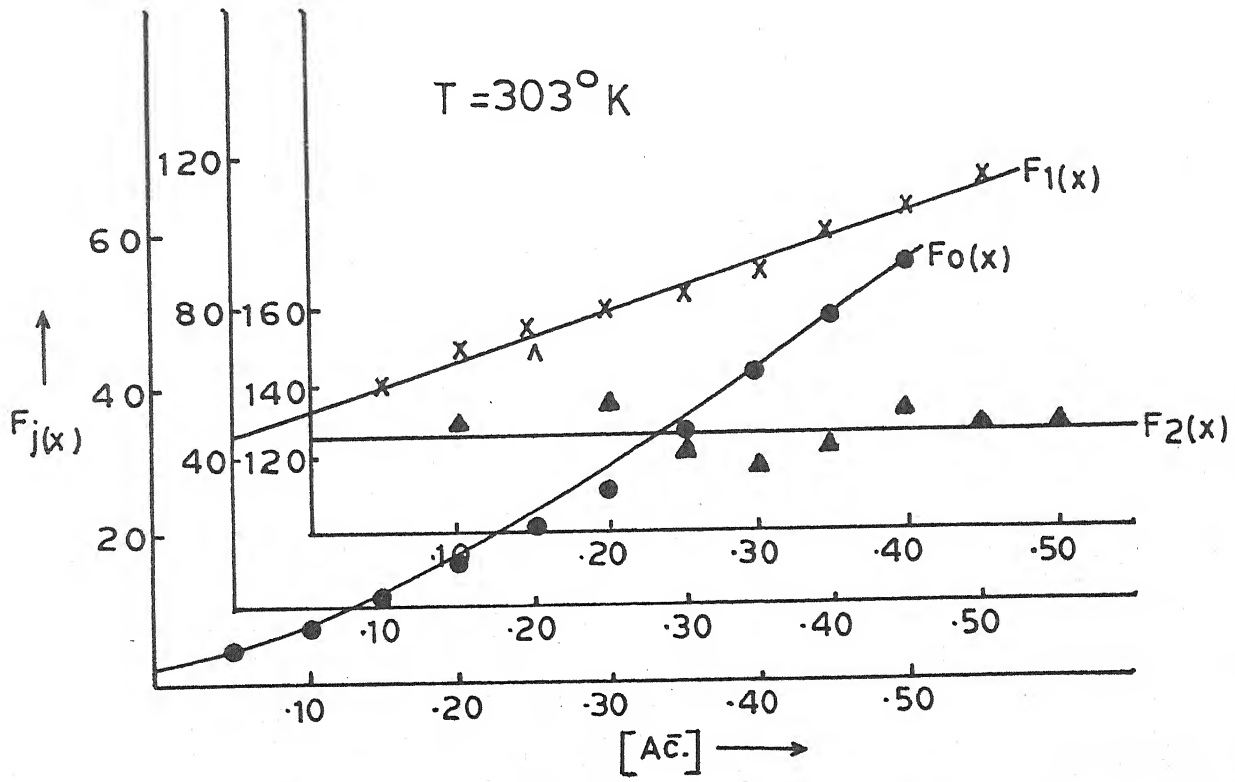

Fig. 6·02 - Plot of $F_{j(x)}$ Vs. $[A\bar{c}.]$; Cd ($A\bar{c}.$) system.

Table 6.01

Polarographic data for Cadmium acetate system

Concn. of Cd^{++} ions = 0.9 mM Ionic strength = 1.0 M ($NaClO_4$)
$E_{1/2}$ of Cd^{++} ions = -0.576 V vs. SCE Temperature = 303° K
Slopes of plots of $-E_{de}$ vs. -log. i/i_d-i = 29-30 mV

$[Ac^-]$ (M)	$\Delta E_{1/2}$ (V)	log. I_M/I_C	$F_0(X)$	$F_1(X)$	$F_2(X)$
0.05	0.018	0.0265	4.22	-	-
0.10	0.024	0.0419	6.92	59.2	132.0
0.15	0.030	0.0547	11.29	68.6	150.6
0.20	0.034	0.0645	15.69	73.45	137.2
0.25	0.037	0.0746	20.20	76.8	123.2
0.30	0.040	0.0780	25.63	82.1	120.3
0.35	0.043	0.0814	32.50	90.0	125.7
0.40	0.046	0.0814	40.90	99.75	134.4
0.45	0.048	0.0849	48.05	104.55	130.1
0.50	0.050	0.0884	56.46	110.92	129.8

$\beta_1 = 46$ $\beta_2 = 126$

Table 6.02

Polarographic data for Cadmium acetate system

Concn. of Cd^{++} ions = 0.9 mM Ionic strength = 1.0 M ($NaClO_4$)
$E_{1/2}$ of Cd^{++} ions = -0.570 V vs. SCE Temperature = 313° K
Slopes of plots of $-E_{de}$ vs. -log. i/i_d-i = 29-30 mV

$[Ac^-]$ (M)	$\Delta E_{1/2}$ (V)	log. I_M/I_C	$F_0(X)$	$F_1(X)$	$F_2(X)$
0.05	0.015	0.0349	3.29	45.8	-
0.10	0.022	0.0521	5.76	47.6	76.0
0.15	0.027	0.0669	8.63	50.86	72.4
0.20	0.031	0.0760	11.86	54.3	71.5
0.25	0.035	0.0822	16.19	60.76	83.0
0.30	0.038	0.0885	20.52	65.06	85.3
0.35	0.041	0.0949	26.02	71.42	87.7
0.40	0.043	0.0982	30.40	73.5	83.7
0.45	0.045	0.1041	35.53	76.7	81.5
0.50	0.047	0.1041	41.52	81.0	82.0

$\beta_1 = 40$ $\beta_2 = 82$

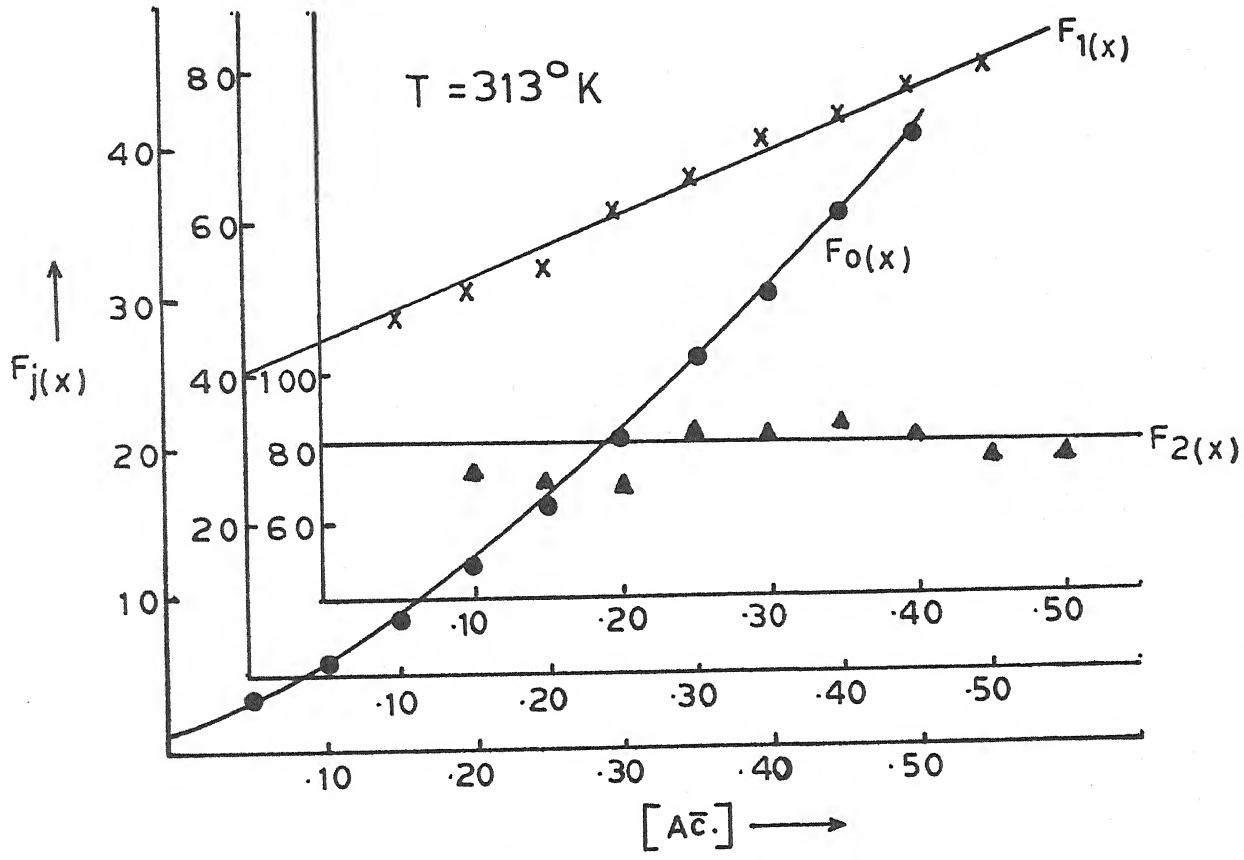

Fig. 6·03 - Plot of $F_{j(x)}$ Vs. $[A\bar{c}.]$; Cd(Ac̄.)system.

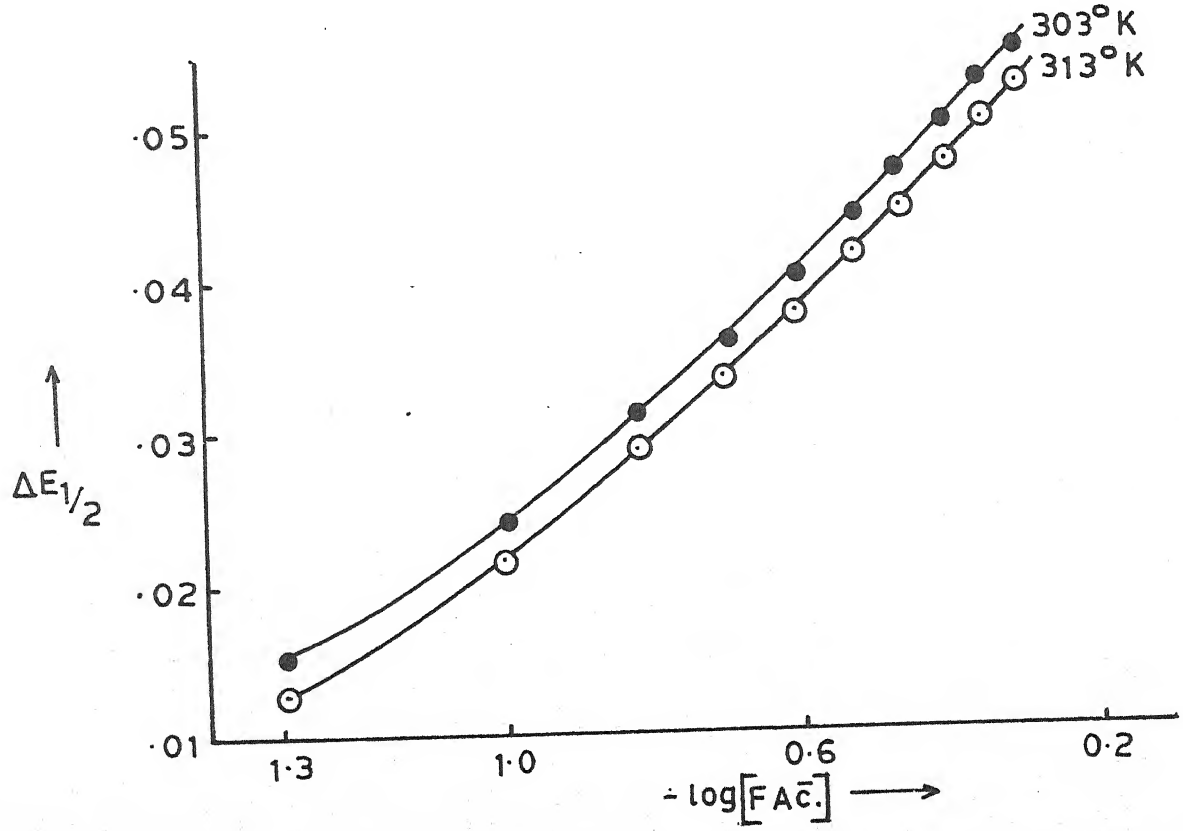

Fig. 6·04 - Plot of $F_{j(x)}$ Vs. $-\log[F A\bar{c}.]$; Cd(FAc̄.)system.

to maintain ionic strength constant at 1.0 M exhibited shift of $E_{1/2}$ to the more negative side and a gradual decrease in i_d to indicate complex formation. The plot of $\Delta E_{1/2}$ vs. -log. $[Ac^-]$ being a curve (figure 6.01) multiple complex formation was inferred and the method of DeFord and Hume[11] as improved by Irving[12] was applied to evaluate overall stability constants which were found to be 46 and 126 for $[Cd(Ac.)]^+$ and $[Cd(Ac.)_2]$ complexes respectively. The corresponding polarographic data and $F_j(X)$ plots appear in table 6.01 and figure 6.02.

(c) Effect of temperature : As reported earlier in this section, the temperature co-efficients of $E_{1/2}$ and i_d were found to be of the order of 0.2 - 0.3 mV per degree and 0.5 $\pm$ 0.1% per degree respectively.

The effect of ligand concentration on $E_{1/2}$ and i_d was reinvestigated at 313° K to obtain $\beta_1 = 40$ and $\beta_2 = 82$ for which the polarographic data and $F_j(X)$ functions have been presented in table 6.02 and figure 6.03.

Table 6.03 contains the thermodynamic functions computed from the knowledge of β_1 at the two temperatures.

Table 6.03

Cadmium acetate system

Temperature (° K)	log β_1	- ΔG (kj)	- ΔH (kj)	- ΔS (kj deg^{-1})x10^3
303	1.6627	9.6466		4.5419
			11.0228	
313	1.6020	9.6012		4.5418

6.3.02 Cadmium monofluoroacete system :

(a) Nature of reduction : The straight line nature of the conventional log. plots with slopes of 29-30 mV, the temperature co-efficients of $E_{1/2}$ (0.2 mV per degree) and i_d (0.5 $\pm$ 0.1% per degree) coupled with constancy of ratio $i_d / \sqrt{h_{eff.}}$ helped us deduce that the reduction of Cd(II) in presence of monofluoroacetate ions is reversible involving two electrons and is fully diffusion controlled.

(b) Effect of ligand concentration : Polarography at 303° K of solutions consisting of 0.9 mM Cd(II) ions, 0.002% gelatin, increasing concentration of monofluoroacetate ions and decreasing concentration of sodium perchlorate (for μ = 1.0 M) revealed a gradual cathodic shift in $E_{1/2}$ and decrease in i_d indicating that complex formation has taken place between Cd(II) and (FAc^-) ions. Successive complex formation was inferred from the curved nature (figure 6.04) of the plot of $\Delta E_{1/2}$ vs. -log. $[FAc^-]$. Consequently, DeFord and Hume's method, yielded the values of overall stability constants as 37 and 250 for $Cd(FAc.)^+$ and $Cd(FAc.)_2$ complexes. The relevant polarographic data and $F_j(X)$ functions have been presented in table 6.04 and figure 6.05.

(c) Effect of temperature : In the reduction of Cd(II) in presence of monofluoroacetate ions, the temperature co-efficient values of $E_{1/2}$ and i_d were found to be 0.2 mV per degree and 0.5 $\pm$ 0.1% per degree respectively.

The stability constants of Cd monofluoroacetate complexes were redetermined at 313° K and were found to be 27.5 and 200 for

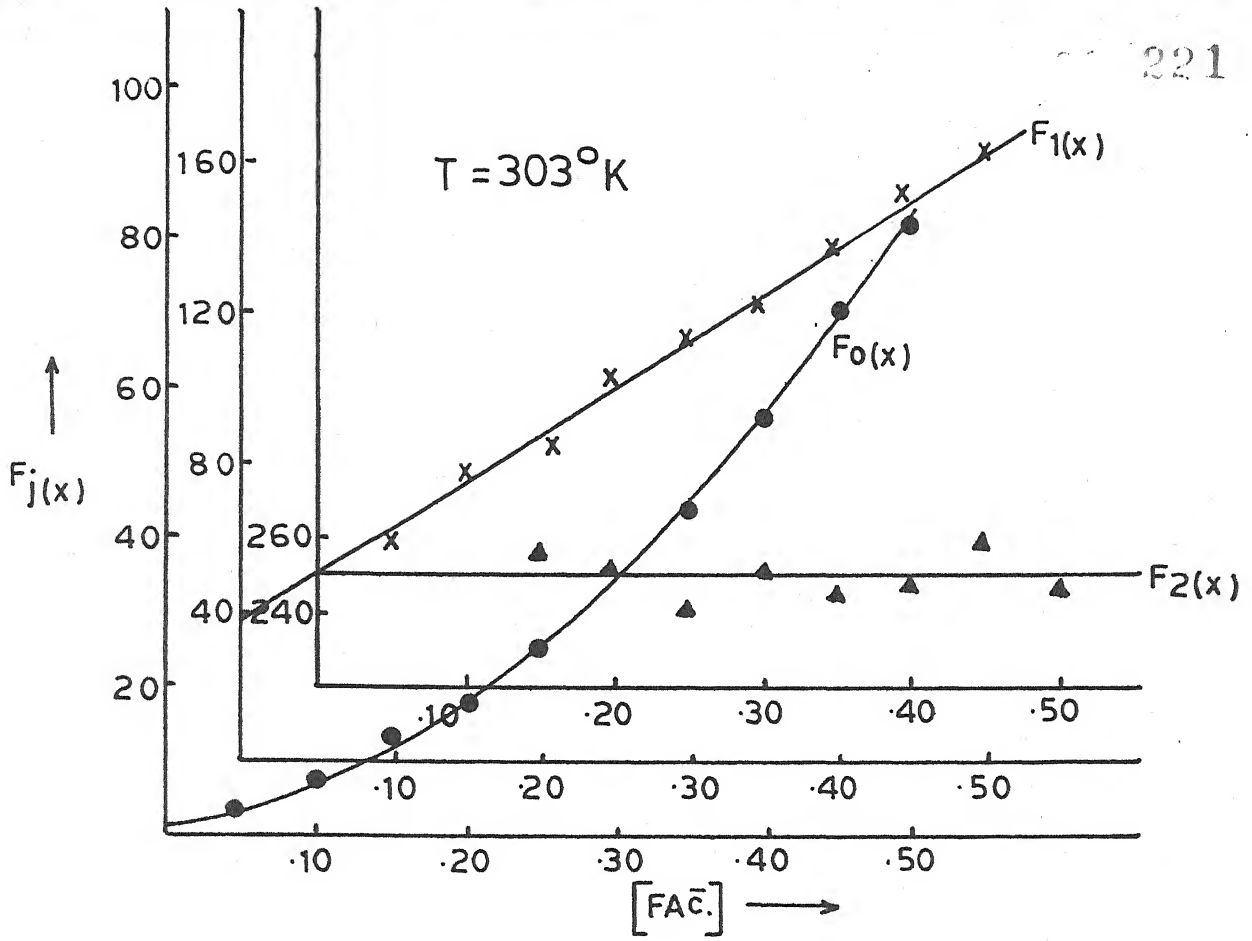

Fig. 6·05 - Plot of $F_{j(x)}$ Vs. $[FAc.]$; Cd(FAc.) system.

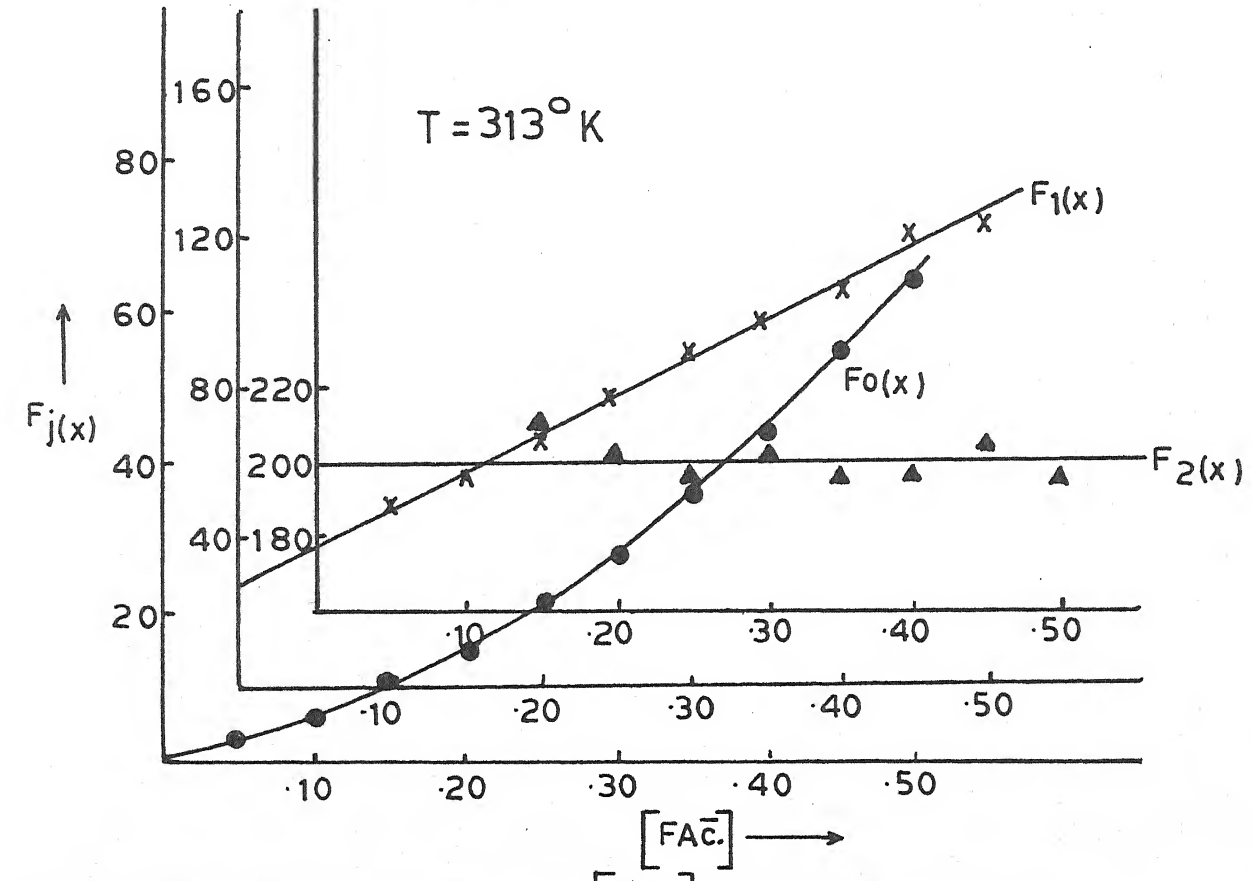

Fig. 6·06 - Plot of $F_{j(x)}$ Vs. $[FAc.]$; Cd(FAc.) system.

Table 6.04

Polarographic data for Cadmium monofluoroacetate system

Concn. of Cd^{++} ions = 0.9 mM Ionic strength = 1.0 M ($NaClO_4$)

$E_{1/2}$ of Cd^{++} ions = -0.576 V vs. SCE Temperature = 303° K

Slopes of plots of $-E_{de}$ vs. - log. i/i_d-i = 29-30 mV

$[FAc^-]$ (M)	$\Delta E_{1/2}$ (V)	log. I_M/I_C	$F_0(X)$	$F_1(X)$	$F_2(X)$
0.05	0.015	0.0285	3.36	47.2	-
0.10	0.024	0.0497	7.05	60.5	-
0.15	0.031	0.0623	12.40	76.0	260.0
0.20	0.036	0.0687	18.46	87.3	251.5
0.25	0.040	0.0753	25.46	97.84	243.3
0.30	0.044	0.0786	34.86	112.86	252.8
0.35	0.047	0.0819	44.21	123.45	247.0
0.40	0.050	0.0853	56.06	137.65	251.6
0.45	0.053	0.0886	71.09	155.75	263.8
0.50	0.055	0.0886	82.87	163.74	252.0

$\beta_1 = 37$ $\beta_2 = 250$

Table 6.05

Polarographic data for Cadmium monofluoroacetate system

Concn. of Cd^{++} ions = 0.9 mM Ionic strength = 1.0 M ($NaClO_4$)

$E_{1/2}$ of Cd^{++} ions = -0.570 V vs. SCE Temperature = 313° K

Slopes of plots of $-E_{de}$ vs. -log. i/i_d-i = 29-30 mV

$[FAc^-]$ (M)	$\Delta E_{1/2}$ (V)	log. I_M/I_C	$F_0(X)$	$F_1(X)$	$F_2(X)$
0.05	0.013	0.0339	2.83	36.6	-
0.10	0.022	0.0505	5.74	47.4	199.0
0.15	0.029	0.0619	9.90	59.33	212.2
0.20	0.034	0.0707	14.64	68.2	203.5
0.25	0.038	0.0796	20.11	76.44	195.7
0.30	0.042	0.0856	27.43	88.1	202.0
0.35	0.045	0.0919	34.76	96.45	197.0
0.40	0.048	0.0981	44.05	107.62	200.3
0.45	0.051	0.0981	55.03	120.06	205.6
0.50	0.053	0.1013	64.29	126.58	198.1

$\beta_1 = 27.5$ $\beta_2 = 200$

1:1 and 1:2 complexes for which the polarographic data and $F_j(X)$ plots appear in table 6.05 and figure 6.06.

The thermodynamic parameters calculated from the knowledge of two sets of β_1 are presented in table 6.06.

Table 6.06

Cadmium monofluoroacetate system

Temperature (° K)	log β_1	- ΔG (kj)	- ΔH (kj)	- ΔS (kj deg^{-1})x10^3
303	1.5682	9.0983		47.2257
			23.4077	
313	1.4393	8.8621		47.2255

6.3.03 Cadmium difluoroacetate system :

(a) Nature of reduction: The reduction at DME of Cd(II) in difluoroacetate medium yielded the following results :

(i) The plots of $-E_{de}$ vs. $-\log \frac{i}{i_d - i}$ are straight lines with slopes of 29-30 mV.

(ii) Per degree rise in temperature, $E_{1/2}$ and i_d vary by 0.1 $\pm$ 0.1 mV and 0.5 $\pm$ 0.1%.

(iii) i_d is directly proportional to the square root of effective height of mercury column of the DME.

These observations combined together to lead us to the conclusion that the two electron reversible reduction is

entirely diffusion controlled.

(b) Effect of ligand concentration : A cathodic shift in $E_{1/2}$ coupled with decrease in i_d with increasing ($F_2A\bar{c}.$) concentrations was observed when solutions also containing 0.9 mM Cd(II) ion, 0.002% gelatin and decreasing amounts of sodium perchlorate to keep ionic strength constant at 1.0 M, were polarographed at 303° K. This indicated complex formation between Cd(II) and difluoroacetate ions. The plot of $\Delta E_{1/2}$ vs. -log. $[F_2A\bar{c}.]$ was a curve (figure 6.07) leading us to conclude that successive complex formation had occurred. Hence the method of DeFord and Hume was applied to yield 12.5 and 138 as the β_1 and β_2 values. The concerned polarographic data is presented in table 6.07 and the $F_j(X)$ functions depicted in figure 6.08.

(c) Effect of temperature : Earlier in this section, the temperature co-efficients of $E_{1/2}$ and i_d have been utilised to help establish the reversible and diffusion controlled nature of reduction of Cd(II) in presence of difluoroacetate ions.

In order to compute thermodynamic functions, it is essential to determine stability constants at atleast one other temperature. The experiment (b) was repeated at 313° K. The overall stability constants for 1:1 and 1:2 metal/ligand ratio complexes were found to be 10 and 85 respectively. The relevant, polarographic data, $F_j(X)$ functions and thermodynamic parameters find place in table 6.08, figure 6.09 and table 6.09 respectively.

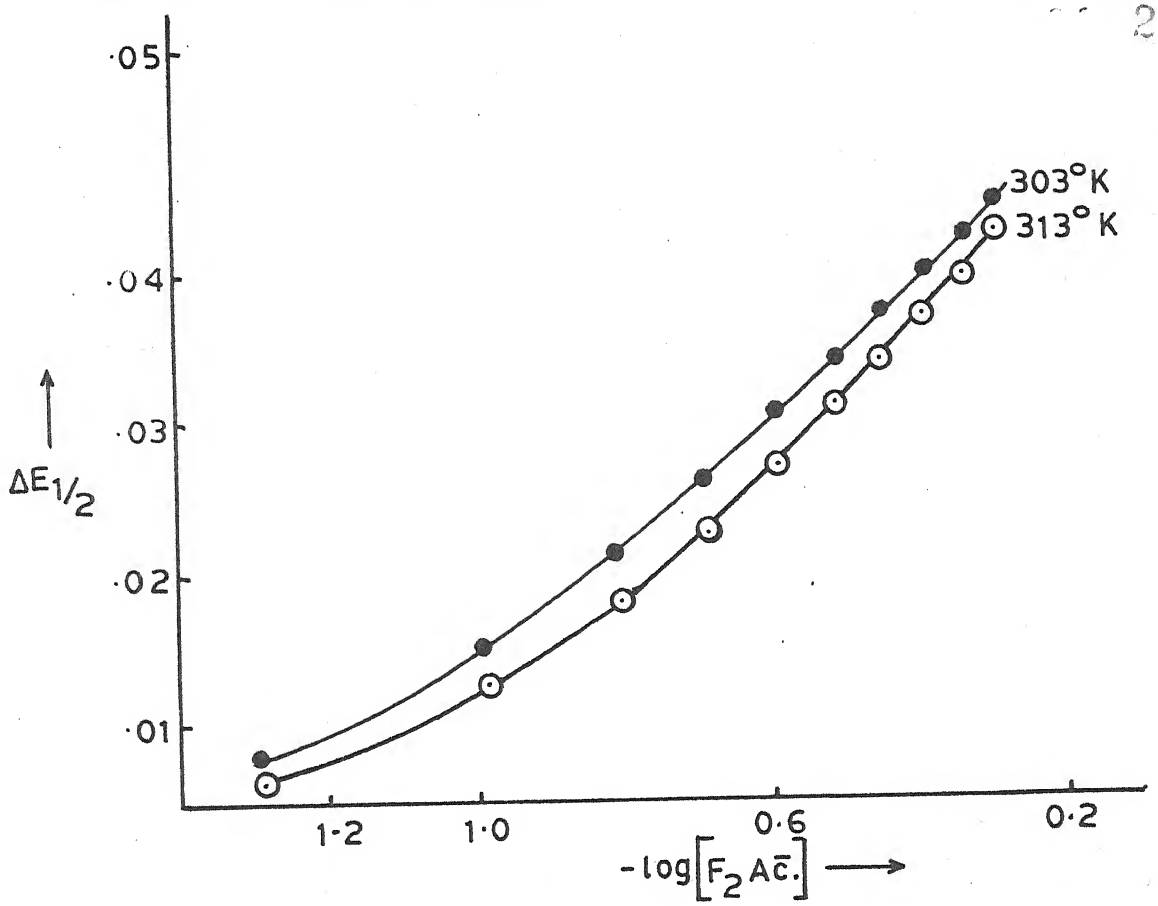

Fig. 6·07 - Plot of $\Delta E_{1/2}$ Vs. $-\log[F_2 A\bar{c}.]$; Cd(F_2 Ac̄.) system.

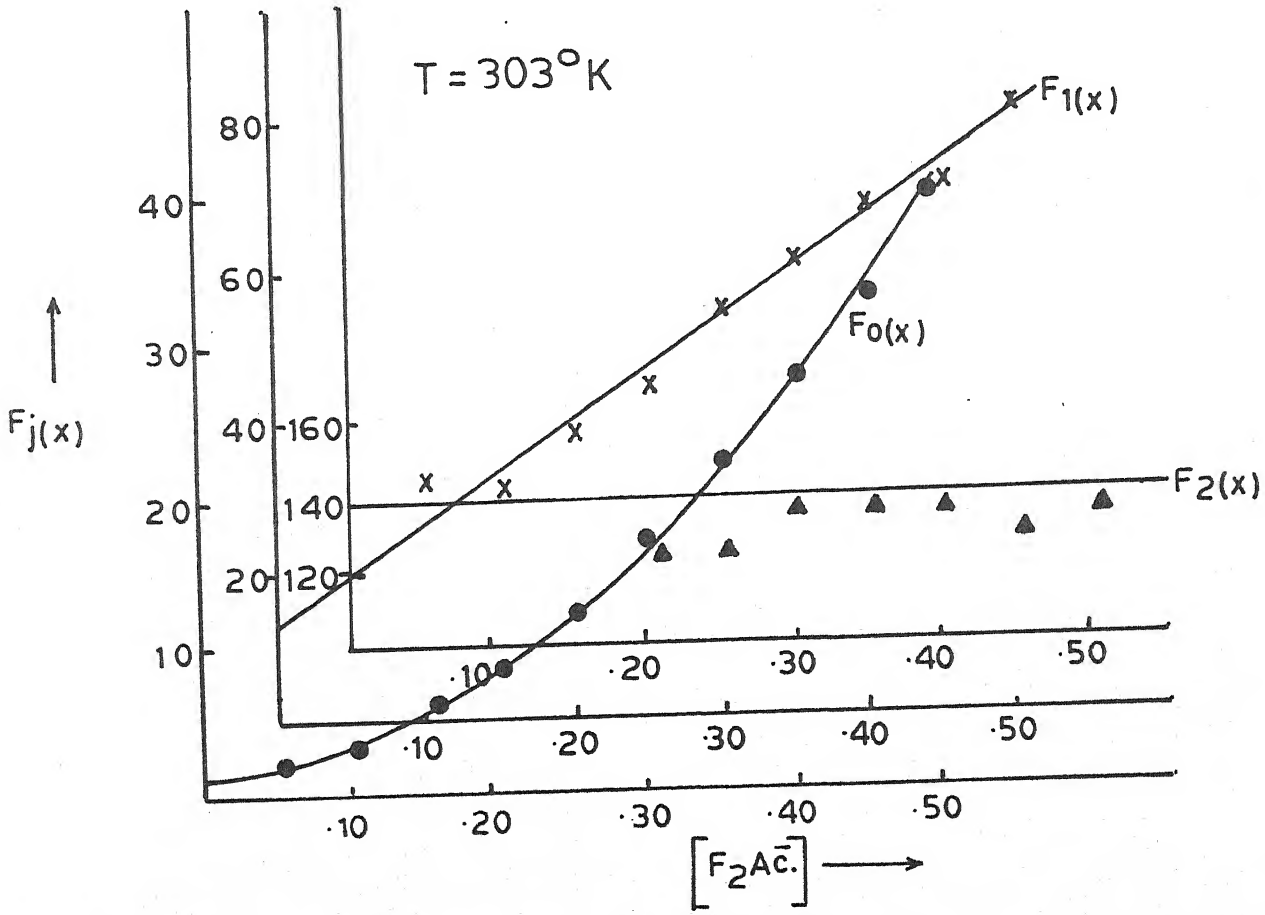

Fig. 6·08 - Plot of $F_{j(x)}$ Vs. $[F_2 A\bar{c}.]$; Cd(F_2 Ac̄.) system.

Table 6.07

Polarographic data for Cadmium difluoroacetate system

Concn. of Cd^{++} ions = 0.9 mM Ionic strength = 1.0 M ($NaClO_4$)

$E_{1/2}$ of Cd^{++} ions = -0.576 V vs. SCE Temperature = 303° K

Slopes of plots of $-E_{de}$ vs. $-\log. i/i_d-i$ = 29-30 mV

$[F_2A\bar{c}.]$ (M)	$\Delta E_{1/2}$ (V)	$\log. I_M/I_C$	$F_0(X)$	$F_1(X)$	$F_2(X)$
0.05	0.008	0.0293	1.97	-	-
0.10	0.014	0.0416	3.21	-	-
0.15	0.021	0.0511	5.62	30.8	-
0.20	0.026	0.0703	8.62	38.1	128.0
0.25	0.030	0.0843	11.93	43.72	124.8
0.30	0.034	0.1055	17.24	54.13	138.7
0.35	0.037	0.1165	22.25	60.71	137.7
0.40	0.040	0.1202	28.24	68.1	139.0
0.45	0.042	0.1239	33.20	71.55	131.2
0.50	0.045	0.1239	41.78	81.56	138.1

$\beta_1 = 12.5$ $\beta_2 = 138$

Table 6.08

Polarographic data for Cadmium difluoroacetate system

Concn. of Cd^{++} ions = 0.9 mM Ionic strength = 1.0 M ($NaClO_4$)

$E_{1/2}$ of Cd^{++} ions = -0.570 V vs. SCE Temperature = 313° K

Slopes of plots of $-E_{de}$ vs. $-\log. i/i_d-i$ = 29-30 mV

$[F_2A\bar{c}.]$ (M)	$\Delta E_{1/2}$ (V)	$\log. I_M/I_C$	$F_0(X)$	$F_1(X)$	$F_2(X)$
0.05	0.006	0.0375	1.7	14.0	-
0.10	0.013	0.0517	2.95	19.5	-
0.15	0.018	0.0576	4.33	22.5	-
0.20	0.022	0.0635	5.91	24.55	-
0.25	0.027	0.0695	8.69	30.76	83.0
0.30	0.031	0.0725	11.77	35.9	86.3
0.35	0.034	0.0755	14.80	39.42	84.0
0.40	0.037	0.0848	18.89	44.72	85.0
0.45	0.040	0.0880	23.77	50.6	90.2
0.50	0.043	0.0880	29.12	56.24	92.5

$\beta_1 = 10$ $\beta_2 = 85$

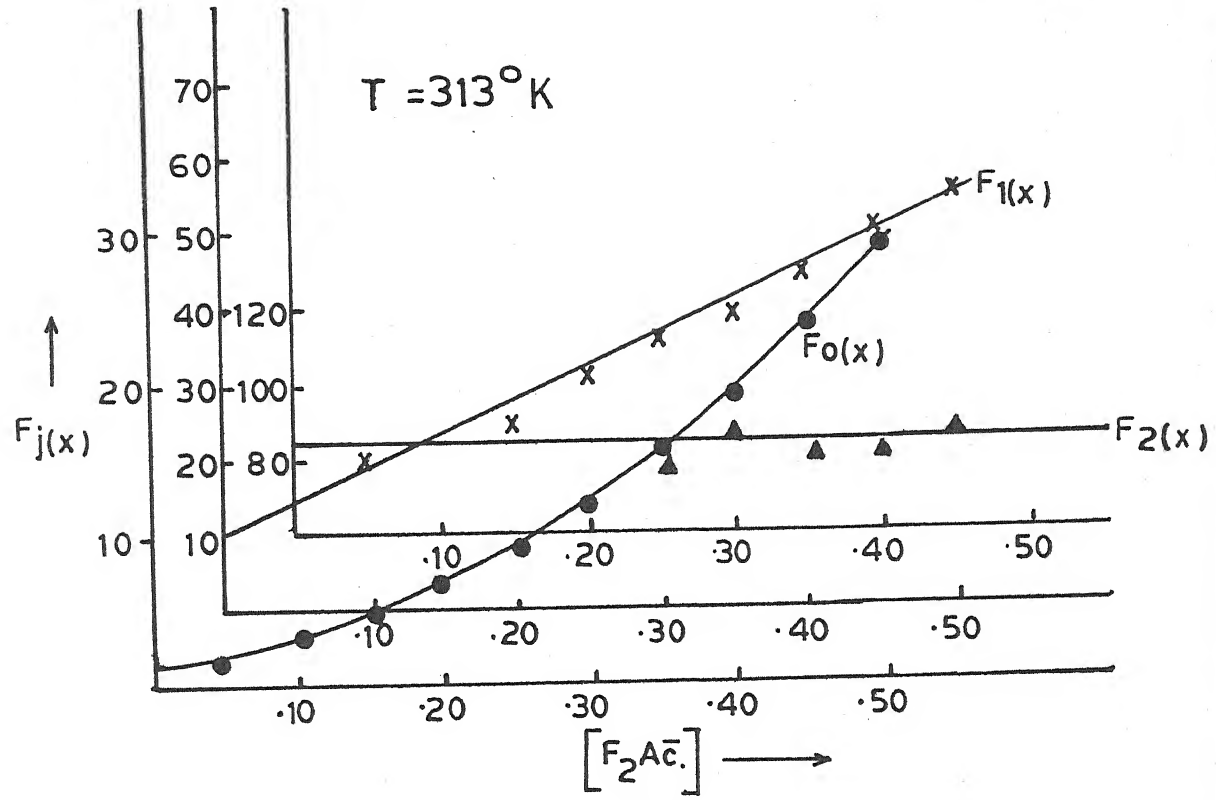

Fig. 6·09 - Plot of $F_{j(x)}$ Vs. $[F_2 A\bar{c}.]$; Cd(F_2 $A\bar{c}$.)system.

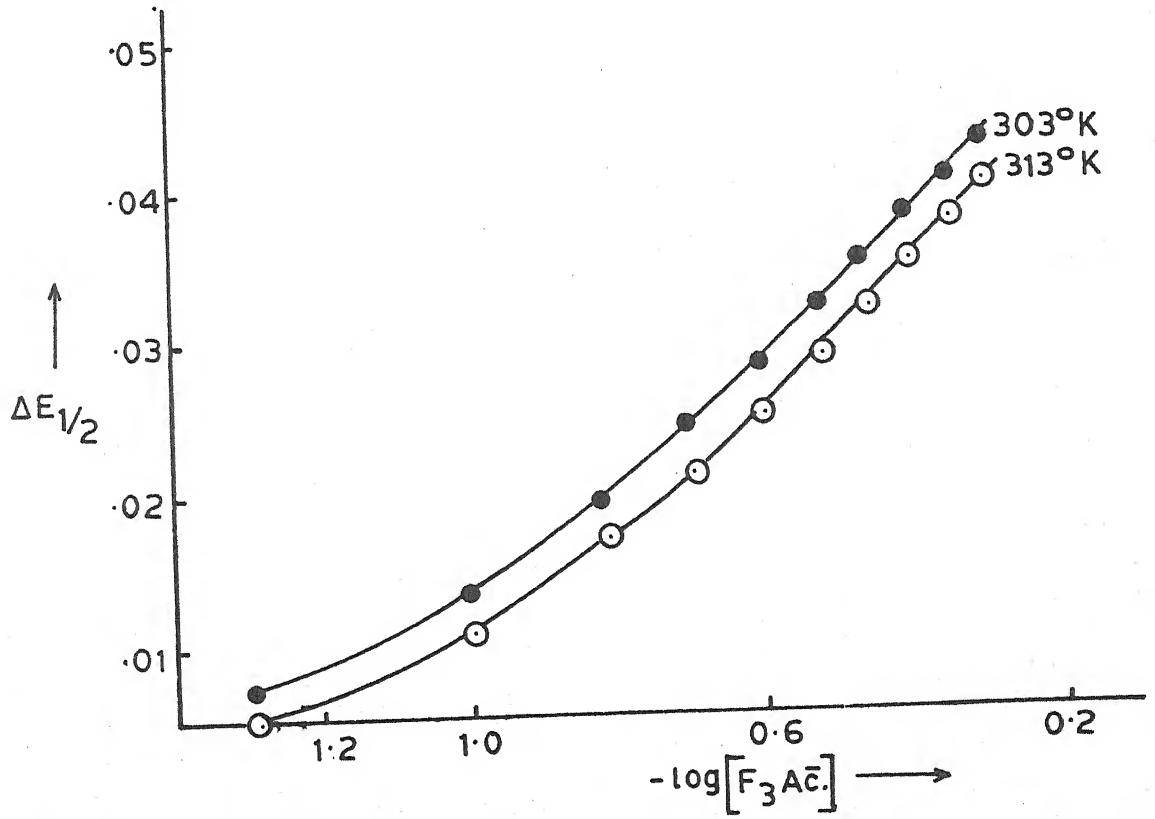

Fig. 6·10 - Plot of $\Delta E_{1/2}$ Vs. $-\log[F_3 A\bar{c}.]$; Cd(F_3 $A\bar{c}$.)system.

Table 6.09

Cadmium difluoroacetate system

Temperature (^{o} K)	log β_1	- ΔG (kj)	- ΔH (kj)	- ΔS (kj deg^{-1})x10^3
303	1.0969	6.3640		37.0715
			17.5966	
313	1.0000	5.9932		37.0715

6.3.04 Cadmium trifluoroacetate system :

(a) Nature of reduction : That the two electron reduction of Cd(II) in presence of trifluoroacetate ions is reversible and diffusion controlled could be inferred from the following observations :

(i) The linearity of conventional log. plots with slopes of 29-30 mV.

(ii) The temperature co-efficient of $E_{1/2}$ was 0.2 - 0.3 mV per degree.

(iii) The temperature co-efficient of i_d was 0.5 $\pm$ 0.1% per degree.

(iv) The ratio of i_d and $\sqrt{h_{eff.}}$ was constant.

(b) Effect of ligand concentration : A successive shift of $E_{1/2}$ in the cathodic direction and decrease in i_d was observed when solutions containing 0.9 mM Cd(II) ions, 0.002% gelatin, increasing concentrations of trifluoroacetate ions and requisite

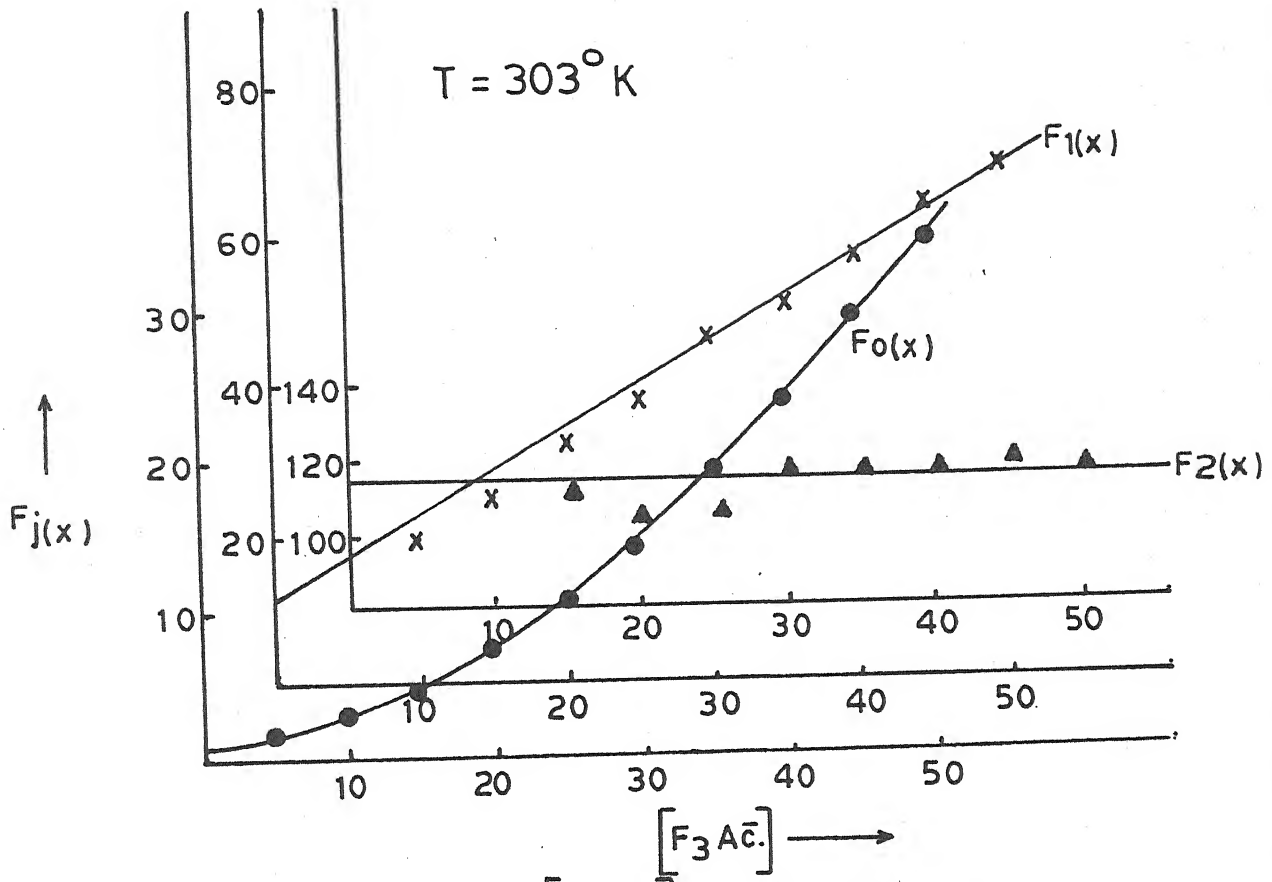

Fig. 6·11 - Plot of $F_{j(x)}$ Vs. $[F_3Ac.]$; Cd $(F_3Ac.)$ system.

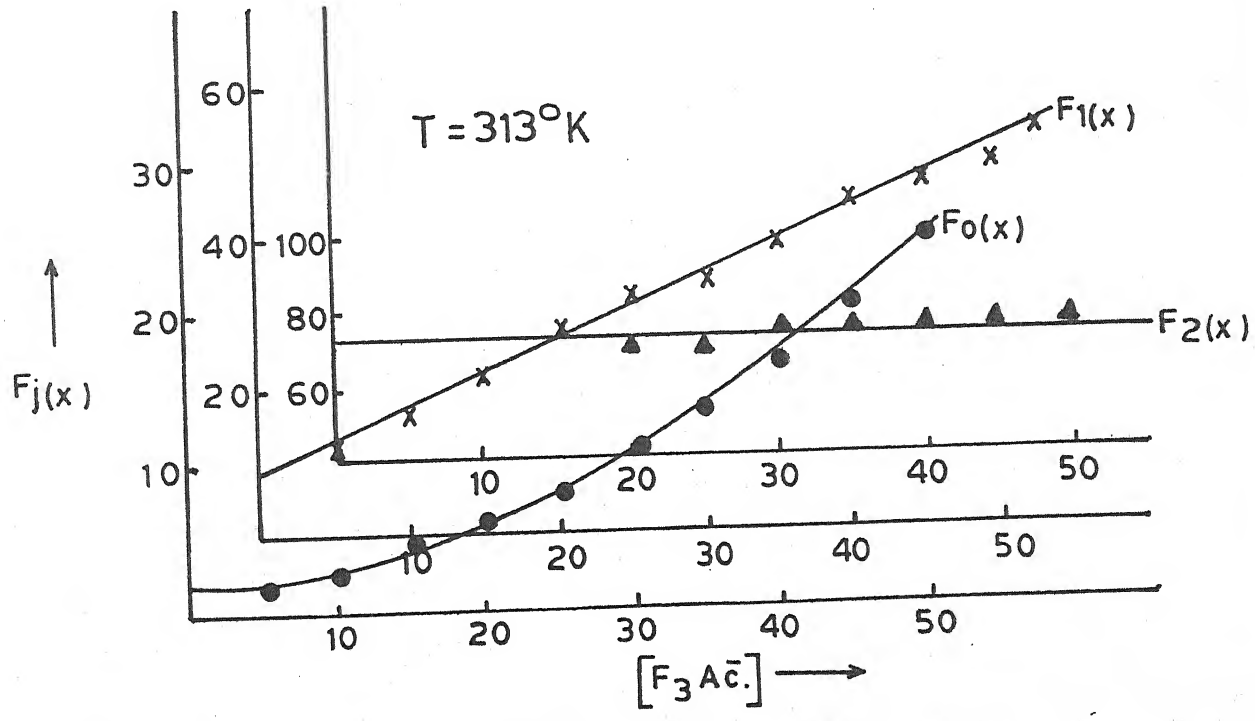

Fig. 6·12 - Plot of $F_{j(x)}$ Vs. $[F_3Ac.]$; Cd $(F_3Ac.)$ system.

Table 6.10

Polarographic data for Cadmium trichloroacetate system

Concn. of Cd^{++} ions = 0.9 mM Ionic strength = 1.0 M ($NaClO_4$)

$E_{1/2}$ of Cd^{++} ions = -0.576 V vs. SCE Temperature = 303° K

Slopes of plots of $-E_{de}$ vs. -log. i/i_d-i = 29-30 mV

$[F_3A\bar{c}.]$ (M)	$E_{1/2}$ (V)	log. I_M/I_C	$F_0(X)$	$F_1(X)$	$F_2(X)$
0.05	0.007	0.0263	1.81	16.2	-
0.10	0.013	0.0385	2.95	19.5	-
0.15	0.019	0.0511	4.82	25.46	113.3
0.20	0.024	0.0641	7.39	31.95	104.7
0.25	0.028	0.0877	10.45	37.8	107.2
0.30	0.032	0.1019	14.67	45.56	115.2
0.35	0.035	0.1128	18.93	51.22	114.9
0.40	0.038	0.1165	24.02	57.55	116.3
0.45	0.041	0.1165	30.23	64.95	119.8
0.50	0.043	0.1202	35.54	69.0	110.0

$\beta_1 = 11$ $\beta_2 = 114$

Table 6.11

Polarographic data for Cadmium trifluoroacetate system

Concn. of Cd^{++} ions = 0.9 mM Ionic strength = 1.0 M ($NaClO_4$)

$E_{1/2}$ of Cd^{++} ions = -0.570 V vs. SCE Temperature = 313° K

Slopes of plots of $-E_{de}$ vs. log. i/i_d-i = 29-30 mV

$[F_3A\bar{c}.]$ (M)	$\Delta E_{1/2}$ (V)	log. I_M/I_C	$F_0(X)$	$F_1(X)$	$F_2(X)$
0.05	0.005	0.0321	1.56	11.2	-
0.10	0.010	0.0492	2.53	15.3	-
0.15	0.017	0.0609	4.05	20.33	-
0.20	0.021	0.0669	5.53	22.05	70.7
0.25	0.025	0.0730	7.55	26.2	70.8
0.30	0.029	0.0760	10.23	30.76	74.2
0.35	0.032	0.0791	12.87	33.91	72.6
0.40	0.035	0.0822	16.19	37.97	73.6
0.45	0.038	0.0854	20.30	43.06	76.8
0.50	0.040	0.0885	23.81	45.62	74.2

$\beta_1 = 8.5$ $\beta_2 = 72$

concentrations of sodium perchlorate ions (for μ = 1.0 M) were reduced at the DME at 303° K to indicate complex formation between Cd(II) and trifluoroacetate ions. The plot of $\Delta E_{1/2}$ vs. -log. $[F_3Ac^-]$ was a curve (figure 6.10). This indicated that more than one complex had been formed. The application of method of DeFord and Hume yielded 11 and 114 as the overall formation constant values for $[Cd(F_3Ac.)]^+$ and $[Cd(F_3Ac.)_2]$ complexes for which the data and the $F_j(X)$ functions are presented in table 6.10 and figure 6.11.

(c) Effect of temperature : The temperature co-efficient values of $E_{1/2}$ and i_d have already been reported earlier in this section to be 0.2-0.3 mV per degree and 0.5 $\pm$ 0.1% per degree.

The effect of ligand concentration on $E_{1/2}$ and i_d was re-investigated at 313° K to obtain 8.5 and 72 as the β_1 and β_2 values for which the polarographic data have been included in table 6.11 and figure 6.12.

Table 6.12 contains the thermodynamic functions evaluated by utilising the knowledge of two sets of β_1 values for the system.

Table 6.12

Cadmium trifluoroacetate system

Temperature (° K)	log β_1	- ΔG (kj)	- ΔH (kj)	- ΔS (kj deg^{-1})x10^3
303	1.0413	6.0412	20.3206	47.1267
313	0.9294	5.5703		47.1255

6.3.05 Cadmium monochloroacetate system :

(a) Nature of reduction : Cd(II) reduced reversibly with two electron transfer process and with full diffusion control. This inference was drawn from the straight line conventional log. plots with slopes of 29-30 mV, temperature co-efficients of $E_{1/2}$ and i_d which were 0.3 $\pm$ 0.1 mV per degree and 0.5 $\pm$ 0.1% per degree respectively coupled with the constancy of ratio of diffusion current and square root of effective height of the mercury column of the DME.

(b) Effect of ligand concentration : Solutions containing 0.9 mM Cd(II) ions, 0.002% gelatin, increasing amounts of monochloroacetate ions and required amounts of sodium perchlorate to maintain ionic strength at 1.0 M, when polarographed at 303° K, exhibited a gradual shift of $E_{1/2}$ towards the more negative side and a successive decrease in i_d to indicate complex formation between Cd(II) and monochloroacetate ions. Multiple complex formation having been deduced from the curved character (figure 6.13) of plot of $\Delta E_{1/2}$ vs. $-\log.[ClAc^-]$, the method of DeFord and Hume could be applied to compute the formation constants ($\beta_1 = 32$, $\beta_2 = 110$) of the complexes so formed. The relevant polarographic data have been presented in table 6.13 and $F_j(X)$ functions plotted in figure 6.14.

(c) Effect of temperature : The reversibility and diffusion controlled behaviour of reduction of Cd(II) in presence of monochloroacetate ions has been, earlier in this section, established from the temperature co-efficients of half wave

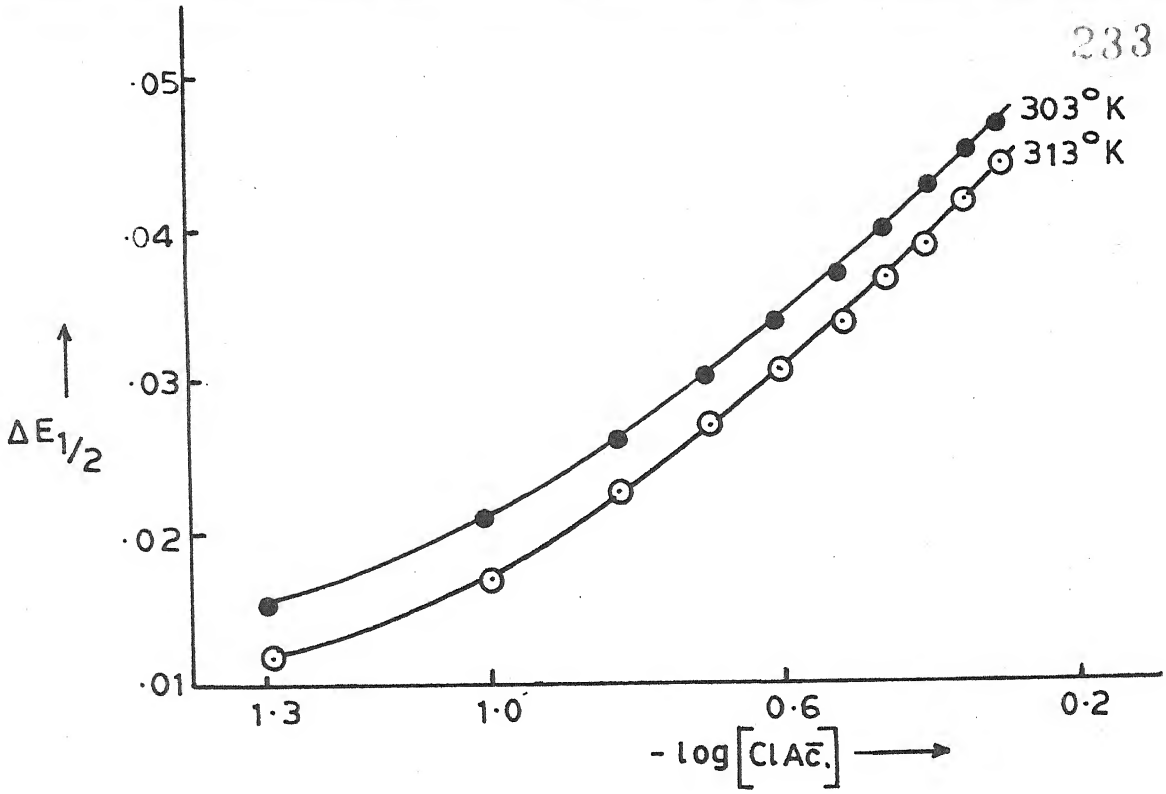

Fig. 6·13 - Plot of $\Delta E_{1/2}$ Vs. $-\log[ClA\bar{c}.]$; Cd(ClAc̄.) system.

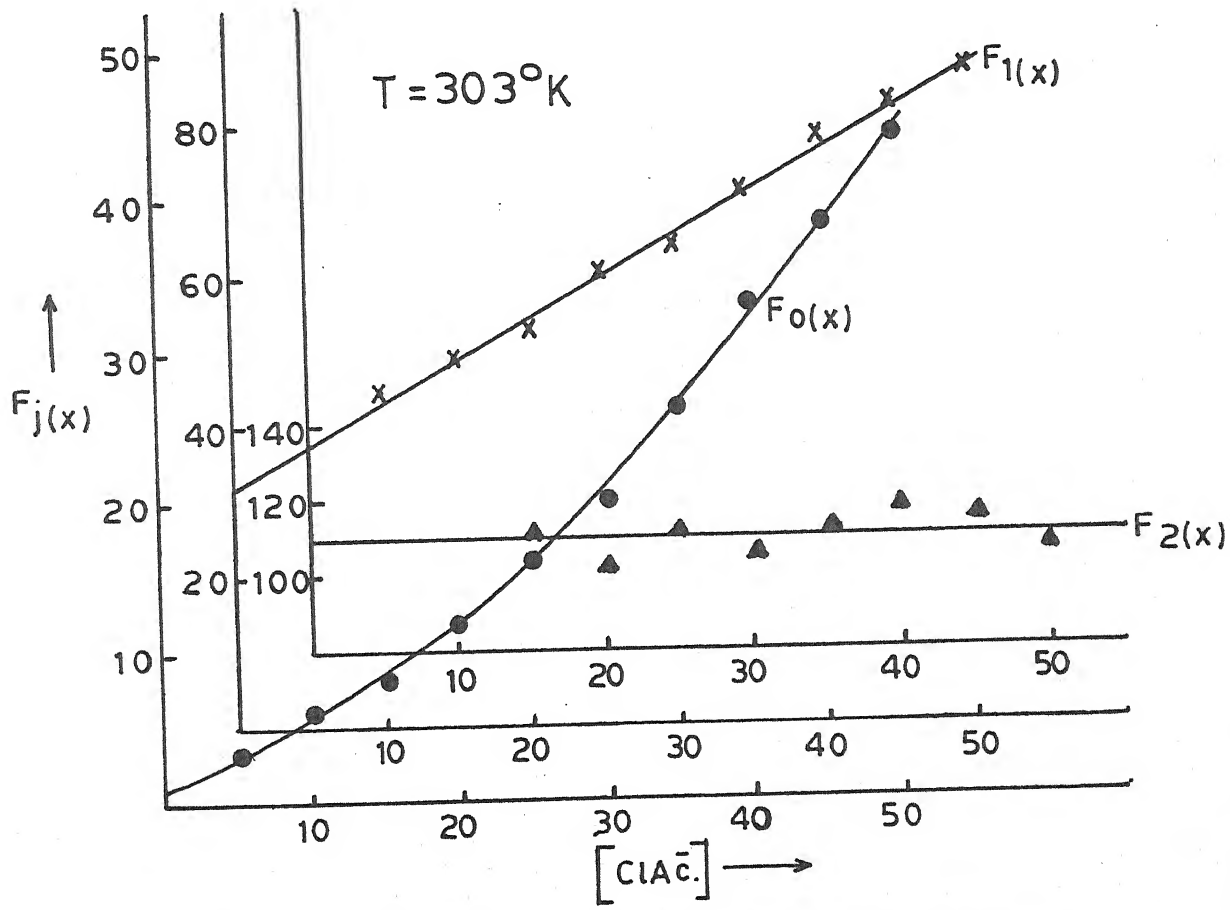

Fig. 6·14 - Plot of $F_{j(x)}$ Vs. $[ClA\bar{c}.]$; Cd(ClAc̄.) system.

Table 6.13

Polarographic data for Cadmium monochloroacetate system

Concn. of Cd^{++} ions = 0.9 mM Ionic strength = 1.0 M ($NaClO_4$)

$E_{1/2}$ of Cd^{++} ions = -0.576 V vs. SCE Temperature = 303° K

Slopes of plots of $-E_{de}$ vs. $-\log. i/i_d-i$ = 29-30 mV

$[ClAc^-]$ (M)	$\Delta E_{1/2}$ (V)	$\log. I_M/I_C$	$F_0(X)$	$F_1(X)$	$F_2(X)$
0.05	0.015	0.0265	3.35	-	-
0.10	0.021	0.0419	5.50	45.0	-
0.15	0.026	0.0547	8.31	48.73	111.5
0.20	0.030	0.0645	11.55	52.77	103.8
0.25	0.034	0.0712	15.93	59.72	110.8
0.30	0.037	0.0780	20.36	64.53	108.4
0.35	0.040	0.0814	25.83	70.94	111.2
0.40	0.043	0.0849	32.76	79.4	118.5
0.45	0.045	0.0849	39.19	82.54	112.3
0.50	0.047	0.0849	44.51	87.02	110.0

$\beta_1 = 32$ $\beta_2 = 110$

Table 6.14

Polarographic data for Cadmium monochloroacetate system

Concn. of Cd^{++} ions = 0.9 mM Ionic strength = 1.0 M ($NaClO_4$)

$E_{1/2}$ of Cd^{++} ions = -0.570 V vs. SCE Temperature = 313° K

Slopes of plots of $-E_{de}$ vs. $-\log. i/i_d-i$ = 29-30 mV

$[ClAc^-]$ (M)	$\Delta E_{1/2}$ (V)	$\log. I_M/I_C$	$F_0(X)$	$F_1(X)$	$F_2(X)$
0.05	0.012	0.0294	2.60	-	-
0.10	0.017	0.0434	4.19	31.9	74.0
0.15	0.023	0.0521	6.20	34.6	67.3
0.20	0.027	0.0579	8.54	37.3	65.0
0.25	0.031	0.0639	11.54	42.16	70.6
0.30	0.034	0.0699	14.61	45.36	69.5
0.35	0.037	0.0730	18.37	49.62	71.7
0.40	0.039	0.0730	21.32	50.8	65.7
0.45	0.042	0.0822	27.71	58.24	74.9
0.50	0.044	0.0854	31.80	61.6	74.2

$\beta_1 = 24.5$ $\beta_2 = 68$

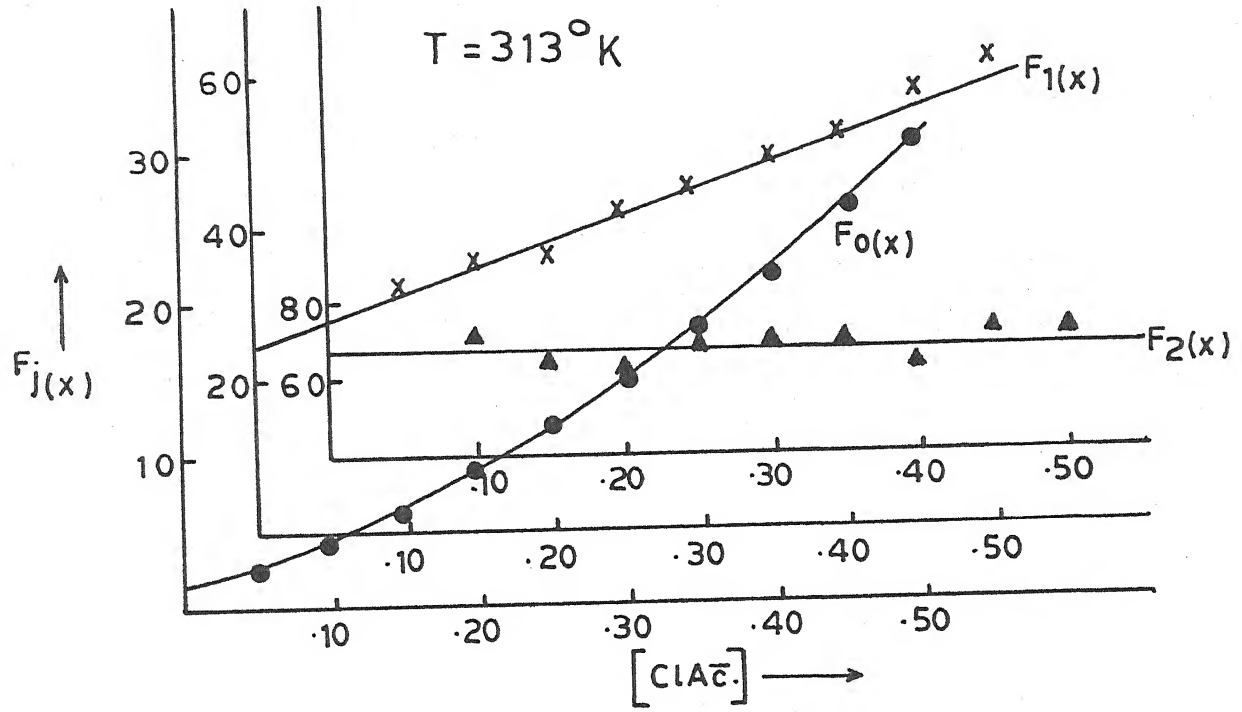

Fig.6·15 - Plot of $F_{j(x)}$ Vs. $[ClA\bar{c}.]$; Cd($ClA\bar{c}.$) system.

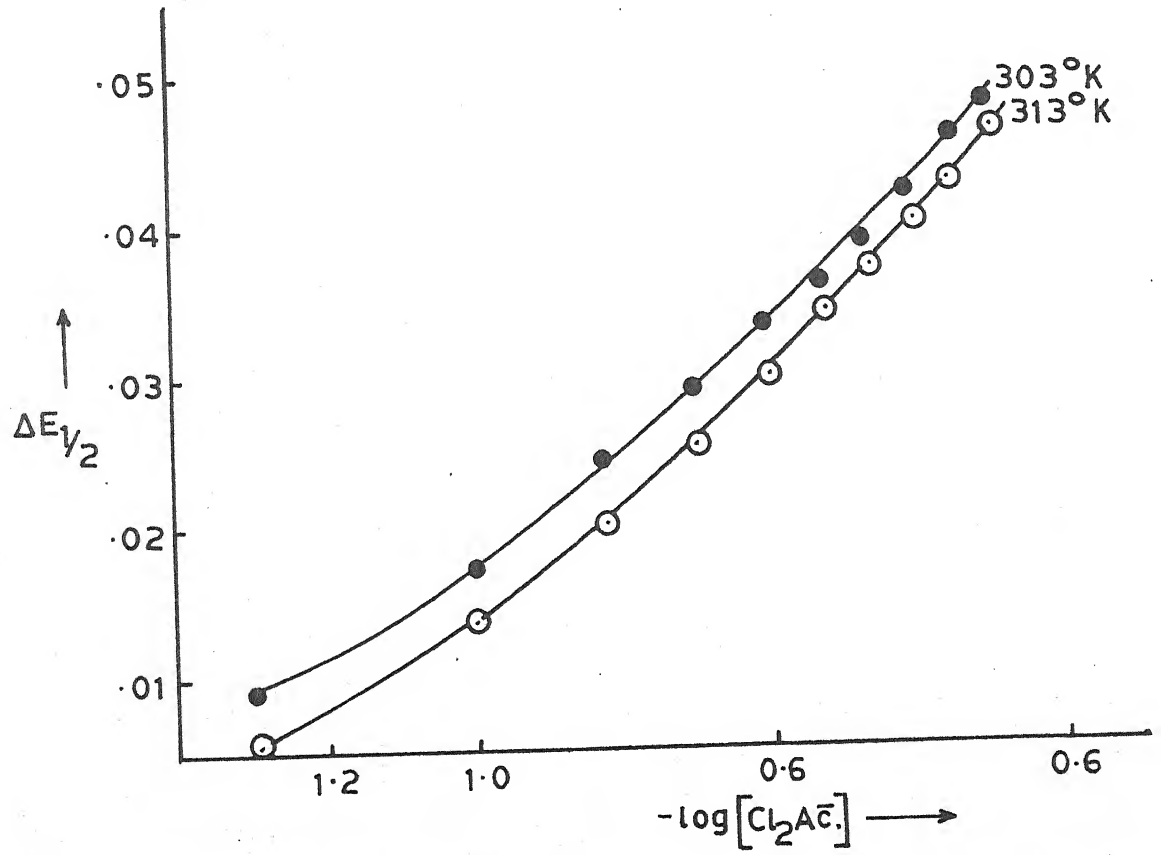

Fig.6·16 - Plot of $\Delta E_{1/2}$ Vs. $-\log[Cl_2A\bar{c}.]$; Cd($Cl_2A\bar{c}.$) system.

potential and diffusion current.

The stability constants of the cadmium monochloroacetate system were redetermined at 313° K and were found to be 24.5 and 68 respectively for $[Cd(ClAc.)]^{+}$ and $[Cd(ClAc.)_2]$ complexes for which the polarographic data and $F_j(X)$ plots are included in table 6.14 and figure 6.15.

Table 6.15 contains the ΔG, ΔH and ΔS values evaluated from the knowledge of the two sets of formation constants.

Table 6.15

Cadmium monochloroacetate system

Temperature (° K)	log β_1	- ΔG (kj)	- ΔH (kj)	- ΔS (kj deg^{-1}) x 10^3
303	1.5051	8.7322		40.7026
			21.0651	
313	1.3891	8.3252		40.7025

6.3.06 Cadmium dichloroacetate system :

(a) Nature of reduction : The following results combined together to conclusively indicate that the reduction of Cd(II) in presence of dichloroacetate ions is reversible involving two electrons and is solely diffusion controlled.

(i) Linear plots of $-E_{de}$ vs. $-\log. i/i_d - i$ with slopes of 29-30 mV.

(ii) Temperature co-efficients of $E_{1/2}$ (0.2-0.3 mV per degree) and i_d (0.5 $\pm$ 0.1% per degree).

(iii) Direct proportionality between i_d and $\sqrt{h_{eff.}}$.

(b) Effect of ligand concentration : Complex formation between Cd(II) and dichloroacetate ions was deduced from the cathodic shift in half wave potential and decrease in i_d with increasing $[Cl_2A\bar{c}.]$ concentration from polarography at 303° K of solutions also containing 0.9 mM Cd(II) ions, 0.002% gelatin and decreasing concentrations of sodium perchlorate to keep ionic strength constant at 1.0 M. The plot of $\Delta E_{1/2}$ vs. -log. $[Cl_2A\bar{c}.]$ being a curve (figure 6.16) symbolising multiple complex formation, the method of DeFord and Hume was conveniently applied to evaluate the overall formation constants of the two complexes so formed. The β_1 and β_2 values obtained are 20 and 152 respectively for which the polarographic data are presented in table 6.16 and figure 6.17.

(c) Effect of temperature : The $E_{1/2}$ decreases by 0.2-0.3 mV and i_d increases by 0.5 $\pm$ 0.1 percent for every degree rise in temperature for the reduction of Cd(II) in $(Cl_2A\bar{c}.)$ ions.

The effect of ligand concentration on $E_{1/2}$ and i_d was reinvestigated at 313° K to determine formation constants at the higher temperature. The values were found to be 12.5 and 154 for 1:1 and 1:2 metal/ligand ratio complexes for which the polarographic data are included in table 6.17 and figure 6.18.

The thermodynamic functions evaluated from these two

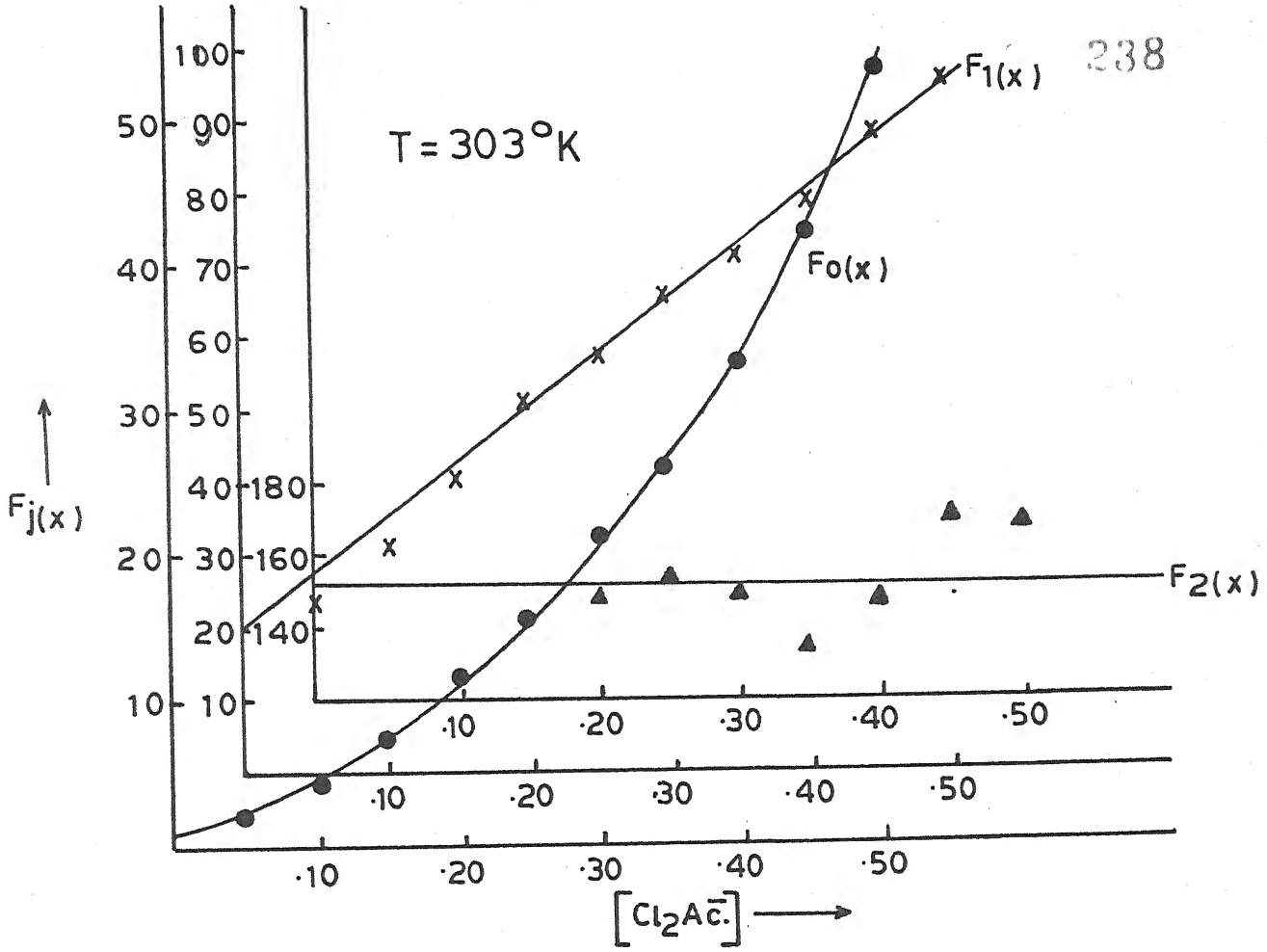

Fig. 6·17 - Plot of $F_{j(x)}$ Vs. $[Cl_2Ac^-]$; Cd(Cl_2Ac^-)system.

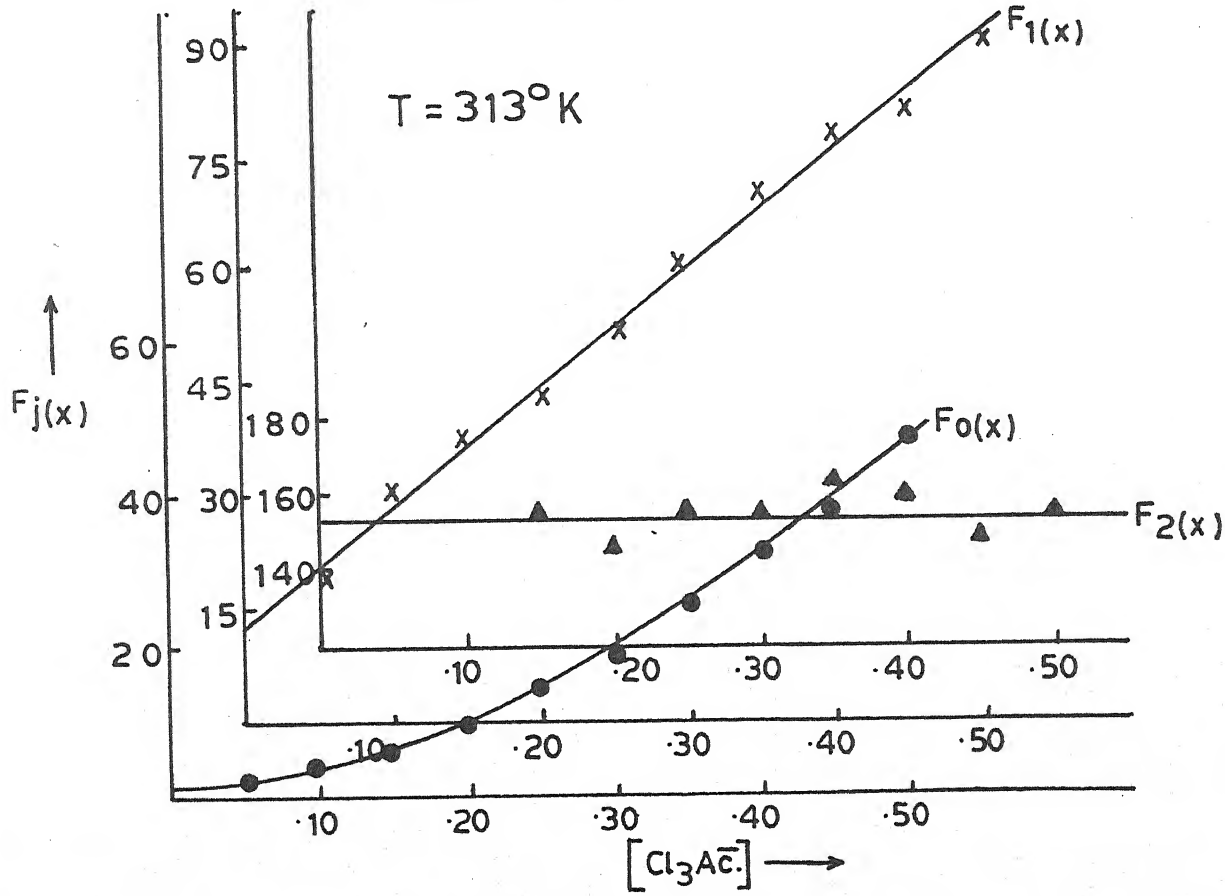

Fig. 6·18 - Plot of $F_{j(x)}$ Vs. $[Cl_2Ac^-]$; Cd(Cl_2Ac^-)system.

Table 6.16

Polarographic data for Cadmium dichloroacetate system

Concn. of Cd^{++} ions = 0.9 mM Ionic strength = 1.0 M ($NaClO_4$)

$E_{1/2}$ of Cd^{++} ions = -0.576 V vs. SCE Temperature = ~~29-30 mV~~ 303°K

Slopes of plots of $-E_{de}$ vs. -log. i/i_d-i = 29-30 mV

$[Cl_2Ac^-]$ (M)	$\Delta E_{1/2}$ (V)	log. I_M/I_C	$F_0(X)$	$F_1(X)$	$F_2(X)$
0.05	0.009	0.0354	2.33	26.6	-
0.10	0.017	0.0511	4.13	31.3	-
0.15	0.024	0.0608	7.23	41.54	-
0.20	0.029	0.0808	11.10	50.5	152.5
0.25	0.033	0.0947	15.88	58.32	153.2
0.30	0.036	0.1202	20.79	65.96	153.2
0.35	0.039	0.1202	26.16	71.8	148.0
0.40	0.042	0.1239	33.2	80.50	153.3
0.45	0.046	0.1277	45.21	98.9	175.3
0.50	0.048	0.1354	53.99	105.98	171.9

$\beta_1 = 20$ $\beta_2 = 152$

Table 6.17

Polarographic data for Cadmium dichloroacetate system

Concn. of Cd^{++} ions =0.9 mM Ionic strength = 1.0 M ($NaClO_4$)

$E_{1/2}$ of Cd^{++} ions = -0.570 V vs. SCE Temperature = 313° K

Slopes of plots of $-E_{de}$ vs. -log. i/i_d-i = 29-30 mV

$[Cl_2Ac^-]$ (M)	$\Delta E_{1/2}$ (V)	log. I_M/I_C	$F_0(X)$	$F_1(X)$	$F_2(X)$
0.05	0.008	0.0347	1.96	19.2	-
0.10	0.017	0.0517	3.97	29.7	-
0.15	0.023	0.0665	6.41	36.06	157.0
0.20	0.028	0.0755	9.49	42.45	149.7
0.25	0.033	0.0817	13.94	51.76	157.0
0.30	0.037	0.0848	18.89	59.63	157.1
0.35	0.041	0.0880	25.60	70.28	165.0
0.40	0.044	0.0911	32.20	78.0	163.7
0.45	0.046	0.0943	37.64	81.42	153.0
0.50	0.049	0.0943	47.0	92.0	159.0

$\beta_1 = 12.5$ $\beta_2 = 154.$

sets of formation constants are presented in table 6.18.

Table 6.18

Cadmium dichloroacetate system

Temperature (° K)	log β_1	- ΔG (kj)	- ΔH (kj)	- ΔS (kj deg^{-1})x10^3
303	1.3010	7.5480		97.4115
			37.0637	
313	1.0969	6.5740		97.4111

6.3.07 Cadmium trichloroacetate system :

(a) Nature of reduction : The observations that the linear conventional log. plots have slopes of 29-30 mV, $E_{1/2}$ and i_d have temperature co-efficient values of 0.2-0.3 mV per degree and 0.5 $\pm$ 0.1% per degree and the linearity of plot of i_d against square root of effective height of mercury column of the DME combine together to conclusively prove that the reduction of cadmium trichloroacetate complex is reversible with two electron transfer and is solely diffusion controlled.

(b) Effect of ligand concentration : Polarographic examination of solutions consisting of 0.9 mM Cd(II) ions, 0.002% gelatin increasing concentration of trichloroacetate ions and requisite amounts of sodium perchlorate (μ = 1.0 M) showed a gradual cathodic shift in $E_{1/2}$ and decrease in i_d. Hence complex formation had taken place between Cd(II) and trichloroacetate

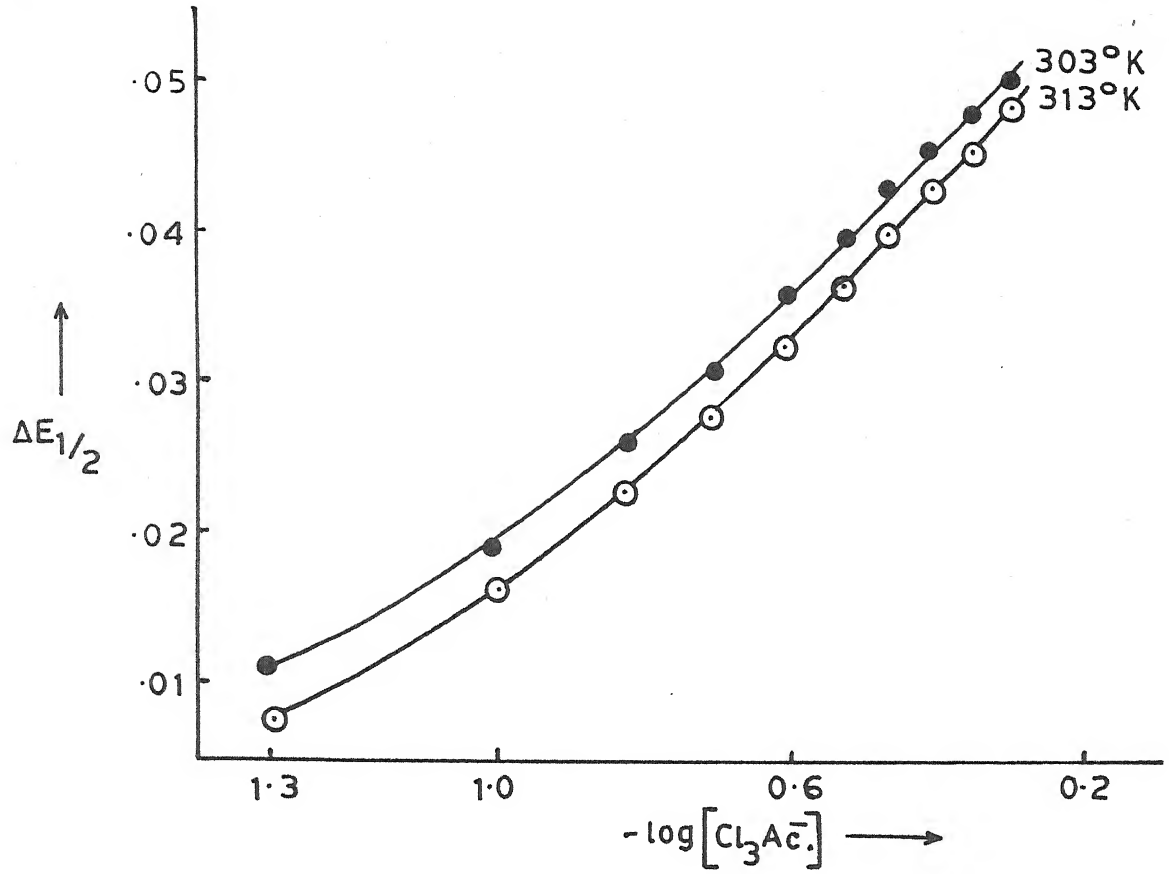

Fig. 6·19 - Plot of $\Delta E_{1/2}$ Vs. $-\log[Cl_3A\bar{c}.]$; $Cd(Cl_3A\bar{c}.)$ system.

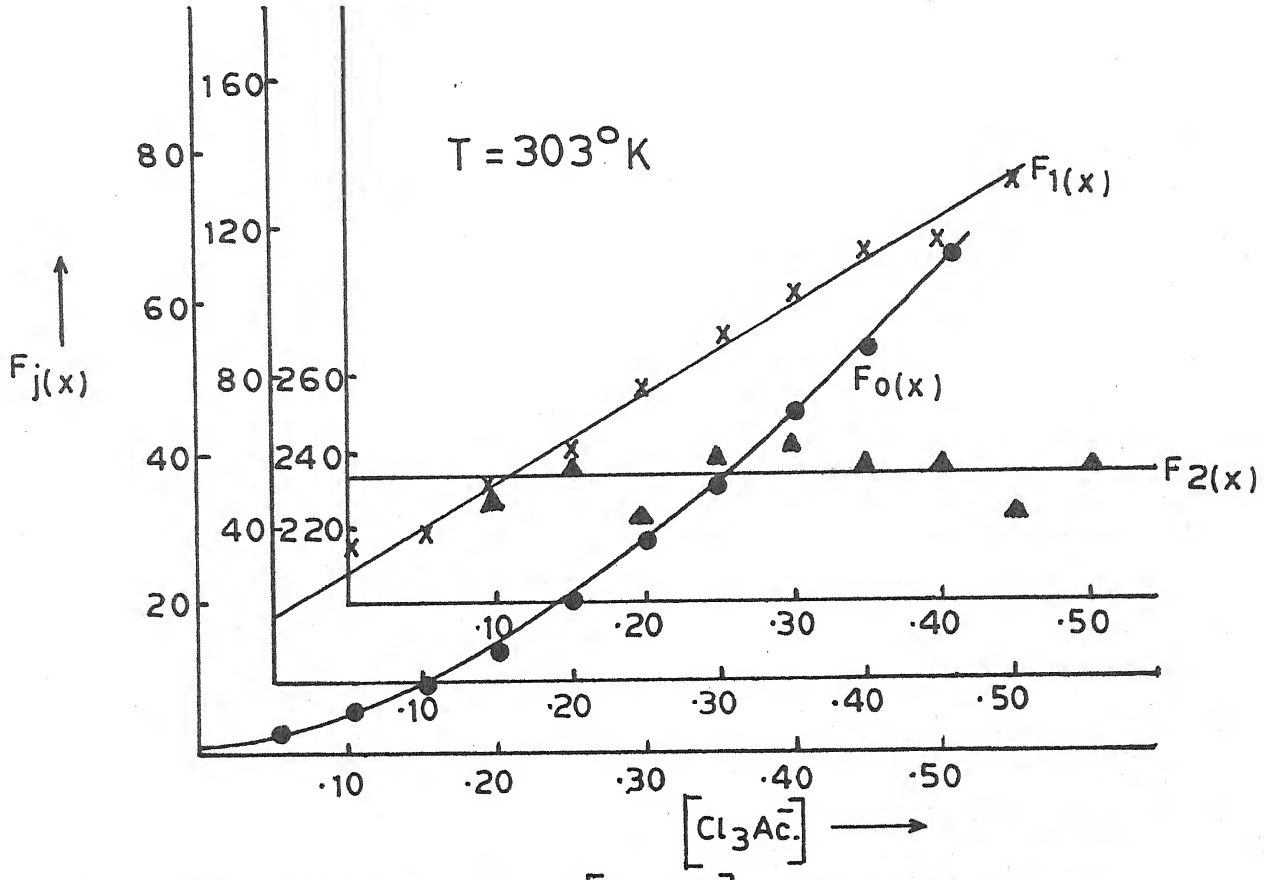

Fig. 6·20 - Plot of $F_{j(x)}$ Vs. $[Cl_3A\bar{c}.]$ $Cd(Cl_3A\bar{c}.)$ system.

Table 6.19

Polarographic data for Cadmium trichloroacetate system

Concn. of Cd^{++} ions = 0.9 mM Ionic strength = 1.0 M ($NaClO_4$)

$E_{1/2}$ of Cd^{++} ions = -0.576 V vs. SCE Temperature = 303° K

Slopes of plots of $-E_{de}$ vs. $-\log. i/i_d-i$ = 29-30 mV

$[Cl_3A\bar{c}.]$ (M)	$\Delta E_{1/2}$ (V)	$\log. I_M/I_C$	$F_0(X)$	$F_1(X)$	$F_2(X)$
0.05	0.011	0.0385	2.53	30.6	-
0.10	0.019	0.0575	4.89	38.9	229.0
0.15	0.026	0.0741	8.69	51.26	235.0
0.20	0.031	0.0877	13.18	60.9	224.5
0.25	0.036	0.1019	19.93	70.72	238.8
0.30	0.040	0.1128	27.76	89.2	244.0
0.35	0.043	0.1202	35.54	98.68	236.2
0.40	0.046	0.1277	45.50	111.25	238.1
0.45	0.048	0.1316	53.51	116.68	223.7
0.50	0.051	0.1354	67.93	133.86	235.7

$\beta_1 = 16$ $\beta_2 = 234$

Table 6.20

Polarographic data for Cadmium trichloroacetate system

Concn. of Cd^{++} ions = 0.9 mM Ionic strength = 1.0 M ($NaClO_4$)

$E_{1/2}$ of Cd^{++} ions = -0.570 V vs. SCE Temperature = 313° K

Slopes of plots of $-E_{de}$ vs. $-\log. i/i_d-i$ = 29 mV

$[Cl_3A\bar{c}.]$ (M)	$\Delta E_{1/2}$ (V)	$\log. I_M/I_C$	$F_0(X)$	$F_1(X)$	$F_2(X)$
0.05	0.006	0.0319	1.67	13.4	-
0.10	0.014	0.0489	3.16	21.6	-
0.15	0.020	0.0665	5.13	27.53	106.8
0.20	0.025	0.0755	7.59	32.95	107.2
0.25	0.030	0.0817	11.16	40.64	116.5
0.30	0.034	0.0848	15.12	47.64	118.5
0.35	0.037	0.0880	19.02	51.51	114.3
0.40	0.040	0.0911	23.14	57.37	114.7
0.45	0.043	0.0943	30.14	64.75	118.3
0.50	0.046	0.0943	37.64	73.28	123.5

$\beta_1 = 11.5$ $\beta_2 = 116$

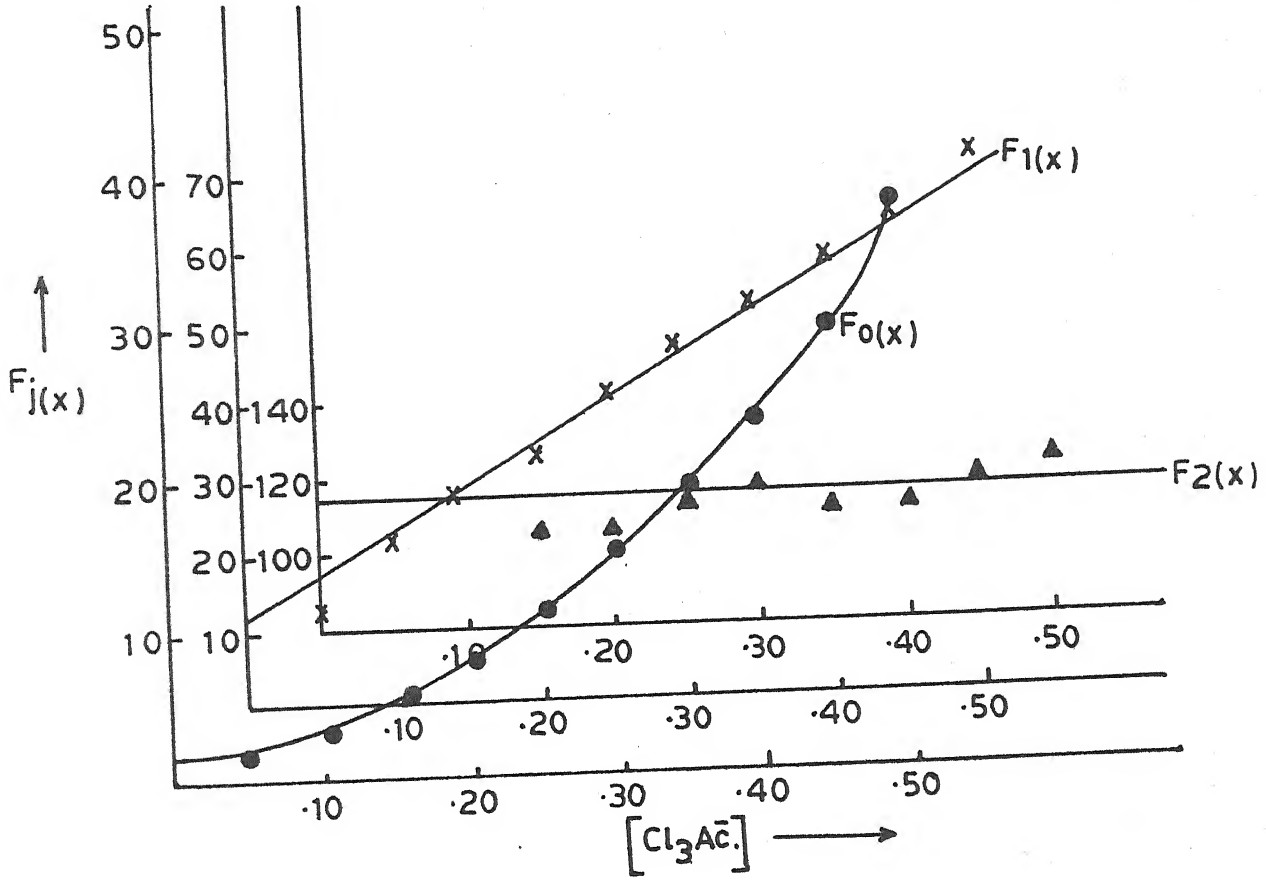

Fig. 6·21 - Plot of $F_{j(x)}$ Vs. $[Cl_3A\bar{c}.]$; Cd $(Cl_3A\bar{c}.)$ system.

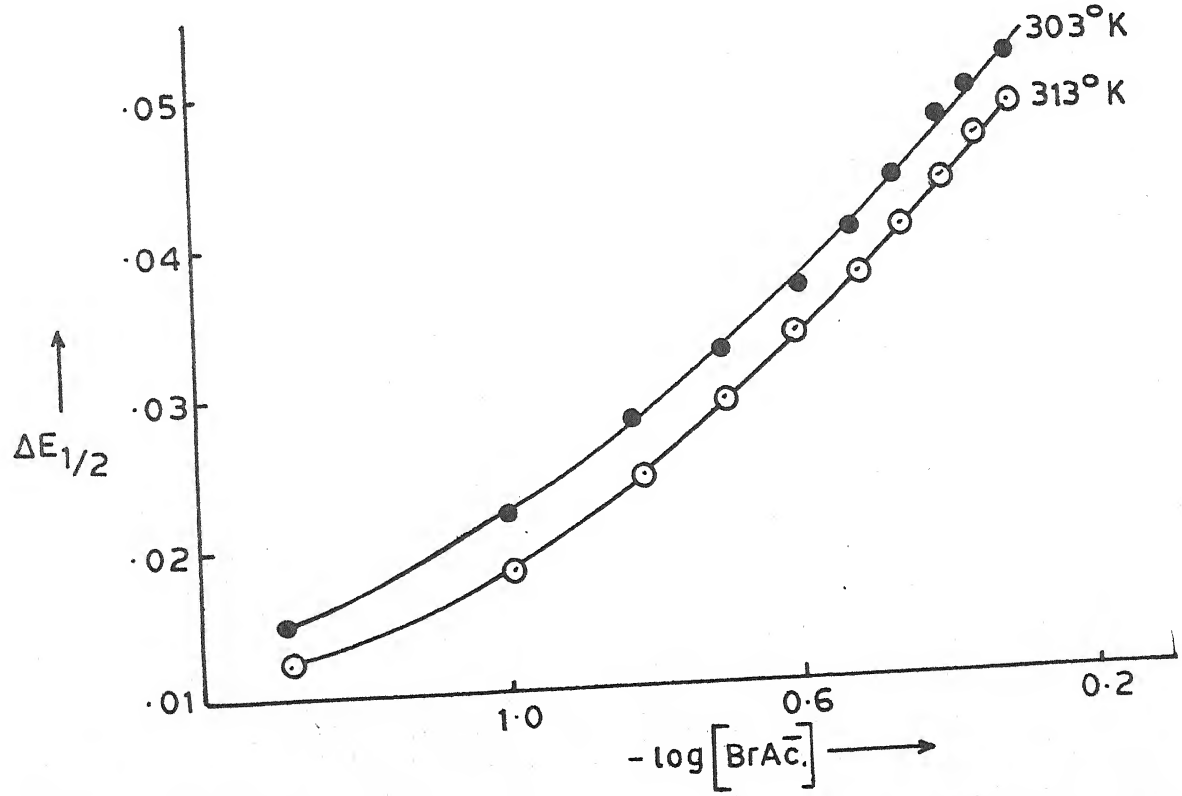

Fig. 6·22 - Plot of $\Delta E_{1/2}$ Vs. $-\log[BrA\bar{c}.]$; Cd $(BrA\bar{c}.)$ system.

ions. Multiple nature of complex formation was inferred from the curved charac-ter (figure 6.19) of plot of $\Delta E_{1/2}$ vs. -log. $[Cl_3Ac^-]$ and consequently method of DeFord and Hume applied to compute the formation constants which were found to be 16 and 234 for $[Cd(Cl_3Ac.)]^+$ and $[Cd(Cl_3Ac.)_2]$ complexes. The relevant polarographic data and $F_j(X)$ functions appear in table 6.19 and figure 6.20.

(c) Effect of temperature : The temperature co-efficient values of $E_{1/2}$ and i_d were found to be of the order of 0.2-0.3 mV per degree and 0.5 $\pm$ 0.1% per degree.

The formation constants were redetermined at a higher temperature i.e. 313° K to enable us to evaluate ΔG, ΔH and ΔS. The β_1 and β_2 values so obtained are 11.5 and 116. The relevant polarographic data, $F_j(X)$ functions and the thermodynamic parameters are presented in table 6.20 figure 6.21.and table 6.21 respectively.

Table 6.21

Cadmium trichloroacetate system

Temperature (° K)	log β_1	- ΔG (kj)	- ΔH (kj)	- ΔS (kj deg^{-1})x10^3
303	1.2041	6.9859		62.9475
			26.0590	
313	1.0606	6.3564		62.9476

6.3.08 Cadmium monobromoacetate system :

(a) Nature of reduction : The straight line plots of conventional log. plots had slopes of 29-30 mV, the temperature co-efficients of half wave potential and diffusion current were 0.3-0.4 mV per degree and 0.5 $\pm$ 0.1 percent per degree respectively and i_d was directly proportional to square root of $h_{eff.}$ leading us to conclude that the reduction of Cd(II) in monochloroacetate ions is reversible, involves two electrons and is solely diffusion controlled.

(b) Effect of ligand concentration : When solutions consisting of 0.9 mM Cd(II) ions, 0.002% of gelatin, increasing concentrations of monobromoacetate ions and required concentrations of sodium perchlorate to keep ionic strength constant at 1.0 M were reduced at DME at 303° K, a gradual cathodic shift in $E_{1/2}$ and decrease in i_d indicated complex formation between Cd(II) and $(BrA\bar{c}.)$ ions. The method of DeFord and Hume could be applied to compute overall stability constants since stepwise complex formation had been indicated by the plot of $\Delta E_{1/2}$ vs. $-\log.[BrA\bar{c}.]$ which was a curve (figure 6.22). The β_1 and β_2 values were found to be 26 and 181 respectively. The relevant polarographic data and $F_j(X)$ functions appear in table 6.22 and figure 6.23.

(c) Effect of temperature : $E_{1/2}$ decreases by 0.3-0.4 mV and i_d increases by 0.5 $\pm$ 0.1 percent for one degree rise in temperature in the reduction at DME of Cd(II) in presence of monobromoacetate ions.

The experiment (b) was repeated at 313° K to determine

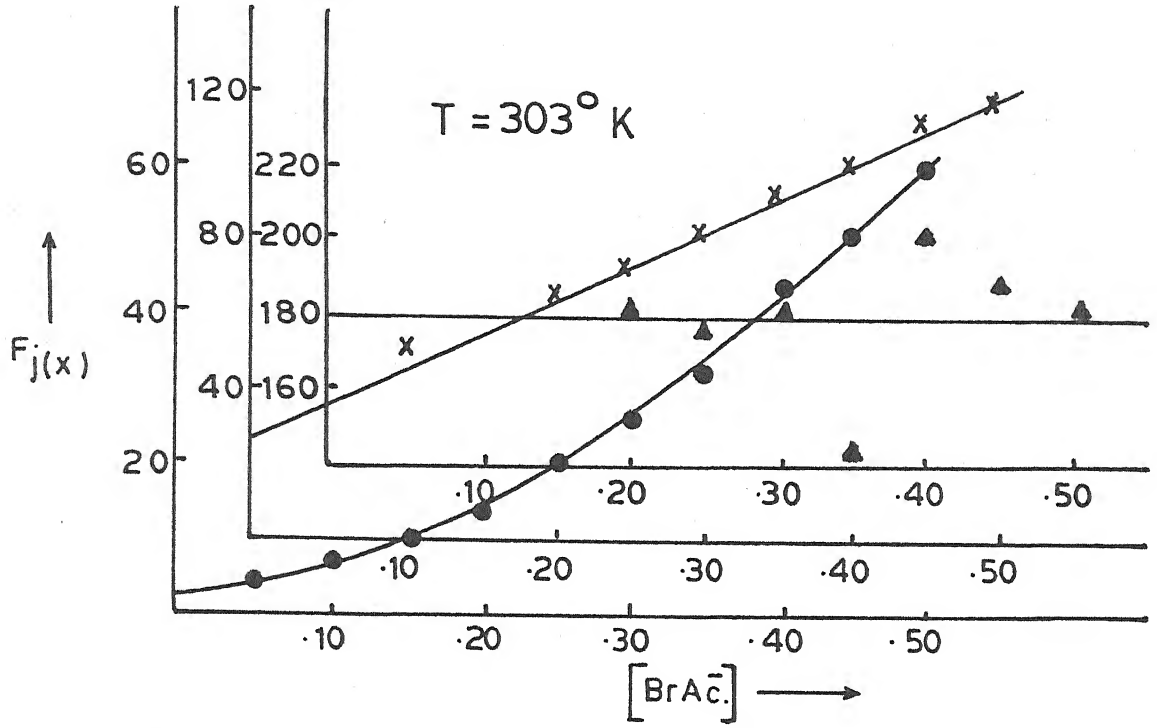

Fig. 6·23 - Plot of $F_{j(x)}$ Vs. [BrAc̄.]; Cd(BrAc̄.)system.

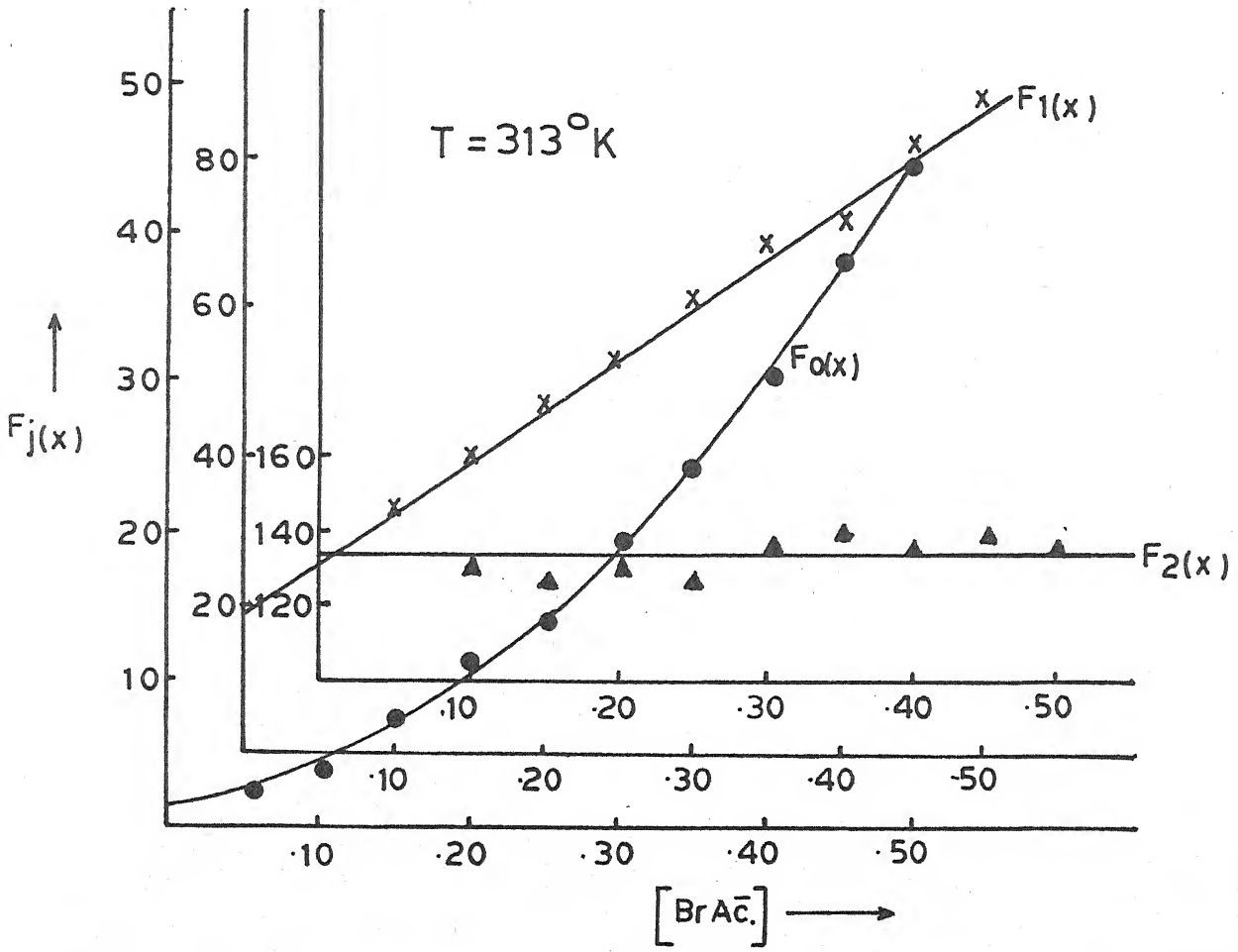

Fig. 6·24 - Plot of $F_{j(x)}$ Vs. [BrAc̄.]; Cd(BrAc̄.)system.

Table 6.22

Polarographic data for Cadmium monobromoacetate system

Concn. of Cd^{++} ions = 0.9 mM Ionic strength = 1.0 M ($NaClO_4$)
$E_{1/2}$ of Cd^{++} ions = -0.576 V vs. SCE Temperature = 303° K
Slopes of plots of $-E_{de}$ vs. $-\log. i/i_d-i$ = 29-30 mV

[BrAc̄.] (M)	$\Delta E_{1/2}$ (V)	$\log. I_M/I_C$	$F_0(X)$	$F_1(X)$	$F_2(X)$
0.05	0.015	0.0324	3.39	47.8	-
0.10	0.022	0.0448	5.97	49.7	-
0.15	0.028	0.0575	9.75	58.33	-
0.20	0.032	0.0676	13.55	62.75	183.7
0.25	0.036	0.0741	18.69	70.76	179.0
0.30	0.040	0.0774	25.59	81.96	186.6
0.35	0.043	0.0774	32.20	89.14	147.1
0.40	0.047	0.0808	44.10	107.75	204.4
0.45	0.049	0.0808	51.40	112.0	191.1
0.50	0.051	0.0808	59.91	117.82	183.3

$\beta_1 = 26$ $\beta_2 = 181$

Table 6.23

Polarographic data for Cadmium monobromoacetate system

Concn. of Cd^{++} ions = 0.9 mM Ionic strength = 1.0 M ($NaClO_4$)
$E_{1/2}$ of Cd^{++} ions = -0.570 V vs. SCE Temperature = 313° K
Slopes of plots of $-E_{de}$ vs. $-\log. i/i_d-i$ = 29-30 mV

[BrAc̄.] (M)	$\Delta E_{1/2}$ (V)	$\log. I_M/I_C$	$F_0(X)$	$F_1(X)$	$F_2(X)$
0.05	0.012	0.0375	2.65	-	-
0.10	0.018	0.0517	4.28	32.8	133.0
0.15	0.024	0.0635	6.86	39.06	130.4
0.20	0.029	0.0755	10.22	46.1	133.0
0.25	0.033	0.0848	14.04	52.16	130.6
0.30	0.037	0.0911	19.17	60.56	136.8
0.35	0.040	0.0943	24.12	69.0	141.4
0.40	0.043	0.0975	30.36	73.4	134.7
0.45	0.046	0.1007	38.21	82.68	140.4
0.50	0.048	0.1047	44.65	87.3	135.6

$\beta_1 = 19.5$ $\beta_2 = 134$

β_1 and β_2 at the higher temperature. The overall formation constant values were found to be 19.5 and 134 for $[Cd(BrAc.)]^+$ and $[Cd(BrAc.)_2]$ complexes respectively. The relevant polarographic data and $F_j(X)$ plots are presented in table 6.23 and figure 6.24.

Thermodynamic parameters ΔG, ΔH and ΔS were evaluated from the knowledge of β_1 at two temperatures and are included in table 6.24.

Table 6.24

Cadmium monobromoacetate system

Temperature (° K)	$\log \beta_1$	$-\Delta G$ (kj)	$-\Delta H$ (kj)	$-\Delta S$ (kj deg^{-1})x10^3
303	1.4149	8.2089		47.7636
			22.6813	
313	1.2900	7.7313		47.7635

6.3.09 Cadmium dibromoacetate system :

(a) Nature of reduction : That two electron of Cd(II) in presence of dibromoacetate ions is reversible and solely diffusion controlled is established from the following observations :

(i) Linear plots of $-E_{de}$ vs. -log. i/i_d-i have slopes of 29-30 mV.

(ii) The temperature co-efficients of $E_{1/2}$ and i_d are 0.4 ± 0.1 mV per degree and 0.5 ± 0.1 mV respectively.

(iii) The plots of i_d against $\sqrt{h_{eff.}}$ of mercury column are straight lines.

(b) Effect of ligand concentration : The half wave potential shifts towards the more negative direction and diffusion current decreases gradually when polarographic investigations at 303° K on solutions containing 0.9 mM Cd(II) ions, 0.002% gelatin, increasing dibromoacetate ion concentration and requisite amounts of sodium perchlorate were carried out. This indicated that the dibromoacetate ions have formed complexes with Cd(II) ions. The plot of $\Delta E_{1/2}$ vs. -log. $[Br_2Ac^-]$ is a curve (figure 6.25). Hence DeFord and Hume's method, when applied, yielded 21.5 and 122 as the β_1 and β_2 values. The polarographic data is presented in table 6.25 and figure 6.26.

(c) Effect of temperature : The temperature co-efficient values of $E_{1/2}$ and i_d were of the order of 0.4 $\pm$ 0.1 mV per degree and 0.5 $\pm$ 0.1 percent per degree respectively.

The effect of ligand concentration was reinvestigated at 313° K to yield 12.5 and 102 as the overall formation constant values of $[Cd(Br_2Ac.)]^+$ and $[Cd(Br_2Ac.)_2]$ complexes respectively for which the polarographic data and $F_j(X)$ functions have been included in table 6.26 and figure 6.27.

Table 6.27 contains the thermodynamic parameters computed from the knowledge of two sets of formation constants.

P.T.O

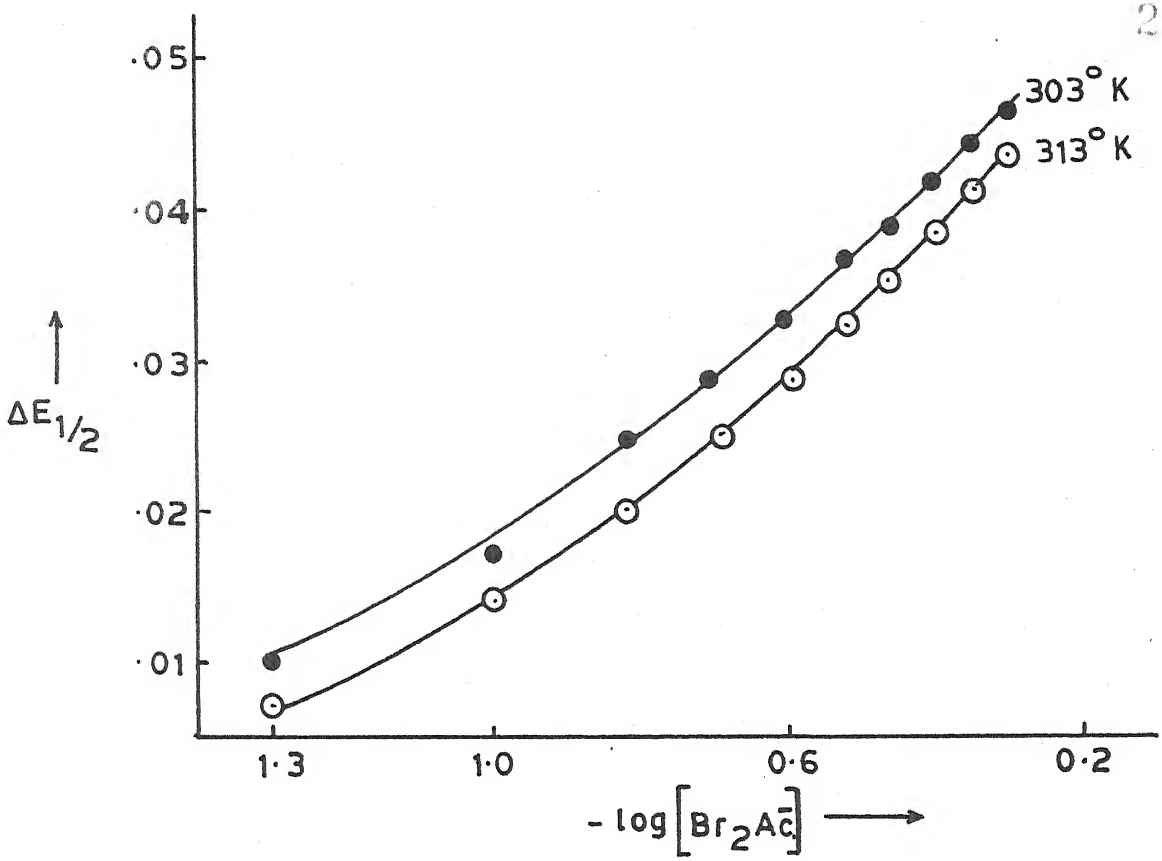

Fig. 6·25 - Plot of $\Delta E_{1/2}$ Vs. $-\log\left[Br_2A\bar{c}.\right]$; Cd($Br_2A\bar{c}.$)system.

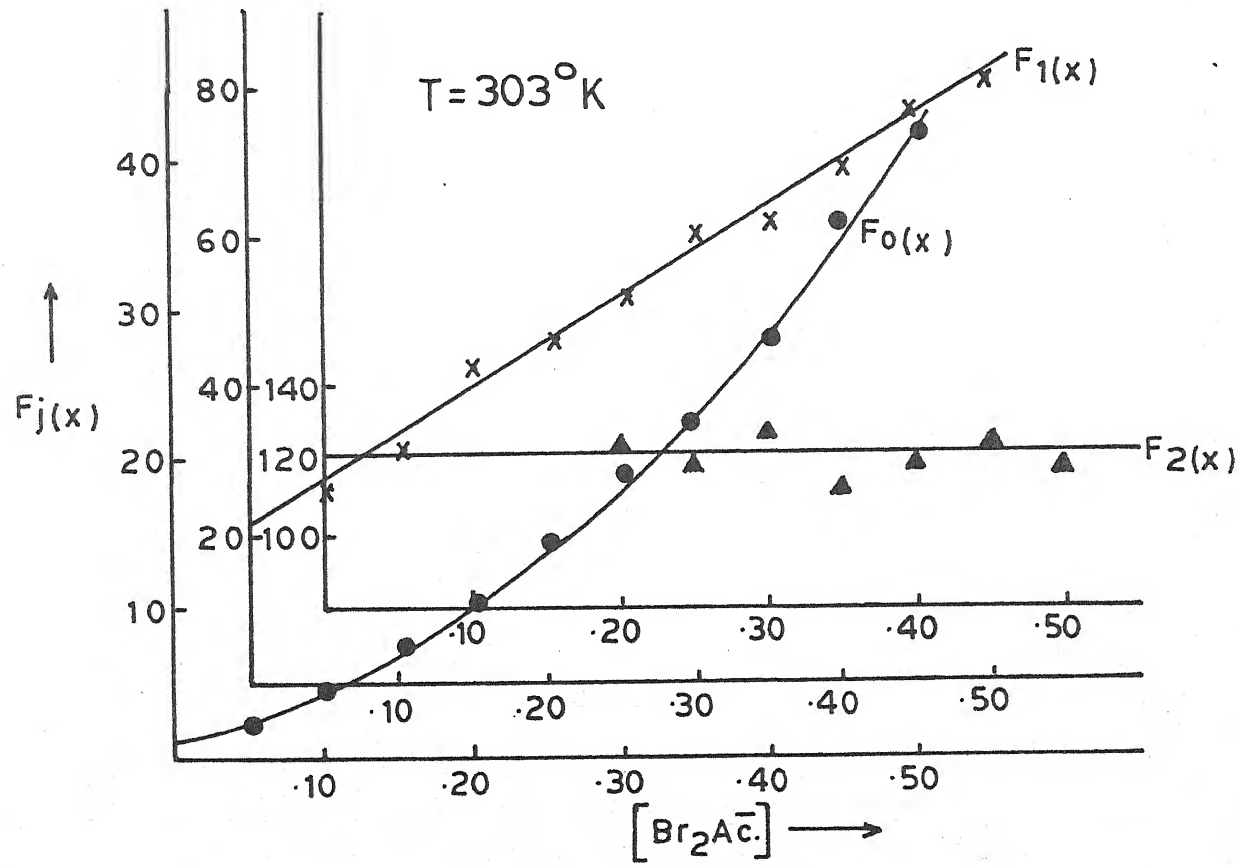

Fig. 6·26 - Plot of $F_{j(x)}$ Vs. $\left[Br_2Ac.\right]$; Cd(Br_2Ac.)system.

Table 6.25

Polarographic data for Cadmium dibromoacetate system

Concn. of Cd^{++} ions = 0.9 mM Ionic strength = 1.0 M ($NaClO_4$)
$E_{1/2}$ of Cd^{++} ions = -0.576 V vs. SCE Temperature = 303° K
Slopes of plots of $-E_{de}$ vs. -log. i/i_d-i = 29-30 mV

$[Br_2A\bar{c}.]$ (M)	$\Delta E_{1/2}$ (V)	log. I_M/I_C	$F_0(X)$	$F_1(X)$	$F_2(X)$
0.05	0.010	0.0179	2.30	26.0	-
0.10	0.017	0.0303	4.03	30.3	-
0.15	0.025	0.0399	7.44	42.93	-
0.20	0.029	0.0464	10.26	46.3	124.0
0.25	0.033	0.0496	14.04	52.0	122.0
0.30	0.037	0.0529	19.22	60.73	130.0
0.35	0.039	0.0529	22.40	61.14	114.0
0.40	0.042	0.0563	28.19	69.75	120.6
0.45	0.045	0.0563	35.75	77.22	123.3
0.50	0.047	0.0563	41.67	81.34	119.7

$\beta_1 = 21.5$ $\beta_2 = 122$

Table 6.26

Polarographic data for Cadmium dibromoacetate system

Concn. of Cd^{++} ions = 0.9 mM Ionic strength = 1.0 M ($NaClO_4$)
$E_{1/2}$ of Cd^{++} ions = -0.570 V vs. SCE Temperature = 313° K
Slopes of plots of $-E_{de}$ vs. -log. i/i_d-i = 29 mV

$[Br_2A\bar{c}.]$ (M)	$\Delta E_{1/2}$ (V)	log. I_M/I_C	$F_0(X)$	$F_1(X)$	$F_2(X)$
0.05	0.007	0.0273	1.78	15.6	-
0.10	0.014	0.0475	3.16	21.6	-
0.15	0.020	0.0595	5.05	27.0	96.6
0.20	0.025	0.0718	7.53	32.65	100.7
0.25	0.029	0.0781	10.28	37.12	98.5
0.30	0.033	0.0845	14.03	43.43	103.1
0.35	0.036	0.0877	17.66	47.6	100.3
0.40	0.039	0.0909	22.23	53.07	101.4
0.45	0.042	0.0942	27.98	59.95	105.4
0.50	0.044	0.0975	32.70	65.4	105.8

$\beta_1 = 12.5$ $\beta_2 = 102$

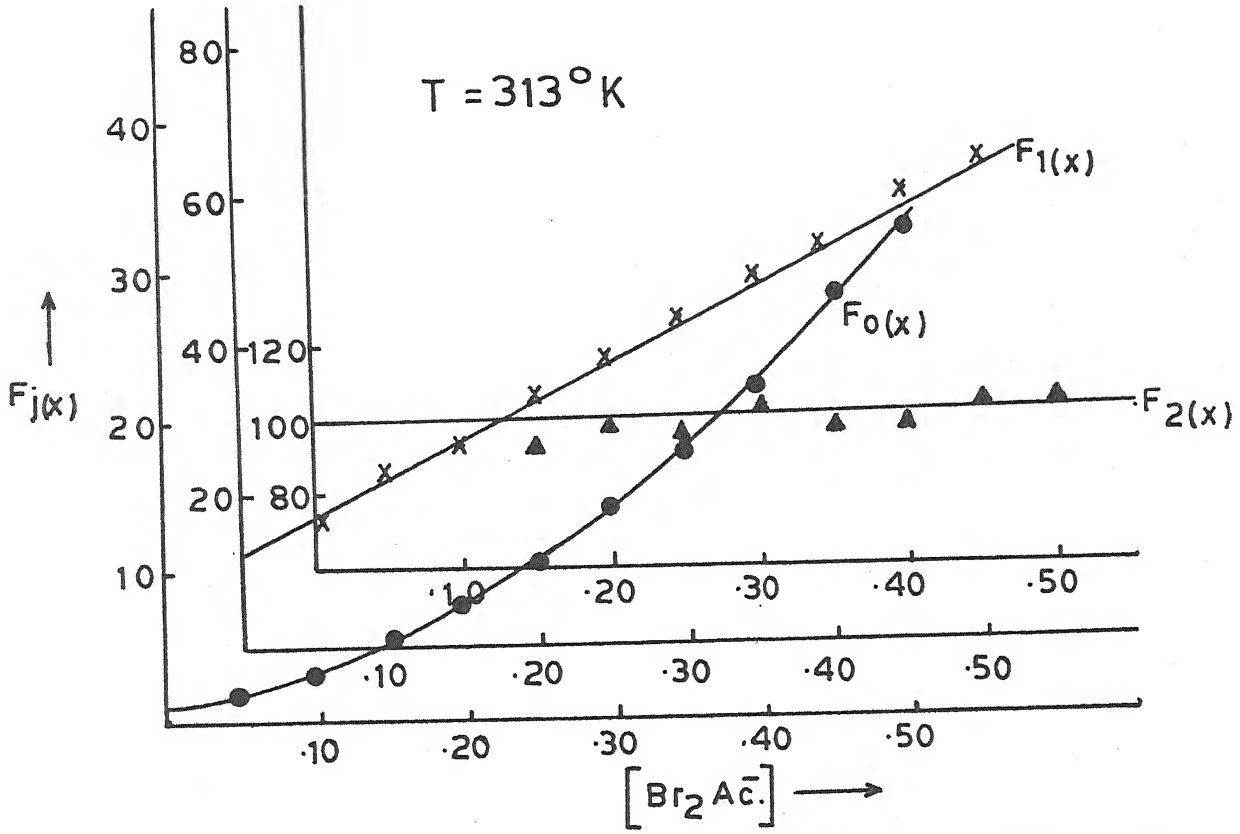

Fig.6·27 - Plot of $F_{j(x)}$ Vs. $[Br_2 A\bar{c}.]$; Cd $(Br_2 A\bar{c}.)$ system.

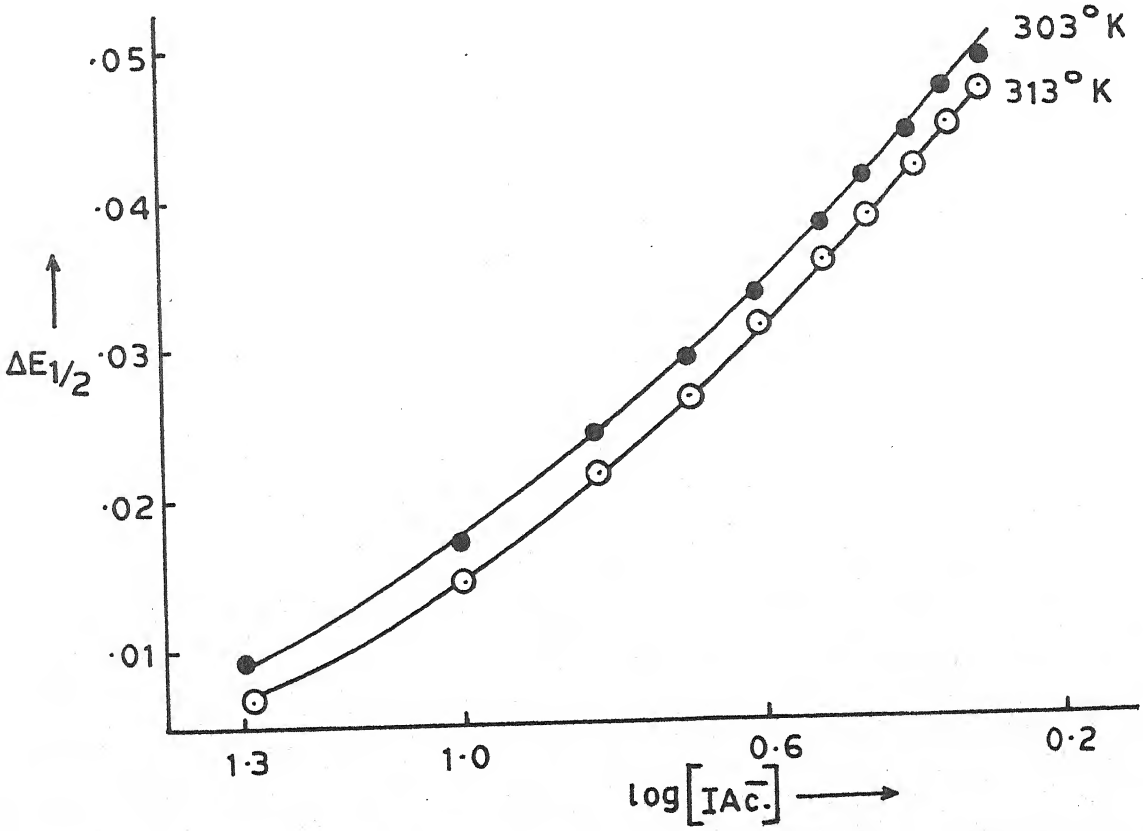

Fig.6·28 - Plot of $\Delta E_{1/2}$ Vs. $-\log[IA\bar{c}.]$; Cd $(IA\bar{c}.)$ system.

Table 6.27

Cadmium dibromoacetate system

Temperature (^{o} K)	$\log \beta_1$	$-\Delta G$ (kj)	$-\Delta H$ (kj)	$-\Delta S$ (kj deg^{-1})x10^3
303	1.3324	7.7303		115.6287
			42.7658	
313	1.0969	6.5740		115.6287

6.3.10 Cadmium monoiodoacetate system :

(a) Nature of reduction : The linear plots of $-E_{de}$ vs. $-\log i/i_d - i$ with slopes of 29-30 mV, the temperature coefficients of $E_{1/2}$ (0.2-0.3 mV per degree) and i_d (0.5 $\pm$ 0.1 percent per degree) coupled with the constancy of ratio of diffusion current and square root of effective height of mercury column lead us to conclude that the two electron reduction of Cd(II) in presence of monoiodoacetate ions is reversible and diffusion controlled.

(b) Effect of ligand concentration : Polarography at 303^{o} K of solutions containing 0.9 mM Cd(II) ions, 0.002% gelatin, increasing amounts of monoiodoacetate ions and decreasing amounts of sodium perchlorate to keep ionic strength constant at 1.0 M showed complex formation between Cd(II) and monoiodoacetate ions as revealed by a cathodic shift in half wave potential and decrease in diffusion current. The plot of $\Delta E_{1/2}$ vs. $-\log.[IAc^-]$ being a curve (figure 6.28) stepwise complex formation was inferred and method of DeFord and Hume applied to evaluate the overall formation constants as 14.5 and 168 respectively for

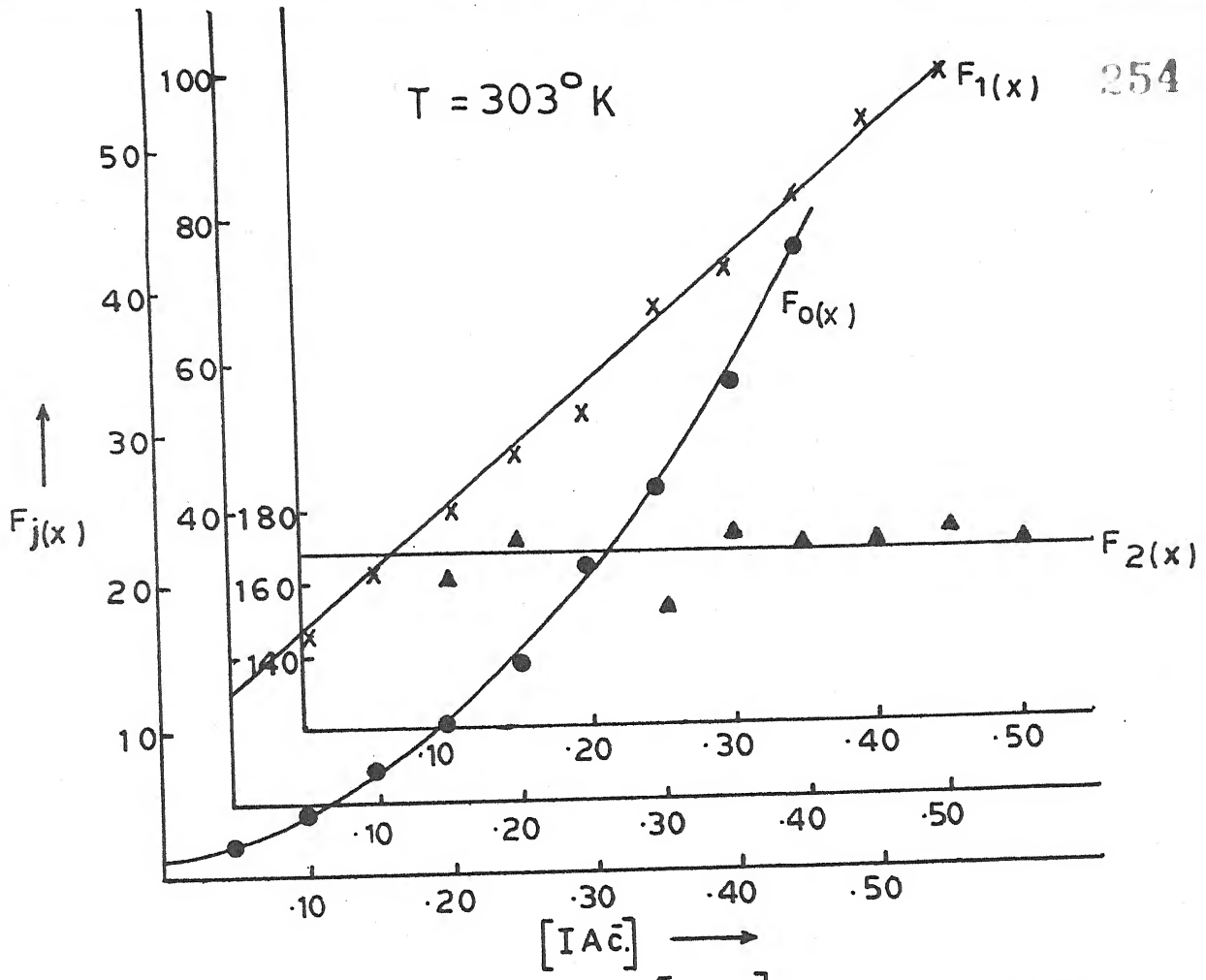

Fig. 6·29 - Plot of $F_{j(x)}$ Vs. $[IA\bar{c}]$; Cd (IAc̄) system.

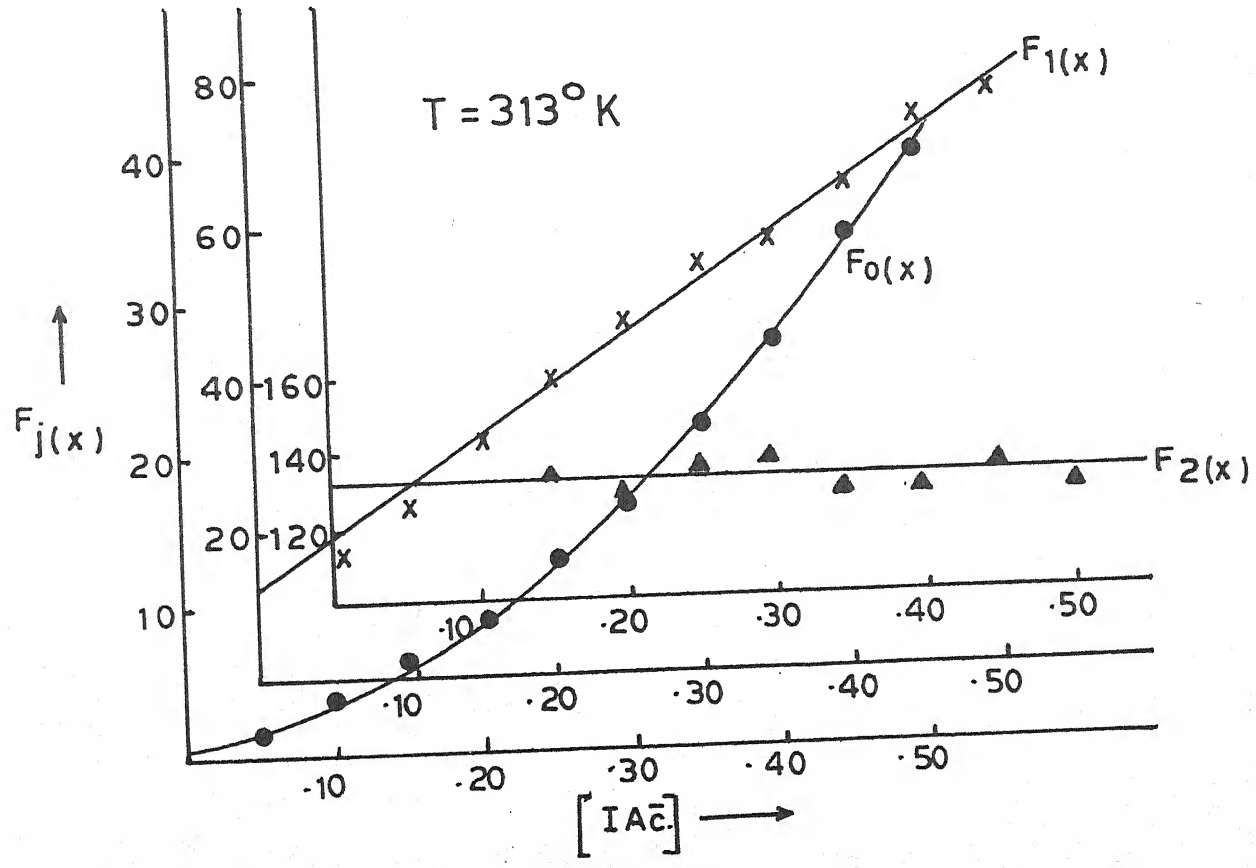

Fig. 6·30 - Plot of $F_{j(x)}$ Vs. $[IA\bar{c}]$; Cd (IAc̄) system.

Table 6.28

Polarographic data for Cadmium monoiodoacetate system

Concn. of Cd^{++} ions = 0.9 mM Ionic strength = 1.0 M ($NaClO_4$)

$E_{1/2}$ of Cd^{++} ions = -0.576 V vs. SCE Temperature = 303° K

Slopes of plots of $-E_{de}$ vs. -log. i/i_d-i = 29-30 mV

$[I\bar{A}c.]$ (M)	$\Delta E_{1/2}$ (V)	log. I_M/I_C	$F_0(X)$	$F_1(X)$	$F_2(X)$
0.05	0.009	0.0321	2.14	22.8	166.0
0.10	0.017	0.0445	4.07	30.7	162.0
0.15	0.024	0.0508	7.06	40.46	173.0
0.20	0.029	0.0539	10.44	47.2	163.5
0.25	0.033	0.0571	14.28	53.12	154.5
0.30	0.038	0.0604	21.11	67.03	175.0
0.35	0.041	0.0636	26.76	73.6	168.9
0.40	0.044	0.0669	33.94	82.35	169.6
0.45	0.047	0.0702	43.03	93.4	175.0
0.50	0.049	0.0735	50.54	99.08	169.1

$\beta_1 = 14.5$ $\beta_2 = 168$

Table 6.29

Polarographic data for Cadmium monoiodoacetate system

Concn. of Cd^{++} ions = 0.9 mM Ionic strength = 1.0 M ($NaClO_4$)

$E_{1/2}$ of Cd^{++} ions = -0.570 V vs. SCE Temperature = 313° K

Slopes of plots of $-E_{de}$ vs. -log. i/i_d-i = 29-30 mV

$[I\bar{A}c.]$ (M)	$\Delta E_{1/2}$ (V)	log. I_M/I_C	$F_0(X)$	$F_1(X)$	$F_2(X)$
0.05	0.007	0.0263	1.78	15.6	-
0.10	0.015	0.0429	3.35	23.5	-
0.15	0.022	0.0543	5.79	31.93	132.9
0.20	0.027	0.0631	8.56	37.8	129.0
0.25	0.032	0.0690	12.57	46.28	137.1
0.30	0.036	0.0751	17.15	53.83	139.4
0.35	0.039	0.0751	21.43	58.37	132.5
0.40	0.042	0.0781	26.96	64.9	132.2
0.45	0.045	0.0812	33.91	73.13	135.8
0.50	0.047	0.0843	39.62	77.24	130.5

$\beta_1 = 12$ $\beta_2 = 132$

$[Cd(IAc.)]^{+}$ and $[Cd(IAc.)_2]$ complexes for which the polarographic data and $F_j(X)$ plots appear in table 6.28 and figure 6.29.

(c) Effect of temperature : The temperature co-efficient values of $E_{1/2}$ and i_d were of the order of 0.2-0.3 mV per degree and 0.5 ± 0.1 percent per degree respectively for the reduction of Cd(II) in monoiodoacetate ions.

The formation constants were redetermined at 313° K and were found to be 12 and 132 for 1:1 and 1:2 metal/ligand ratio complexes. The relevant polarographic data and $F_j(X)$ plots are presented in table 6.29 and figure 6.30.

Table 6.30 presents the thermodynamic functions evaluated from the knowledge of formation constants at the two temperatures.

Table 6.30

Cadmium monoiodoacetate system

Temperature (° K)	$\log \beta_1$	$-\Delta G$ (kj)	$-\Delta H$ (kj)	$-\Delta S$ (kj deg^{-1})x10^3
303	1.1613	6.7376		27.0283
			14.9272	
313	1.0791	6.4673		27.0284

6.4 DISCUSSION :

As already discussed in earlier chapters, the subject of study of formation constants of metal complexes is very complicated because there are a number of variables

involving the central metal, the ligand, the composition of the solvent and the temperature at which the investigations are undertaken. The only reasonable and logical approach to the stability is to keep as many variables constant as possible and then examine a small area of the subject.

We, too have, in our present investigations, attempted to determine the stability of haloacetate complexes of Cd(II) under almost identical conditions so that we can make comparisons and look into various factors affecting the relative stability of complexes.

It was, however, not possible to study the complexes of tribromo-, diiodo- and triiodoacetic acids because they get hydrolysed when their sodium salts are prepared. Their easy tendency to hydrolysis is due to the lower carbon/halogen bond energy and greater intramolecular repulsions between halogen atoms to render them unstable and susceptible to hydrolysis to yield more stable products. The bond energies and bond lengths of carbon-halogen bonds are listed[13] below :

Bond	Bond length (A^{o})	Bond energy (kj)
C - F	1.42	447.7
C - Cl	1.77	326.4
C - Br	1.91	284.5
C - I	2.13	213.4

Cd(II) forms the weakest complexes among the four cations under investigation in accord with the Mellor and Maley

order.[1] A comparative account of stability constants of various haloacetate complexes of Cd(II) is given below :

System	At 303° K		At 313° K	
	β_1	β_2	β_1	β_2
Cd acetate	46	126	40	82
Cd monofluoroacetate	37	250	27.5	200
Cd difluoroacetate	12.5	138	10	85
Cd trifluoroacetate	11	114	8.5	72
Cd monochloroacetate	32	110	24.5	68
Cd dichloroacetate	20	152	12.5	154
Cd trichloroacetate	16	234	11.5	116
Cd monobromoacetate	26	181	19.5	134
Cd dibromoacetate	21.5	122	12.5	102
Cd monoiodoacetate	14.5	168	12	132

In no case more than two stepwise complexes have been formed due probably to the smaller concentration range (0.00 to 0.50 M) used in the investigations.

A survey of the formation constants reveals that in each case β_1 (or K_1) is greater than β_2/β_1 (or K_2). This decrease in second stepwise formation constant can be explained on the basis of the following considerations.

(a) Statistical factors : Cd(II) can have a maximum co-ordination number of six so that the free metal ion $[Cd(H_2O)_6]^{++}$ has six

sites for the first ligand to choose from , to form $[Cd(H_2O)_5L]^+$ complex. When the second ligand is to enter the co-ordination sphere, there are only five sites available to it to co-ordinate with the metal ion. Statistically, therefore, there is lesser probability for the formation of the 1:2 complex than the 1:1 complex.

(b) Steric hindrance : When 1:1 complex has been formed, a smaller H_2O molecule has been replaced by bulkier haloacetate ions to restrict space around the central metal ion. So, when the second ligand is to enter the co-ordination sphere, it has lesser space available to accomodate itself. Hence it suffers steric hindrance which was not so for the entry of the first ligand.

(c) Coulombic factors : For the attachment of the first uninegative ligand, there is a bipositive free metal ion i.e. $[Cd(H_2O)_6]^{2+}$ so that there is considerable attraction between the two. But for the entry of the second uninegative ligand, there is only unipositive 1:1 complex i.e. $[Cd(H_2O)_5L]^+$, for attraction between the two. Hence there is lesser attraction for the second ligand to attach to the 1:1 complex. These three factors combine together to explain why K_2 is less than K_1 in each case.

It is also noticed that the formation constant for monosubstituted haloacetate complex is less than that of non-substituted haloacetate complex, that of disubstituted haloacetate complex is less than the monosubstituted haloacetate complex and finally the trisubstituted haloacetate complex has

less stability than the disubstituted haloacetate complex for each halogen to yield the trend:

$$[CdAc.]^{+} > [Cd(XAc.)]^{+} > [Cd(X_2Ac.)]^{+} > [Cd(X_3Ac.)]^{+}$$

The following considerations are able to explain the trend.

Each substitution of the hydrogen atom by halogen atom from the acetate ion reduces its basicity due to inductive effect depending upon the halogen introduced.

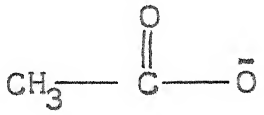

acetate ion

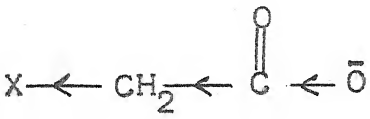

monohaloacetate ion

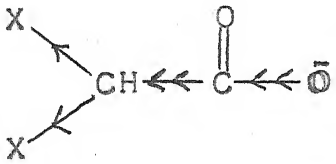

dihaloacetate ion

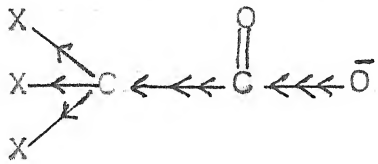

trihaloacetate ion

The acetate ion itself has low basicity. Its basic nature is further reduced due to replacement of H by more electronegative halogen by inductive effect which results in electron withdrawal form the co-ordinating O atom of the substituted haloacetate ions. Replacement of one, two and three

H atoms successively reduces the basicity of the parent acetate ions so that their co-ordinating ability gets correspondingly decreased.

Further the successively bulkier mono-, di- and triacetate ions experience greater steric hindrance while entering the co-ordination sphere. Hence the following trend of formation constants gets explained.

$[Cd(Ac.)]^+ = 46 > [Cd(FAc.)]^+ = 37 > [Cd(F_2Ac.)]^+ = 12.5 > [Cd(F_3Ac.)]^+ = 11$ for each halogen at a given temperature (303° K in this case).

Another discernible order to emerge from the survey can be stated as in the form of the following trends of formation constants :

(a) $[Cd(FAc.)]^+ > [Cd(ClAc.)]^+ > [Cd(BrAc.)]^+ > [Cd(IAc.)]^+$

(b) $[Cd(F_2Ac.)]^+ < [Cd(Cl_2Ac.)]^+ < [Cd(Br_2Ac.)]^+$

(c) $[Cd(F_3Ac.)]^+ < [Cd(Cl_3Ac.)]^+$

From the point of view of electronegativity and consequent inductive effect only in halosubstituted acetate ion, the trends (b) and (c) are logical. But the trend (a) is exactly reverse of what is expected.

The situation may be explained as follows :

The stronger inductive effect of more electronegative

halogen substituted acetate ion is more than counterbalanced by the smaller size of the ligand (due to the size trend F < Cl < Br < I)as a result of which lesser steric hindrance increases the stability of the complex.

In other words, single halogen substitution is not able to exert an inductive effect strong enough to counter easier formation of the complex due to lesser steric hindrance. Hence the trend (a) is justified.

But when successively two and three halogens substitute in acetate ion, the inductive effect is doubled and tripled while the size of the ligand has also increased. The size of the ligand becomes greater as we move from fluoro to bromo - substituted acetate ions. But now inductive effect more than cancels the relatively smaller increase in ligand size.The increase in ligand size is maximum for mono haloacetate ion and is relatively less as we go from mono- to di- and di- to trisubstituted haloacetate ions. Hence inductive effect predominates over the size increase to justify the trends (b) and (c).

In short while the size of the ligand determines trend (a), the trends (b) and (c) are determined by inductive effect.

In each case we have obtained lesser value of β_1 at the higher temperature. This is because there is greater dissociation and hence lesser formation of the complex at the

elevated temperature. We have obtained almost no change in ΔS of the 1:1 complex at both the temperatures. It may appear to be surprising. However, it is possible to explain the phenomenon in terms of number of particles available in the system when the complex partially dissociates at the higher temperature.

$$\left[Cd(H_2O)_5(XAc.)\right]^{+} + H_2O \rightleftharpoons \left[Cd(H_2O)_6\right]^{++} + (XAc^{-}.)$$

Since the number of particles determine the disorder or entropy of a system, there is no change in ΔS as the number of particles remain the same even on partial dissociation of the complex at the higher temperature.

The positive shift in ΔG of the 1:1 complex at the higher temperature is obviously due to lesser stability of the complex at the raised temperature so that its free energy registers an increase.

The negative ΔH or enthalpy value for the formation of each complex results from the replacement of weaker Cd(II) - H_2O bonds by stronger Cd - haloacetate bonds. Thus heat content of the system is reduced.

LITERATURE CITED

1. D.P. Mellor and L.E. Maley, Nature, 159, 370 (1947).
2. R.S. Kolat and J.E. Powell, Inorg. Chem., 1, 293 (1962).
3. D.W. Archer and C.B. Monk, J. Chem. Soc., 3117 (1964).
4. S. Gobon, Acta Chem. Scand., 17, 1814 (1963).
5. P. Gerding, Acta Chem. Scand., 22, 1283 (1968).
6. N. Janaka, M. Kamada, H. Osawa and G. Sato, Bull. Chem. Soc., Japan, 33, 1412 (1960).
7. G.R. Goel and N.K. Jha, Can. J. Chem., 59, 3267 (1981).
8. A.I. Khokhlora, A.M. Robov and V.A. Fedorov, Neorg. Khim., 26, 258 (1981).
9. P.H. Tedesco and J. Martinez, An Asoc. Quim. Argent., 32, 144 (1983).
10. H. Matsui, Nagoy Kogyo Gijutsu Shiken Sho Hokoku, 32, 144 (1983).
11. D.D. DeFord and D.N. Hume, J. Am. Chem. Soc., 5321, 73, (1951).
12. H. Irving, 'Advances in Polarography', Pergamon Press, Oxford, 49 (1960).
13. I.L. Finar, 'Organic Chemistry', Vol. 1, ELBS/Longman, 36-37 (1985).